

HEAT TRANSFER MEASUREMENT OF SLUG
TWO-PHASE FLOW IN A HORIZONTAL AND
A SLIGHTLY UPWARD INCLINED TUBE

By

KAPIL MALHOTRA

Bachelor of Science

Siddaganga Institute of Technology

Tumkur, Karnataka (India)

2000

Submitted to the Faculty of the
Graduate College of the
Oklahoma State University
in partial fulfillment of
the requirements for
the Degree of
MASTER OF SCIENCE
December 2004

HEAT TRANSFER MEASUREMENT OF SLUG
TWO-PHASE FLOW IN A HORIZONTAL AND
A SLIGHTLY UPWARD INCLINED TUBE

Thesis Approved:

Dr. Afshin A. Ghajar

Thesis Advisor

Dr. Frank W. Chambers

Dr. P. M. Moretti

Dr. A. Gordon Emslie

Dean of the Graduate College

ACKNOWLEDGEMENTS

I would like to thank my advisor Dr. A.J. Ghajar for his friendship, advice and endless support during my graduate career. Special thanks go to my colleagues, Steve Trimble, Jae-yong Kim and Samit Nabar for their help and sacrifice.

I will also like to thank Dr. P.M.Moretti and Dr. F.W.Chambers for their advice and support during my masters program.

This thesis is dedicated to my parents Mr. J.L.Malhotra, Mrs. Neeru Malhotra and my brother Manav Malhotra for their cooperation and love.

TABLE OF CONTENTS

CHAPTER	PAGE
CHAPTER I INTRODUCTION	1
1.1 Background.....	1
1.2 Objectives of Study.....	2
1.3 Scope and Limitations.....	3
CHAPTER II LITERATURE SURVEY	5
2.1 Flow Regime Mapping	6
2.2 Single-Phase Heat Transfer in a Pipe.....	10
2.3 Two-Phase Heat Transfer in a Pipe.....	10
CHAPTER III EXPERIMENTAL EQUIPMENT, CALIBRATION AND DATA REDUCTION	20
3.1 Test Section Descriptions	20
3.1.1 Test Cradle.....	20
3.1.2 Water Supply.....	22
3.1.3 Pump	22
3.1.4 Heat Exchanger	22
3.1.5 Flow Meters and Flow Regulation	23
3.1.6 Air Supply.....	23
3.1.7 Controls.....	24
3.1.8 Mixing Section	25
3.1.9 Test Section.....	25
3.1.10 Power/Uniform Heat Source.....	27
3.1.11 Data Acquisition System	27
3.2 Thermocouples and Thermocouple Calibration.....	27
3.2.1 Thermocouples.....	27
3.2.2 Thermocouple and Probe Calibration.....	30
3.2.3 Thermocouple Attachment	31
3.3 Isothermal Trials, Pre and Post Heat Checks.....	33
3.3.1 Isothermal Trials.....	33
3.4 Other Calibrations.....	33
3.4.1 Air and Water Mass Flow Rate Calibration.....	33
3.4.2 Voltmeter and Ammeter Measurements	35

3.5 Data Reduction Program.....	36
3.5.1 Input Data.....	36
3.5.2 Finite-Difference Formulations.....	37
3.5.3 Physical Properties of the Fluids.....	42
3.5.4 Output.....	43
3.6 Heat Transfer in a Horizontal Pipe.....	45
3.6.1 Single-Phase Flow Heat Transfer.....	45
3.6.2 Colburn (1933).....	46
3.6.3 Sieder & Tate (1936).....	46
3.6.4 Gnielinski (1976).....	47
3.6.5 Heat Transfer in Two-Phase Flow.....	48
3.7 Uncertainty Analysis.....	49
3.8 Experimental Procedures.....	50
3.8.1 Reliability.....	53
CHAPTER IV RESULTS AND DISCUSSION.....	55
4.1 General.....	55
4.1.1 Heat Transfer Coefficient.....	56
4.1.2 Horizontal Experimental Data.....	61
4.1.3 Two Degree Data.....	77
4.1.4 Five Degree Data.....	89
4.1.5 Seven Degree Data.....	101
4.2 Comparison of Slug-Flow Data at Different Tube Inclinations.....	112
4.2.1 Low Liquid Reynolds Number Analysis.....	114
4.2.2 Medium Liquid Reynolds Number Analysis.....	122
4.2.3 High Liquid Reynolds Number Analysis.....	133
4.2.4 Modified Froude Number.....	152
4.3 Slug Flow Heat Transfer Correlation.....	154
4.3.1 Slug Flow Heat Transfer Correlation Development.....	155
CHAPTER V CONCLUSIONS AND RECOMMENDATIONS.....	160
5.1 Conclusions.....	160
5.2 Recommendations.....	161
BIBLIOGRAPHY.....	162
APPENDIX A SOURCE CODE.....	166
APPENDIX B UNCERTAINTY ANALYSIS.....	212

LIST OF TABLES

TABLE		PAGE
Table 2.1	Air-water mass flow rate values for various flow patterns and number of data points taken from Kim and Ghajar (2002)	9
Table 2.2	Correlations for two-phase heat transfer, Kim <i>et al</i> (1999)	15
Table 2.3	Limitations of the heat transfer correlations found by Kim <i>et al</i> (1999).....	16
Table 2.4	Ranges of experimental data used by Kim <i>et al</i> (1999).....	17
Table 2.5	Recommended correlations for two-phase heat transfer, Kim <i>et al</i> (1999).....	18
Table 2.6	Horizontal correlation and respective parameters of Kim and Ghajar (2002).....	19
Table 3.1	Physical properties of the fluids used in this study.....	43
Table 3.2	Colburn (1933) single-phase heat transfer results	46
Table 3.3	Sieder and Tate (1936) single-phase heat transfer results	47
Table 3.4	Gnielinski (1976) [3] single-phase heat transfer results	48
Table 3.5	Two-phase comparison runs	49
Table 3.6	Stabilization time	51
Table 3.7	Random repeat runs to check the reliability	54
Table 4.1	Heat transfer results for horizontal position	62
Table 4.2	Heat transfer results for the two degree tube inclination.....	78
Table 4.3	Heat transfer results for the five degree tube inclination.....	90
Table 4.4	Heat transfer results for the seven degree tube inclination.....	102
Table 4.5	Average change of h_{TP} for various tube inclinations	112
Table 4.6	Horizontal and two degree experimental data comparison.....	146
Table 4.7	Horizontal and five degree experimental data comparison	147
Table 4.8	Horizontal and seven degree experimental data comparison	148
Table 4.9	Two degree and five degree experimental data comparison	149
Table 4.10	Two degree and seven degree experimental data comparison.....	150
Table 4.11	Five degree and seven degree experimental data comparison.....	151
Table 4.12	Recommended values for modified Kim and Ghajar (2002) correlation for slug flow data.....	156

LIST OF FIGURES

FIGURE	PAGE
Figure 2.1	9
Figure 3.1	21
Figure 3.2	26
Figure 3.3	28
Figure 3.4	29
Figure 3.5	31
Figure 3.6	34
Figure 3.7	35
Figure 3.8	38
Figure 3.9	45
Figure 3.10	51
Figure 3.11	52
Figure 4.1	57
Figure 4.2	57
Figure 4.3	64
Figure 4.4	65
Figure 4.5	65
Figure 4.6	67
Figure 4.7	67

Figure 4.8	Variation of the superficial liquid Froude number (Fr_{SL}) with the increase of superficial gas Reynolds number (Re_{SG}) for horizontal slug flow data.....	69
Figure 4.9(a)	Flow visualization picture for horizontal position, ($Re_{SL}=5000, Re_{SG}=1500$).....	70
Figure 4.9(b)	Flow visualization picture for horizontal position, ($Re_{SL}=5000, Re_{SG}=3000$).....	71
Figure 4.9(c)	Flow visualization picture for horizontal position, ($Re_{SL}=5000, Re_{SG}=5000$).....	71
Figure 4.10	Variation of the overall mean heat transfer coefficient of horizontal flow over superficial gas Reynolds number (Re_{SG}) with fixed superficial liquid Reynolds number.....	73
Figure 4.11	Variation of the overall mean heat transfer coefficient with the increase of Re_{SL} and Re_{SG} for horizontal data	74
Figure 4.12	Kim and Ghajar's et al (2002) slug flow heat transfer behavior with Re_{SL} and Re_{SG}	75
Figure 4.13	Two-phase heat transfer coefficient as a function of Re_{SL} for horizontal slug data (Trimble et al 2002).....	76
Figure 4.14	Variation of the overall mean heat transfer coefficient with the increase of superficial liquid Reynolds number (Re_{SL}) for the coordinated two degree slug flow data	79
Figure 4.15	Variation of the overall mean heat transfer coefficient with the increase of superficial gas Reynolds number (Re_{SG}) for the coordinated two degree slug flow data	80
Figure 4.16	Variation of the overall mean heat transfer coefficient with the increase of superficial liquid velocity (u_{SL}) for two degree slug flow data.....	81
Figure 4.17	Variation of the overall mean heat transfer coefficient with the increase of superficial gas velocity (u_{SG}) for two degree slug flow data.....	81
Figure 4.18	Variation of the superficial liquid Froude number (Fr_{SL}) with the increase of superficial gas Reynolds number (Re_{SG}) for two degree slug flow data	82
Figure 4.19(a)	Flow visualization picture for two degree tube inclination, ($Re_{SL}=5000, Re_{SG}=1500$).....	83
Figure 4.19(b)	Flow visualization picture for two degree tube inclination, ($Re_{SL}=5000, Re_{SG}=3000$).....	83
Figure 4.19(c)	Flow visualization picture for two degree tube inclination, ($Re_{SL}=5000, Re_{SG}=5000$).....	84
Figure 4.20	Back flow effects on heat transfer characteristics in inclined tube position.....	85
Figure 4.21	Variation of overall mean heat transfer coefficient of two degree inclined flow over superficial gas Reynolds number (Re_{SG}) for fixed superficial liquid Reynolds number (Re_{SL})	86
Figure 4.22	Variation of the overall mean heat transfer coefficient with the increase of Re_{SL} and Re_{SG} for two degree data	87

Figure 4.23	Two-phase heat transfer coefficient as a function of Re_{SL} for two degree slug data (Trimble et al 2002)	88
Figure 4.24	Variation of the overall mean heat transfer coefficient with the increase of superficial liquid Reynolds number (Re_{SL}) for the coordinated five degree slug flow data	91
Figure 4.25	Variation of the overall mean heat transfer coefficient with the increase of superficial gas Reynolds number (Re_{SG}) for the coordinated five degree slug flow data	92
Figure 4.26	Variation of the overall mean heat transfer coefficient with the increase of superficial liquid velocity (u_{SL}) for five degree slug flow data	93
Figure 4.27	Variation of the overall mean heat transfer coefficient with the increase of superficial gas velocity (u_{SG}) for five degree slug flow data	93
Figure 4.28	Variation of the superficial liquid Froude number (Fr_{SL}) with the increase of superficial gas Reynolds number (Re_{SG}) for five degree slug flow data	94
Figure 4.29(a)	Flow visualization picture for five degree tube inclination, ($Re_{SL}=5000$, $Re_{SG}=1500$)	95
Figure 4.29(b)	Flow visualization picture for five degree tube inclination, ($Re_{SL}=5000$, $Re_{SG}=3000$)	95
Figure 4.29(c)	Flow visualization picture for five degree tube inclination, ($Re_{SL}=5000$, $Re_{SG}=5000$)	96
Figure 4.30	Retarded flow effects on heat transfer characteristics in inclined tube position	97
Figure 4.31	Variation of overall mean heat transfer coefficient of five degree inclined flow over superficial gas Reynolds number (Re_{SG}) for fixed superficial liquid Reynolds number (Re_{SL})	98
Figure 4.32	Variation of the overall mean heat transfer coefficient with the increase of Re_{SL} and Re_{SG} for five degree data	99
Figure 4.33	Two-phase heat transfer coefficient as a function of Re_{SL} for five degree slug data (Trimble et al 2002)	100
Figure 4.34	Variation of the overall mean heat transfer coefficient with the increase of superficial liquid Reynolds number (Re_{SL}) for the coordinated seven degree slug flow data	103
Figure 4.35	Variation of the overall mean heat transfer coefficient with the increase of superficial gas Reynolds number (Re_{SG}) for the coordinated five degree slug flow data	103
Figure 4.36	Variation of the overall mean heat transfer coefficient with the increase of superficial liquid velocity (u_{SL}) for seven degree slug flow data	104
Figure 4.37	Variation of the overall mean heat transfer coefficient with the increase of superficial gas velocity (u_{SG}) for seven degree slug flow data	105

Figure 4.38	Variation of the superficial liquid Froude number (Fr_{SL}) with the increase of superficial gas Reynolds number (Re_{SG}) for seven degree slug flow data	106
Figure 4.39(a)	Flow visualization picture for seven degree tube inclination, ($Re_{SL}=5000$, $Re_{SG}=1500$).....	107
Figure 4.39(b)	Flow visualization picture for seven degree tube inclination, ($Re_{SL}=5000$, $Re_{SG}=3000$).....	107
Figure 4.39(c)	Flow visualization picture for seven degree tube inclination, ($Re_{SL}=5000$, $Re_{SG}=5000$).....	108
Figure 4.40	Variation of overall mean heat transfer coefficient of seven degree inclined flow over superficial gas Reynolds number (Re_{SG}) for fixed superficial liquid Reynolds number (Re_{SL})	109
Figure 4.41	Variation of the overall mean heat transfer coefficient with the increase of Re_{SL} and Re_{SG} for seven degree data.....	111
Figure 4.42	Variation of overall mean heat transfer coefficient for $Re_{SL}=5000$ series for varying Re_{SG} values.....	114
Figure 4.43	Visual observations ($Re_{SL}=5000$, $Re_{SG}=1500$).....	115
Figure 4.43(a)	Five degree slug flow at time=0.0 sec, ($Re_{SL}=5000$, $Re_{SG}=1500$).....	119
Figure 4.43(b)	Seven degree slug flow at time=0.0 sec, ($Re_{SL}=5000$, $Re_{SG}=1500$).....	119
Figure 4.44	Horizontal slug flow pattern.....	117
Figure 4.45	Variation of superficial liquid Froude number with the variation of superficial gas Reynolds number for $Re_{SL}=5000$ series	120
Figure 4.46	Variation of overall mean heat transfer coefficient for $Re_{SL}=7000$ series for varying Re_{SG} values.....	121
Figure 4.47	Variation of superficial liquid Froude number for $Re_{SL}=7000$ series for varying Re_{SG} values	122
Figure 4.48	Variation of overall mean heat transfer coefficient for $Re_{SL}=15000$ series for varying Re_{SG} values.....	123
Figure 4.49	Visual observations ($Re_{SL}=15000$, $Re_{SG}=2200$).....	125
Figure 4.49(a)	Five degree slug flow at time=0.0 sec, ($Re_{SL}=15000$, $Re_{SG}=2200$).....	127
Figure 4.49(b)	Seven degree slug flow at time=0.0 sec, ($Re_{SL}=15000$, $Re_{SG}=2200$).....	128
Figure 4.50	Variation of superficial liquid Froude number for $Re_{SL}=15000$ series for varying Re_{SG} values	129
Figure 4.51	Variation of overall mean heat transfer coefficient for $Re_{SL}=9500$ series for varying Re_{SG} values.....	130
Figure 4.52	Variation of superficial liquid Froude number for $Re_{SL}=9500$ series for varying Re_{SG} values	130
Figure 4.53	Variation of overall mean heat transfer coefficient for $Re_{SL}=12000$ series for varying Re_{SG} values.....	131
Figure 4.54	Variation of superficial liquid Froude number for $Re_{SL}=12000$ series for varying Re_{SG} values	131

Figure 4.55	Variation of overall mean heat transfer coefficient for $Re_{SL}=17000$ series for varying Re_{SG} values.....	132
Figure 4.56	Variation of superficial liquid Froude number for $Re_{SL}=17000$ series for varying Re_{SG} values	132
Figure 4.57	Variation of overall mean heat transfer coefficient for $Re_{SL}=26000$ series for varying Re_{SG} values.....	134
Figure 4.58	Visual observations ($Re_{SL}=26000, Re_{SG}=4000$).....	136
Figure 4.58(a)	Horizontal slug flow at time=0.0 sec, ($Re_{SL}=26000, Re_{SG}=4000$).....	139
Figure 4.58(b)	Two degree slug flow at time=0.0 sec, ($Re_{SL}=26000, Re_{SG}=4000$).....	139
Figure 4.58(c)	Five degree slug flow at time=0.0 sec, ($Re_{SL}=26000, Re_{SG}=4000$).....	140
Figure 4.58(d)	Seven degree slug flow at time=0.0 sec, ($Re_{SL}=26000, Re_{SG}=4000$).....	140
Figure 4.59	Variation of superficial liquid Froude number for $Re_{SL}=26000$ series for varying Re_{SG} values	141
Figure 4.60	Variation of overall mean heat transfer coefficient for $Re_{SL}=22000$ series for varying Re_{SG} values.....	142
Figure 4.61	Variation of superficial liquid Froude number for $Re_{SL}=22000$ series for varying Re_{SG} values	143
Figure 4.62	Variation of overall mean heat transfer coefficient for varying Re_{SL} values.....	144
Figure 4.63	Variation of overall mean heat transfer coefficient for varying superficial liquid Froude number for complete slug flow data (0, 2, 5, 7 degree tube inclinations).....	145
Figure 4.64	Variation of overall mean heat transfer coefficient with changing superficial liquid Froude number (Using Eq. 4.5 to calculate Fr_{SL})	153
Figure 4.65	Variation of overall mean heat transfer coefficient with changing superficial liquid Froude number (Using Eq. 4.6 to calculate Fr_{SL})	153
Figure 4.66	Slug flow correlation prediction of complete data set (141 data points) using new exponents for the modified Kim and Ghajar (2002) correlation.....	157
Figure 4.67	Slug flow correlation prediction of inclined data set (105 data points) using new exponents for the modified Kim and Ghajar (2002) correlation.....	158
Figure 4.68	Slug flow correlation prediction of horizontal data set (36 data points) using new exponents for the modified Kim and Ghajar (2002) correlation.....	159

NOMENCLATURE

English Letter Symbols

A	cross sectional area, ft ² or m ²
A	annular
ABS	annular/bubbly slug
atm	atmosphere or atmospheric
AW	annular wavy
AWG	American Wire Gauge
BS	bubbly slug
BTU	British thermal unit
C	Celsius
C _p , C _{pl} , c	specific heat at constant pressure, Btu/(lb _m ·°F) or J/kg·K
C _f , c _f	coefficient of friction
D, d	inside diameter of a circular tube, ft or m
f	f-stop setting for camera shutter speed
F	Fahrenheit
Fr _{SL}	superficial liquid Froude number
ft	foot or feet
g	acceleration due to gravity, ft/s ² or m/s ²
gpm	gallons per minute
Heat _{in}	power input through by the test section

Heat _{taken}	power taken by the test fluid, Btu/hr or W
h	heat transfer coefficient, Btu/(s·ft ² ·°F) or W/(m ² ·K)
h _i	local peripheral heat transfer coefficient, Btu/(s·ft ² ·°F) or W/(m ² ·K)
hr	hour
Hz	Hertz or cycles (s ⁻¹)
i	enthalpy
I	electrical current, Amps, A
I.D.	inner diameter
in	inches
K	wavy flow, dimensionless
K	velocity ratio (=U _G /U _L), dimensionless
k	thermal conductivity, Btu/(hr·ft·°F) or W/(m·K)
kg	kilograms
L	liter
L, l	length of test section, ft or m
Lb, lb	pounds
m	mass flow rate, lb _m /s or kg/s
m	meters
Nu	Nusselt number (=hD/k), dimensionless
N _{th}	number of finite-difference sections in the theta-direction (peripheral) which is equal to the number of thermocouples at each station
P	pressure

Pr	Prandtl number
psi	pounds per square inch (lb/in ²), unit of pressure
PT	pressure tap
Q,q	rate of heat transfer, Btu/hr or W
Q	generated heat, Btu/hr or W
Q	volumetric flow rate, ft ³ /min, or m ³ /min
q"	heat flux, Btu/(hr·ft ²) or W/m ²
R	resistance ($=\gamma l/A$), Ω
R	Rankine
Re	Reynolds number ($=DG/\mu$), dimensionless
Re _{SL}	superficial liquid Reynolds number, dimensionless
Re _{SG}	superficial gas Reynolds number, dimensionless
r _i	tube inside radius, ft or m
RMS	root mean square
SCFM	standard cubic feet per minute, (ft ³ /min)
SL	slug
St	stratified
St.	station
T	dispersed bubble flow, dimensionless
T	temperature, °F or °C
TC	thermocouple
TMP	temporary
V	velocity, ft/s or m/s

u_{SL}	superficial liquid velocity, ft/s or m/s
u_{SG}	superficial gas velocity, ft/s or m/s
U	uncertainty interval, dimensionless
V	voltage drop through the test section, Volts, V
W	watt or watts
W	wavy
WS	wavy/slug
X	distance from the pipe inlet to the thermocouple station, ft or m
X	Martinelli parameter, dimensionless
x	local distance along the test section from the inlet, ft or m
x	flow quality ($=m_g/m_t$), dimensionless
x^+	axial distance inside a tube ($=(x/r_o)/(RePr)$), dimensionless
Y	dimensionless inclination parameter
y	local weigh fraction vapor, dimensionless
δz	length of element, ft or m

Greek Letter Symbols

α	angle between the pipe axis and the horizontal, positive for downward flow, rad
γ	electric resistivity of the element, $\mu\Omega\cdot\text{in}$ or $\Omega\cdot\text{m}$
Δ	change in...
Θ	radial dimension of pipe, rads
Δr	incremental radius, ft or m

ρ	density, lb _m /ft ³
μ	viscosity, lb _m /ft-hr

Subscripts and Superscripts

a	denotes air
b,bulk	bulk or mixed-mean fluid condition
cal	evaluated based on calculation or correlation
D	evaluated based on diameter
exp	evaluated based on experimental data
FR	denotes flow rate
f	denotes fluid
G,g	denotes gas
i	evaluated based on the inside wall
i	index of the finite-difference grid points radial direction starting from the outside surface of the tube
in	evaluated on inlet condition
j	index of the finite-difference grid points radial peripheral direction starting from top of the tube and increasing clockwise
L,l	denotes liquid
m	mean
out	evaluated at the outlet condition
o	evaluated based on the outside wall
SG	denotes superficial gas
SL	denotes superficial liquid

TP	two-phase
w,wall	denotes condition at inside wall of tube
w	denotes water
x	evaluated at a particular point along the surface

CHAPTER 1

INTRODUCTION

This chapter starts with the basic definition of two-phase slug flow. It touches on the applications of this type of flow pattern and then discusses the main focus of this study. It describes the objectives and finally concludes with the discussion on the scope and limitations of this study.

1.1 Background

Two-phase flow is a characteristic term for a gas-liquid, gas-solid, or a liquid-solid flow, flowing simultaneously in a pipe, channel, or other conduit. Such a flow can be created by flowing two separate fluids or species or by a single fluid or species that has undergone a physical change of state, from solid to liquid or from liquid to a gas. This type of flow can be observed in long pipelines containing petroleum, oil, and natural gas products, or in well bores and refrigeration processes.

This study focuses on the application and measurement of heat transfer on a flow experiencing a slug flow pattern at the horizontal and at slightly upward inclined angles. The test apparatus used was built and tested during the Ph.D. work of Dongwoo Kim (2000), and the Masters work of Jae-yong Kim (1999), Venkata Ryali (1999) and Durant (2003). This thesis is a continuation of the work that was started during their graduate studies.

In order to understand the two-phase flow heat transfer phenomenon, a mental picture of the flow patterns must be established. Flow patterns determine hydrodynamic and thermal conditions of these fluids and the respective heat transfer properties are dependent upon the types of fluids present in the flow. So it is of the utmost importance to understand the effects that two-phase flow has on the fluids so that a better understanding of the heat transfer properties can be made.

Two-phase flow creates a multitude of flow patterns. This specific study focuses on the slug flow pattern. Many researchers have defined this flow pattern but no unique definition exists. Shaharabany (1976) defined slug flow as a flow in which liquid slugs bridge the pipe and are accelerated to the gas phase velocity separated by gas zones flowing over a slow moving film. Kim (2000) defined slug flow as one in which most of the gas is located in large bullet shaped bubbles which have a diameter almost equal to the pipe diameter. They move uniformly upward and are sometimes designated as “Taylor bubbles”. Taylor bubbles are separated by slugs of continuous liquid which bridge the pipe and contain small gas bubbles. Between the Taylor bubbles and the pipe wall, liquid flows downward in the form of a thin falling film.

Many other definitions exist for the slug flow pattern, but in this study we are following the definition given by Kim (2000).

1.2 Objectives of Study

The main objective of this study is to take controlled slug flow data so that the heat transfer behavior could be better understood. The data has been systematically controlled and recorded for horizontal, 2 degree, 5 degree and 7 degree tube inclinations.

The use of flow visualization has been incorporated so as to explain the intricacies of heat transfer behavior which cannot be explained effectively otherwise. An explanation fortified with flow visualization pictures has been put forward to explain how the heat transfer behaves when a comparative study is carried out for various tube inclinations. In the end a unified correlation for slug flow heat transfer prediction has been suggested for horizontal and inclined tube positions. To summarize in points, the main objectives of this study are:

- 1) Record systematically controlled slug flow data for horizontal, 2 degree, 5 degree and 7 degree tube inclination.
- 2) Carry out systematic analysis of the heat transfer behavior for the horizontal and inclined tube positions and explain the intricacies of this behavior.
- 3) Develop a unified correlation for prediction of horizontal and inclined slug flow heat transfer.

1.3 Scope and Limitations

The results that are reported in this thesis are:

- 1) Developed, systematic approach to securing the test setup and recording data.
- 2) Heat transfer measurement data for horizontal, 2°, and 5° and 7° tests.
- 3) Analysis of the heat transfer data for horizontal, 2°, and 5° and 7° tests.
- 4) A unified correlation for the prediction of the heat transfer for horizontal and inclined slug flow data.
- 5) Conclusions and recommendations for further development.

This test-up was made by moving the old test setup to a new and more research-oriented facility. This work was done in the Masters work of Jae-yong Kim (1999), Venkata Ryali (1999) and Durant (2003). Also, the contribution of Mr. Steve Trimble and Mr. Sameet Nabar is greatly appreciated. During this move, the integrity of the original test setup was jeopardized. While repairing the setup, modifications were approved to further the scope and abilities of the research. Newer, more sophisticated and accurate devices, which are discussed in Chapter 3, were incorporated into the apparatus. With these additions, the full scope of two-phase flow patterns and measurements could be made.

CHAPTER II

LITERATURE REVIEW

The primary objective of this thesis is to gather accurate and controlled data concerning heat transfer properties in horizontal, two degree, five degree and seven degree air-water, slug flow in a pipe. The data has been systematically controlled so that a better understanding of heat transfer characteristics for this particular flow pattern could be made.

Literature describing the physical properties of two-phase flow has been investigated, which requires an understanding of what flow rates do the slug flow patterns develop and stabilize. Such a method would require the use of a flow regime map. Since very few consistent profiles exist it is very difficult to set the basis of the determination of flow pattern. Many investigators have published data for different types of fluid flows and tube sizes, yet there is little agreement as to the classifications of the flow patterns. Thus, we have used visualization as a tool to identify and explore many different cases which will allow the slug flow to be characterized.

Heat Transfer studies for two-phase flows are dominated by the presence of vertically oriented tests. Few researchers have studied horizontal two-phase flow and still fewer have experimented with inclined two-phase air-water heat transfer. These facts alone make this experiment a significant contribution to the understanding of two-phase flow heat transfer.

2.1 Flow Regime Mapping

We first focus on the open literature to see what important factors have been used to determine for the two-phase flow pattern mapping. Many investigators have tackled this subject, Bergelin *et al* (1949) suggested one of the first flow pattern maps. Their diagram, based on air-water system in a 1-in. pipe uses the liquid and gas mass flow rates, M_L and M_G , as the coordinates.

Johnson and Abou-Sabe (1952) proposed a flow pattern map which is very similar to that of Bergelin and Gazley. Their research was based on air-water data in a 0.87-in. pipe.

Alves (1954) suggested a map based on data for air-water and air-oil mixtures using superficial liquid and gas velocities, V_{SL} and V_{SG} , as the coordinates. The research was based on a pipe of 1-in. diameter.

Baker (1954) proposed a flow pattern map based on the data of Alves (1954) and Kosterin (1949). The research was based on air-water fluid mixture. He plotted gas mass velocity to the ratio of liquid to gas velocity.

White and Huntington (1955) proposed a flow pattern map. The research utilized pipes with diameters of 1-in., 1.5-in., and 2-in. They used gas-oil and air-water as fluids for their research. They used liquid and gas mass velocities as the coordinates.

Hoogendoorn (1959) presented a paper that focused on the gathering of information on two-phase air-water and air-oil mixtures in horizontal smooth pipes with diameters ranging from 24 mm to 140 mm, and rough pipes with inner diameters of 50 mm. Hoogendoorn (1959) used flow rates of approximately 0.02 to 320 m³/hr for the

liquid side, which was produced using four centrifugal pumps and a pressure vessel. Air was used from a 6.5 atm supply producing a maximum flow rate of 1800 kg/hr. With these specifications and mechanical power, the scope of Hoogendoorn (1959) was far greater than this research.

Govier and Omer (1962) presented a map based on their data for air-water system. They used liquid and gas mass velocities as coordinates similar to what White and Huntington (1955) did. The research was based on a 1.026-in. pipe diameter.

Scott (1963) modified Baker's (1954) diagram. He utilized the more recent data of Hoogendoorn (1959) and Govier and Omer (1962). His modified diagram shows relatively wide bands depicting regions of transition from one flow pattern to another.

Govier and Aziz (1972) included the data of Baker (1954) and Hoogendoorn (1959) to create a better flow pattern map. They used superficial liquid and gas velocities as coordinates similar to what was used by Alves (1954).

Mandhane *et al* (1974) presented a study, which was an extension of the work of Govier and Aziz (1972). They used superficial velocities, V_{SL} and V_{SG} , as the coordinate axes, so that the effect of pipe diameter can be adequately taken care of.

Taitel and Dukler (1976) presented their data in a model that represented five basic flow regimes. These regimes were stratified, intermittent, dispersed bubble, wavy, and annular flow. Five dimensionless groups were discussed and each of the respective patterns was formulated into a dimensionless quantity, X, T, Y, F, and K. In order of appearance, the variables are the Martinelli parameter (X), dispersed bubble flow parameter (T), inclination parameter (Y), modified Froude number (F), and the wavy flow parameter (K). Each of these dimensionless quantities could be determined from the

operating conditions. These five equations could then be solved to produce a flow regime map for any type of operating condition at any inclination.

Barnea *et al* (1983) later performed more tests on smaller diameter pipes, less than 12.3 mm. Again, these tests proved that the formulations created by Taitel and Dukler (1976), were accurate and predict numerous flow patterns for a multitude of flow setups.

Kim *et al* (2000) developed a seven-pattern description for two-phase flow that consisted of stratified, wavy, wavy/slug, slug, wavy/annular, annular/bubbly and or annular/bubbly/slug, and bubbly/slug. This pattern can be seen in Figure 2.1. Kim *et al* (2000) presented research that was performed on the same test apparatus described herein.

Kim *et al* (2000) also created a table containing data on minimum and maximum flow rates for specific types of flow patterns. This data can be seen in Table 2.1. This study is a continuation of the work done by Kim *et al* (2000), and is unique in its own way, since the flow pattern identification has been fortified using flow visualization pictures and videos.

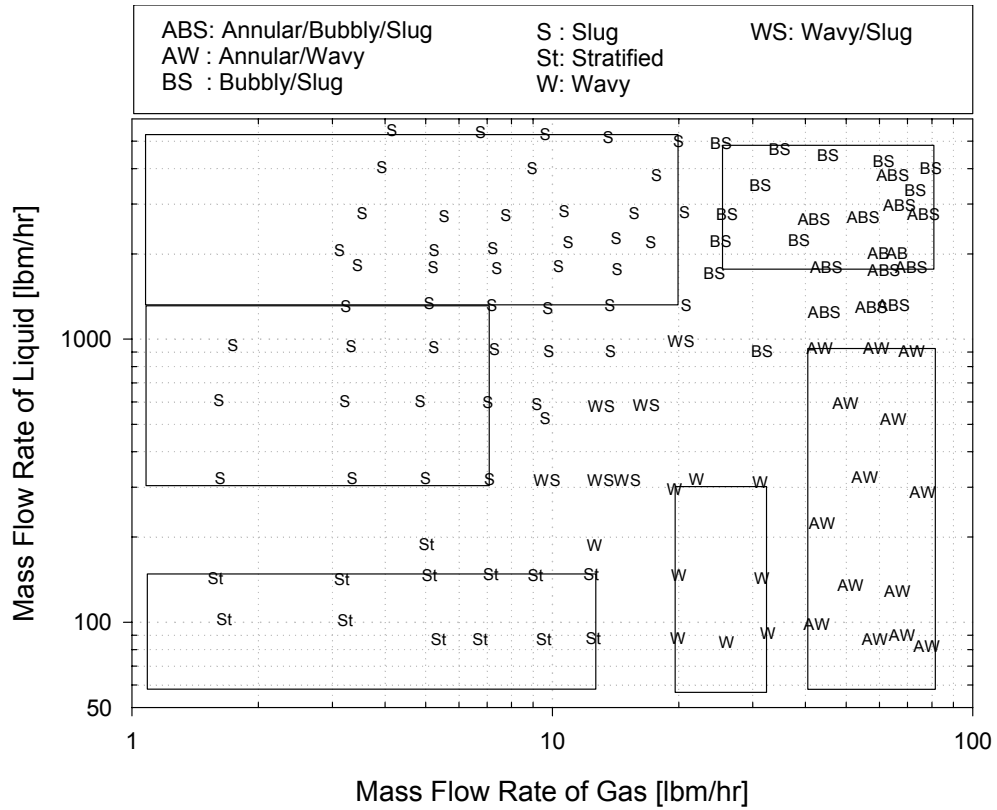


Figure 2.1 Observed flow pattern data versus the corresponding mass flow rates of air and water, Kim *et al* (2000)

Table 2.1 Air-Water mass flow rate values for various flow patterns and number of data points taken from Kim *et al* (2000)

\dot{m}_G [lbm/hr]		\dot{m}_L [lbm/hr]		Expected Flow Pattern	Prospective Number of Data Points
Min.	Max.	Min.	Max.	All of the Flow Patterns	150
0	12	0	147	Stratified	-
0	7	300	1300	Slug	25
0	20	1300	5460	Slug	30
20	32	0	310	Wavy	20
10	30	300	800	Wavy/Slug	-
24	80	1080	4890	Bubbly/Slug or Annular/Bubbly/Slug	35
43	80	0	925	Annular/Wavy	40

2.2 Single-Phase Heat Transfer in a Pipe

Single-phase experiments are essential to validate the equipment. So, before any two-phase experiments were made, single-phase analysis has been carried out to confirm the integrity of the equipment.

The procedure has been taken from Kim (2000). In his thesis he mentions five correlations which have been used as a reference for comparison purposes. These were Colburn (1933), Sieder and Tate (1936), Gnielinski [1] (1976), Gnielinski [3] (1976) and Ghajar and Tam (1994). More detailed analysis about single-phase heat transfer has been discussed in Experimental procedure and calibration.

2.3 Two-Phase Heat Transfer in a Pipe

After establishing the flow rates essential to create slug flow, we shall now investigate the open literature for heat transfer in a horizontal and slightly inclined tube. Few authors have done research in horizontal two-phase slug flow heat transfer and still fewer have done research on inclined two-phase heat transfer slug flow.

Oliver and Wright (1964) studied horizontal slug flow heat transfer experimentally. They used 88% by weight glycol in water, 1.5% sodium carboxymethylcellulose in water, and 0.5% by weight Polox in water. It was suggested in their paper that the heat transfer rise obtained during two-phase slug flow might be due to the increase of liquid velocity and partly due to the presence of circulation within liquid slugs. It was explained that the circulation effect was directly dependent on liquid slug length and might be expected to be of greatest importance when liquid slugs were short enough to permit several cycles of circulation within the heated test section of the tube.

Hughmark (1965) studied horizontal gas-liquid slug flow heat transfer and developed a two-phase heat transfer coefficient correlation. In developing the correlation he used the velocity of gas slug and the liquid slug Reynolds number. He assumed that the entire wall is wet with liquid and there is a continuous liquid phase in the region of the wall to the liquid phase, thus the heat transfers between the wall and the slug only.

Oliver and Young Hoon (1968) studied horizontal slug flow heat transfer using pseudoplastic liquids. They used Graetz number in their analysis and observed that at low Graetz numbers the heat transfer was found to be higher than that predicted by single-phase correlation. They observed that the small heat transfer benefits gained in slug flow contradicts the work of Oliver and Wright (1964). They stated that the possible break up of liquid slugs might be the reason for higher heat transfer rates in Oliver and Wright's work.

Duckler and Hubbard (1975) proposed a hydrodynamic model for the unsteady heat transfer process in slug flow. They suggested that a typical slug unit consists of four zones: (1) a mixing eddy at the front of the slug, in which the slow moving film in front of the slug is scooped up and mixed with the body of the slug; (2) a region behind the mixing eddy consisting of the main body of the liquid slug in which the liquid moves as if in full pipe flow; (3) a liquid film zone, in which the liquid is shed from the back of the slug and decelerates over a length, this liquid flows in a stratified configuration with the depth varying with distance behind the slug; (4) a gas region, flowing over the film and of the same length. This model combined with the model by Taitel and Duckler (1977) permits the prediction of all of these characteristic lengths, as well as velocities in the slug, at various positions in the film and in the gas.

Shaharabany (1976) conducted research on heat transfer for horizontal air-water slug flow. They observed that the heat transfer in the nose of the slug was higher than that in the slug body.

Duckler and Shaharabany (1977) suggested a method for calculating average heat transfer coefficient to be expected in slug flow without the use of complex program. Heat transfer coefficient predictions were compared with Shaharabany (1976) and were found to be in good agreement.

Taitel and Duckler (1977) conducted research on horizontal and near horizontal gas-liquid slug flow. They presented a fundamental model which predicted slug frequency for entry sections in which natural slugging is permitted to take place. The agreement with experimental data was within probable limits of data uncertainty. Five dimensionless groups were shown to control the dimensionless frequency.

Shoham and Duckler (1982) conducted research on horizontal gas-liquid slug flow. They reported the time variation of temperature, heat transfer coefficients, and heat flux for the different zones of slug flow. The authors observed substantial differences in heat transfer coefficient between the bottom and top of the slug and explained the fact that each slug is effectively a thermally developing entry region caused by the presence of a hot upper wall just upstream of each slug. They presented a qualitative theory which explains this behavior.

Barnea and Yacoub (1983) conducted research on heat transfer in vertical gas-liquid slug flow. They developed a mathematical model based on the method of slug characteristic lines for heat transfer analysis.

Hetsroni *et al* (1998a) and Hetsroni *et al* (1998b) analyzed two-phase air-water heat transfer behavior in horizontal and upward inclined tubes. They used Froude number to present their results and analyzed the variation of Froude number on heat transfer analysis in two-phase flow. They observed an enhancement in heat transfer properties as the tube was inclined from two degree to five degree. The research done by them emphasized more on the qualitative results and lacked quantitative explanation. This study is unique since emphasis has been given on quantitative results in analyzing the two-phase slug flow heat transfer in inclined tube positions.

Kim *et al* (1999a) compared all of the correlations with data that was found in the open literature for each of the different types of flows and mixtures.

Trimble *et al* (2002) performed research on two-phase air-water slug flow and observed the pattern of heat transfer behavior when the tube was inclined from horizontal to two degree and five degree positions. The observations made by him were similar to what Hetsroni *et al* (1998b) observed. They both observed an enhancement in heat transfer when the tube is inclined from horizontal to two degree and five degree.

Kim *et al* (1999a) gathered twenty of the identified correlations and the same has been presented in Table 2.2. Also, the limitations of the twenty correlations used in the comparisons as proposed by the original authors are tabulated in Table 2.3. The ranges of the experimental data used to assess the general validity of the correlations listed in Table 2.2 are provided in Table 2.4. Table 2.5 gives the summary of the suggested heat transfer correlations for different flow patterns and different fluid combinations.

Table 2.6 gives the summary of the correlation developed by Kim and Ghajar (2002) for horizontal pipes, based on the doctoral work of Kim (2000). This correlation

was designed to encompass a wide range of flow patterns, including wavy-annular and slug flows, by changing the given parameters and exponential values according to flow pattern. The unified slug flow heat transfer correlation for horizontal and slightly upward inclined tube positions for slug flow in this work will be an extension of the heat transfer correlation developed by Kim and Ghajar (2002).

In analyzing the work done by researchers, we observe that no systematic controlled runs have been carried out for horizontal and slightly inclined tube positions. Also, the use of flow visualization to explain the intricacies of slug flow heat transfer behavior is missing. This forms the basis for this study.

In this study, we have systematically controlled the slug flow heat transfer runs and conducted study on horizontal, two degree, five degree and seven degree tube inclinations. All the parameters are kept same, so as to better understand the heat transfer behavior. The use of flow visualization videos and pictures fortifies the explanation of two-phase slug flow heat transfer and provides insight to the intricacies of the flow. This fact in itself makes this study unique in its own way.

Table 2.2 Heat transfer correlations chosen for the preliminary comparisons by Kim *et al*(1999)

Source	Heat Transfer Correlations	Source	Heat Transfer Correlations
Aggour (1978)	$h_{TP} / h_L = (1 - \alpha)^{-1/3}$ Laminar (L)	Knott et al (1959)	$\frac{h_{TP}}{h_L} = \left(1 + \frac{V_{SG}}{V_{SL}}\right)^{1/3}$ where h_L is from Sieder & Tate (1936)
	$Nu_L = 1.615 (Re_{SL} Pr_L D / L)^{1/3} (\mu_B / \mu_W)^{0.14}$		
Chu & Jones (1980)	$h_{TP} / h_L = (1 - \alpha)^{-0.83}$ Turbulent (T)	Kudirka et al (1965)	$Nu_{TP} = 125 \left(\frac{V_{SG}}{V_{SL}}\right)^{1/8} \left(\frac{\mu_G}{\mu_L}\right)^{0.6} (Re_{SL})^{1/4} (Pr_L)^{1/3} \left(\frac{\mu_B}{\mu_W}\right)^{0.14}$
	$Nu_L = 0.0155 Re_{SL}^{0.83} Pr_L^{0.5} (\mu_B / \mu_W)^{0.33}$		
Davis & David (1964)	$Nu_{TP} = 0.060 \left(\frac{\rho_L}{\rho_G}\right)^{0.28} \left(\frac{DG_{TX}}{\mu_L}\right)^{0.87} Pr_L^{0.4}$	Martin & Sims (1971)	$\frac{h_{TP}}{h_L} = 1 + 0.64 \sqrt{\frac{V_{SG}}{V_{SL}}}$ where h_L is from Sieder & Tate (1936)
Dorresteyn (1970)	$h_{TP} / h_L = (1 - \alpha)^{-1/3}$ (L)	Oliver & Wright (1964)	$Nu_{TP} = Nu_L \left(\frac{1.2}{R_L^{0.36}} - \frac{0.2}{R_L}\right)$ $Nu_L = 1.615 \left[\frac{(Q_G + Q_L)\rho D}{A\mu} Pr_L D / L\right]^{1/3} (\mu_B / \mu_W)^{0.1}$
	$h_{TP} / h_L = (1 - \alpha)^{-0.8}$ (T)		
Dusseau (1968)	$Nu_L = 0.0123 Re_{SL}^{0.9} Pr_L^{0.33} (\mu_B / \mu_W)^{0.14}$	Ravipudi & Godbold (1978)	$Nu_{TP} = 0.56 \left(\frac{V_{SG}}{V_{SL}}\right)^{0.3} \left(\frac{\mu_G}{\mu_L}\right)^{0.2} (Re_{SL})^{0.6} (Pr_L)^{1/3} \left(\frac{\mu_B}{\mu_W}\right)^{0.14}$
	$Nu_{TP} = 0.029 (Re_{TP})^{0.87} (Pr_L)^{0.4}$		
Elamvaluthi & Srinivas (1984)	$Nu_{TP} = 0.5 \left(\frac{\mu_G}{\mu_L}\right)^{1/4} (Re_{TP})^{0.7} (Pr_L)^{1/3} \left(\frac{\mu_B}{\mu_W}\right)^{0.14}$	Rezkallah & Sims (1987)	$h_{TP} / h_L = (1 - \alpha)^{-0.9}$ where h_L is from Sieder & Tate (1936)
Groothuis & Hendaal (1959)	$Nu_{TP} = 0.029 (Re_{TP})^{0.87} (Pr_L)^{1/3} (\mu_B / \mu_W)^{0.14}$ (for water-air)	Serizawa et al (1975)	$\frac{h_{TP}}{h_L} = 1 + 462 X_{TP}^{-1.27}$ where h_L is from Sieder & Tate (1936)
	$Nu_{TP} = 2.6 (Re_{TP})^{0.39} (Pr_L)^{1/3} (\mu_B / \mu_W)^{0.14}$ (for gas-oil-air)		
Hughmark (1965)	$Nu_{TP} = 1.75 (R_L)^{-1/2} \left(\frac{\dot{m}_L c_L}{R_L k_L L}\right)^{1/3} \left(\frac{\mu_B}{\mu_W}\right)^{0.14}$	Shah (1981)	$\frac{h_{TP}}{h_L} = \left(1 + \frac{V_{SG}}{V_{SL}}\right)^{1/4}$ $Nu_L = 1.86 (Re_{SL} Pr_L D / L)^{1/3} (\mu_B / \mu_W)^{0.14}$ (L) $Nu_L = 0.023 Re_{SL}^{0.8} Pr_L^{0.4} (\mu_B / \mu_W)^{0.14}$ (T)
Khoze et al (1976)	$Nu_{TP} = 0.26 Re_{SG}^{0.2} Re_{SL}^{0.55} Pr_L^{0.4}$	Ueda & Hanaoka (1967)	$Nu_{TP} = 0.075 (Re_M)^{0.6} \frac{Pr_L}{1 + 0.035(Pr_L - 1)}$
King (1952)	$\frac{h_{TP}}{h_L} = \frac{R_L^{-0.52}}{1 + 0.025 Re_{SG}^{0.5}} \left[\left(\frac{\Delta P}{\Delta L}\right)_{TP} / \left(\frac{\Delta P}{\Delta L}\right)_L\right]^{0.32}$	Vijay et al (1982)	$h_{TP} / h_L = (\Delta P_{TP} / \Delta P_L)^{0.451}$ $Nu_L = 1.615 (Re_{SL} Pr_L D / L)^{1/3} (\mu_B / \mu_W)^{0.14}$ (L) $Nu_L = 0.0155 Re_{SL}^{0.83} Pr_L^{0.5} (\mu_B / \mu_W)^{0.33}$ (T)
	$Nu_L = 0.023 Re_{SL}^{0.8} Pr_L^{0.4}$		
		Sieder & Tate (1936)	$Nu_L = 1.86 (Re_{SL} Pr_L D / L)^{1/3} (\mu_B / \mu_W)^{0.14}$ (L) $Nu_L = 0.027 Re_{SL}^{0.8} Pr_L^{0.33} (\mu_B / \mu_W)^{0.14}$ (T)

Note: α and R_L are taken from the original experimental data for this study. $Re_{SL} < 2000$ implies laminar flow, otherwise turbulent. For Shah (1980), replace 2000 by 170. With regard to the eqs. given for Shah (1980) above, the laminar two-phase correlation was used along with the appropriate single-phase correlation, since Shah recommended a graphical turbulent two-phase correlation.

Table 2.3 Limitations of the heat transfer correlations used in the preliminary comparisons
(See nomenclature for abbreviations) by Kim *et al* (1999)

Source	Fluids	L/D	Orient.	\dot{m}_G / \dot{m}_L	V_{SG}/V_{SL}	Re_{SG}	Re_{SL}	Pr_L	Flow Pattern(s)
Aggour (1978)	A-W, Helium-W, Freon12-W	52.1	V	7.5×10^{-3} - 5.72×10^{-2}	0.02-470	13.95- 2.09×10^5		5.42-6.36	B, S, A, B-S, B-F, S-A, A-M
Chu & Jones (1980)	W-A	34	V		0.12-4.64	540-2700	16000- 112000		B, S, F-A
Davis & David (1964)	Gas-Liquid		H & V						A, M-A
Dorrestein (1970)	A-Oil	16	V		0.004-4500		300-66000		B, S, A
Dusseau (1968)	A-W	67	V	45-350		$0-4.29 \times 10^4$	1.4×10^4 - 4.9×10^4		F
Elamvaluthi & Srinivas (1984)	A-W A-Glycerin	86	V		0.3-2.5 0.6-4.6		300-14300		B, S
Groothuis & Hendal	A-W Gas-Oil-A	14.3	V	244-977 269-513	1-250 0.6-80		>5000 1400-3500		
Hughmark (1965)	Gas-Liquid		H						S
Khoze et al (1976)	A-W, A-Poly methylsiloxane, A-Diphenyloxide	60-80	V			4000-37000	3.5-210	4.1-90	A
King (1952)	A-W	252	H		1.21-6.94	1570- 8.28×10^4	22500- 11.9×10^4		S
Knott et al (1959)	Petroleum oil- Nitrogen gas	118.6	V	1.57×10^{-3} - 1.19	0.1-40	6.7-162	126-3920		B
Kudirka et al (1965)	A-W, A-Ethylene glycol	17.6	V	1.92×10^{-4} - 0.1427 0-0.11	0.16-75 0.25-67		5.5×10^4 - 49.5×10^4 380-1700	140 @ 37.8°C	B, S, F
Martin & Sims (1971)	A-W	17	H		0.08-276				B, S, A
Oliver & Wright (1964)	A-85% Glycol, A-1.5% SCMC, A-0.5% Polyox		H				500-1800		S
Ravipudi & Godbold (1978)	A-W, A-Toluene, A-Benzene, A-Methanol		V		1-90	3562-82532	8554-89626		F
Rezkallah & Sims (1987)	A, W, Oil, etc.; 13 Liquid-Gas combinations	52.1	V		0.01-7030		$1.8-1.3 \times 10^5$	4.2-7000	B, S, C, A, F, B-S, B-F, S-C, S-A, C- A, F-A
Serizawa et al (1975)	A-W	35	V						B
Shah (1980)	A, W, Oil, Nitrogen, Glycol, etc.; 10 combinations		H & V		0.004-4500		7-253000		B, S, F, F-A, M
Ueda & Hanaoka (1967)	A-Liquid	67	V	9.4×10^{-4} - 0.059	4-50			4-160	S, A
Vijay et al (1982)	A-W, A-Glycerin, Helium-W, Freon12-W	52.1	V		0.005-7670		1.8-130000	5.5-7000	B, S, F, A, M, B-F, S-A, F-A, A-M

Table 2.4 Ranges of the experimental data used in the preliminary comparisons by
Kim *et al* (1999)

Water-Air Vertical Data (139 Points) of Vijay (1978)	$16.71 \leq \dot{m}_L \text{ (lbm/hr)} \leq 8996$ $0.058 \leq \dot{m}_G \text{ (lbm/hr)} \leq 216.82$ $0.007 \leq X_{TT} \leq 433.04$ $0.061 \leq \Delta P_{TP} \text{ (psi)} \leq 17.048$ $5.503 \leq Pr_L \leq 6.982$ $101.5 \leq h_{TP} \text{ (Btu/hr-ft}^2\text{-}^\circ\text{F)} \leq 7042.3$	$0.06 \leq V_{SL} \text{ (ft/sec)} \leq 34.80$ $0.164 \leq V_{SG} \text{ (ft/sec)} \leq 460.202$ $59.64 \leq T_{MIX} \text{ (}^\circ\text{F)} \leq 83.94$ $0.007 \leq \Delta P_{TPF} \text{ (psi)} \leq 16.74$ $0.708 \leq Pr_G \leq 0.710$ $0.813 \leq \mu_W/\mu_B \leq 0.933$	$231.83 \leq Re_{SL} \leq 126630$ $43.42 \leq Re_{SG} \leq 163020$ $14.62 \leq P_{MIX} \text{ (psi)} \leq 74.44$ $0.033 \leq \alpha \leq 0.997$ $11.03 \leq Nu_{TP} \leq 776.12$ $L/D = 52.1, D = 0.46 \text{ in.}$
Glycerin-Air Vertical Data (57 Points) of Vijay (1978)	$100.5 \leq \dot{m}_L \text{ (lbm/hr)} \leq 1242.5$ $0.085 \leq \dot{m}_G \text{ (lbm/hr)} \leq 99.302$ $0.15 \leq X_{TT} \leq 407.905$ $1.317 \leq \Delta P_{TP} \text{ (psi)} \leq 20.022$ $6307.04 \leq Pr_L \leq 6962.605$ $54.84 \leq h_{TP} \text{ (Btu/hr-ft}^2\text{-}^\circ\text{F)} \leq 159.91$	$0.31 \leq V_{SL} \text{ (ft/sec)} \leq 3.80$ $0.217 \leq V_{SG} \text{ (ft/sec)} \leq 117.303$ $80.40 \leq T_{MIX} \text{ (}^\circ\text{F)} \leq 82.59$ $1.07 \leq \Delta P_{TPF} \text{ (psi)} \leq 19.771$ $0.708 \leq Pr_G \leq 0.709$ $0.513 \leq \mu_W/\mu_B \leq 0.610$	$1.77 \leq Re_{SL} \leq 21.16$ $63.22 \leq Re_{SG} \leq 73698$ $17.08 \leq P_{MIX} \text{ (psi)} \leq 62.47$ $0.0521 \leq \alpha \leq 0.9648$ $12.78 \leq Nu_{TP} \leq 37.26$ $L/D = 52.1, D = 0.46 \text{ in.}$
Silicone-Air Vertical Data (162 points) of Rezkallah (1986)	$17.3 \leq \dot{m}_L \text{ (lbm/hr)} \leq 196$ $0.07 \leq \dot{m}_G \text{ (lbm/hr)} \leq 157.26$ $72.46 \leq T_W \text{ (}^\circ\text{F)} \leq 113.90$ $0.037 \leq \Delta P_{TP} \text{ (psi)} \leq 9.767$ $61.0 \leq Pr_L \leq 76.5$ $29.9 \leq h_{TP} \text{ (Btu/hr-ft}^2\text{-}^\circ\text{F)} \leq 683.0$	$0.072 \leq V_{SL} \text{ (ft/sec)} \leq 30.20$ $0.17 \leq V_{SG} \text{ (ft/sec)} \leq 363.63$ $66.09 \leq T_B \text{ (}^\circ\text{F)} \leq 89.0$ $0.094 \leq \Delta P_{TPF} \text{ (psi)} \leq 9.074$ $0.079 \leq Pr_G \leq 0.710$ $L/D = 52.1, D = 0.46 \text{ in.}$	$47.0 \leq Re_{SL} \leq 20930$ $52.1 \leq Re_{SG} \leq 118160$ $13.9 \leq P_{MIX} \text{ (psi)} \leq 45.3$ $0.011 \leq \alpha \leq 0.996$ $17.3 \leq Nu_{TP} \leq 386.8$
Water-Air Horizontal Data (48 points) of Pletcher (1966)	$0.069 \leq \dot{m}_L \text{ (lbm/sec)} \leq 0.3876$ $0.22 \leq \Delta P_M/L \text{ (lbf/ft}^3\text{)} \leq 26.35$ $7.23 \leq \phi_l \leq 68.0$ $7372 \leq q'' \text{ (Btu/hr-ft}^2\text{)} \leq 11077$	$0.03 \leq \dot{m}_G \text{ (lbm/sec)} \leq 0.2568$ $0.021 \leq X_{TT} \leq 0.490$ $73.6 \leq T_W \text{ (}^\circ\text{F)} \leq 107.1$ $433 \leq h_{TP} \text{ (Btu/hr-ft}^2\text{-}^\circ\text{F)} \leq 1043.8$	$7.84 \leq \Delta P/L \text{ (lbf/ft}^3\text{)} \leq 137.5$ $1.45 \leq \phi_g \leq 3.54$ $64.9 \leq T_{MIX} \text{ (}^\circ\text{F)} \leq 99.4$ $L/D = 60.0, D = 1.0 \text{ in.}$
Water-Air Horizontal Data (21 points) of King (1952)	$1375 \leq \dot{m}_L \text{ (lbm/hr)} \leq 6410$ $1570 \leq Re_{SG} \leq 84200$ $136.8 \leq T_{MIX} \text{ (}^\circ\text{F)} \leq 144.85$ $147.9 \leq \Delta P_{TP} \text{ (psf)} \leq 3226$ $1.35 \leq h_{TP} / h_L \leq 3.34$	$0.82 \leq \dot{m}_G \text{ (SCFM)} \leq 43.7$ $0.41 \leq X_{TT} \leq 29.10$ $184.3 \leq T_W \text{ (}^\circ\text{F)} \leq 211.3$ $1462 \leq h_{TP} \text{ (Btu/hr-ft}^2\text{-}^\circ\text{F)} \leq 4415$ $1.35 \leq \phi_l \leq 8.20$	$22500 \leq Re_{SL} \leq 119000$ $0.117 \leq R_L \leq 0.746$ $15.8 \leq P_{MIX} \text{ (psi)} \leq 55.0$ $1.08 \leq V_{SG}/V_{SL} \leq 6.94$ $L/D = 252, D = 0.737 \text{ in.}$

Table 2.6 Horizontal correlation and respective parameters of Kim and Ghajar (2002)

General Form of the Two-Phase Heat Transfer Coefficient Correlation:

$$h_{TP} = (1 - \alpha)h_L \left[1 + C \left(\frac{x}{1-x} \right)^m \left(\frac{\alpha}{1-\alpha} \right)^n \left(\frac{Pr_G}{Pr_L} \right)^p \left(\frac{\mu_G}{\mu_L} \right)^q \right]$$

Experimental Data	Value of C and Exponents (m, n, p, q)				Mean Dev. (%)	rms Dev. (%)	Number of Data within $\pm 20\%$	Range of Dev. (%)	Range of Parameter				
	C	m	n	p					q	ResL	$\left(\frac{x}{1-x} \right)$	$\left(\frac{\alpha}{1-\alpha} \right)$	$\left(\frac{Pr_G}{Pr_L} \right)$
Slug and Bubbly/Slug Bubbly/Slug/Annular or 89 data points from Kim (2000)	2.86	0.42	0.35	0.66	-0.72	12.29	82	-25.17 and 31.31	2468 and 35503	6.9×10^{-4} and 0.03	0.36 and 3.45	0.102 and 0.137	0.015 and 0.028
Slug 21 data points from King (1952)						20.78	10	-31.13 and 35.13	22500 and 119000	7.1×10^{-4} and 0.11	0.34 and 7.55	0.23 and 0.25	0.041 and 0.044
Wavy-Annular 41 data points from Kim (2000)	1.58	1.40	0.54	-1.93	-0.09	3.38	41	-12.77 and 19.26	2163 and 4985	0.05 and 0.13	3.10 and 4.55	0.10 and 0.11	0.015 and 0.018
Wavy 20 data points from Kim (2000)	27.89	3.10	-4.44	-9.65	1.56	16.49	16	-19.79 and 34.42	636 and 1829	0.08 and 0.25	4.87 and 8.85	0.102 and 0.107	0.016 and 0.021
All of the Data Points for Kim (2000) 150 data points	See Above for the Values for Each Flow Pattern				1.01	12.08	139	-25.17 and 34.42	636 and 35503	6.9×10^{-4} and 0.25	0.36 and 8.85	0.102 and 0.137	0.015 and 0.028

CHAPTER III

EXPERIMENTAL EQUIPMENT, CALIBRATION AND DATA REDUCTION

In this chapter we have discussed the vital components of the test set-up and provided requisite description of the components. Calibration procedures of the vital components are discussed. Details have been provided on the data reduction program used in this study using the finite difference formulations. We have then carried out single-phase validation runs by comparing the single phase runs carried out on this equipment with the well known single-phase heat transfer correlations. In the end the experimental procedures adopted for this study have been discussed and the system is checked for repeatability.

3.1 Test Section Description

The test set-up is shown in Figure 3.1. Details of individual parts are described below, for more details on the experimental set-up and calibration, refer to Durant (2003).

3.1.1 Test Cradle

The test section rests on an aluminum I-beam. The beam is supported by a pivoting foot and a stationary foot that is incorporated with a small electronic jack.

The I-beam is approximately 9.14 m in length and can be inclined up to eight degree above horizontal. This method is especially beneficial in keeping the test section free from stresses that might be caused while lifting it manually and placing static pillars underneath one end to elevate it. This method keeps the entire beam free from stresses that might crack or loosen joints causing leaks.

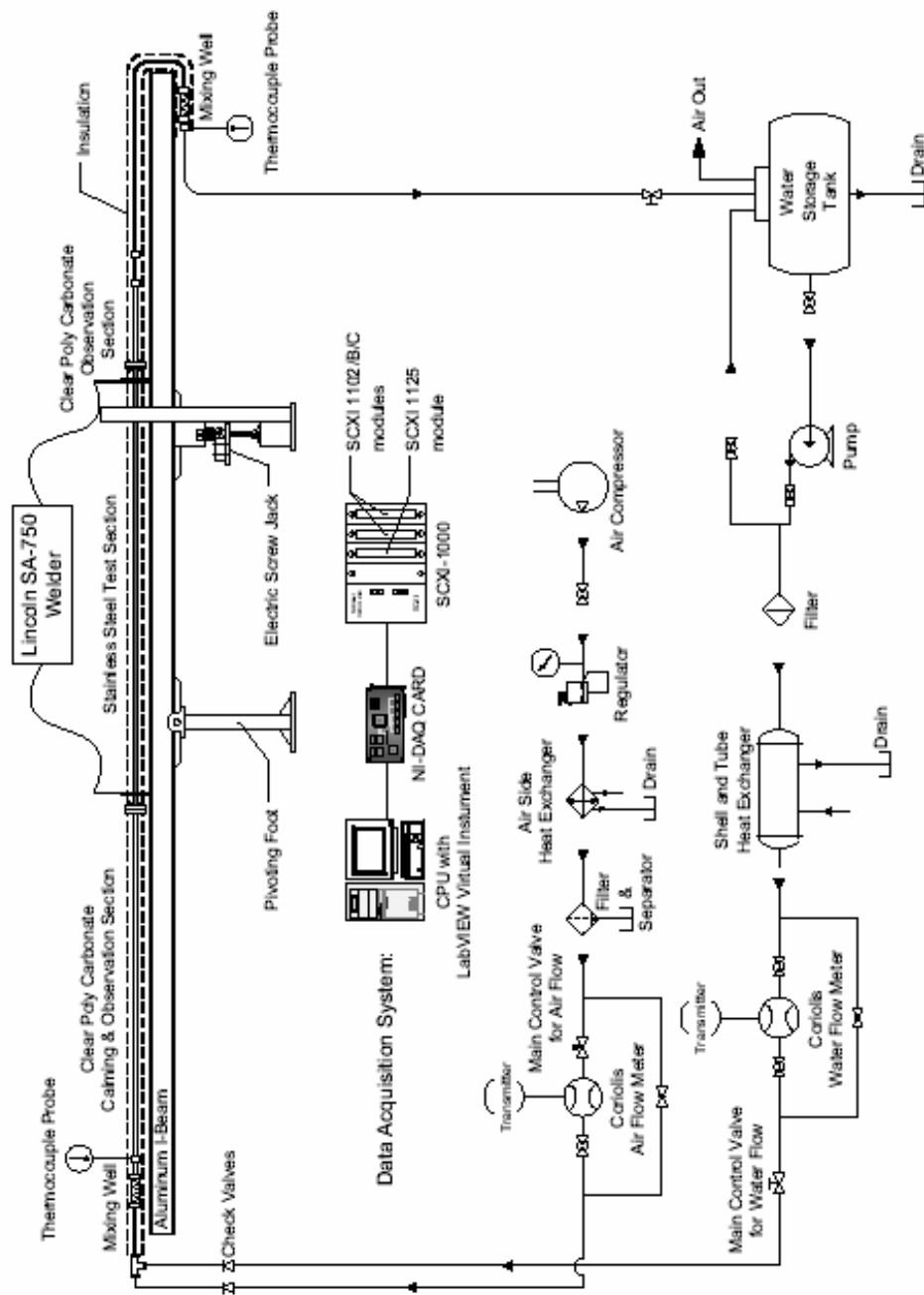


Figure 3.1 Experimental set-up, Ghajar *et al* (2004)

3.1.2 Water Supply

The two fluids used in this research are air and water. The water used is distilled water which is stored in a 0.21 cubic meter cylindrical polyethylene tank. The water is drawn by a pump from this tank and is either bypassed back into the 0.21 cubic meter tank or pushed into a cross-flow heat exchanger. The bypass is one of the ways that the regulation of the flow is controlled. The other is the gate valve that is located directly after the Coriolus flow meter.

Cooling water used for the heat exchanger is drawn from the city utilities. The water flows at an average rate of $0.038\text{m}^3/\text{min}$ through the heat exchanger. Once the water leaves the heat exchanger, it is dumped into the drain.

3.1.3 Pump

The pump used is a Bell and Gosset series 1535 coupled centrifugal pump. The size of the pump is 3545 D 10 and it produces desired flow rates so as to produce any flow pattern desired. The flow rate can range from the miniscule stratified flow rate of $0.011\text{ m}^3/\text{min}$ to plug flow rate of $0.303\text{ m}^3/\text{min}$. The pump has the capacity to produce $0.606\text{ m}^3/\text{min}$, if the full capacity of the pump is used and assuming that the pressure drops across the filters are at minimal values.

3.1.4 The Heat Exchanger

The heat exchanger is an ITT standard model BCF 4063 one shell and two-tube pass heat exchanger. The heat exchanger has been purchased from Thermal Engineering Company in Tulsa. The heat exchanger has been used in this research to cool the test

water and it has an effective shell area of 1.97 m^2 and a maximum duty of 19.7 KW. Water was passed at an approximate rate of $0.038 \text{ m}^3/\text{min}$ through the heat exchanger to ensure maximum heat transfer.

3.1.5 Flow Meters and Flow Regulation

The flow meter used in this research is a Coriolus flow meter Model CMF125 and it has been donated by Micro Motion. The water from the heat exchanger flows into this flow meter or if it is desired to by pass the flow meter, a bypass loop is incorporated in the design of the set-up. To ensure that no air or abrupt pressure change damage the inner working of the flow meter, the by pass loop is opened and the pathway to the flow meters closed upon startup.

In describing the flow meter, a Digital Field-Mount Transmitter Model RFT9739 displays the flow rate in lb_m/min , L/min , density of the fluid in g/cm^3 , temperature in $^\circ\text{C}$, total lb_m , total L, and an inventory of total lb_m/min and L/min . The water after passing through the flow meter, flows through a 1 inch. twelve turn gate valve. The gate valve helps to regulate the flow rate of the water entering the test section. From this point, the water travels through a 1 inch I.D. hose, through a check valve, and enters the test section.

3.1.6 Air Supply

The air compressor is an Ingersoll-Rand T30 Model 2545 industrial air compressor. This air compressor is located in an adjacent room next to the test facility

and it provides the requisite airflow for producing the air-water flow patterns. Placing the air compressor in the adjacent room served the following purposes:

1. Kept the noise to a minimum.
2. Reduced the chances of any physical hazard.

The maximum pressure possible is approximately 170 psi and a minimum of 50 psi. The air compressor is fitted with an unloader valve and a dump valve to keep the air pressure as constant as possible with no dramatic fluctuations.

The outside air is sucked in through the compressor and brought inside. The air once inside is passed through a copper coil. The copper coil is kept submerged in running water and takes care of the following:

1. The outside air if heated gets cooled by the running water.
2. Water in the tank serves as a safety in case of any undue happening due to loose connection or leak.

Also, cooling outside air is important since energy in the form of heat from the compressor, and the high temperatures of the Oklahoma summer raised the air temperature drastically. The air temperature desired was near what the inlet water temperature was. Hence, to achieve it was mandatory to submerge the coil in water.

3.1.7 Controls

The air and water flow rates are measured using two Model CFM025 and CFM125 Coriolus flow meters donated by Micro Motion Inc. Two model RFT9739 Field-Mount Transmitters from Micro Motion/Fisher-Rosemount are used to read the flow rates of both the Coriolus flow meters.

3.1.8 Mixing Section

The mixer is a point of the test section where the water and air are introduced simultaneously in the tube and mixed. The schematic of the mixing section is shown in Figure 3.2. The mixer used in this test setup is similar to that used by Ewing *et al* (1999) in their two-phase experimental setup for generating varied flow patterns.

The water is injected in the system through a 1 inch. copper Tee. Through the other end of the Tee a reducer bushing is in place to hold the compression fitting that secures the ½ inch I.D. 304 Stainless Steel tube that the air will be pushed through. The other end of the copper Tee is connected to the observation section of the test setup.

3.1.9 Test Section

The test section of this setup is a 1.097 inch. I.D. 304 10S Stainless Steel Pipe. Both ends of the test section are connected to the plastic observation and calming section by a nylon flange. The flange was made in the machine lab at Oklahoma State University. Figure 3.3 shows the schematic of the Nylon flange assembly. Special provision has been made in the flange so that an O-ring can be placed in it. Each flange contains two O-rings. One O-ring contains the flow in the radial direction while the other contains the flow in the lateral direction. The lateral controlling O-ring is located on the plastic tubing side. The flange located on the steel side is threaded and therefore Teflon tape can be added to prevent leakage.

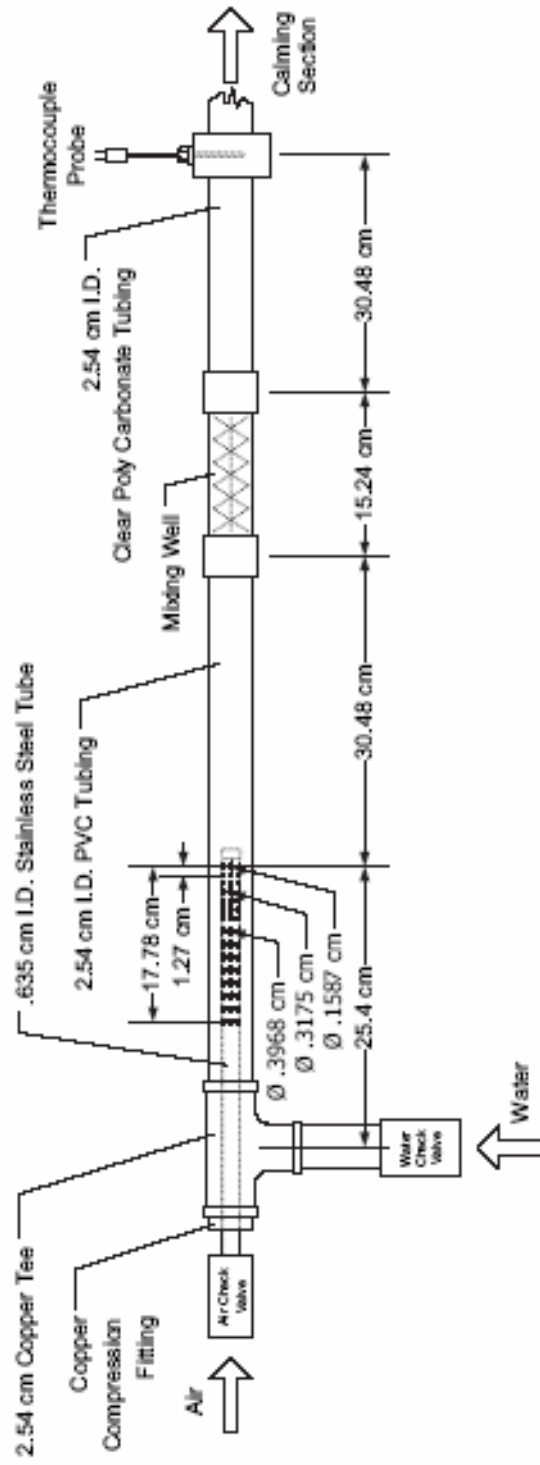


Figure 3.2 Air-water mixing section, Ghajar *et al* (2004)

3.1.10 Power (Uniform Heat Source)

High amperage current was passed through the stainless steel section to generate the uniform heat flux around the periphery. Two copper plates were silver soldered on the stainless steel test section and the current was flowed through it. A LINCOLDWELD SA-750 arc welder provided this current with a maximum of 750 Amperes. The welder was placed outside the laboratory to reduce noise and vibration in the laboratory.

3.1.11 Data Acquisitions

Data acquisition system was taken from National Instruments. This acquisition system was used to record all requisite information like temperatures readings, current, voltage drop and flow rates measured by flow meters. The software that ran the thermocouple programs was a LabView interface created by Jae-yong Kim (PhD Candidate).

The acquisition system is house in an AC powered four-slot SCXI 1000 chassis that serves as a low noise environment for signal conditioning. Three NI SCXI control modules are housed inside the chassis. There are two SCXI 1102/B/C modules and one SCXI 1125 module. From these three modules input signals for all 40 thermocouples, two thermocouple probes, voltmeter and flow meters are gathered and recorded.

3.2 Thermocouples and Thermocouple Calibration

3.2.1 Thermocouples

The thermocouples used to measure the temperature of the test section were Omega TT-T-30, T-Type Thermocouples. Figure 3.4 shows the arrangement of stainless steel section indicating the thermocouple station locations. To ensure equal error, if any, in all thermocouples, each thermocouple extension was kept of same length.

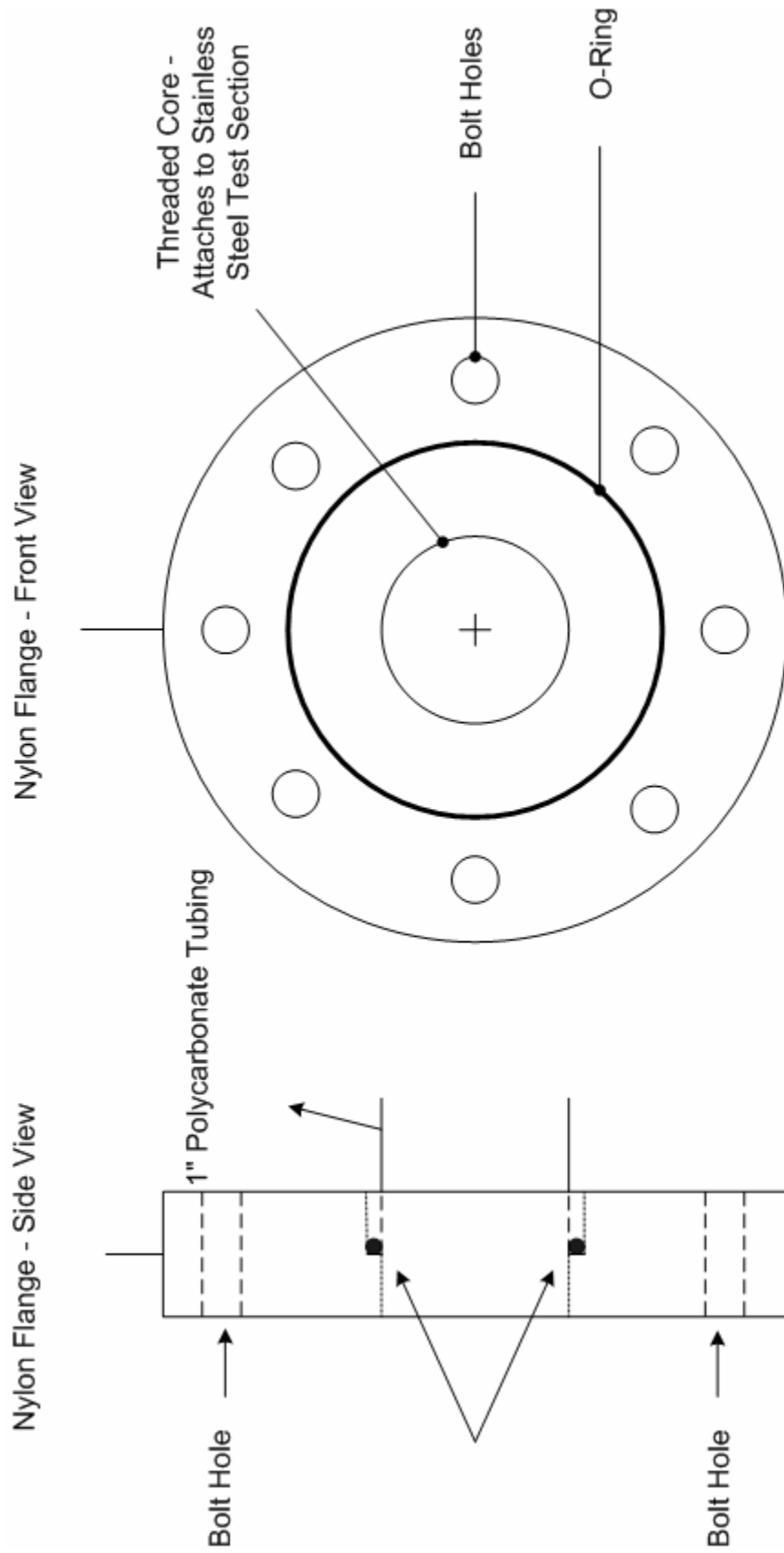


Figure 3.3 Nylon flange assemblies, Durant (2003)

The extension wire was 20 ft piece of EXPP-T-20-SLE make. The thermocouples were attached to the extension wire by wrapping a bare connection from the T-type thermocouple to the bare connection of extension wire. Contact was made between the wires by twisting them, and then they were soldered together. Omega SMPW-T-M and SMPW-T-F connectors were used to attach the wires. A 16 inch. lead was wired from the data acquisition board to a female end of the connector for each thermocouple and probe. This was to prevent from removing the data card when wishing to replace a thermocouple. Instead, the 20 ft extension wire could be removed and fixed with a new thermocouple while never having to disturb the data acquisition devices.

Water temperature was measured using three Omega TMQSS-125U-6 thermal probes. They were placed in the mixing section, the end of the test section located just before the return to the storage tank and the last one to measure the ambient air temperature of the room. The thermal probes were attached with the connectors with the same 20 ft piece extension to maintain uniformity in the measurements.

3.2.2 Thermocouple and Probe Calibration

Probe calibration was done by Durant (2003) and no modification has been made since then. The test setup has 10 stations and each station has four thermocouples, which counts to 40 thermocouples just in the test section. A total of 55 thermocouples were made with three OMEGA TMQSS-125U-6 thermal probes. The oil bath was used to calibrate the thermocouples. The oil bath was a Neslab RTE 740 with a Digital Plus readout. The fluid used for calibration was Ethylene Glycol.

As a process of calibration, seven temperatures were measured with the thermocouples starting with 10⁰C to 40⁰C at an increment of 5⁰C. The thermocouples were not calibrated for extremely low or high temperatures. The desired range for an acceptable thermocouple deviation was ± 0.5⁰C. Once the calibration is completed, all the thermocouple probes were compared against the bath temperature in an Excel spreadsheet. The data is then fitted with a regression equation which takes care of any deviations. This Excel obtained equation is then fed in the data acquisition code for an adjusted fit. Figure 3.5 shows the simple calibration curve for Thermocouple 1 at Station 1.

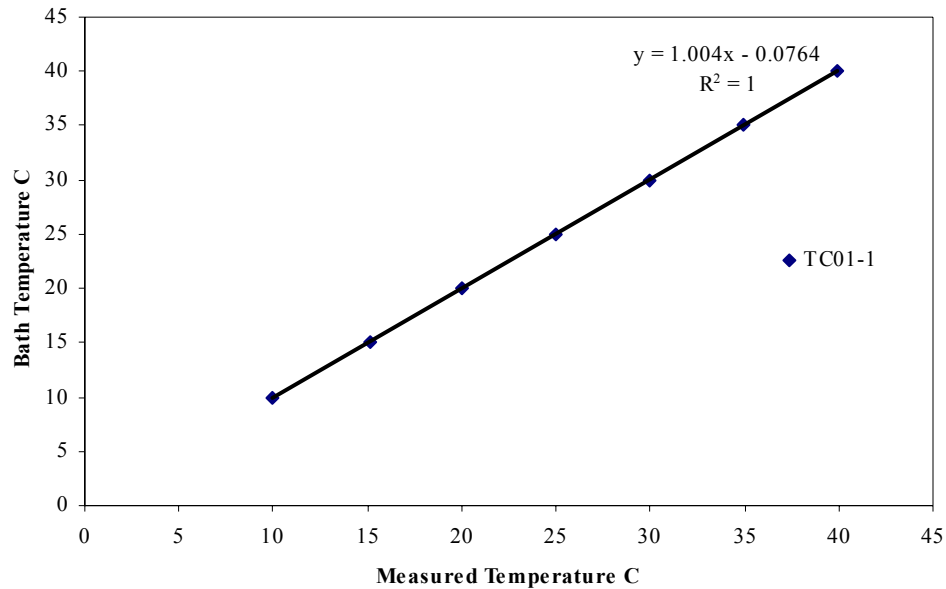


Figure 3.5 Calibration curve for Thermocouple 1, TC01-1, Durant (2003)

3.2.3 Thermocouple Attachment

No modifications have been made in the Thermocouple attachment and it was formerly done by Durant (2003). After the calibration was done, the thermocouples were

attached to the test section with OMEGABOND 101 epoxy, and the probes were inserted into the inlet and outlet areas and secured with Omega BRLK-18-14 compression fittings.

To obtain a good bond we first clean the area where the thermocouple will be attached. Low concentration ammonia or other cleaning solvent should be applied and allowed to dry. Once dry wipe the area clean with a rubbing alcohol to remove all film and dirt that may have been left behind. After the alcohol has evaporated, mix the OMEGABOND 101 and apply a small drop, approximately 1 to 2 mm in diameter, and allow it to dry for 24 hrs. Four drops were placed at each station for the four thermocouples that were to be attached. After the epoxy had dried the hardened drops were lightly filed to create a flat surface for the thermocouples to rest in. The filing was minimal and great care was taken to ensure that the thermocouple bead would not touch the pipe.

The thermocouple extension wires were attached to the test setup and secured. The actual thermocouple wires were then taped to the stainless steel test section in a position where the bead was atop of its respective station epoxy droplet. Once the bead was in place, another small 1 to 2 mm droplet of OMEGABOND 101 was placed over the bead and allowed it to dry for 24 hrs. While the epoxy was curing, no electrical or fluid movement was sent through the pipe.

After the 24 hour drying period, the tape used to secure the thermocouple wire was removed so that no adverse heating or cooling effects could be contributed to it. The thermocouples were then insulated with fiberglass, vinyl backed, pipe insulation. Two insulation layers were used and then the insulation was contained with a plastic wrapping to keep the insulation in place.

3.3 Isothermal Trials, Pre and Post Heat Checks

3.3.1 Isothermal Trials

After the complete process of thermocouple attachment, isothermal runs were carried out to ensure that the thermocouples were reading correctly. In these isothermal runs, we ran single-phase water flow, and recorded the temperatures of all the thermocouples. Raw data was adjusted using the calibrated thermocouple equation using the Visual Basic Applications program written by Durant (2003). Once the data was adjusted and replaced into the spreadsheet, the values of each thermocouple were averaged and final adjustments were made. These final adjustments were made by Jae-yong Kim (PhD Candidate). These values were then plotted against the thermocouple position. Since the profile was similar and repeatable, the thermocouples were assumed to be working properly with no substantial alterations due to the epoxy. For more details, refer to Durant (2003).

3.4 Other Calibrations

Calibration of water flow meter, air flow meter, voltmeter and ammeter was done by Durant (2003) and no modification has been done since then.

3.4.1 Air and Water Mass Flow Rate Calibration

The data acquisition system is designed to read the flow transmitters and record data automatically. In order to do this accurately, the readings had to be calibrated. The data acquisition devices have a range of 4-20 mA. In order for the computer to distinguish the correct flow rate, the flow rates had to be set and then the amperage read

from the computer console. Once the data had been established, a line was fitted to the comparison of the flow rate and the current measured by the computer and then fitted with an equation that would relate the amperage to a corresponding flow rate. Figures 3.6 and 3.7 represent the calibration curves for the air and water mass flow rates.

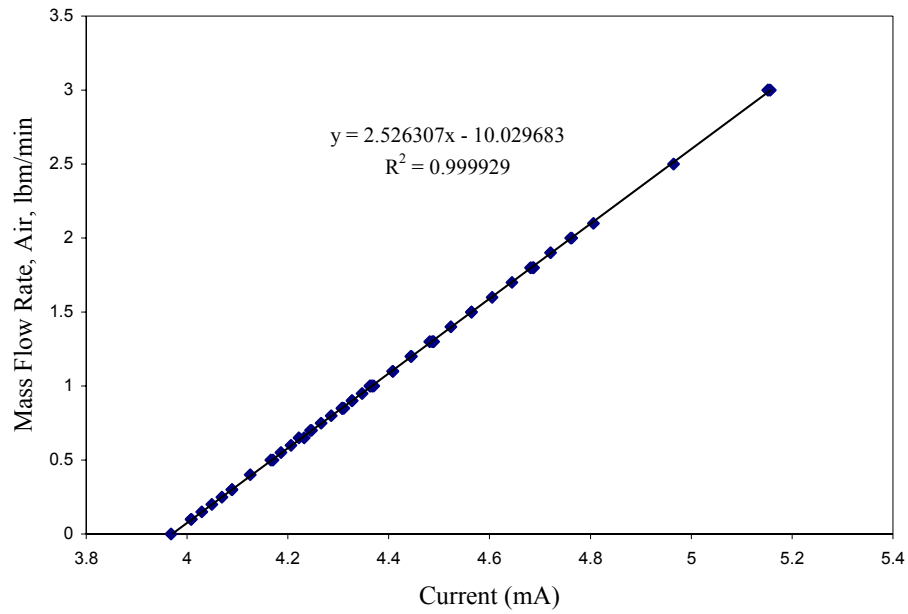


Figure 3.6 Air mass flow rate calibration curve, Durant (2003)

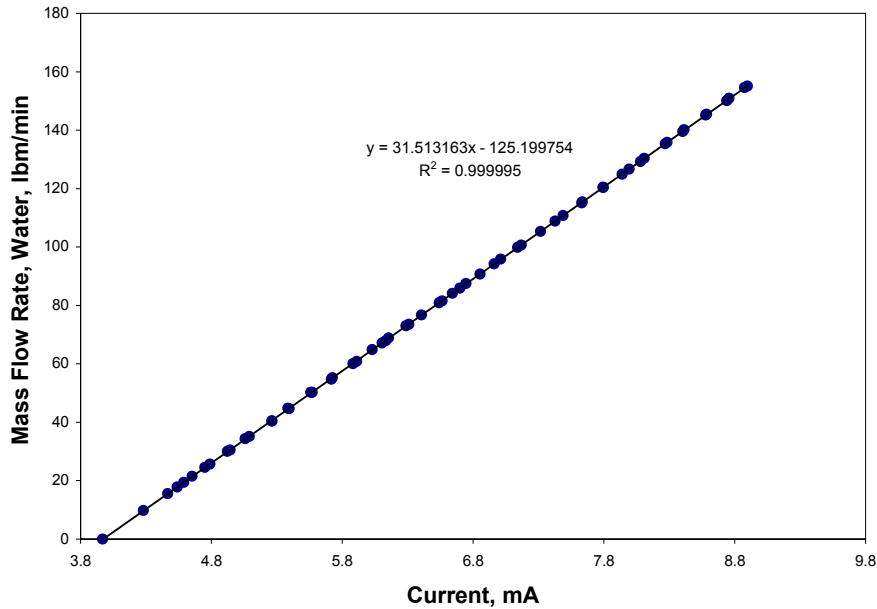


Figure 3.7 Water mass flow rate calibration curve, Durant (2003)

3.4.2 Voltmeter and Ammeter Measurements

The voltmeter was incorporated into the measurement system to calculate the voltage drop across the test section. The voltage drop was used in conjunction with the amperage to determine the average heat flux that was passed through the system.

The voltage drop was determined by measuring the voltage at the inlet and outlet of the test section. This was done by wiring 26 AWG wire to the silver soldered connections located at each end of the test section and connecting it directly into the data acquisition system. The two values were then subtracted from one another to get the overall voltage drop.

The ammeter used to collect the amperage readings during testing was created by using a 50 millivolt shunt that was installed on the silver solder connection on the exit end of the test section. Knowing the voltage drop and the resistance, the amperage of the test section could be determined by using the equation, $I = V/R$. This was done using the data acquisition system.

3.5 Data Reduction Program

The data reduction program used a finite-difference formulation to determine the inside wall temperature and the inside wall heat flux. It utilized measurements of the outside wall temperature, the heat generation within the pipe wall, and the thermophysical properties of the pipe material (electrical resistivity and thermal conductivity). In these calculations, axial conduction was assumed negligible, but peripheral and radial conduction of heat in the tubewall were included. The bulk fluid temperature was assumed to increase linearly from inlet to outlet. The computer program was named 2HT03FALL, which was developed by Jae-yong Kim (PhD Candidate) based on the work of Ghajar and Zurigat (1991). Details of this program can be found in Appendix A.

3.5.1 Input Data

The inputs of this program included the voltage drop across the pipe, the current carried by the pipe, the volumetric flow rates of the air and water, the bulk fluid temperatures at the inlet and exit, and the outside wall temperature data for all 44 thermocouple locations.

3.5.2 Finite-Difference Formulations

No modifications were made to the development of the finite-difference calculations. The procedures are exactly the same of what was followed by Kim (2000). This information can also be found in the research papers by Kim *et al* (2000) and Kim *et al* (2002).

The numerical solution of the conduction equation with internal heat generation, variable thermal conductivity, and variable electrical resistivity was based on the following assumptions:

- Steady state conditions exist.
- Peripheral and radial wall conduction exists.
- Axial conduction is negligible.
- The electrical resistivity and thermal conductivity of the tube wall are functions of temperature.

Based on these assumptions, the expressions for the calculation of the local inside wall temperatures, heat flux, and the local peripheral heat transfer coefficients are developed.

- Local Inside Wall Temperature and Local Inside Wall Heat Flux

The heat balance on a segment of the tube wall at any particular station is given by Equation (3.1) and is illustrated by Figure 3.8:

$$Q_g = Q_1 + Q_2 + Q_3 + Q_4 \quad (3.1)$$

From Fourier's law of heat conduction in a given direction the following equation applies

$$Q = -kA \frac{dT}{dn} \quad (3.2)$$

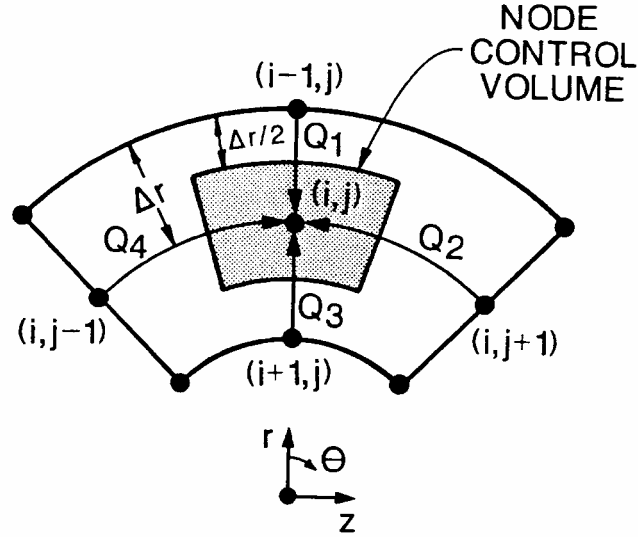


Figure 3.8 Finite-difference grid arrangement (Ghajar and Zurigat, 1991)

Now substituting Fourier's law into Equation (3.1) and applying the finite-difference formulation for the radial (i) and peripheral (j) directions:

$$Q_1 = \frac{(k_{i,j} + k_{i-1,j})}{2} \frac{2\pi \left(r_i + \frac{\Delta r}{2} \right) \Delta z}{N_{TH}} \frac{(T_{i,j} - T_{i-1,j})}{\Delta r} \quad (3.3)$$

$$Q_2 = \frac{(k_{i,j} + k_{i,j+1})}{2} (\Delta r \Delta z) \frac{(T_{i,j} - T_{i,j+1})}{\left(\frac{2\pi r_i}{N_{TH}} \right)} \quad (3.4)$$

$$Q_3 = \frac{(k_{i,j} + k_{i+1,j})}{2} \frac{2\pi \left(r_i - \frac{\Delta r}{2} \right) \Delta z}{N_{TH}} \frac{(T_{i,j} - T_{i+1,j})}{\Delta r} \quad (3.5)$$

$$Q_4 = \frac{(k_{i,j} + k_{i,j-1})}{2} (\Delta r \Delta z) \frac{(T_{i,j} - T_{i,j-1})}{\left(\frac{2\pi r_i}{N_{TH}} \right)} \quad (3.6)$$

where

k = thermal conductivity

r_i = tube inside radius

Q = rate of heat transfer

T = temperature

Δz = length of element

Δr = incremental radius

N_{TH} = number of finite-difference sections in the θ -direction (peripheral)
which is equal to the number of thermocouples at each station.

i and j = the indices of the finite-difference grid points, i is the radial direction starting from the outside surface of the tube and j is the peripheral direction starting from top of the tube and increasing clockwise.

The heat generated at i, j element volume is given by equation (3.7):

$$Q_g = I^2 R \quad (3.7)$$

Where

I = Current

R = $\gamma l / A$ = resistance

γ = electrical resistivity of the element

$l = \Delta z = \text{length of the element}$

$A = (2\pi r_i / N_{TH})\Delta r = \text{cross-sectional area of the element}$

Substituting the above definitions into Equation (3.7) gives:

$$Q_g = I^2 \frac{\gamma \Delta z}{\left(\frac{2\pi r_i}{N_{TH}}\right) \Delta r} \quad (3.8)$$

Substitution of Equations (3.3) through (3.6), and Equation (3.8) into Equation (3.1) and solving for $T_{i+1,j}$ yields Equation (3.9):

$$T_{i+1,j} = T_{i,j} - \left\{ \frac{I^2 \gamma N_{TH}}{(2\pi r_i \Delta r)} - \frac{(k_{i,j} + k_{i-1,j})}{\Delta r} \frac{\pi \left(r_i + \frac{\Delta r}{2} \right)}{N_{TH}} (T_{i,j} - T_{i-1,j}) \right. \\ \left. - (k_{i,j} + k_{i,j+1}) \frac{\Delta r N_{TH}}{4\pi r_i} (T_{i,j} - T_{i,j+1}) - (k_{i,j} + k_{i,j+1}) \frac{\Delta r N_{TH}}{4\pi r_i} (T_{i,j} - T_{i,j+1}) \right\} \quad (3.9) \\ \left\{ \frac{\Delta r N_{TH} (k_{i,j} + k_{i+1,j})}{\pi \left(r_i - \frac{\Delta r}{2} \right)} \right\}$$

Equation (3.9) was used to calculate the temperature of the interior nodes, such as those seen in Figure 3.8. In Equation (3.9), the thermal conductivity (k) and electrical resistivity (γ) of each node control volume, were determined as a function of temperature from the following equations given by Ghajar and Zurigat (1991), for a pipe of 316 stainless steel:

$$k = 7.27 + 0.0038T \quad (3.10)$$

$$\gamma = 27.67 + 0.0213T \quad (3.11)$$

where T is the temperature in °F, k is the thermal conductivity in Btu/hr-ft-°F, and γ is the electrical resistivity in micro-ohm-in.

Once the local inside wall temperatures were calculated from Equation (3.9), the local peripheral inside wall heat flux could be calculated from the heat balance equation, Equation (3.1).

- Calculation of Local Peripheral and Local Average Heat Transfer Coefficients

From the local inside wall temperature, the local peripheral inside wall heat flux and the local bulk fluid temperature, the local peripheral heat transfer coefficient could be calculated using Equation (3.12):

$$h_i = \dot{q}_i'' / (T_{wi} - T_b) \quad (3.12)$$

where

- h_i = local peripheral heat transfer coefficient
- \dot{q}_i'' = local peripheral inside wall heat flux
- T_{wi} = local inside wall temperature
- T_b = bulk fluid temperature at the thermocouple station

Using Equation (3.12) it was assumed that the bulk fluid temperature increased linearly from the inlet of the pipe to the outlet. This linear increase was calculated according to Equation (3.13):

$$T_b = T_{in} + (T_{out} - T_{in}) X/L \quad (3.13)$$

Where

- T_b = bulk temperature

- T_{in} = bulk inlet temperature
 T_{out} = bulk outlet temperature
 X = distance from the pipe inlet to the thermocouple station
 L = total length of the test section

The local average heat transfer coefficient at each station could then be calculated by Equation (3.14):

$$\bar{h}_i = \bar{q}_i'' / (\bar{T}_{wi} - T_b) \quad (3.14)$$

where

- \bar{h}_i = local average heat transfer coefficient
 \bar{q}_i'' = average peripheral inside wall heat flux at a station
 \bar{T}_{wi} = average inside wall temperature at a station

3.5.3 Physical Properties of the Fluids

The correlation equations used for the fluid properties of air and water, which were used in this research, are given in Table 3.1. These correlations were developed by Vijay (1978).

Table 3.1 Physical properties of the fluids used in this study, Kim (2000)

Fluid	Equation for the Physical Property (T = Temperature in °F except where noted)	Range of Validity & Accuracy	Source
Air	ρ (lbm/ft ³) = P/RT where P in lbf/ft ² , T in °R, and R = 53.34 ft-lbf/lbm°R C_p (Btu/lbm-°F) = 7.540x10 ⁻⁶ T + 0.2401 μ (lbm/ft-hr) = -2.673x10 ⁻⁸ T ² + 6.819x10 ⁻⁵ T + 0.03936 k (Btu/hr-ft-°F) = -6.154x10 ⁻⁹ T ² + 2.591x10 ⁻⁵ T + 0.01313	P ≤ 150 psi -10 ≤ T ≤ 242, 0.2% -10 ≤ T ≤ 242, 0.1% -10 ≤ T ≤ 242, 0.2%	Vijay (1978)
Water	ρ (lbm/ft ³) = {2.101x10 ⁻⁸ T ² - 1.303x10 ⁻⁶ T + 0.01602} ⁻¹ C_p (Btu/lbm-°F) = 1.337x10 ⁻⁶ T ² - 3.374x10 ⁻⁴ T + 1.018 μ (lbm/ft-hr) = {1.207x10 ⁻⁵ T ² + 3.863x10 ⁻³ T + 0.09461} ⁻¹ k (Btu/hr-ft-°F) = 4.722x10 ⁻⁴ T + 0.3149 σ (lbf/ft) = 5.52288x10 ⁻¹² T ³ - 8.05936x10 ⁻⁹ T ² - 4.75886x10 ⁻⁶ T + 5.346x10 ⁻³ T	32 ≤ T ≤ 212, 0.1% 32 ≤ T ≤ 212, 0.3% 32 ≤ T ≤ 212, 1.0% 32 ≤ T ≤ 176, 0.2% 68 ≤ T ≤ 150	Vijay (1978)

3.5.4 Output

Figure 3.9 shows a sample output data file of Run No. # 4501 using the computer program, 2HT03FALL. The output sheet starts with the summary list of the important parameters showing flow rates, temperatures, average Reynolds and Prandtl numbers, viscosities, conductivities, heat flux and the heat balance error for that particular run.

It then describes the details of outside surface temperatures of tube, inside surface temperatures, superficial Reynolds numbers of liquid and gas and heat fluxes of inside tube. It also shows the peripheral heat transfer coefficients. The details are shown for all the 40 thermocouples in the test section.

In the end it sums up the results and provide details of total mass flux, quality, slip ratio, void fraction, superficial liquid and gas velocities and Taitel and Dukler parameters.

RUN NUMBER 4501
Air-Water Two-phase Heat Transfer
Test Date: 12-16-2003
SI UNIT VERSION

```

=====
LIQUID VOLUMETRIC FLOW RATE : 0.466 [m^3/hr]
GAS VOLUMETRIC FLOW RATE : 3.823 [m^3/hr]
LIQUID MASS FLOW RATE : 465.71 [kg/hr]
GAS MASS FLOW RATE : 5.152 [kg/hr]
LIQUID V_SL : 0.212 [m/s]
GAS V_SG : 1.742 [m/s]
ROOM TEMPERATURE : 15.59 [C]
INLET TEMPERATURE : 13.11 [C]
OUTLET TEMPERATURE : 15.24 [C]
AVG REFERENCE GAGE PRESSURE : 9792.00 [Pa]
AVG LIQUID RE_SL : 5101
AVG GAS RE_SG : 3662
AVG LIQUID PR : 8.220
AVG GAS PR : 0.712
AVG LIQUID DENSITY : 1000.2 [kg/m^3]
AVG GAS DENSITY : 1.348 [kg/m^3]
AVG LIQUID SPECIFIC HEAT : 4.199 [kJ/kg-K]
AVG GAS SPECIFIC HEAT : 1.007 [kJ/kg-K]
AVG LIQUID VISCOSITY : 115.88e-05 [Pa-s]
AVG GAS VISCOSITY : 17.86e-06 [Pa-s]
AVG LIQUID CONDUCTIVITY : 0.592 [W/m-K]
AVG GAS CONDUCTIVITY : 25.27e-03 [W/m-K]
CURRENT TO TUBE : 403.37 [A]
VOLTAGE DROP IN TUBE : 3.08 [V]
AVG HEAT FLUX : 5371.87 [W/m^2]
Q = AMP*VOLT : 1242.17 [W]
Q = M*C*(T2 -T1) : 1155.24 [W]
HEAT BALANCE ERROR : 7.00 [%]

```

OUTSIDE SURFACE TEMPERATURE OF TUBE [C]

	1	2	3	4	5	6	7	8	9	10
1	21.27	21.88	22.10	22.36	22.56	22.87	23.05	23.41	23.49	23.72
2	19.03	18.76	20.07	19.79	20.41	20.50	21.15	21.03	21.39	21.43
3	15.76	16.10	16.26	16.50	16.88	17.01	17.35	17.39	17.59	17.77
4	19.11	19.21	19.46	19.97	20.11	20.70	21.02	21.42	21.10	21.61

INSIDE SURFACE TEMPERATURES [C]

	1	2	3	4	5	6	7	8	9	10
1	20.77	21.39	21.61	21.86	22.07	22.38	22.55	22.91	22.99	23.22
2	18.50	18.23	19.55	19.27	19.89	19.97	20.63	20.51	20.87	20.91
3	15.18	15.53	15.68	15.92	16.30	16.42	16.76	16.80	17.00	17.18
4	18.59	18.68	18.93	19.45	19.59	20.18	20.50	20.90	20.58	21.10

SUPERFICIAL REYNOLDS NUMBER OF GAS AT THE INSIDE TUBE WALL

	1	2	3	4	5	6	7	8	9	10
1	3598	3592	3590	3588	3586	3583	3581	3578	3577	3575
2	3620	3622	3610	3612	3607	3606	3599	3601	3597	3597
3	3652	3649	3647	3645	3641	3640	3637	3636	3634	3633
4	3619	3618	3616	3611	3609	3604	3601	3597	3600	3595

SUPERFICIAL REYNOLDS NUMBER OF LIQUID AT THE INSIDE TUBE WALL

	1	2	3	4	5	6	7	8	9	10
1	6017	6106	6136	6174	6202	6247	6272	6325	6336	6369
2	5697	5658	5844	5804	5891	5904	5998	5979	6031	6037
3	5237	5285	5305	5339	5391	5408	5454	5460	5488	5512
4	5709	5722	5757	5829	5849	5933	5979	6036	5990	6063

INSIDE SURFACE HEAT FLUXES [W/m^2]

	1	2	3	4	5	6	7	8	9	10
1	4830	4732	4815	4796	4823	4829	4875	4845	4837	4846
2	5078	5185	5028	5105	5061	5082	5028	5076	5044	5069
3	5628	5569	5661	5644	5646	5679	5702	5717	5692	5708
4	5065	5121	5116	5080	5104	5052	5047	5019	5085	5042

PERIPHERAL HEAT TRANSFER COEFFICIENT [W/m^2-K]

	1	2	3	4	5	6	7	8	9	10
1	643	597	606	600	603	596	604	589	597	596
2	968	1087	854	945	871	892	817	872	843	871
3	2928	2690	2815	2749	2537	2645	2501	2700	2693	2733
4	950	981	971	911	926	855	838	807	894	840

=====

RUN NUMBER 4501 continued

Air-Water Two-phase Heat Transfer

Test Date: 12-16-2003

SI UNIT VERSION

=====

ST	MU_L[E-5 Pa-s]		MU_G[E-6 Pa-s]		CP[kJ/kg-K]		K[W/m-K]		RHO[kg/m^3]	
	Bulk	Wall	Bulk	Wall	Lqd	Gas	Lqd	Gas(E-3)	Lqd	Gas
1	118.76	104.39	17.81	18.05	4.201	1.007	0.591	25.20	1000.4	1.352
2	118.11	103.88	17.82	18.06	4.200	1.007	0.591	25.21	1000.3	1.351
3	117.47	102.66	17.83	18.09	4.200	1.007	0.591	25.23	1000.3	1.350
4	116.83	102.20	17.84	18.09	4.200	1.007	0.592	25.24	1000.3	1.349
5	116.20	101.38	17.85	18.11	4.200	1.007	0.592	25.26	1000.3	1.348
6	115.57	100.69	17.86	18.12	4.199	1.007	0.592	25.28	1000.2	1.347
7	114.95	99.80	17.87	18.14	4.199	1.007	0.592	25.29	1000.2	1.346
8	114.34	99.40	17.88	18.15	4.199	1.007	0.593	25.31	1000.2	1.345
9	113.73	99.21	17.89	18.15	4.198	1.007	0.593	25.32	1000.2	1.344
10	113.12	98.64	17.90	18.17	4.198	1.007	0.593	25.34	1000.1	1.343

ST	X/D	RESL	RESG	PRL	PRG	MUB/W(L)	MUB/W(G)	HT/HB	HFLUX	TB[C]	TW[C]	HCOEFF	NU_L
1	6.38	4977	3671	8.45	0.712	1.138	0.987	0.220	5150	13.26	18.26	1029.3	48.56
2	15.50	5005	3669	8.40	0.712	1.137	0.987	0.222	5152	13.46	18.46	1030.9	48.61
3	24.61	5032	3667	8.34	0.712	1.144	0.986	0.215	5155	13.67	18.94	976.8	46.03
4	33.73	5060	3665	8.29	0.712	1.143	0.986	0.218	5156	13.87	19.13	981.0	46.21
5	42.84	5087	3663	8.24	0.712	1.146	0.986	0.238	5159	14.07	19.46	957.7	45.09
6	51.96	5115	3661	8.20	0.712	1.148	0.985	0.225	5160	14.28	19.74	944.7	44.45
7	61.08	5142	3659	8.15	0.712	1.152	0.985	0.242	5163	14.48	20.11	916.9	43.12
8	70.19	5170	3657	8.10	0.711	1.150	0.985	0.218	5164	14.68	20.28	922.8	43.38
9	79.31	5198	3655	8.05	0.711	1.146	0.985	0.222	5165	14.89	20.36	943.9	44.35
10	88.42	5226	3653	8.00	0.711	1.147	0.985	0.218	5166	15.09	20.60	937.8	44.04

```

=====
RUN NUMBER 4501 continued
Air-Water Two-phase Heat Transfer
QUANTITIES OF MAIN PARAMETERS
Test Date: 12-16-2003
=====
INCLINATION ANGLE : 0.000 [DEG]
TOTAL MASS FLUX(Gt): 214.496 [kg/m^2-s]
QUALITY (x) : 0.011
SLIP RATIO(K) : 3.018
VOID FRACTION(alpa): 0.731
V_SL : 0.212 [m/s]
V_SG : 1.742 [m/s]
RE_SL : 5101
RE_SG : 3662
RE_TP : 8763
X(Taitel & Dukler) : 3.210
T(Taitel & Dukler) : 0.052
Y(Taitel & Dukler) : 0.000
F(Taitel & Dukler) : 0.122
K(Taitel & Dukler) : 8.739
X (Breber) : 3.210
j*g(Breber) : 0.122
=====

```

```

=====
RUN NUMBER 4501 continued
Two-phase flow Darcy Friction factor
Test Date: 12-16-2003
=====
PRESSURE DROP ALONG TUBE [psia]
PT# 5 10
6.2950 6.2780
TWO-PHASE FLOW FRICTION FACTOR TUBE
PT# 5 10
4.5449 2.2663
=====

```

Figure 3.9 Sample output file Run # 4501 from program 2HT03FALL.

3.6 Heat Transfer in Horizontal Pipe

Heat transfer analysis in single-phase and two-phase was carried out to validate the equipment. Many tests were repeated to confirm the reliability of the equipment.

3.6.1 Heat Transfer in Single-Phase Flow

Single-phase heat transfer runs were made and the results were compared with the well known single-phase heat transfer correlations available in the open literature. In this research we carried out a few extra single-phase runs, since the equipment was formerly

validated by Durant (2003). The correlations used to compare the single-phase heat transfer runs were Colburn (1933), Sieder and Tate (1936) and Gnielinski [3](1976) correlation.

Since the system was formerly validated by Durant (2003), only a few extra runs have been carried out to validate the system.

3.6.2 Colburn (1933)

Six runs were made to compare with the Colburn correlation. Table 3.2 shows the data that was measured and calculated.

Colburn (1933) correlation:

$$Nu = 0.023 Re^{0.8} Pr^{1/3} \quad (3.15)$$

where $Re \geq 10,000, 0.6 \leq Pr \leq 160$

Table 3.2 Colburn (1933) single-phase heat transfer results

Runs #	Prandtl Number	Reynolds Number	Experimental Nusselt Number	Colburn (ReD>10000)	% Devn
4041	8.67	10300	91.69	76.67	16.38
4043	8.79	19410	126.99	127.89	-0.71
4044	9.02	19827	131.41	131.18	0.17
4045	8.90	6395	52.79	52.83	-0.09
4046	8.93	8729	71.46	67.82	5.09
4047	8.98	16919	118.04	115.38	2.25

We observe that the deviation is well within the accepted limits of $\pm 20\%$.

3.6.3 Sieder & Tate (1936)

Six runs were made to compare with the Sieder and Tate correlation.

Table 3.3 shows the data that was measured and calculated.

Sieder and Tate (1936) correlation:

$$Nu = 0.023 Re^{0.8} Pr^{1/3} (\mu_b / \mu_w)^{0.14} \quad (3.16)$$

where $Re \geq 10,000, 0.7 \leq Pr \leq 16,700$

Table 3.3 Sieder and Tate (1936) single-phase heat transfer results

Runs #	Prandtl Number	Reynolds Number	Experimental Nusselt Number	Sieder & Tate (ReD>10000)	% Devn
4041	8.67	10300	91.69	77.05	15.96
4043	8.79	19410	126.99	128.53	-1.21
4044	9.02	19827	131.41	131.83	-0.32
4045	8.90	6395	52.79	53.09	-0.58
4046	8.93	8729	71.46	68.16	4.62
4047	8.98	16919	118.04	115.95	1.77

We observe that the deviation is well within the accepted limits of $\pm 20\%$.

3.6.4 Gnielinski (1976)

Six runs were made to compare with the Gnielinski correlation. Table 3.4 shows the data that was measured and calculated.

Gnielinski [3] (1976) correlation:

$$Nu = 0.012(Re^{0.87} - 280)Pr^{0.4} \quad (3.17)$$

where $1.5 \leq Pr \leq 500, 3,000 \leq Re \leq 1 \times 10^6$

Table 3.4 Gnielinski single-phase heat transfer results

Runs #	Prandtl Number	Reynolds Number	Experimental Nusselt Number	Gnielinski [3] (ReD>3000)	% Devn
4041	8.67	10300	91.69	80.24	12.49
4043	8.79	19410	126.99	145.94	-14.92
4044	9.02	19827	131.41	150.32	-14.39
4045	8.90	6395	52.79	50.84	3.70
4046	8.93	8729	71.46	69.22	3.14
4047	8.98	16919	118.04	129.67	-9.86

We observe that the deviation is well within the accepted limits of $\pm 20\%$.

3.6.5 Heat Transfer in Two-Phase Flow

After validating the system using single-phase heat transfer correlations. It was essential to make comparison runs with other investigators, to check the system response for the two-phase data. In this study we carried out two-phase runs and compared with Trimble *et al* (2002). A total to 11 runs were made and compared. Attempt was made to keep the conditions exactly same as those of Trimble *et al* (2002). Table 3.5 gives the details of the two-phase comparison runs.

We observe from Table 3.5 that the % difference of the overall mean two-phase heat transfer coefficient was well within the acceptable limits of $\pm 20\%$.

Table 3.5 Two-phase comparison runs

	Run No.	Re _{SL}	Re _{SG}	Current	Voltage	h (Btu/Ft ² -Hr-F)
Current study	RN4001	5023	3710	402.1	4.4	216
Trimble <i>et al</i> (2002)	RN8311	5155	3729	411.2	3.3	257
% Deviation		2.6	0.5	2.2	-31.2	15.8
Current study	RN4002	7809	1115	416.7	4.5	282
Trimble <i>et al</i> (2002)	RN8313	7809	1048	421.4	3.4	275
% Deviation		0	-6.4	1.1	-30.1	-2.4
Current study	RN4003	13276	4914	462.6	4.9	484
Trimble <i>et al</i> (2002)	RN8323	12976	4893	466.9	3.8	601
% Deviation		-2.3	-0.4	0.9	-27.7	19.5
Current study	RN4004	4560	2752	392.5	4.1	198
Trimble <i>et al</i> (2002)	RN8310	4382	2716	404.4	3.2	208
% Deviation		-4.1	-1.3	2.9	-27.2	4.8
Current study	RN4005	21434	2145	504.4	5.1	727
Trimble <i>et al</i> (2002)	RN8327	21131	2051	524.9	4.4	646
% Deviation		-1.4	-4.6	3.9	-16.3	-12.6
Current study	RN4006	25388	2147	493.7	4.9	822
Trimble <i>et al</i> (2002)	RN8337	24764	2187	494.7	4.1	804
% Deviation		-2.5	1.8	0.2	-18	-2.2
Current study	RN4008	10473	3484	426.4	4.2	401
Trimble <i>et al</i> (2002)	RN8316	10253	3454	426.6	3.6	401
% Deviation		-2.1	-0.9	0	-17.5	0
Current study	RN4009	18119	3000	511.8	4.7	691
Trimble <i>et al</i> (2002)	RN8329	17794	2975	511.1	4.2	597
% Deviation		-1.8	-0.8	-0.1	-12.9	-15.7
Current study	RN4010	4657	2312	423.3	4.1	200
Trimble <i>et al</i> (2002)	RN8318	4428	2230	420.7	3.5	204
% Deviation		-5.2	-3.7	-0.6	-17.7	2
Current study	RN4011	8498	2307	435.1	4.1	321
Trimble <i>et al</i> (2002)	RN8314	8340	2226	438.2	3.6	339
% Deviation		-1.9	-3.6	0.7	-15.8	5.1
Current study	RN4012	11087	727	432.6	4	382
Trimble <i>et al</i> (2002)	RN8317	10958	804	431.4	3.5	380
% Deviation		-1.2	9.6	-0.3	-15.1	-0.5

3.7 Uncertainty Analysis

Uncertainty calculations were performed using the methodology described by Kline and McClintock (1953). From the uncertainty analysis, it was found that the maximum error corresponding to the experimental heat transfer coefficient is approximately 9.65 %. The methodology and details about the uncertainty analysis can be found in Appendix B.

3.8 Experimental Procedures

Once the system validation was done it was essential to set-up a standard procedure to record data, so that the data recorded shows consistency. This guideline will also be helpful for future studies that will be carried on this set-up. To set-up the guideline for data taking, it was essential that the system attains steady state before final data recording is done. To check for the steady state two-phase flow in this setup, we observed the variation of temperatures of each thermocouple series. When the temperatures followed a consistent horizontal path with the passage of time, the system was said to have reached steady state. Experimentally the voltage drops a little initially when the heat flux is applied to the set-up and this also corresponds to the drop in the temperatures of the thermocouple series. But, with the passage of time, the voltage stabilizes and no further current or voltage variations were noticed in the system, at this time no fluctuations in temperatures were observed. This was an indication of the steady state two-phase flow.

To set the time limits of how long the heat flux should be applied and when the data recording be done, a simple experimental test was carried out. We repeated a two-phase slug flow heat transfer run and observed the voltage variation with the passage of time. We used the following stabilization times:

1. Apply heat flux for 15 min, and then record the data for another 15 min.
2. Apply heat flux for 30 min, and then record the data for another 15 min
3. Apply heat flux for 45 min, and then record the data for another 15 min.

Table 3.6, gives the summary of the results of the heat transfer runs. We observe very small difference in the two-phase mean overall heat transfer coefficients. Figures 3.10

and 3.11 show the variation of voltage in the recording phase of last 15 min. for Run Nos. 4054 and 4055.

Table 3.6 Stabilization time

	Re _{SL}	Re _{SG}	Current	Voltage	h (Btu/Ft ² -Hr-F)
RN.4031	8498	2307	435.1	4.11	321.32
Repeat - [Stabilization time (15 Min) + Data record time(15 Min)]					
	Re _{SL}	Re _{SG}	Current	Voltage	h (Btu/Ft ² -Hr-F)
RN4054	8537	2463	436.8	4.07	319.54
Repeat - [Stabilization time (30 Min) + Data record time(15 Min)]					
	Re _{SL}	Re _{SG}	Current	Voltage	h (Btu/Ft ² -Hr-F)
RN4055	8510	2467	439	4.09	317.35
Repeat - [Stabilization time (45 Min) + Data record time(15 Min)]					
	Re _{SL}	Re _{SG}	Current	Voltage	h (Btu/Ft ² -Hr-F)
RN4056	8503	2459	435.5	4.07	313.43

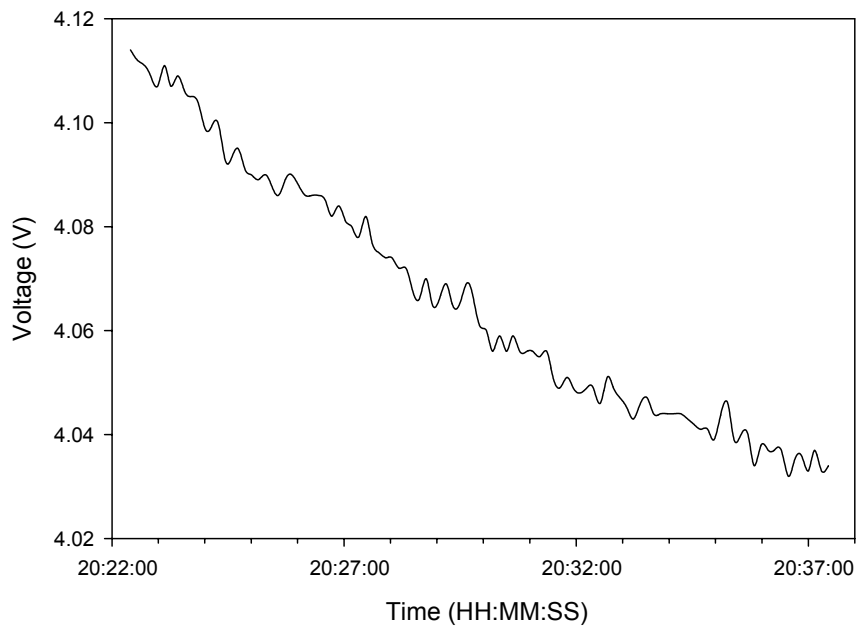


Figure 3.10 Behavior of voltage in the last 15 min recording phase after applying heat flux to the test set up for 15 min (RN4054)

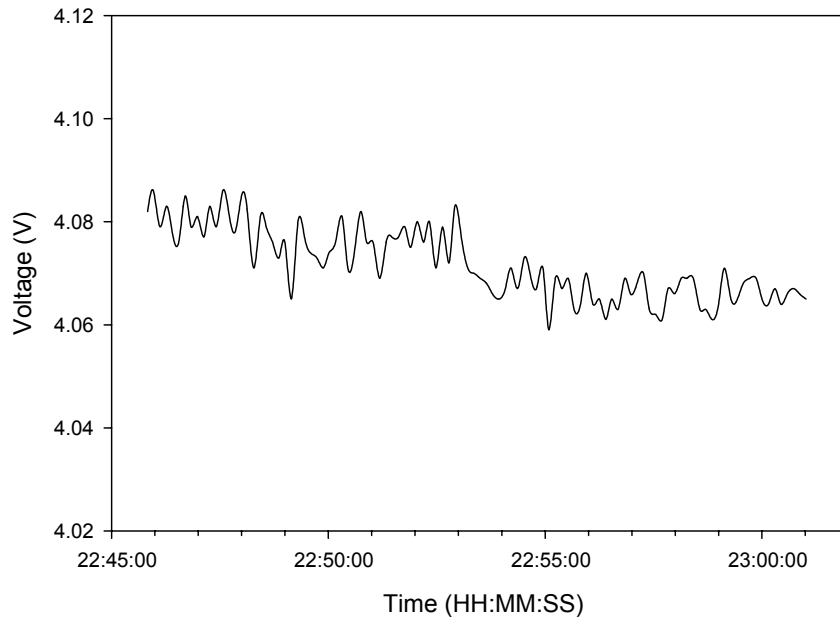


Figure 3.11 Behavior of voltage in the last 15 min recording phase after applying heat flux to the test set up for 30 min (RN4055)

We observe from Figure 3.10 that the voltage is still dropping in the last 15 minutes of recording phase. We concluded that 15 minutes of stabilization was not sufficient to achieve a steady state two-phase flow. Figure 3.11 shows that the voltage has stabilized and no significant drop in voltage is observed. The small drop observed in the voltage is negligible. Hence, this stabilization time was deemed appropriate for all single and two-phase runs.

Based on the above analysis, and the operating instructions for all other equipments. The following test procedure was established:

Test Procedure

- 1) Start all the instruments in the beginning.
- 2) Start the Compressor.
- 3) Start the Water Pump.

- 4) Adjust the Re_{SL} & Re_{SG} that you want to set using flow meters.
- 5) Wait for 5 – 6 min, to let the flow stabilize, check again for the Re_{SL} & Re_{SG} .
- 6) Once the stabilized flow has been achieved with the requisite Re_{SL} & Re_{SG} , turn the welder on.
- 7) Wait for a minute and apply the current that you feel is enough to achieve a reasonable temperature difference ($T_{in} - T_{out}$) (preferably more than 2 degree)
- 8) Once the required current is applied, wait for 30 mins, to let the system stabilize completely.
- 9) After 30 mins, start recording the data, and record it for 15 minutes.
- 10) After recording the data, bring down the current regulator to its minimum, and then put it in the close mode.
- 11) Let the apparatus cool down for approximately 15 minutes, before you repeat the same procedure to take the next reading.

Following the test procedure developed, it required approximately an hour to record one data point.

3.8.1 Reliability

After validating the single-phase flow, two-phase flows and setting up the standard test procedure, it was felt essential to check the system for reliability. To ensure reliability, random two-phase test runs were made and compared with some previous runs made in this current study. A total of 6 two-phase heated runs were made. All the repeated runs followed the same standard test procedure developed for this test set-up. Table 3.7 gives the details of the repeat runs. We observe from the Table 3.7, a maximum deviation of 5.96% and a minimum deviation of -3.10% in the overall mean two-phase

heat transfer coefficient. The deviations observed are well within the experimental uncertainty of 9.65% determined for this set-up.

Table 3.7 Random repeat runs carried out to check the setup for reliability

Run #	Re _{SL}	Re _{SG}	Current	Voltage	h (Btu/Ft ² -Hr-F)
RN 4212	9605	4978	457.1	4.38	394.83
Repeat Run RN4237	9794	4917	445.1	3.43	397.47
% Deviation	1.97	-1.23	-2.63	-21.69	0.67
Run #	Re _{SL}	Re _{SG}	Current	Voltage	h (Btu/Ft ² -Hr-F)
RN 4031	8498	2307	435.1	4.11	321.32
Repeat Run RN4238	8611	2238	433.6	3.34	325.53
% Deviation	1.33	-2.99	-0.34	-18.73	1.31
Run #	Re _{SL}	Re _{SG}	Current	Voltage	h (Btu/Ft ² -Hr-F)
RN 4084	15915	2480	483.6	4.71	594.83
Repeat Run RN4239	16145	2450	475.5	3.66	559.38
% Deviation	1.45	1.21	1.67	22.29	5.96
Run #	Re _{SL}	Re _{SG}	Current	Voltage	h (Btu/Ft ² -Hr-F)
RN 4199	12026	1508	465.0	4.43	419.48
Repeat Run RN4240	12063	1455	462.5	3.56	420.14
% Deviation	0.31	-3.51	-0.54	-19.64	0.16
Run #	Re _{SL}	Re _{SG}	Current	Voltage	h (Btu/Ft ² -Hr-F)
RN4192	26005	3493	501.66	4.78	843.17
Repeat Run RN4452	25525	3399	501.72	3.83	817.01
% Deviation	-1.85	-2.70	-12.16	-29.14	-3.10
Run #	Re _{SL}	Re _{SG}	Current	Voltage	h (Btu/Ft ² -Hr-F)
RN4193	26070	5074	500.878	4.72206	824.97
Repeat Run RN4253	25949	5097	440.64	3.39	830.46
% Deviation	-0.46	0.45	-12.03	-28.21	0.67

CHAPTER IV

RESULTS AND DISCUSSION

This chapter discusses the intricate details of slug flow heat transfer behavior and explains the phenomenon in detail. It touches upon the methodology of calculating the average heat transfer coefficient and then presents all the systematic controlled slug flow runs recorded in this study. The data has been systematically controlled so that the slug flow heat transfer behavior could be better understood. Then a comparative analysis has been carried out to investigate the change of heat transfer behavior for various tube inclinations. Flow visualization has been utilized as a tool to capture the fine intricacies of slug flow heat transfer behavior and explain the physics of the flow at various tube inclinations. Superficial liquid Froude number analysis has been carried out to see its effect on the heat transfer behavior. In the end a unified slug flow heat transfer correlation has been developed which encompasses all the tube inclinations.

4.1 General

In this study a total of 174 data points in slug region were measured for all tube inclinations, 69 data points at the horizontal position, 37 at the 2-degree position, 34 at the 5-degree position, and 34 at the 7-degree position. For these data the superficial gas Reynolds number ranged from 1055 to 6634 and the superficial liquid Reynolds number ranged from 3161 to 28631. The gas flow rate ranged from 0.015 kg/min to 0.16 kg/min

and the water flow rate ranged from 4.63 kg/min to 42.55 kg/min. The heat flux ranged from 2734 W/m² to 10787 W/m². The overall mean heat transfer coefficient ranged from 641 W/m²-K to 4907 W/m²-K. The flow pattern was visually observed to ensure that the pattern remained constant throughout the test section and did not collapse before the outlet of the test pipe. All the runs carried out remained consistently slug.

4.1.1 Heat Transfer Coefficient:

The heat transfer measurement for this study with uniform heat flux has been carried out by measuring the local outside wall temperatures at 10 stations and the inlet and outlet bulk temperatures.

Typical results of a single-phase experiment comparing the bulk temperatures and the wall temperatures should show the bulk temperature line rising at a gentle slope, while the wall temperature line rises sharply and eventually becomes parallel to the bulk temperature line. Figure 4.1 shows the trend of the bulk temperature and the variation of the wall temperatures of a single phase flow. Figure 4.2 shows the thermocouple readings along the test section at different stations in two-phase slug flow ($Re_{SL}=7087$, $Re_{SG}=1564$).

The inside wall surface temperature and inside wall heat flux has been obtained from a data reduction program written and developed exclusively for this type of experiments by Jae-yong Kim (PhD candidate) . Based on the local peripheral inside wall heat flux and the local bulk fluid temperature, the local peripheral heat transfer coefficient has been calculated using the following equation :

$$h_i = \dot{q}_i'' / (T_{wi} - T_b) \quad (4.1)$$

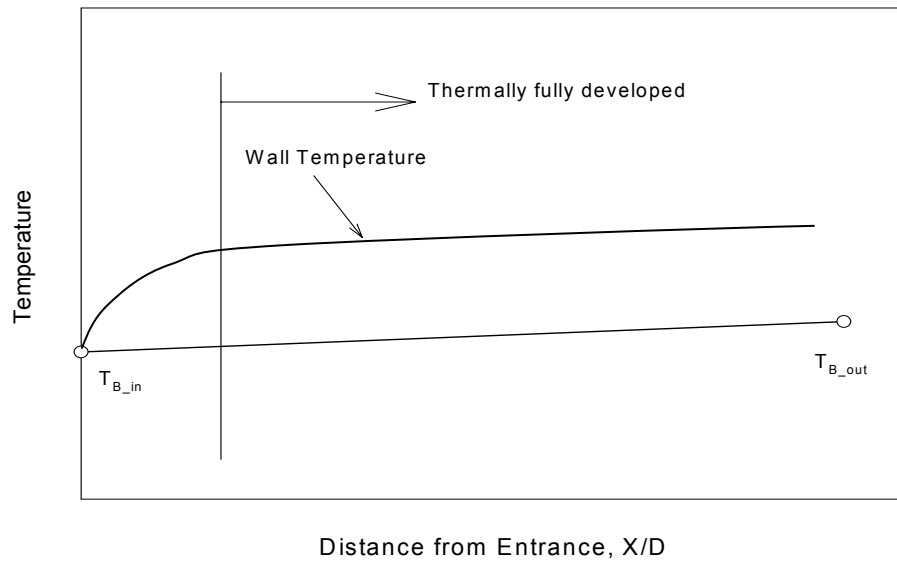


Figure 4.1 Characteristic wall and bulk temperature variation for single-phase flow

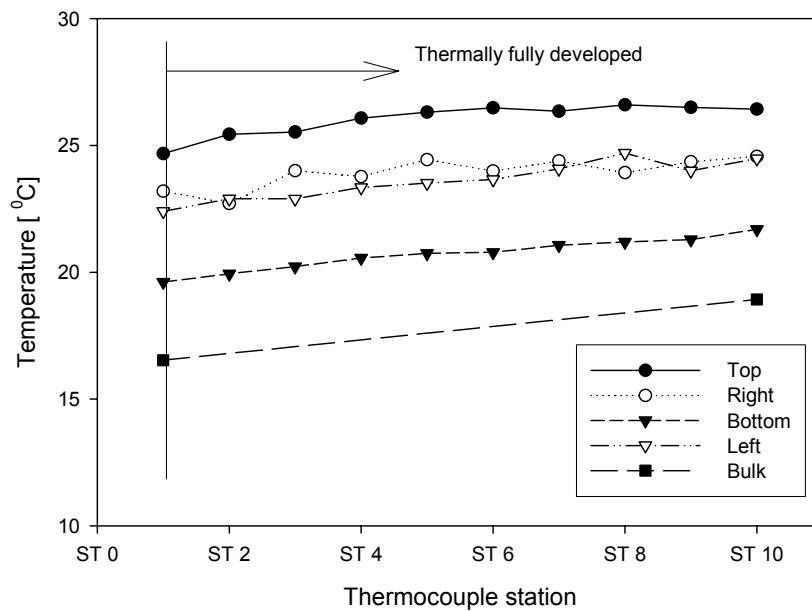


Figure 4.2 Thermocouple readings along the test section for a test case in two-phase flow ($Re_{SL}=7087$, $Re_{SG}=1564$)

where,

- h_i = local peripheral heat transfer coefficient
- \dot{q}_i = local peripheral inside wall heat flux
- T_{wi} = local inside wall temperature
- T_b = bulk fluid temperature at the thermocouple station

The bulk fluid temperature is calculated using the equation :

$$T_b = T_{in} + (T_{out} - T_{in}) X / L \quad (4.2)$$

where,

- T_{in} = bulk inlet temperature
- T_{out} = bulk outlet temperature
- X = distance from the pipe inlet to the thermocouple station
- L = total length of the test section

The local average heat transfer coefficient at each station could be calculated by the following equation:

$$\bar{h}_i = \bar{q}_i / (T_{wi} - T_b) \quad (4.3)$$

where,

- \bar{h}_i = local average heat transfer coefficient
 \bar{q}_i = average peripheral inside wall heat flux at a station
 \bar{T}_{wi} = average inside wall temperature at a station

The large variation in the circumferential wall temperature distribution, which is typical for two-phase gas-liquid flow in horizontal and slightly inclined tubes, leads to different heat transfer coefficients depending on which circumferential wall temperature selected for calculations. In order to overcome the unbalanced circumferential heat transfer coefficient, the overall mean two-phase heat transfer coefficient ($h_{TP_{EXP}}$) for each run was calculated by the equation:

$$h_{TP_{EXP}} = \frac{1}{N} \sum_1^N \left[\frac{\frac{1}{M} \sum_j^M \dot{q}''_{i,j}}{\frac{1}{M} \sum_j^M (T_w)_{i,j} - (T_B)_i} \right] \quad (4.4)$$

where,

- $h_{TP_{EXP}}$ = overall mean two-phase heat transfer coefficient
 N = number of thermocouple stations
 M = number of thermocouples in a stations
 T_B = bulk temperature, K
 T_w = wall temperature, K
 \dot{q}'' = heat flux, W/m²

Further, we shall present the systematically controlled slug flow heat transfer data for various tube inclinations under this study.

4.1.2 Horizontal Experimental Data

In this study, a total of 69 slug flow data points in the horizontal position have been analyzed. Among the 69 slug data points, 36 data points were taken by carefully coordinating the superficial liquid and superficial gas Reynolds numbers in order to better understand the slug flow heat transfer behavior. Each test run is characterized by its specific superficial gas and liquid Reynolds numbers. All the results are first tabulated and then the key elements of the data are discussed. The data is then compared against the slug flow data of Kim and Ghajar (2000) and Trimble *et al* (2002).

Table 4.1 gives the complete summary of the runs made in the horizontal position, stating their run numbers, superficial gas and liquid Reynolds numbers, mass flow rates of gas and liquid, their corresponding heat flux (including current and voltage), the overall mean two-phase heat transfer coefficient and corresponding superficial liquid Froude numbers obtained for each run.

Table 4.1 Heat transfer results for the horizontal position

Run #	Gas Mass Flow Rate (Kg/s)	Re _{SG}	Liquid Mass Flow Rate (Kg/s)	Re _{SL}	Heat Flux [W/m ²]	Current [A]	Voltage [V]	Avg. h _{hp} [W/m ² -K]	Superficial Liquid Froude No (F _{SL})
4014	0.00144	3709	0.13747	5020	7596	402.1	4.37	798	0.4310
4015	0.00043	1113	0.22004	7960	8025	416.7	4.45	1438	0.6899
4017	0.00190	4909	0.37260	13319	9754	462.6	4.88	2476	1.1682
4023	0.00107	2751	0.12551	4556	6993	392.5	4.12	789	0.3935
4028	0.00135	3480	0.28966	10509	7682	426.4	4.17	2055	0.9082
4057	0.00120	3093	0.49651	18774	10481	507.2	4.78	3630	1.5570
4030	0.00090	2312	0.12812	4658	7425	423.2	4.06	847	0.4017
4031	0.00089	2305	0.23595	8529	7740	435.1	4.11	1638	0.7398
4049	0.00041	1055	0.22209	8003	7430	419.6	4.09	1454	0.6963
4060	0.00227	5837	0.14763	5598	7105	415.9	3.95	859	0.4630
4066	0.00175	4481	0.14583	5720	7338	422.9	4.01	859	0.4574
4067	0.00172	4420	0.15469	6018	7273	420.1	4.00	912	0.4851
4068	0.00173	4441	0.16155	6279	7503	424.0	4.09	957	0.5067
4069	0.00173	4430	0.16699	6535	7524	422.0	4.12	1001	0.5237
4070	0.00172	4410	0.17329	6748	7625	424.8	4.15	1041	0.5435
4071	0.00173	4440	0.18443	7207	7652	425.4	4.16	1104	0.5784
4072	0.00172	4408	0.19263	7568	8144	440.1	4.28	1182	0.6042
4075	0.00174	4442	0.23001	9077	8300	440.6	4.36	1478	0.7214
4076	0.00174	4441	0.24772	9762	8536	446.7	4.42	1642	0.7770
4077	0.00173	4439	0.26088	10267	8592	451.5	4.40	1751	0.8183
4078	0.00174	4443	0.27880	10973	8653	451.8	4.43	1908	0.8744
4079	0.00173	4436	0.29397	11579	8793	456.8	4.45	2060	0.9220
4080	0.00166	4241	0.31221	12365	8934	459.6	4.50	2222	0.9793
4081	0.00166	4248	0.32189	12727	8999	459.8	4.53	2302	1.0096
4085	0.00174	4451	0.40495	15983	9660	477.9	4.67	3048	1.2701
4086	0.00145	3712	0.42410	16885	10706	504.1	4.91	3184	1.3303
4087	0.00135	3453	0.43455	17280	10638	499.7	4.92	3308	1.3630
4088	0.00121	3093	0.45046	17915	10639	500.6	4.91	3440	1.4129
4089	0.00121	3092	0.46229	18419	11139	515.2	5.00	3594	1.4500
4107	0.00080	2031	0.10581	4322	8869	459.0	4.47	741	0.3319
4108	0.00071	1801	0.09031	3770	9147	462.6	4.57	635	0.2834
4109	0.00069	1760	0.07711	3161	6266	369.5	3.92	521	0.2419
4114	0.00199	5049	0.67802	28631	13366	573.4	5.39	5602	2.1274

Table 4.1 Heat transfer results for the horizontal position (continued)

Run #	Gas Mass Flow Rate (Kg/s)	Re _{SG}	Liquid Mass Flow Rate (Kg/s)	Re _{SL}	Heat Flux [W/m ²]	Current [A]	Voltage [V]	Avg. Htp [W/m ² -K]	Superficial Liquid Froude No (Fr _{SL})
4128	0.00062	1565	0.16443	7099	8285	436.4	4.39	1159	0.5160
4224	0.00088	2204	0.14668	7045	7331	415.8	4.08	1095	0.4606
4129	0.00116	2935	0.16707	7180	7724	424.5	4.21	1133	0.5243
4197	0.00162	4062	0.14663	6914	7342	413.5	4.11	943	0.4604
4225	0.00204	5110	0.14403	6929	7296	415.2	4.06	946	0.4523
4199	0.00060	1518	0.25616	12041	8911	465.0	4.43	2052	0.8043
4187	0.00091	2287	0.25541	11992	9306	469.5	4.58	2097	0.8020
4195	0.00124	3128	0.25826	12069	8964	466.3	4.45	2016	0.8109
4188	0.00162	4065	0.25576	11981	9237	467.8	4.57	1847	0.8030
4198	0.00196	4931	0.25831	12100	8868	461.5	4.44	1892	0.8110
4146	0.00059	1477	0.10896	4911	4074	294.4	3.20	738	0.3358
4231	0.00089	2238	0.10347	4912	3921	296.8	3.05	721	0.3249
4147	0.00120	3028	0.10819	4954	4104	293.1	3.24	651	0.3396
4202	0.00160	4029	0.10567	4891	3827	292.7	3.02	648	0.3317
4196	0.00201	5050	0.10846	4926	3877	290.9	3.08	641	0.3342
4157	0.00123	3100	0.37153	17119	10291	493.5	4.82	3077	1.1664
4158	0.00085	2126	0.36336	17162	10038	486.5	4.77	3279	1.1410
4159	0.00159	3997	0.36099	17056	10294	494.5	4.81	2898	1.1335
4161	0.00205	5140	0.36319	17139	10258	493.3	4.81	2804	1.1404
4223	0.00122	3057	0.46364	22073	10337	504.6	4.74	4147	1.4559
4170	0.00160	4030	0.47372	21887	10623	500.9	4.90	3907	1.4872
4171	0.00203	5113	0.46870	21928	10787	508.2	4.91	3816	1.4716
4205	0.00260	6521	0.46711	21868	10333	504.8	4.73	3900	1.4666
4192	0.00139	3494	0.55968	26005	10379	501.7	4.78	4785	1.7572
4194	0.00171	4296	0.56054	26061	10228	500.9	4.72	4705	1.7599
4193	0.00202	5074	0.56241	26070	10279	500.5	4.75	4681	1.7657
4222	0.00265	6634	0.53860	25755	10120	502.2	4.66	4611	1.6852
4208	0.00063	1586	0.20180	9566	8719	456.2	4.42	1564	0.6337
4209	0.00090	2250	0.19958	9462	8612	453.2	4.39	1542	0.6267
4210	0.00123	3094	0.20049	9521	8729	455.8	4.43	1453	0.6296
4211	0.00162	4069	0.20327	9663	8539	452.8	4.36	1426	0.6383
4212	0.00200	5005	0.20126	9583	8658	457.1	4.38	1409	0.6320
4384	0.00088	2212	0.31272	15023	7301	469.4	3.60	2668	0.9821
4385	0.00126	3149	0.31164	14985	7301	469.3	3.60	2587	0.9787
4386	0.00165	4131	0.31284	15051	7161	464.8	3.56	2511	0.9825
4387	0.00204	5110	0.31054	14950	7350	470.9	3.61	2421	0.9753

The superficial liquid Reynolds numbers ranged from a minimum of 3161 to a maximum of 28631 (water mass flow rates varied from 4.62 kg/min to 40.68 kg/min) and superficial gas Reynolds numbers varied from a minimum of 1055 to a maximum of 6634 (gas mass flow rates varied from 0.0245 kg/min to 0.1588 kg/min). The uniform heat flux ranged from 3827 W/m² to 13366 W/m² and the resulting overall mean heat transfer coefficients ranged from 521 W/m²-K to 5602 W/m²-K.

Figure 4.3 shows the variation of the overall mean heat transfer coefficient with the increase of superficial liquid Reynolds number for the complete slug flow data (69 data points).

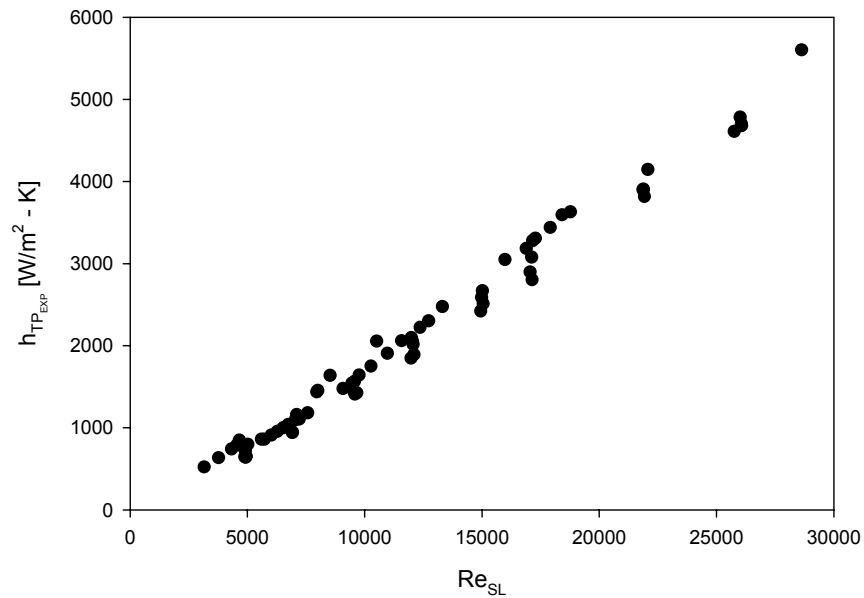


Figure 4.3 Variation of the overall mean heat transfer coefficient with the increase of superficial liquid Reynolds number for the complete horizontal slug flow data (69 data points)

Further, Figures 4.4 and 4.5 show the variation of the overall mean heat transfer coefficient over the superficial liquid and gas Reynolds numbers for the coordinated slug flow data, which comprise of 36 data points.

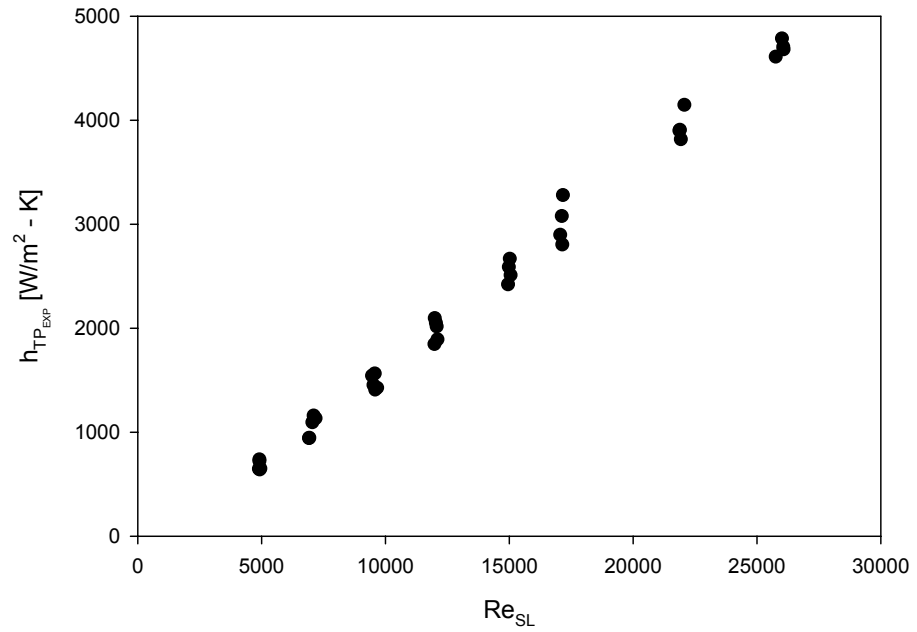


Figure 4.4 Variation of the overall mean heat transfer coefficient with the increase of superficial liquid Reynolds number for the coordinated horizontal slug flow data (36 data points)

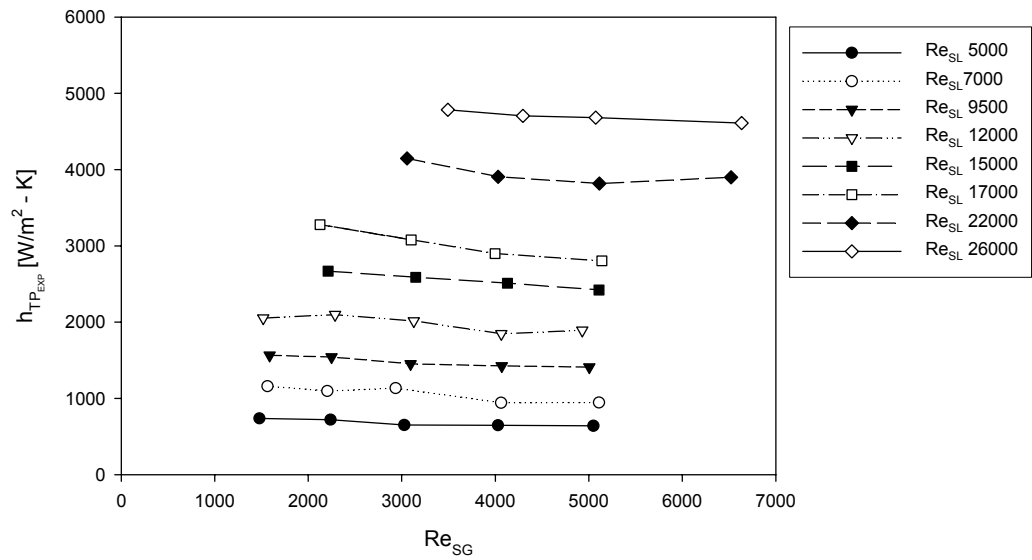


Figure 4.5 Variation of the overall mean heat transfer coefficient with the increase of superficial gas Reynolds number for the coordinated horizontal slug flow data (36 data points)

From Figure 4.3, we can observe that the overall mean heat transfer coefficient increases linearly with the increase of superficial liquid Reynolds number for the 69 slug flow data points. Figure 4.4, clearly indicates that the liquid phase plays a dominant role in heat transfer in the slug flow.

Figures 4.6 and 4.7, we have analyzed the variation of overall mean heat transfer coefficient with the increase of superficial liquid velocity and superficial gas velocity to see its effect with these dimensional parameters. From Figure 4.6, we observe that the superficial liquid velocity plays a dominant role on the heat transfer in slug flow. Hetsroni *et al* (1998b) observed that the heat transfer mainly depends on the liquid velocity. Similar conclusions were drawn by Kago *et al* (1986).

However, analyzing Figure 4.5, we see a slight gradual decrease in the mean overall heat transfer coefficient for fixed superficial gas Reynolds number, which indicates the influence of superficial gas Reynolds number, and hence this effect cannot be neglected. Similar observation is recorded from Figure 4.7, indicating the effect of gas phase on overall mean transfer coefficient.

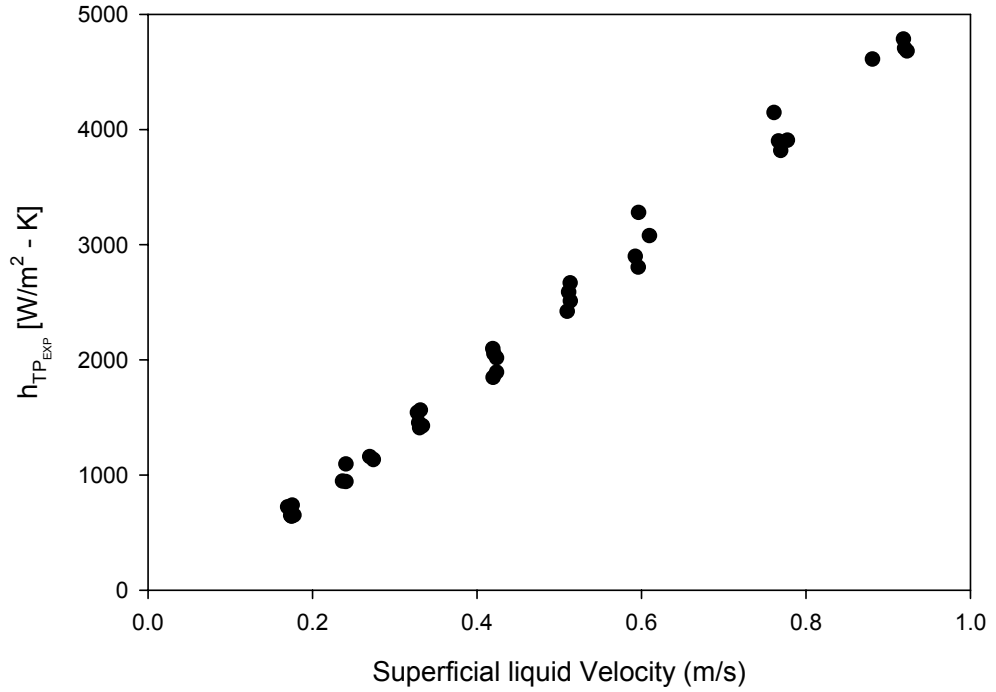


Figure 4.6 Variation of the overall mean heat transfer coefficient with the increase of superficial liquid velocity (m/s) for horizontal data

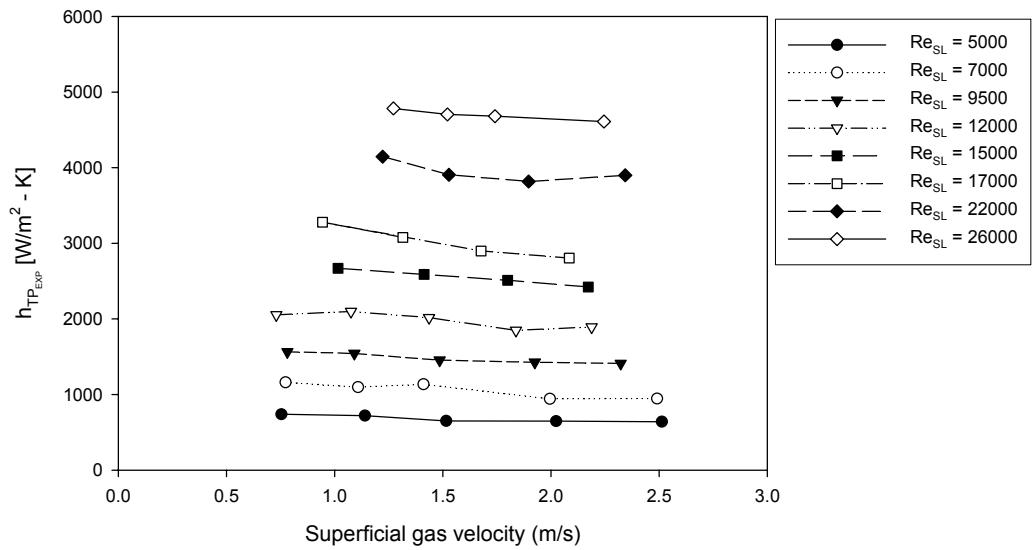


Figure 4.7 Variation of the overall mean heat transfer coefficient with the increase of superficial gas velocity (m/s) for horizontal data

To further investigate the parameters that contribute to the two-phase heat transfer, we have analyzed the effect using the non-dimensional superficial liquid Froude number. Hetsroni *et al* (1998b) used Froude number to represent his results.

$$\text{Superficial liquid Froude number: } Fr_{SL} = \frac{u_{SL}}{\sqrt{gD}} \quad (4.5)$$

Where, Fr_{SL} = superficial liquid Froude number

u_{SL} = superficial liquid velocity

g = acceleration due to gravity (= 9.80665 m/s²)

D = diameter of the pipe (= 0.0278638 m)

Superficial liquid Froude number depicts the *ratio of inertial force to gravitational force*. Figure 4.8 shows the variation of superficial gas Reynolds number with the superficial liquid Froude number.

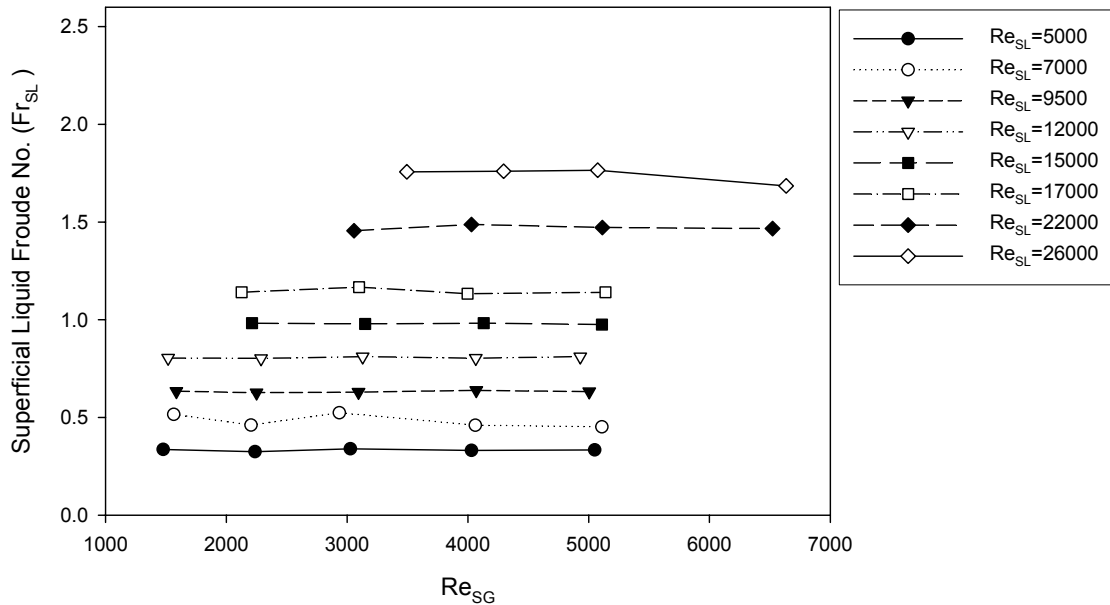


Figure 4.8 Variation of the superficial liquid Froude number with the increase of superficial gas Reynolds number for horizontal data

Comparing Figures 4.5, 4.7 and 4.8, we observe similar trends for overall mean heat transfer coefficient and superficial liquid Froude number with the variation of superficial gas velocity and Reynolds number. It is noted that each superficial liquid Reynolds number series shows its own specific trend with the variation of superficial gas Reynolds number.

Superficial liquid Froude number is dependent on the superficial liquid velocity, as the other two parameters (gravity and diameter) remain constant. Hence, variation in superficial liquid Froude number can also be referred to as a non-dimensional variation of superficial liquid velocity.

In order to better understand the physics of the flow we have used flow visualization as a tool. We have used Adobe Premiere Professional version 7.0 to analyze

the videos, in which the films were observed at an increment of 0.031 sec in piece-wise photographic form. Intricate details like the shape of the slug, formation of bubbles, back flow characteristics were carefully recorded from one photographic slide to the other.

Figures 4.9 (a) [$Re_{SL}=5000$, $Re_{SG}=1500$), 4.9(b) [$Re_{SL}=5000$, $Re_{SG}=3000$] and 4.9(c) [$Re_{SL}=5000$, $Re_{SG}=5000$] show the selected flow visualization pictures recorded for horizontal tube position for $Re_{SL}=5000$ series to explain the heat transfer phenomenon.

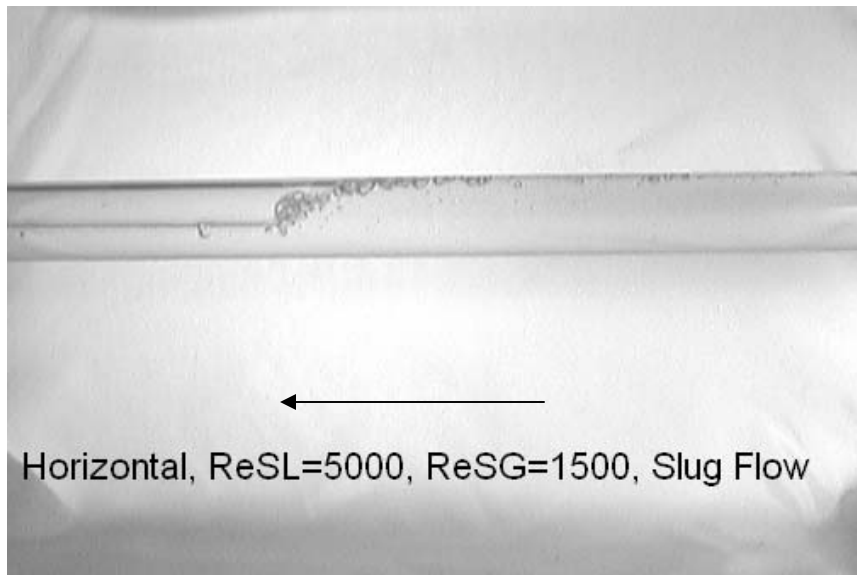


Figure 4.9(a) Horizontal, $Re_{SL}=5000$, $Re_{SG}=1500$ (Slug flow)

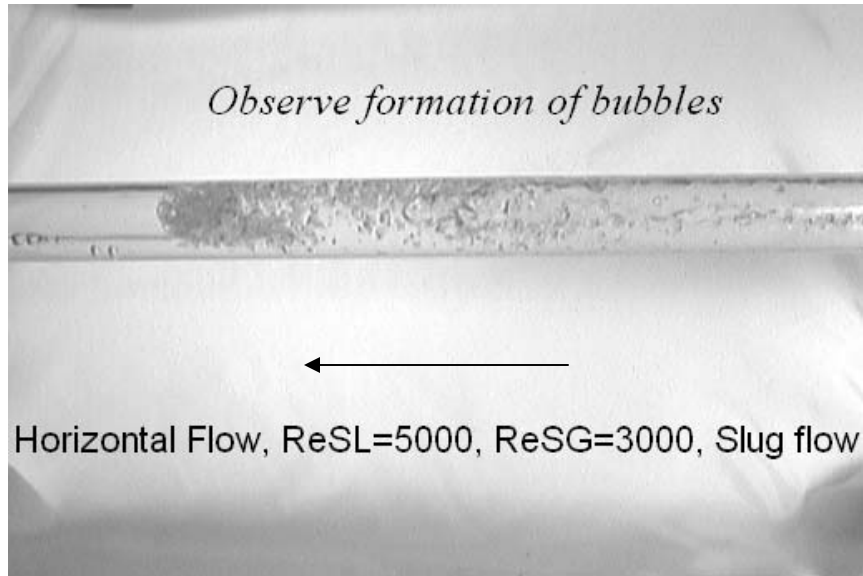


Figure 4.9(b) Horizontal, $Re_{SL}=5000$, $Re_{SG}=3000$ (Slug flow)

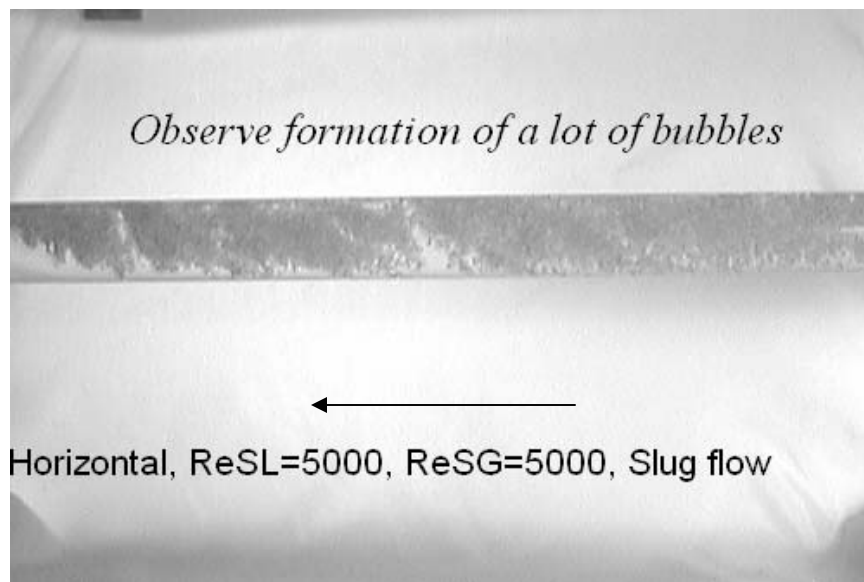


Figure 4.9(c) Horizontal, $Re_{SL}=5000$, $Re_{SG}=5000$ (Slug flow)

We observe from Figure 4.9(a), a normal slug flow pattern with very little formation of bubbles. Figure 4.9(b) shows more formation of bubbles, this is because the high gas velocity creates rigorous turbulence which results in a lot of formation of bubbles. These bubbles hinder the heat transfer and we observe a slight decrease in heat transfer coefficient, as it can be seen in Figure 4.7. Figure 4.9(c) shows formation of a lot of bubbles, which are uniformly distributed throughout the slug. Higher gas velocity for this case results in uniform distribution of lot of bubbles, which lead to the decrease of the heat transfer in slug flow.

It should be noted that liquid plays a dominant role in the heat transfer analysis, but the effect of gas phase results in the change of flow appearance, which in turn results in the change of heat transfer of the slug. Hence the effect of gas phase cannot be neglected.

It has been observed in this study that turbulence generally results in increase of heat transfer characteristics (better mixing), but turbulence caused with the formation of lot of bubbles results in decrease of heat transfer characteristics because excessive bubbles uniformly distributed in the slug hinder the heat transfer.

Although the analysis presented in this thesis is only limited to slug flow pattern, but extra controlled runs were carried out to investigate effect of the superficial gas Reynolds numbers on overall mean heat transfer coefficient for other flow patterns. Figure 4.10 shows the variation of overall mean heat transfer coefficients of horizontal flow over superficial gas Reynolds numbers with fixed superficial liquid Reynolds number.

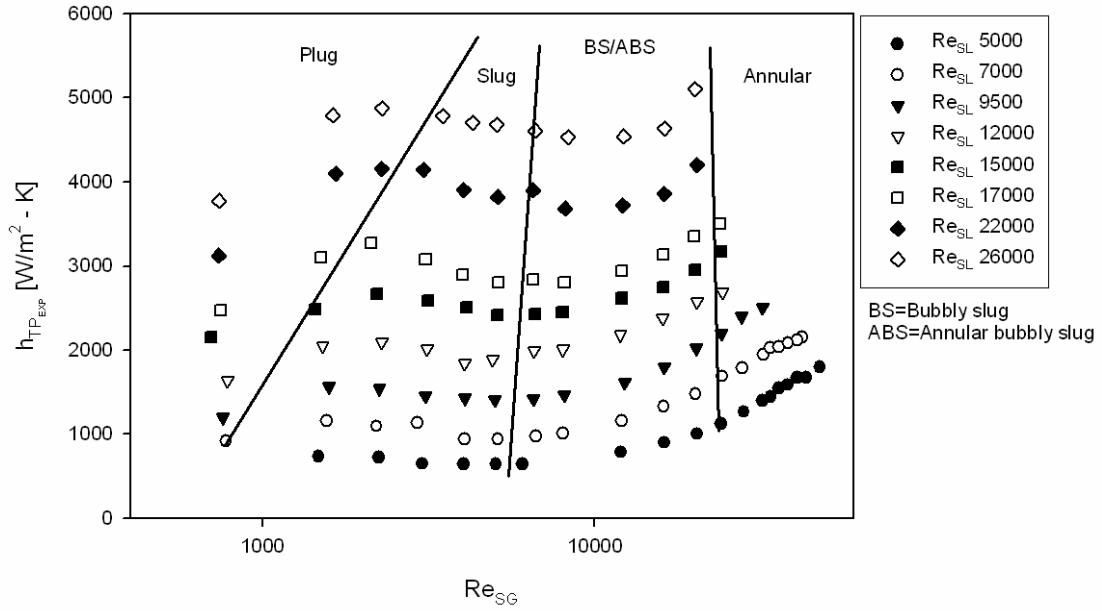


Figure 4.10 Variation of overall mean heat transfer coefficients of horizontal flow over superficial gas Reynolds numbers with fixed superficial liquid Reynolds number

It is observed that the overall mean heat transfer coefficient is dependent on the superficial gas Reynolds number which shows its own trend for different flow patterns. For the slug transitional flow pattern and the annular flow pattern, the overall mean heat transfer coefficient increases with the increase of superficial gas Reynolds number for fixed superficial liquid Reynolds number. However, from Figure 4.5, the slug flow pattern shows a slight decrease in overall mean heat transfer coefficient with the increase of superficial gas Reynolds number.

The combined effect of superficial liquid and superficial gas Reynolds numbers on overall mean heat transfer characteristics can be better analyzed by the three-dimensional plot with superficial liquid Reynolds number on its abscissa, superficial gas Reynolds number on its ordinate and the overall mean heat transfer coefficient on the “z” axis. The graph can be seen in Figure 4.11.

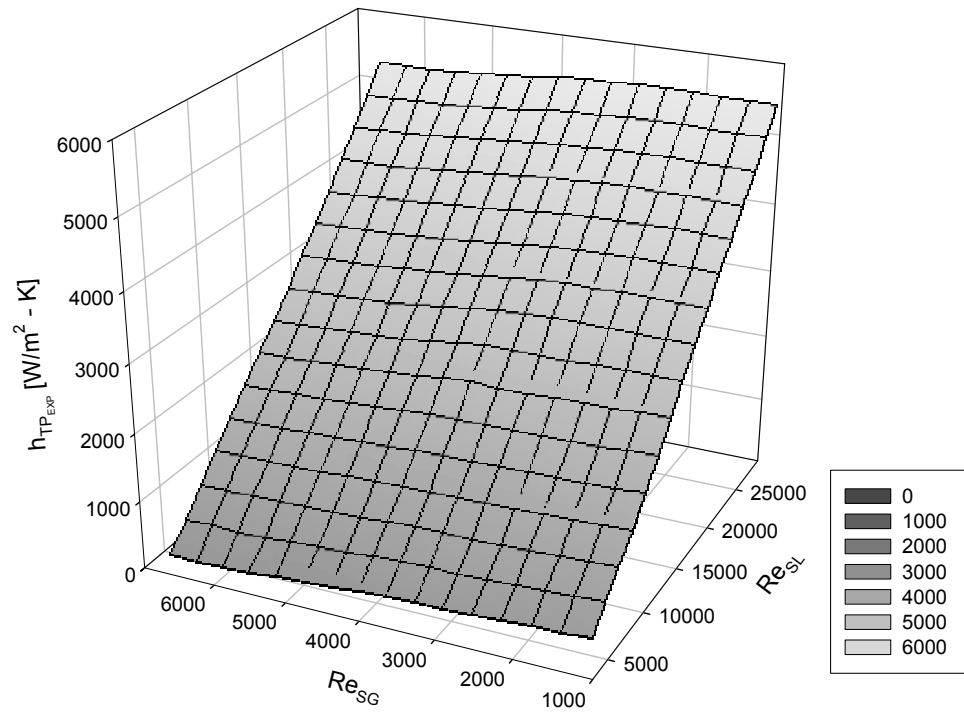


Figure 4.11 Variation of overall mean heat transfer coefficient with the increase of Re_{SL} and Re_{SG} for horizontal data

Kim and Ghajar (2002) obtained a large quantity of slug flow data for air-water, two-phase flow. The pattern of the heat transfer properties as a function of the liquid and gas Reynolds number has been presented in a three-dimensional graph; the graph can be seen in Figure 4.12.

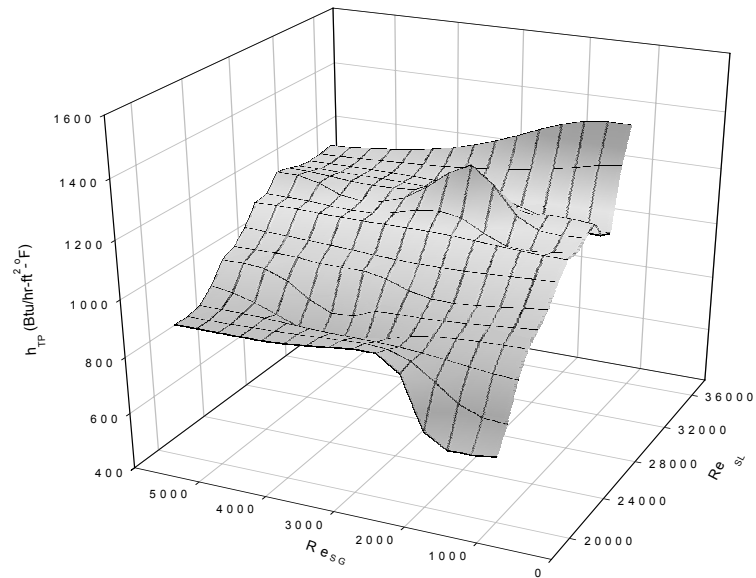


Figure 4.12 Kim and Ghajar's *et al* (2002) slug flow heat transfer behavior with Re_{SL} and Re_{SG}

It can be seen from Figures 4.11 and 4.12, that both plots show an increasing trend of heat transfer characteristics with the increase on superficial liquid Reynolds number.

Trimble *et al* (2002), collected many slug flow data as shown in Figure 4.13, is the trend of heat transfer behavior observed by him for his horizontal slug flow data.

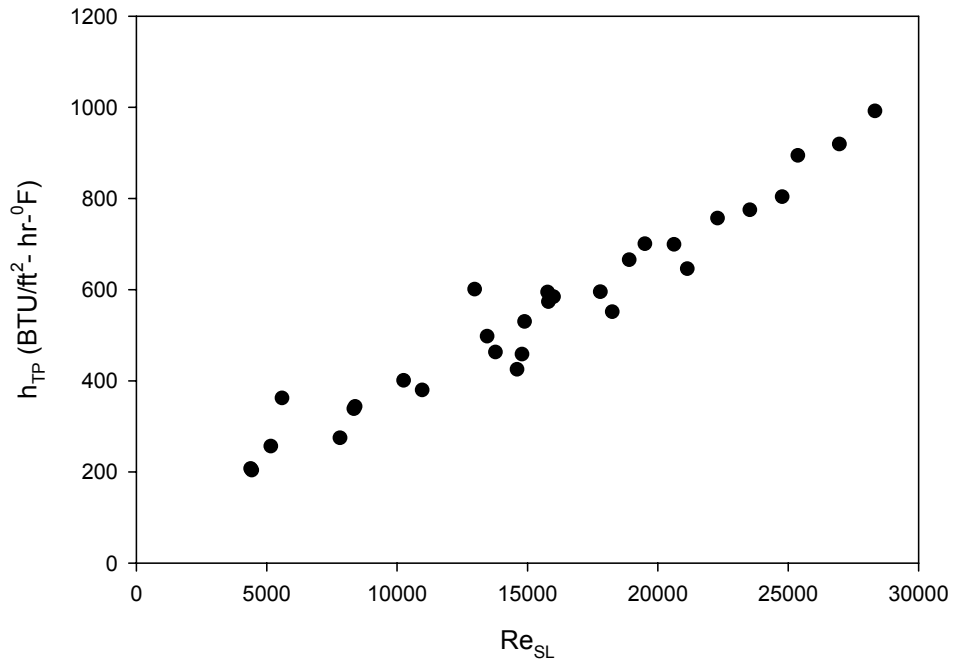


Figure 4.13 Two-phase heat transfer coefficient as a function of Re_{SL} for horizontal slug data (Trimble *et al* 2002)

Referring to Figure 4.4, we observe that the trend of heat transfer behavior observed by Trimble *et al* (2002) as shown in Figure 4.13, is similar to the observations in this study, where liquid phase plays a dominant role in the heat transfer characteristics of two-phase slug flow.

4.1.3 Two Degree Data

In this study a total of 37 controlled slug flow data points have been analyzed. The superficial liquid and gas Reynolds numbers are matched closely (98% of the data points are within $\pm 5\%$ deviation range) with the slug flow horizontal data points and all other parameters are kept the same, so that the effect of inclination on overall mean heat transfer heat coefficient can be analyzed systematically. The data points were taken by carefully coordinating the superficial liquid and superficial gas Reynolds numbers. Each test run is characterized by its specific superficial gas and liquid Reynolds numbers.

Table 4.2 gives the complete summary of the runs made in the two degree tube inclination position, stating their run numbers, superficial gas and liquid Reynolds numbers, mass flow rates of gas and liquid, their corresponding heat flux (including current and voltage), the overall mean two-phase heat transfer coefficient and corresponding superficial liquid Froude numbers obtained for each run.

Table 4.2 Heat transfer results for the two degree tube inclination

Run #	Gas Mass Flow Rate (Kg/s)	Re _{SG}	Liquid Mass Flow Rate (Kg/s)	Re _{SL}	Heat Flux [W/m ²]	Current [A]	Voltage [V]	Avg. h _{tp} [W/m ² -K]	Superficial Liquid Froude No (Fr _{SL})
4577	0.00060	1549	0.13140	5007	3145	309.3	2.35	1039	0.4121
4578	0.00086	2219	0.13111	4996	3141	309.1	2.35	999	0.4112
4579	0.00119	3044	0.13050	4999	3105	307.3	2.34	963	0.4093
4580	0.00156	4006	0.12974	4956	3135	308.8	2.35	931	0.4069
4581	0.00195	5008	0.12965	4948	3094	306.8	2.33	898	0.4066
4598	0.00059	1500	0.18227	7056	5873	422.5	3.21	1432	0.5716
4599	0.00088	2264	0.18363	7093	5786	419.3	3.19	1432	0.5759
4600	0.00119	3055	0.18268	7062	5734	417.4	3.18	1422	0.5729
4601	0.00157	4031	0.18341	7075	5712	416.6	3.17	1361	0.5752
4602	0.00195	4995	0.18314	7113	5837	421.0	3.21	1288	0.5744
4622	0.00058	1492	0.24129	9568	6908	458.0	3.49	1940	0.7568
4623	0.00089	2282	0.24141	9523	6910	458.1	3.49	1956	0.7572
4635	0.00121	3101	0.24328	9542	6842	455.9	3.47	1939	0.7630
4625	0.00159	4060	0.24697	9677	6765	453.4	3.45	1951	0.7746
4626	0.00192	4921	0.24561	9636	6995	460.9	3.51	1863	0.7703
4636	0.00062	1590	0.30561	12029	7097	464.5	3.53	2463	0.9585
4637	0.00089	2267	0.30514	12008	7253	469.5	3.57	2436	0.9571
4654	0.00027	696	0.31274	12335	7264	469.8	3.58	2371	0.9809
4638	0.00128	3269	0.30658	12052	7227	468.7	3.57	2401	0.9616
4639	0.00159	4060	0.30657	12048	7197	467.7	3.56	2380	0.9615
4640	0.00196	5029	0.30702	12049	7199	467.8	3.56	2326	0.9629
4648	0.00059	1504	0.37849	14887	7200	468.0	3.56	3049	1.1871
4649	0.00089	2287	0.38128	14977	7208	468.3	3.56	3020	1.1959
4650	0.00129	3294	0.38414	15005	7188	467.6	3.55	2994	1.2048
4651	0.00167	4279	0.38419	14997	7165	466.9	3.55	2936	1.2050
4652	0.00198	5076	0.38348	14978	7160	466.7	3.55	2907	1.2027
4663	0.00085	2173	0.44240	16925	7962	492.6	3.74	3614	1.3874
4664	0.00123	3155	0.44346	16963	7914	491.0	3.73	3533	1.3907
4665	0.00154	3958	0.44587	17044	7929	491.6	3.73	3526	1.3983
4666	0.00197	5047	0.44373	16917	7938	491.9	3.73	3419	1.3915
4676	0.00115	2953	0.57424	21942	8079	496.3	3.76	4261	1.8008
4677	0.00160	4106	0.57145	21879	8170	499.1	3.79	4359	1.7921
4678	0.00199	5110	0.57148	21900	8193	499.8	3.79	4356	1.7922
4679	0.00253	6499	0.58095	21881	8096	496.9	3.77	4218	1.8218
4688	0.00167	4300	0.68908	25797	8160	499.1	3.78	4846	2.1608
4689	0.00197	5071	0.69127	25881	8215	500.7	3.79	4881	2.1677
4690	0.00252	6491	0.69232	25917	8151	498.8	3.78	4904	2.1710

The superficial liquid Reynolds numbers ranged from a minimum of 4948 to a maximum of 25917 (water mass flow rates varied from 7.78 kg/min to 41.53 kg/min) and superficial gas Reynolds numbers varied from a minimum of 696 to a maximum of 6499 (gas mass flow rates varied from 0.016 kg/min to 0.1516 kg/min). The uniform heat flux ranged from 3094 W/m² to 8215 W/m² and the resulting overall heat transfer coefficients ranged from 898 W/m²-K to 4904 W/m²-K.

Figures 4.14 and 4.15 show the variation of the overall mean heat transfer coefficient with the increase of superficial liquid and gas Reynolds numbers for the coordinated slug flow data (37 data points).

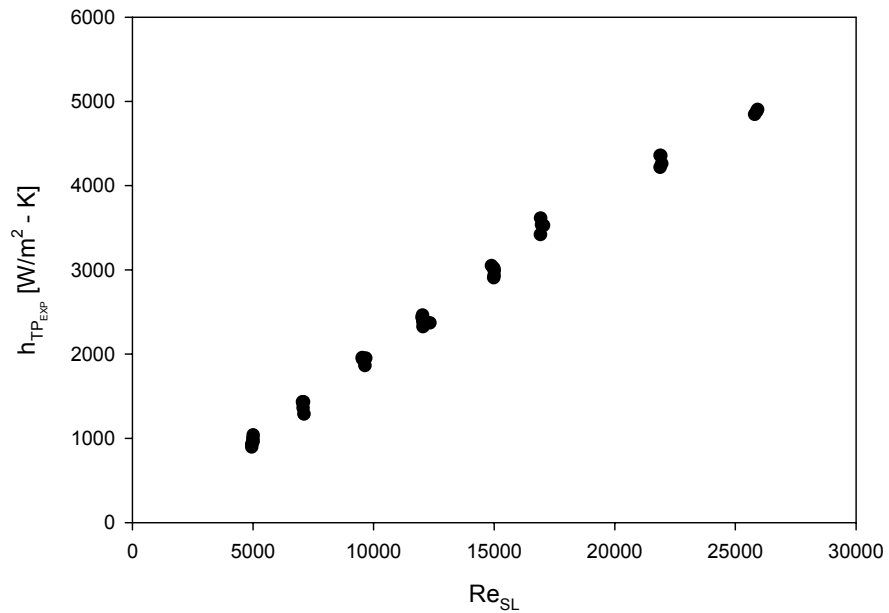


Figure 4.14 Variation of the overall mean heat transfer coefficient with the increase of superficial liquid Reynolds number for the coordinated two degree slug flow data (37 data points)

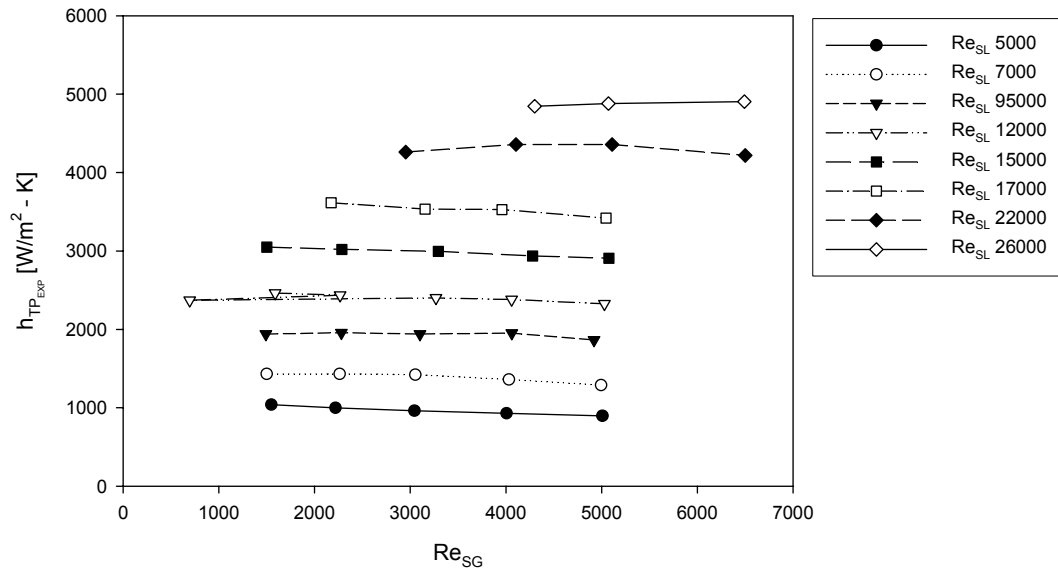


Figure 4.15 Variation of the overall mean heat transfer coefficient with the increase of superficial gas Reynolds number for the coordinated two degree slug flow data (37 data points)

In Figures 4.16 and 4.17, we have analyzed the variation of overall mean heat transfer coefficient with the increase of liquid velocity and gas velocity.

From Figures 4.14 and 4.16, we note that the liquid phase being a dominant factor in slug flow heat transfer for the two degree tube inclination. Analyzing Figures 4.16 and 4.17, we also observe that the gas phase affects the overall mean heat transfer coefficient slightly, and follows the same systematic trend for different superficial liquid Reynolds numbers and gas velocities. Hence, the effect of gas phase cannot be neglected.

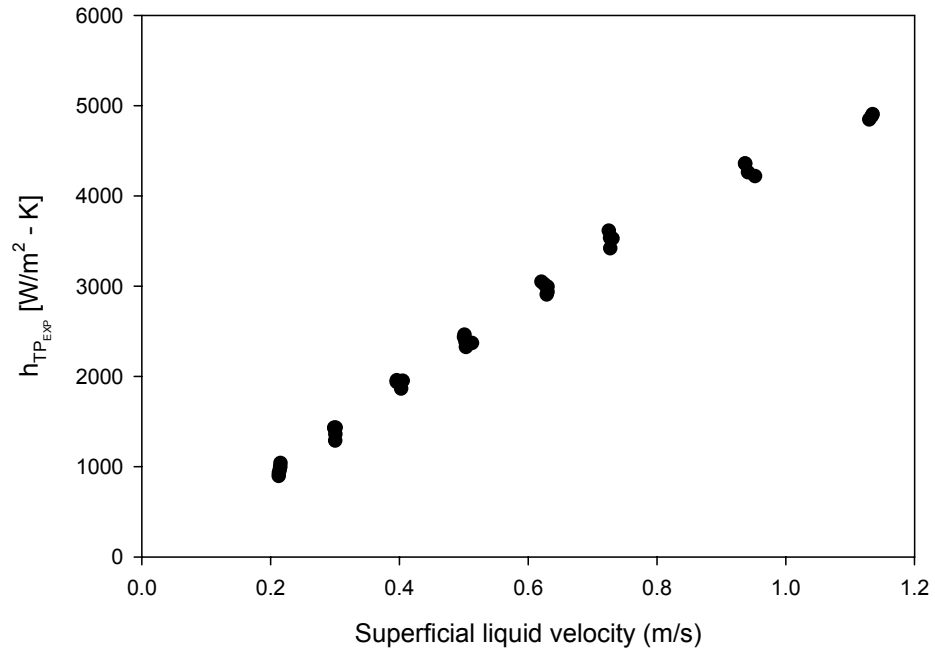


Figure 4.16 Variation of the overall mean heat transfer coefficient with the increase of superficial liquid velocity (m/s) for two degree data

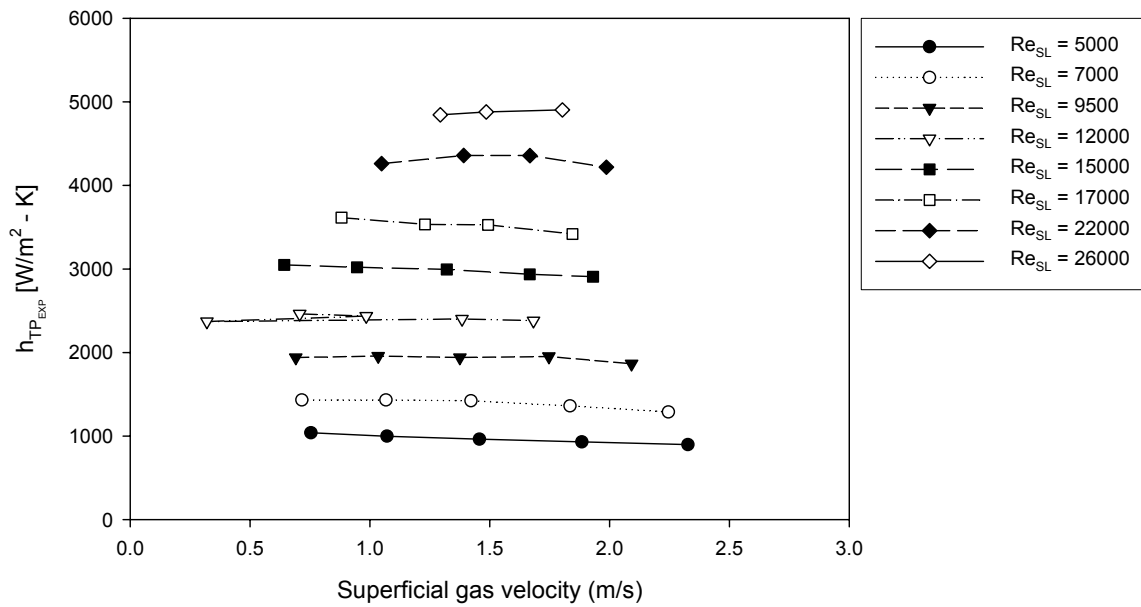


Figure 4.17 Variation of the overall mean heat transfer coefficient with the increase of superficial gas velocity (m/s) for two degree data

Figure 4.18 shows the variation of superficial gas Reynolds number with the superficial liquid Froude number.

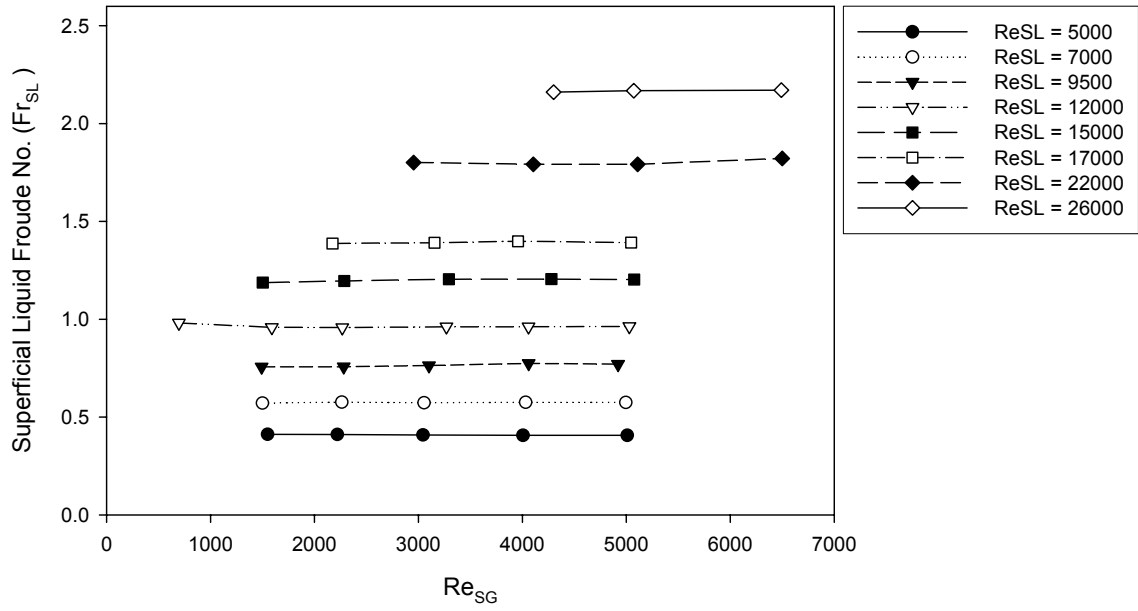


Figure 4.18 Variation of the superficial liquid Froude number with the increase of superficial gas Reynolds number for two degree data

Comparing Figures 4.15, 4.17 and 4.18, we observe similar trends for overall mean heat transfer coefficient and superficial liquid Froude number with the variation of superficial gas velocity and Reynolds number. It is noted that each superficial liquid Reynolds number series shows its own specific trend with the variation of superficial gas Reynolds number.

Using flow visualization, Figures 4.19 (a) [$Re_{SL}=5000, Re_{SG}=1500$], 4.19(b) [$Re_{SL}=5000, Re_{SG}=3000$] and 4.19(c) [$Re_{SL}=5000, Re_{SG}=5000$] show the selected flow

visualization pictures recorded for the two degree tube position for $Re_{SL}=5000$ series to explain the heat transfer phenomenon.

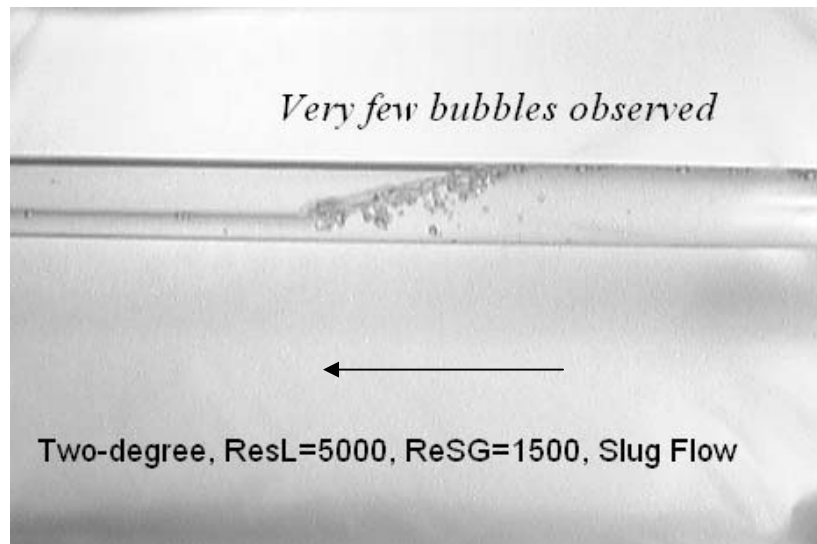


Figure 4.19(a) 2 Degree, $Re_{SL}=5000$, $Re_{SG}=1500$ (Slug flow)

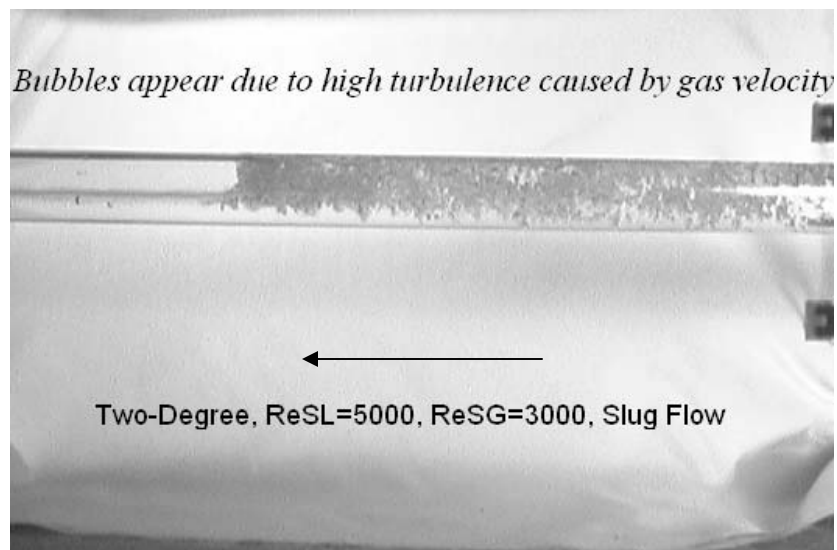


Figure 4.19(b) 2 Degree, $Re_{SL}=5000$, $Re_{SG}=3000$ (Slug flow)

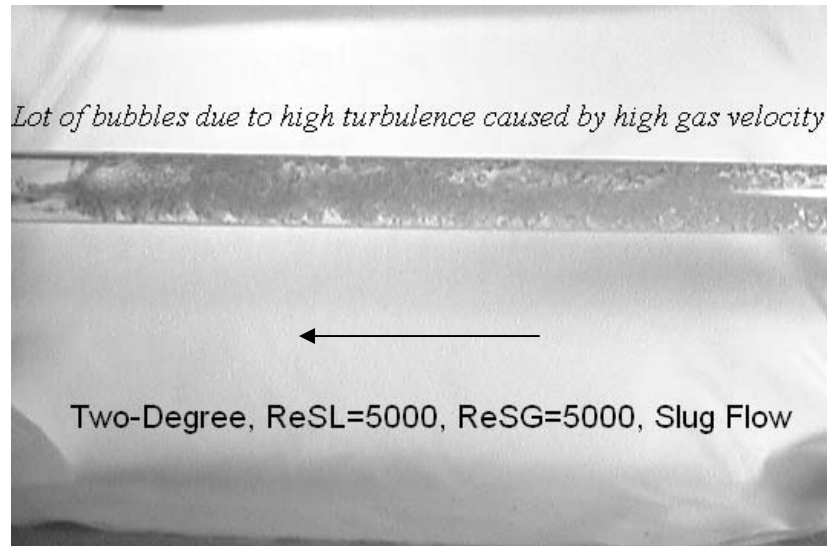
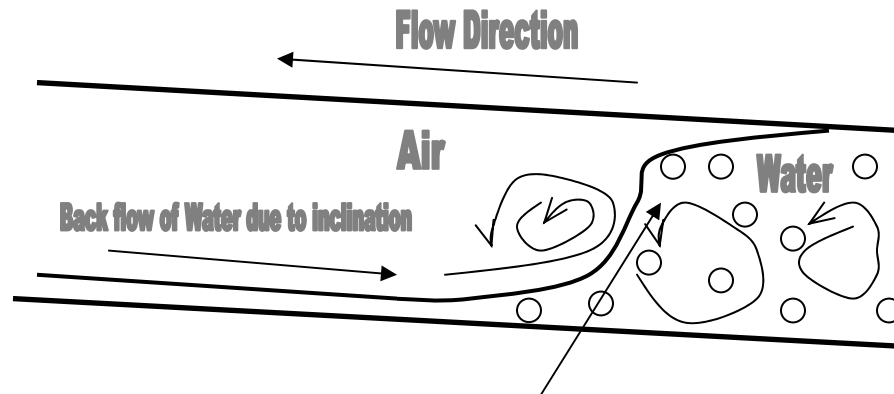


Figure 4.19(c) 2 Degree, $Re_{SL}=5000$, $Re_{SG}=5000$ (Slug flow)

We observe from Figure 4.19(a), a normal slug flow pattern with some formation of bubbles. These formation of bubbles results from the fact that there is a back flow observed in this two degree flow. The back flow causes rigorous turbulence with the oncoming fast slug and hence the formation of lot of bubbles. These bubbles are uniformly distributed in the slug, and hence impede the heat transfer characteristics of the slug flow pattern. We note an increase in the formation of bubbles in Figures 4.19(b) and 4.19(c), with the increase of superficial gas Reynolds number. Figure 4.20 shows a schematic of what was observed in Figure 4.19(a to c). The schematic explains the physics of the back flow characteristics.



Back flow causes resistance to fast moving slug, hence turbulence and higher heat transfer, It also results in formation of bubbles

Figure 4.20 Back flow effects on heat transfer characteristics in inclined tube position

Analysis of back flow and its effect on heat transfer characteristics has been discussed in Section 4.1.3, when a comparative study is done for various Re_{SL} series at various tube inclinations. We shall limit our discussion on the basics in this section.

Similar observations were recorded in this tube inclination position to what we observed in horizontal position. Liquid phase plays a dominant role in the heat transfer analysis, but the effect of gas phase results in the change of flow appearance, which in turn results in the change of heat transfer of the slug. Hence gas phase effect cannot be neglected. The turbulence caused by the back flow (better mixing) tends to enhance the heat transfer characteristics, but strong turbulence results in the formation of many bubbles, which in-turn hinder the heat transfer characteristics.

Extra controlled runs were carried out to investigate the effect of superficial gas Reynolds number on the overall mean heat transfer coefficient for other flow patterns for

two degree tube inclination. Figure 4.21 shows the variation of overall mean heat transfer coefficients of two degree flow over superficial gas Reynolds numbers with fixed superficial liquid Reynolds number.

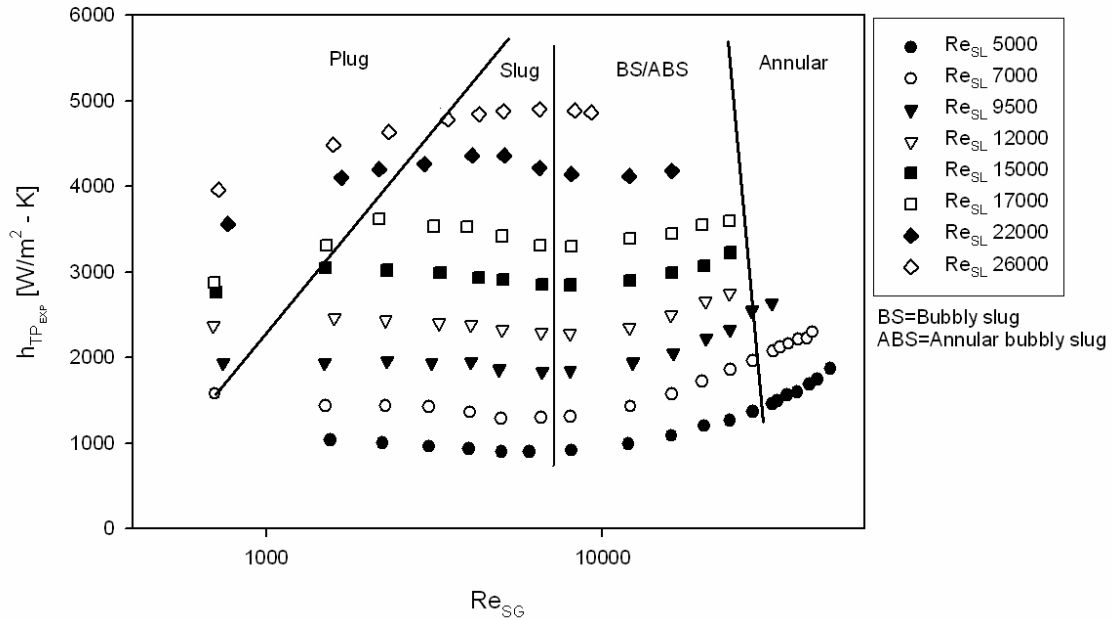


Figure 4.21 Variation of overall mean heat transfer coefficients of two degree inclined flow over superficial gas Reynolds numbers with fixed superficial liquid Reynolds number

It is observed that the overall mean heat transfer coefficient is dependent on the superficial gas Reynolds number which shows its own trend for different flow patterns. For the slug transitional flow pattern and the annular flow pattern, the overall mean heat transfer coefficient increases with the increase of superficial gas Reynolds number for fixed superficial liquid Reynolds number. However, from Figure 4.15, the slug flow pattern shows a slight decrease in overall mean heat transfer coefficient with the increase of superficial gas Reynolds number.

The combined effect of superficial liquid and superficial gas Reynolds numbers on the overall mean heat transfer characteristics can be better analyzed by the three-

dimensional plot with superficial liquid Reynolds number on its abscissa, superficial gas Reynolds number on its ordinate and the overall mean heat transfer coefficient on the “z” axis. The graph can be seen in Figure 4.22.

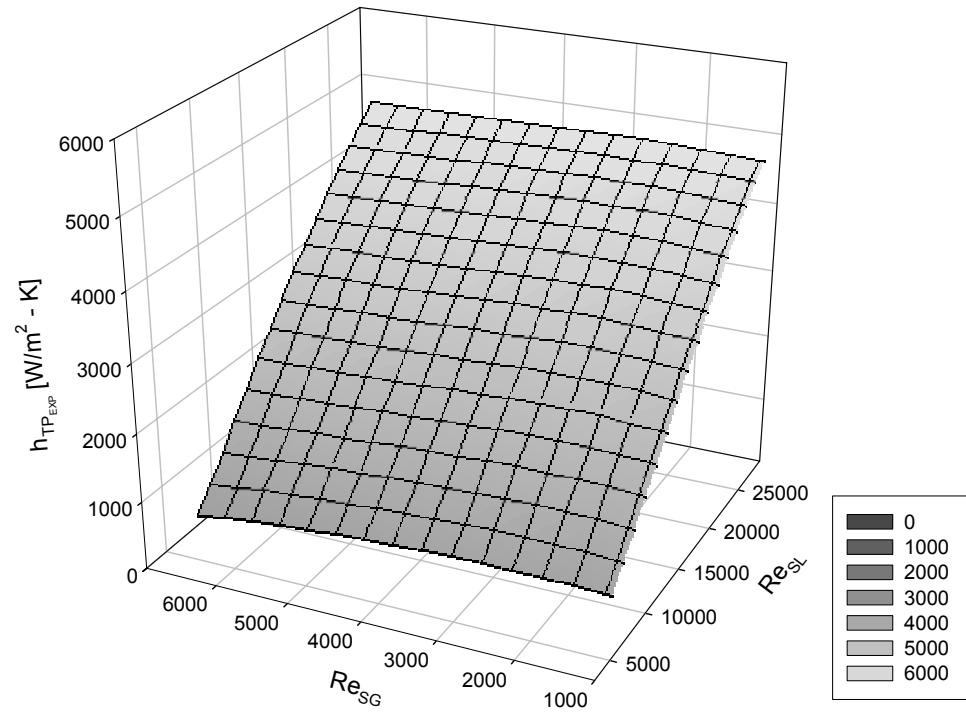


Figure 4.22 Variation of overall mean heat transfer coefficient with the increase of Re_{SL} and Re_{SG} for two degree data

Trimble *et al* (2002), collected many slug flow data points, Figure 4.23 shows the trend of heat transfer behavior observed by him for his two degree slug flow data points.

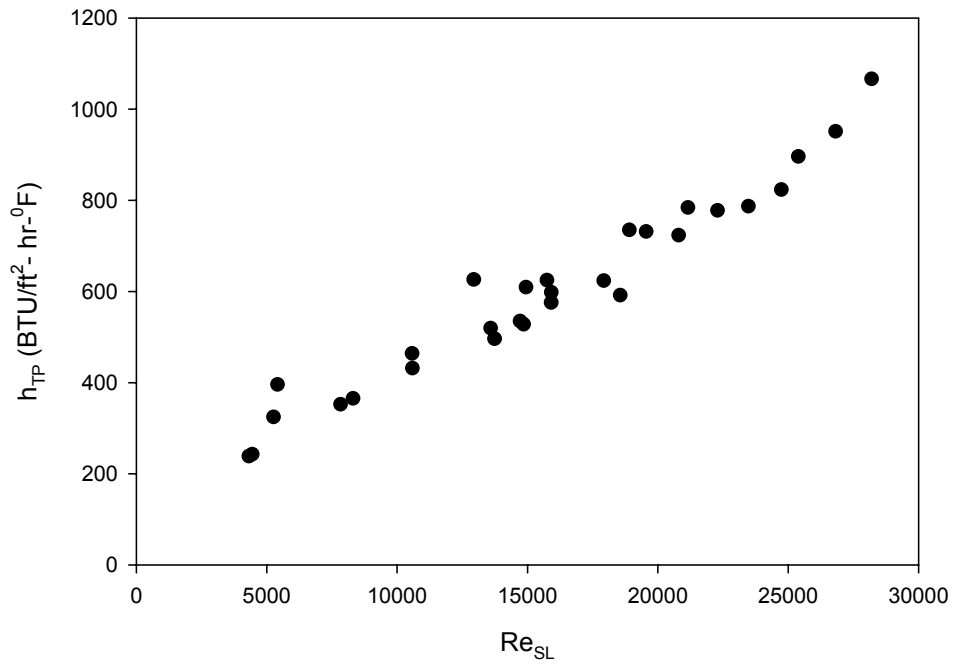


Figure 4.23 Two-phase heat transfer coefficient as a function of Re_{SL} for two degree data (Trimble *et al* 2002)

The observations made by Trimble *et al* (2002) are similar to the observations recorded in this study.

4.1.4 Five Degree Data

In this study a total of 34 controlled slug flow data points have been analyzed. The superficial liquid and gas Reynolds numbers are matched closely (98% of the data points are within $\pm 5\%$ deviation range) with the slug flow horizontal and two degree data points and all other parameters are kept the same, so that the effect of inclination on overall mean heat transfer heat coefficient can be analyzed systematically. The data points were taken by carefully coordinating the superficial liquid and superficial gas Reynolds numbers. Each test run is characterized by its specific superficial gas and liquid Reynolds numbers.

Table 4.3 gives the complete summary of the runs made in the five degree tube inclination, stating their run numbers, superficial gas and liquid Reynolds numbers, mass flow rates of gas and liquid, their corresponding heat flux (including current and voltage), the overall mean two-phase heat transfer coefficient and corresponding superficial liquid Froude numbers obtained for each run.

The superficial liquid Reynolds numbers ranged from a minimum of 4966 to a maximum of 25997 (water mass flow rates varied from 7.99 kg/min to 42.54 kg/min) and superficial gas Reynolds numbers varied from a minimum of 634 to a maximum of 6541 (gas mass flow rates varied from 0.014 kg/min to 0.1519 kg/min). The uniform heat flux ranged from 3110 W/m^2 to 8286 W/m^2 and the resulting overall heat transfer coefficients ranged from $1159 \text{ W/m}^2\text{-K}$ to $4659 \text{ W/m}^2\text{-K}$.

Table 4.3 Heat transfer results for the five degree tube inclination

Run #	Gas Mass Flow Rate (kg/s)	Re _{SG}	Liquid Mass Flow Rate (kg/s)	Re _{SL}	Heat Flux [W/m ²]	Current [A]	Voltage [V]	Avg. h _{hp} [W/m ² -K]	Superficial Liquid Froude No (Fr _{SL})
4701	0.00057	1462	0.13459	5021	3287	316.5	2.40	1271	0.4220
4702	0.00087	2247	0.13421	5008	3209	312.6	2.37	1190	0.4208
4703	0.00118	3035	0.13364	4987	3157	310.1	2.35	1159	0.4191
4704	0.00157	4030	0.13325	4966	3110	307.7	2.34	1161	0.4178
4720	0.00034	871	0.19063	7108	5797	420.2	3.19	1888	0.5978
4721	0.00058	1480	0.19035	7103	5968	426.3	3.24	1693	0.5969
4722	0.00088	2274	0.18933	7059	5844	421.9	3.20	1618	0.5937
4723	0.00119	3059	0.19075	7111	5974	426.5	3.24	1612	0.5981
4724	0.00157	4045	0.18947	7038	5921	424.6	3.22	1591	0.5941
4745	0.00025	634	0.26768	9645	6808	455.8	3.45	2289	0.8393
4746	0.00063	1629	0.26632	9563	6912	459.2	3.48	2197	0.8350
4747	0.00093	2398	0.26727	9573	6847	457.1	3.46	2158	0.8380
4748	0.00124	3196	0.26841	9578	6908	459.1	3.48	2139	0.8415
4749	0.00162	4193	0.26867	9578	6846	457.2	3.46	2143	0.8423
4760	0.00055	1434	0.34373	12050	7039	463.8	3.51	2740	1.0776
4761	0.00090	2339	0.34312	12009	6939	460.6	3.48	2752	1.0757
4762	0.00124	3212	0.34461	12090	7217	469.6	3.55	2732	1.0804
4763	0.00160	4137	0.34179	11984	7136	467.0	3.53	2668	1.0715
4773	0.00095	2463	0.43754	15022	7154	467.9	3.54	3484	1.3716
4774	0.00127	3300	0.43444	14927	7103	466.2	3.52	3394	1.3619
4775	0.00159	4119	0.43490	14941	7061	464.9	3.51	3345	1.3634
4776	0.00196	5094	0.43582	14977	7044	464.3	3.51	3299	1.3662
4786	0.00085	2192	0.48884	16933	8136	498.9	3.77	3802	1.5325
4787	0.00121	3148	0.48983	16947	8004	494.9	3.74	3798	1.5356
4788	0.00154	4001	0.49082	17002	8016	495.2	3.74	3767	1.5387
4789	0.00193	5004	0.49022	16996	8008	495.0	3.74	3673	1.5368
4799	0.00119	3067	0.61692	22058	8286	503.2	3.81	4321	1.9342
4800	0.00157	4054	0.61232	21927	8198	500.6	3.79	4324	1.9198
4801	0.00194	5003	0.61600	22057	8265	502.5	3.80	4364	1.9313
4802	0.00253	6541	0.61067	22007	8187	500.1	3.79	4307	1.9147
4808	0.00126	3253	0.70912	25997	8092	497.0	3.76	4638	2.2235
4809	0.00157	4038	0.70700	25894	8036	495.3	3.75	4636	2.2168
4810	0.00196	5046	0.70829	25871	8001	494.2	3.74	4618	2.2208
4811	0.00250	6444	0.70309	25623	8197	500.3	3.79	4659	2.2045

Figures 4.24 and 4.25, show the variation of the overall mean heat transfer coefficient with the increase of superficial liquid and gas Reynolds numbers for the coordinated slug flow data (37 data points).

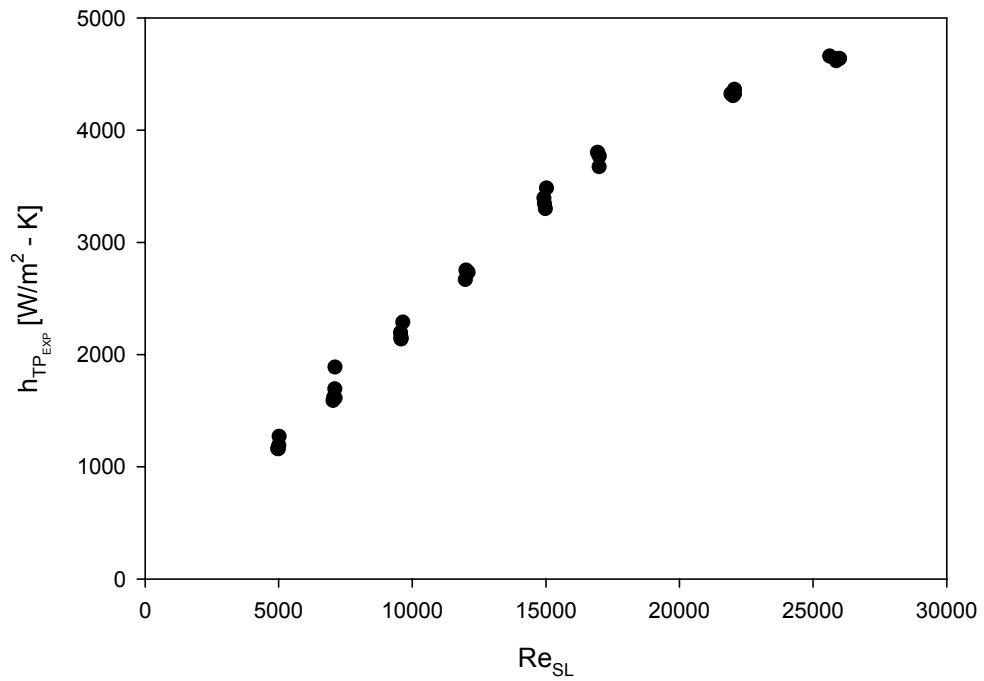


Figure 4.24 Variation of the overall mean heat transfer coefficient with the increase of superficial liquid Reynolds number for the coordinated five degree slug flow data (34 data points)

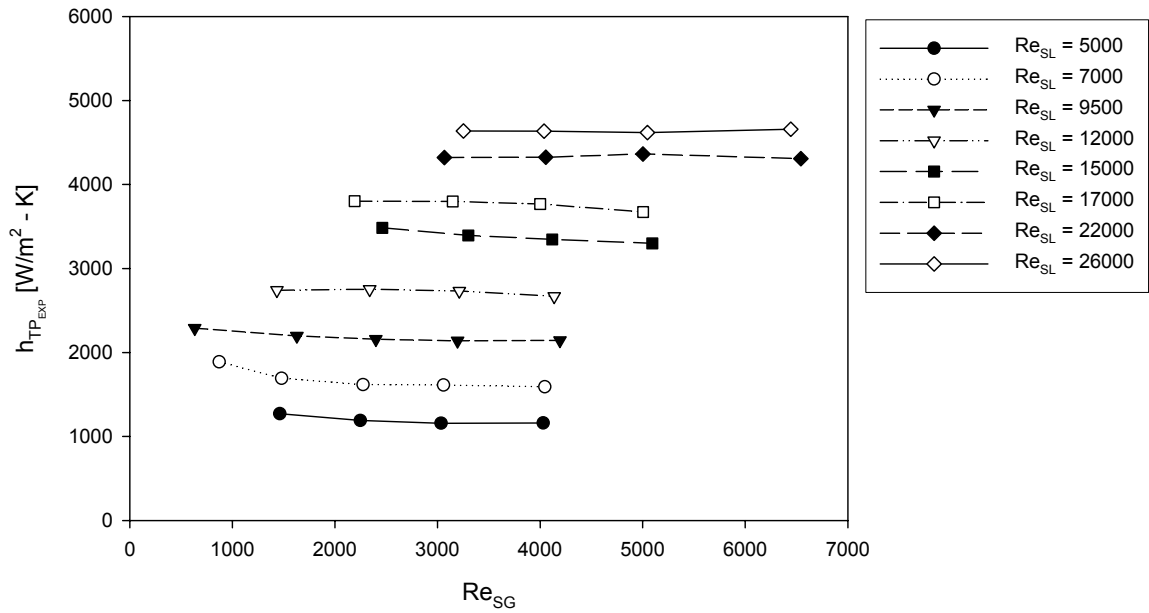


Figure 4.25 Variation of the overall mean heat transfer coefficient with the increase of superficial gas Reynolds number for the coordinated five degree slug flow data (34 data points)

Figures 4.26 and 4.27, we have analyzed the variation of overall mean heat transfer coefficient with the increase of liquid velocity and gas velocity.

From Figures 4.24 and 4.26, we observe the liquid phase being a dominant factor in slug flow heat transfer for the five degree tube inclination. Analyzing Figures 4.25 and 4.27, we also observe that the gas phase affects the overall mean heat transfer coefficient slightly, and follows the same systematic trend for different superficial liquid Reynolds numbers and gas velocities. Hence, the effect of gas phase cannot be neglected.

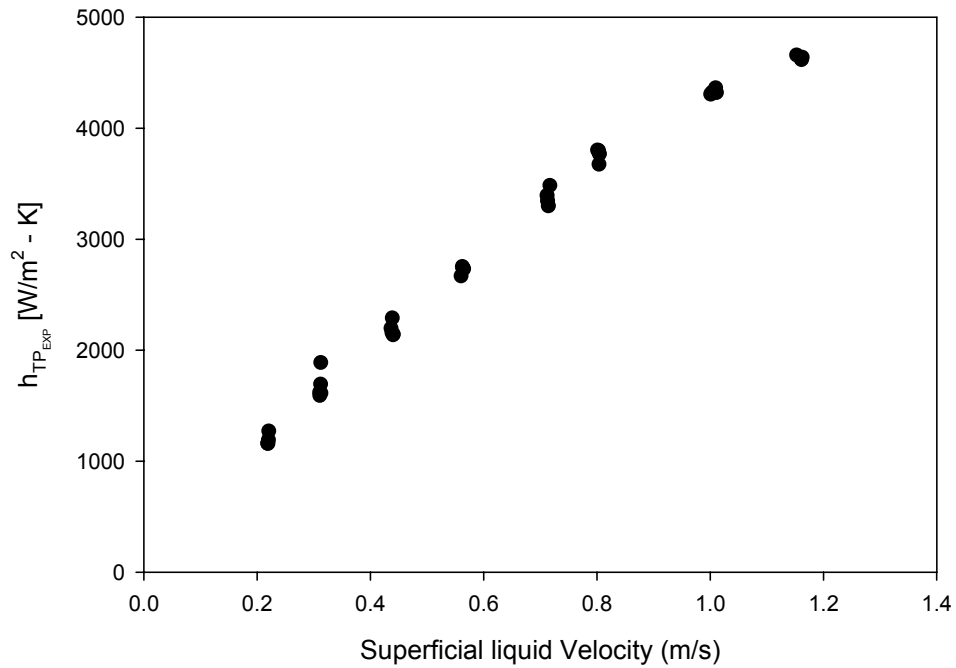


Figure 4.26 Variation of the overall mean heat transfer coefficient with the increase of superficial liquid velocity (m/s) for five degree data

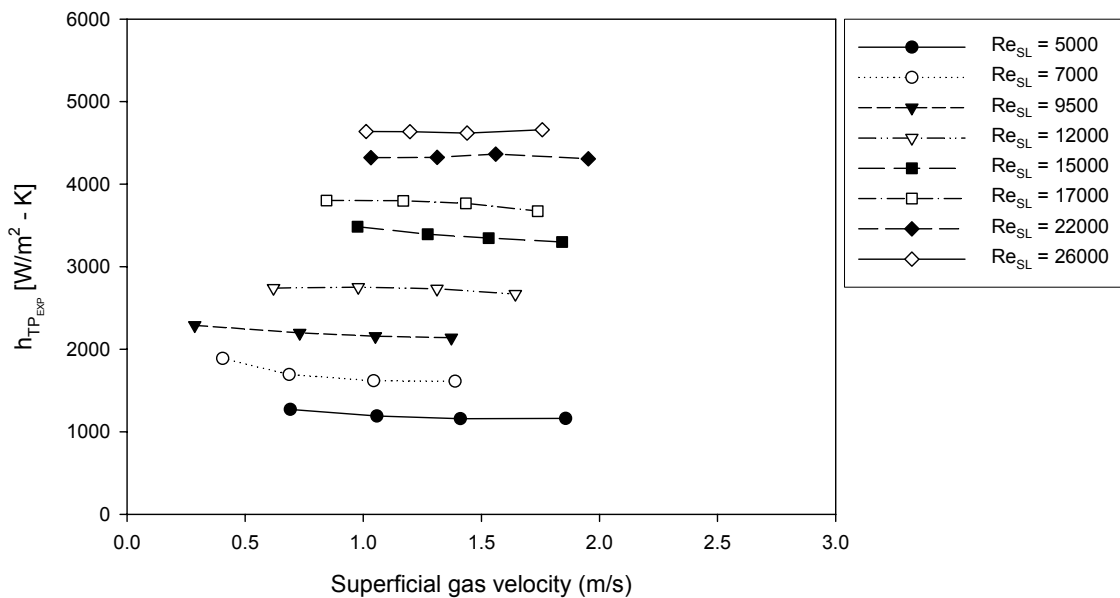


Figure 4.27 Variation of the overall mean heat transfer coefficient with the increase of superficial gas velocity (m/s) for five degree data

Figure 4.28 shows the variation of superficial gas Reynolds number with the superficial liquid Froude number.

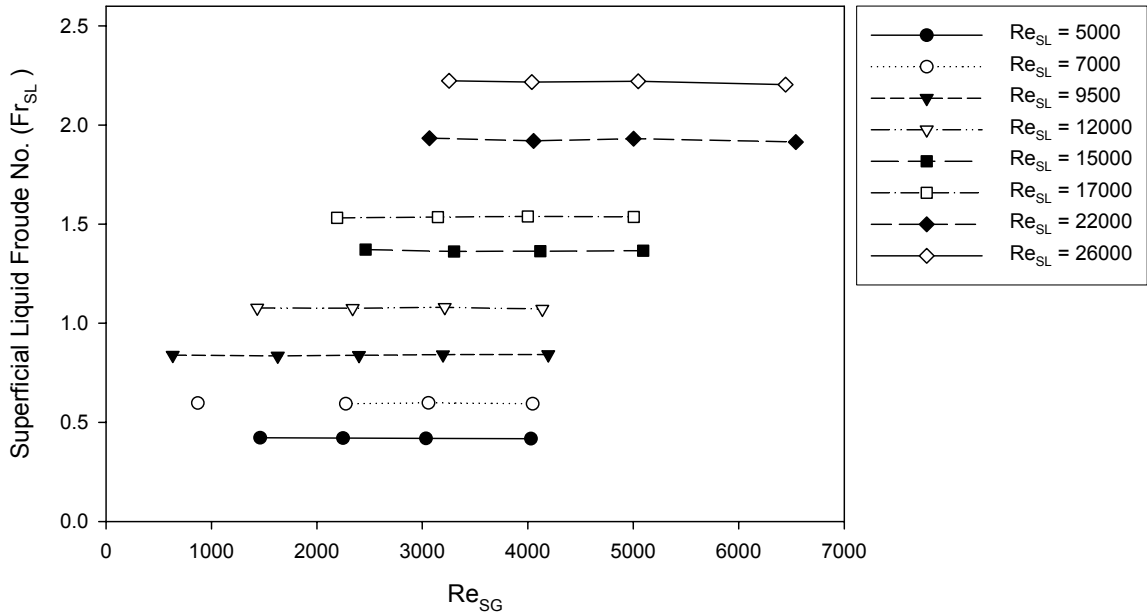


Figure 4.28 Variation of the superficial liquid Froude number with the increase of superficial gas Reynolds number for five degree data

Comparing Figures 4.25, 4.27 and 4.28, we observe similar trends for overall mean heat transfer coefficient and superficial liquid Froude number with the variation of superficial gas velocity and Reynolds number. It is noted that each superficial liquid Reynolds number series shows its own specific trend with the variation of superficial gas Reynolds number.

Using flow visualization, Figures 4.29 (a) [$Re_{SL}=5000$, $Re_{SG}=1500$], 4.29(b) [$Re_{SL}=5000$, $Re_{SG}=3000$] and 4.29(c) [$Re_{SL}=5000$, $Re_{SG}=5000$] show the selected flow

visualization pictures recorded for the five degree tube position for $Re_{SL}=5000$ series to explain the heat transfer phenomenon.

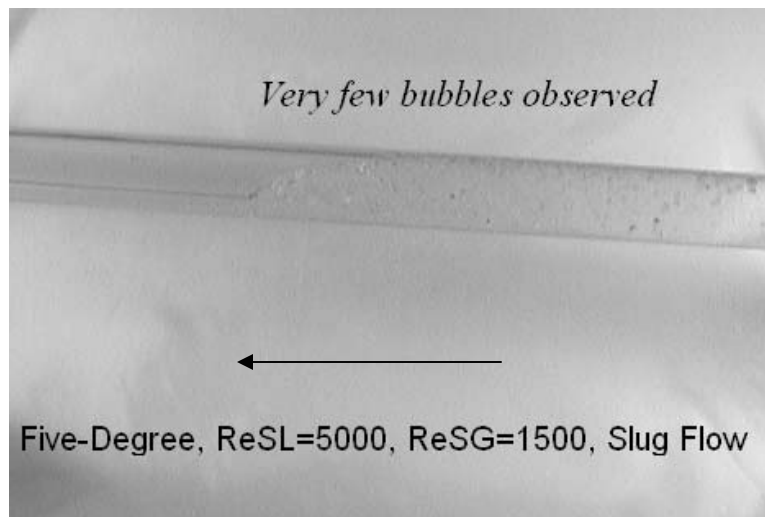


Figure 4.29(a) 5 Degree, $Re_{SL}=5000$, $Re_{SG}=1500$ (Slug flow)

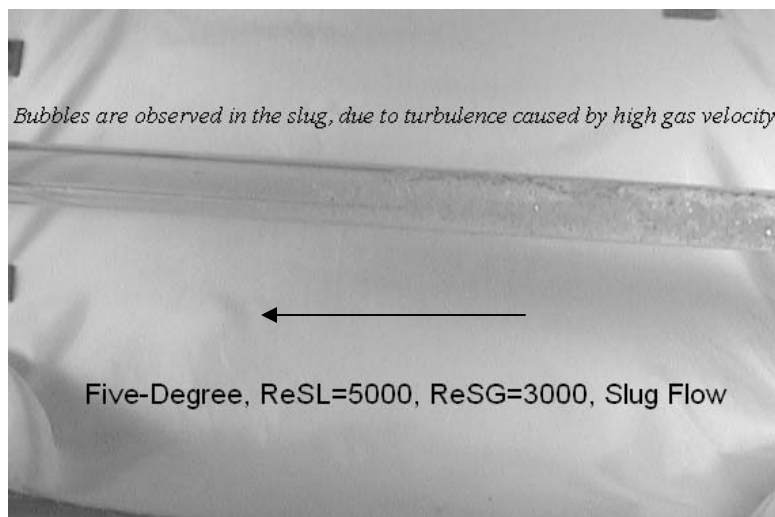


Figure 4.29(b) 5 Degree, $Re_{SL}=5000$, $Re_{SG}=3000$ (Slug flow)

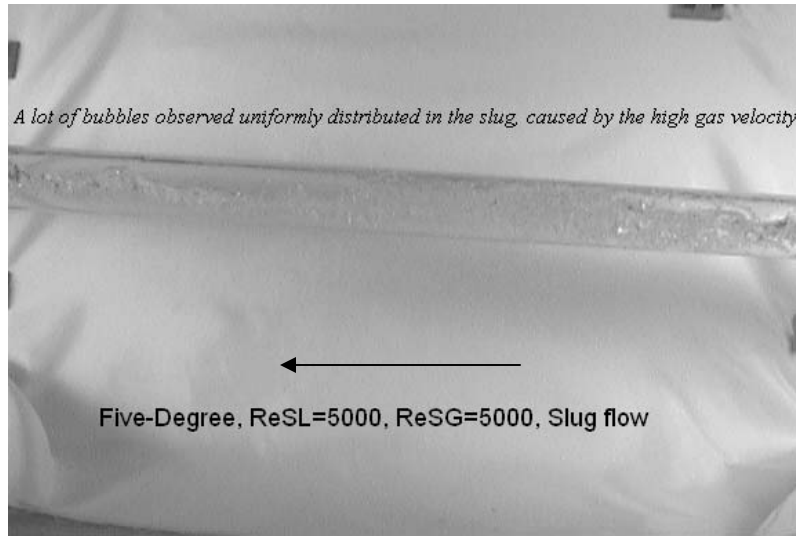
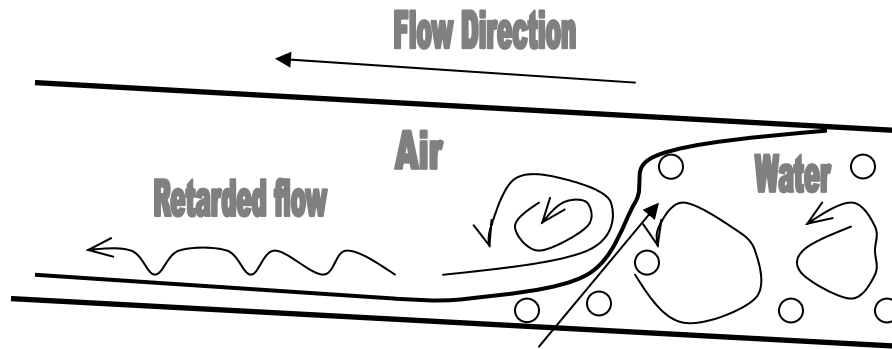


Figure 4.29(c) 5 Degree, $Re_{SL}=5000$, $Re_{SG}=5000$ (Slug flow)

We observe from Figure 4.29(a), a normal slug flow pattern with some formation of bubbles. These formations of bubbles results from the fact that there is a retarded flow observed in this five degree tube inclination. The retarded flow causes turbulence with the oncoming fast slug and hence the formation of lots of bubbles. These bubbles are uniformly distributed in the slug, and hence impede the heat transfer characteristics of the slug flow pattern. Figures 4.29(b) and 4.29(c) show an increase of bubbles in the slug flow with the increase in superficial gas velocity. Figure 4.30 shows a schematic of what was observed in Figures 4.29 (a to c). The schematic explains the physics of the retarded flow characteristics.



Retarded flow causes resistance, hence turbulence & better mixing, it also results in small formation of bubbles

Figure 4.30 Retarded flow effects on heat transfer characteristics in inclined tube position

Analysis of retarded flow and its effect on heat transfer characteristics has been discussed in Section 4.1.4, when a comparative study is done for various Re_{SL} series at the tube inclinations under this study. We shall limit our discussion on the basics in this section.

Similar observations were recorded in this tube inclination position to what we observed in horizontal and two degree tube inclination. Liquid phase plays a dominant role in the heat transfer analysis, but the effect of gas phase results in the change of flow appearance, which in turn results in the change of heat transfer of the slug. Hence gas phase effect cannot be neglected.

Extra controlled runs were carried out to investigate the effect of superficial gas Reynolds number on the overall mean heat transfer coefficient for other flow patterns for this five degree tube inclination. Figure 4.31 shows the variation of overall mean heat transfer coefficients of five degree flow over superficial gas Reynolds numbers with fixed superficial liquid Reynolds number.

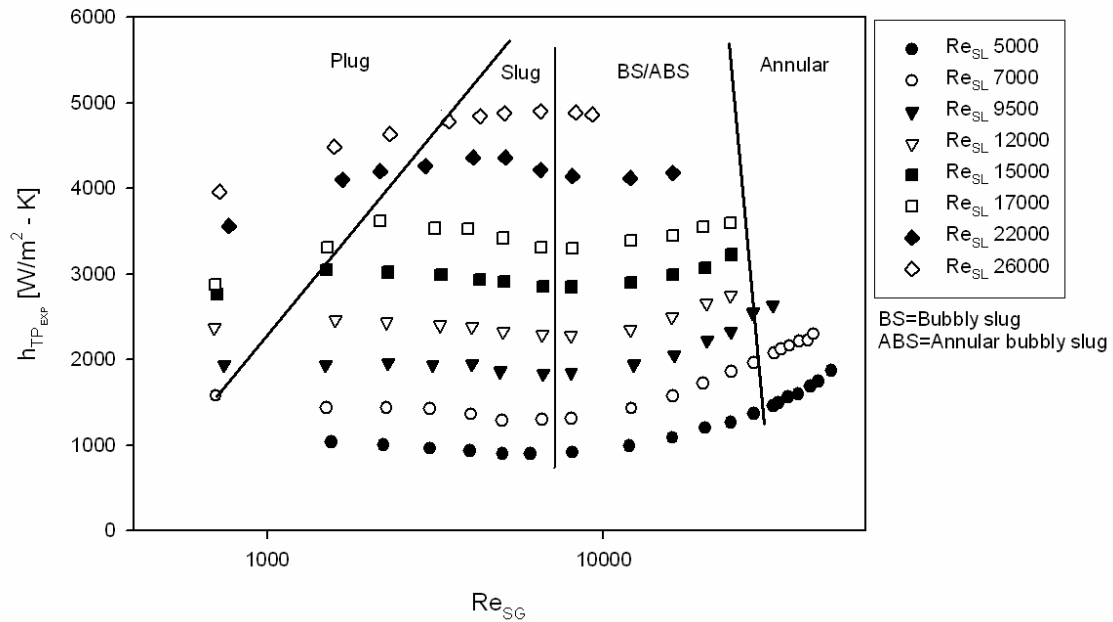


Figure 4.31 Variation of overall mean heat transfer coefficients of five degree inclined flow over superficial gas Reynolds numbers with fixed superficial liquid Reynolds number

It is observed that the overall mean heat transfer coefficient is dependent on the superficial gas Reynolds number which shows its own trend for different flow patterns. For the slug transitional flow pattern and the annular flow pattern, the overall mean heat transfer coefficient increases with the increase of superficial gas Reynolds number for fixed superficial liquid Reynolds number. However, from Figure 4.25, the slug flow pattern shows a slight decrease in overall mean heat transfer coefficient with the increase of superficial gas Reynolds number.

The combined effect of superficial liquid and superficial gas Reynolds numbers on the overall mean heat transfer characteristics can be better analyzed by the three-dimensional plot with superficial liquid Reynolds number on its abscissa, superficial gas

Reynolds number on its ordinate and the overall mean heat transfer coefficient on the “z” axis. The graph can be seen in Figure 4.32.

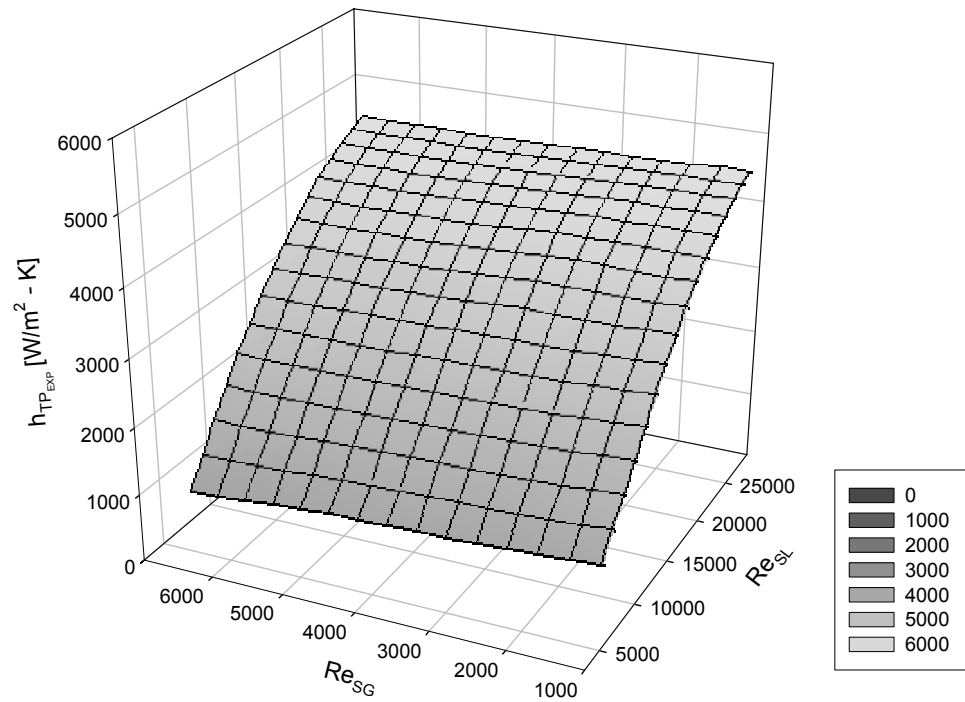


Figure 4.32 Variation of overall mean heat transfer coefficient with the increase of Re_{SL} and Re_{SG} for five degree data

Trimble *et al* (2002), collected many slug flow data points, below is trend of heat transfer behavior observed by him for his five degree slug flow data points.

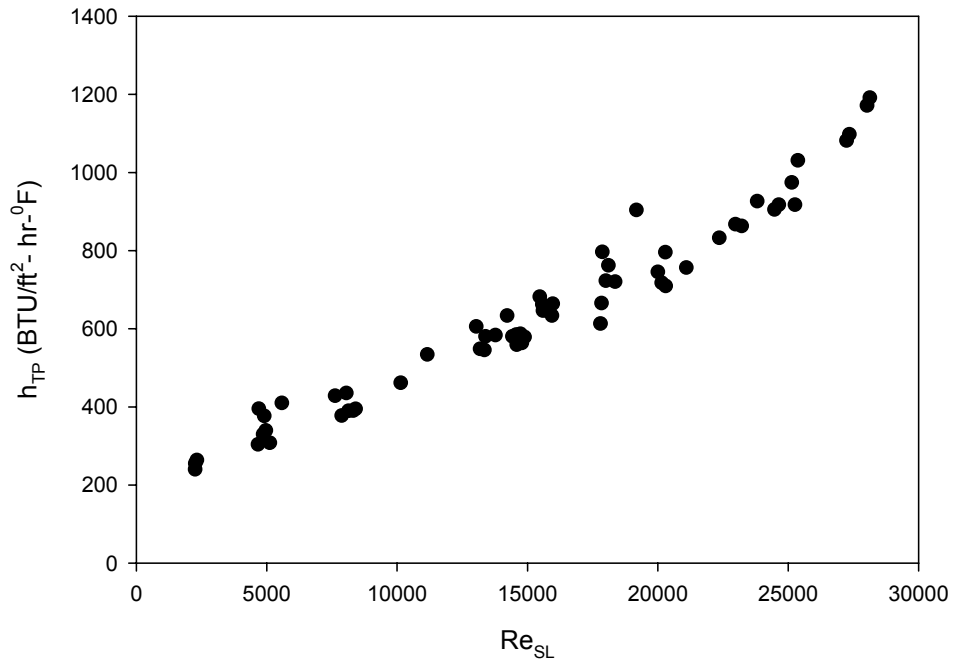


Figure 4.33 Two-phase heat transfer coefficient as a function of Re_{SL} for five degree data (Trimble *et al* 2002)

The observations made by Trimble *et al* (2002) are similar to the observations recorded in this study.

4.1.5 Seven Degree Data

In this study a total of 34 controlled slug flow data points have been analyzed. The superficial liquid and gas Reynolds numbers are matched closely (98% of the data points are within $\pm 5\%$ deviation range) with the slug flow horizontal, two degree and five degree data points and all other parameters are kept the same, so that the effect of inclination on overall mean heat transfer heat coefficient can be analyzed systematically. The data points were taken by carefully coordinating the superficial liquid and superficial gas Reynolds numbers. Each test run is characterized by its specific superficial gas and liquid Reynolds numbers.

Table 4.4 gives the complete summary of the runs made in the seven degree tube inclination, stating their run numbers, superficial gas and liquid Reynolds numbers, mass flow rates of gas and liquid, their corresponding heat flux (including current and voltage), the overall mean two-phase heat transfer coefficient and corresponding superficial liquid Froude numbers obtained for each run.

The superficial liquid Reynolds numbers ranged from a minimum of 5042 to a maximum of 26043 (water mass flow rates varied from 7.88 kg/min to 38.84 kg/min) and superficial gas Reynolds numbers varied from a minimum of 634 to a maximum of 6484 (gas mass flow rates varied from 0.0148 kg/min to 0.1523 kg/min). The uniform heat flux ranged from 2734 W/m² to 8505 W/m² and the resulting overall heat transfer coefficients ranged from 1169 W/m²-K to 4907 W/m²-K.

Table 4.4 Heat transfer results for the seven degree tube inclination

Run #	Gas Mass Flow Rate (Kg/s)	Re _{SG}	Liquid Mass Flow Rate (Kg/s)	Re _{SL}	Heat Flux [W/m ²]	Current [A]	Voltage [V]	Avg. h _{tp} [W/m ² -K]	Superficial Liquid Froude No (Fr _{SL})
4821	0.00060	1544	0.13230	5068	2788	291.3	2.21	1276	0.4149
4822	0.00083	2143	0.13225	5066	2762	289.9	2.20	1190	0.4148
4823	0.00119	3042	0.13162	5042	2746	289.1	2.20	1169	0.4128
4824	0.00157	4025	0.13134	5048	2734	288.4	2.19	1193	0.4119
4840	0.00026	674	0.17993	7086	5736	417.5	3.18	1886	0.5643
4841	0.00057	1453	0.17968	7079	5756	418.1	3.18	1695	0.5636
4842	0.00088	2243	0.17904	7053	5669	414.9	3.16	1561	0.5615
4843	0.00119	3036	0.18035	7103	5746	417.7	3.18	1557	0.5657
4844	0.00157	4007	0.17954	7060	5691	415.7	3.17	1567	0.5631
4859	0.00025	634	0.24113	9563	6782	453.9	3.45	2280	0.7563
4860	0.00055	1400	0.24049	9559	7041	462.5	3.52	2164	0.7543
4861	0.00093	2379	0.24104	9585	7036	462.3	3.52	2043	0.7561
4862	0.00121	3088	0.23984	9545	7043	462.5	3.52	1997	0.7523
4863	0.00161	4103	0.24088	9598	6872	456.8	3.48	1987	0.7555
4864	0.00161	4123	0.24070	9597	6868	456.7	3.48	1981	0.7550
4875	0.00054	1372	0.30248	12033	7026	462.1	3.52	2559	0.9488
4876	0.00085	2173	0.30283	12039	6940	459.3	3.49	2483	0.9499
4877	0.00128	3284	0.30292	12038	6896	457.8	3.48	2414	0.9501
4878	0.00170	4338	0.30432	12095	7078	463.8	3.53	2387	0.9545
4888	0.00091	2338	0.37849	15028	7054	463.2	3.52	3040	1.1872
4889	0.00116	2960	0.37908	15040	7004	461.6	3.51	3003	1.1890
4890	0.00162	4150	0.37912	15025	7183	467.4	3.55	2943	1.1891
4891	0.00201	5138	0.37653	14915	7115	465.2	3.54	2870	1.1810
4900	0.00091	2320	0.42515	16990	7841	488.3	3.71	3396	1.3336
4901	0.00122	3112	0.42488	16873	7970	492.4	3.74	3344	1.3327
4902	0.00161	4109	0.42687	16938	8012	493.6	3.75	3301	1.3389
4903	0.00199	5096	0.42633	16930	8280	501.8	3.82	3251	1.3372
4913	0.00122	3119	0.55386	21954	8329	503.5	3.82	4266	1.7372
4914	0.00161	4119	0.54589	22020	8319	503.1	3.82	4277	1.7124
4915	0.00200	5105	0.54263	21896	8505	508.6	3.87	4218	1.7021
4922	0.00116	2968	0.64473	25910	8230	500.4	3.80	4874	2.0224
4923	0.00156	3990	0.64737	26043	8399	505.5	3.84	4907	2.0307
4924	0.00200	5113	0.64156	25816	8383	505.0	3.84	4862	2.0124
4925	0.00254	6484	0.64333	25915	8381	504.9	3.84	4841	2.0180

Figures 4.34 and 4.35 show the variation of the overall mean heat transfer coefficient with the increase of superficial liquid and gas Reynolds number for the coordinated slug flow data (34 data points).

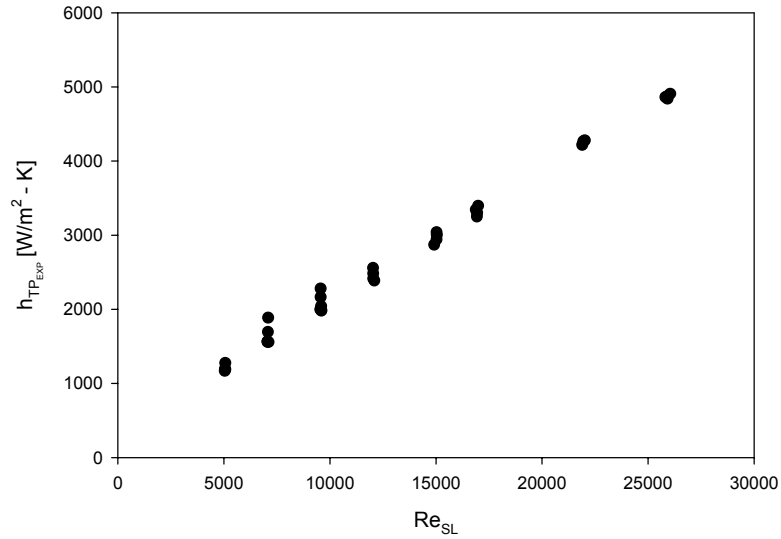


Figure 4.34 Variation of the overall mean heat transfer coefficient with the increase of superficial liquid Reynolds number for the coordinated seven degree slug flow data (34 data points)

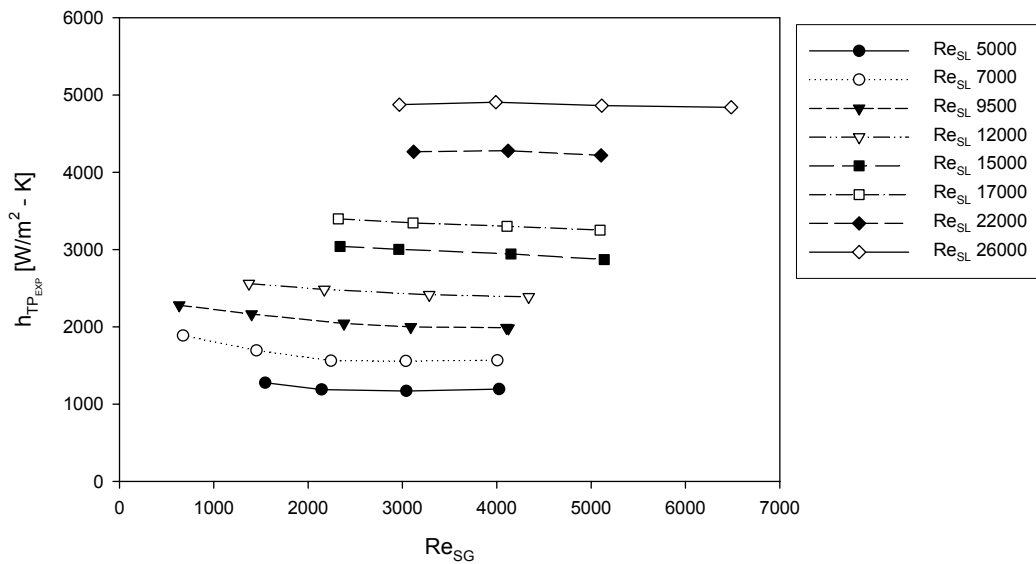


Figure 4.35 Variation of the overall mean heat transfer coefficient with the increase of superficial gas Reynolds number for the coordinated seven degree slug flow data (34 data points)

Figures 4.36 and 4.37, we have analyzed the variation of overall mean heat transfer coefficient with the increase of superficial liquid velocity and superficial gas velocity.

From Figures 4.34 and 4.36, we observe that the liquid phase being a dominant factor in slug flow heat transfer for the seven degree tube inclination. Analyzing Figures 4.35 and 4.37, we also observe that the gas phase affects the overall mean heat transfer coefficient slightly, and follows the same systematic trend for different superficial liquid Reynolds numbers and gas velocities. Hence, the effect of gas phase cannot be neglected.

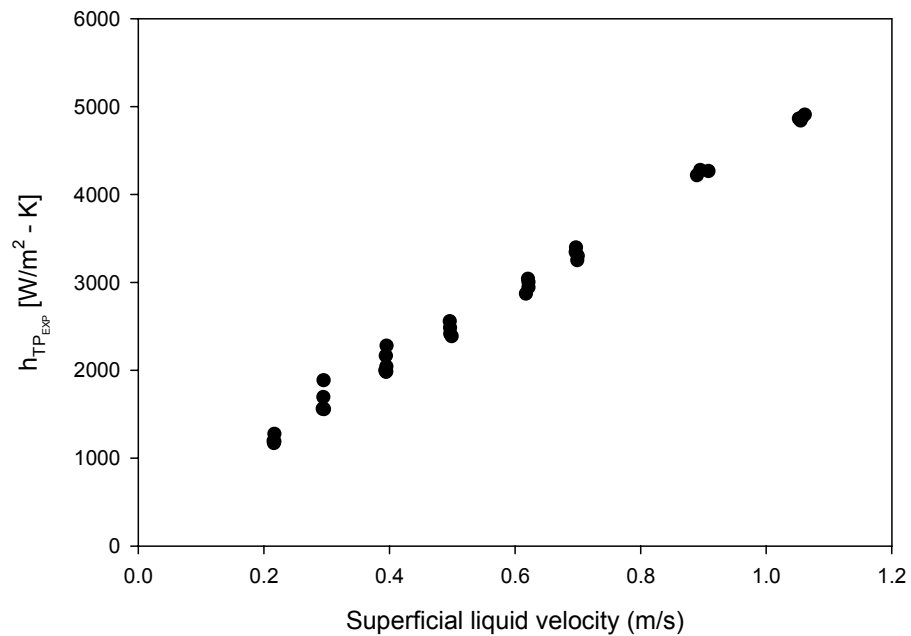


Figure 4.36 Variation of the overall mean heat transfer coefficient with the increase of superficial liquid velocity (m/s) for seven degree data

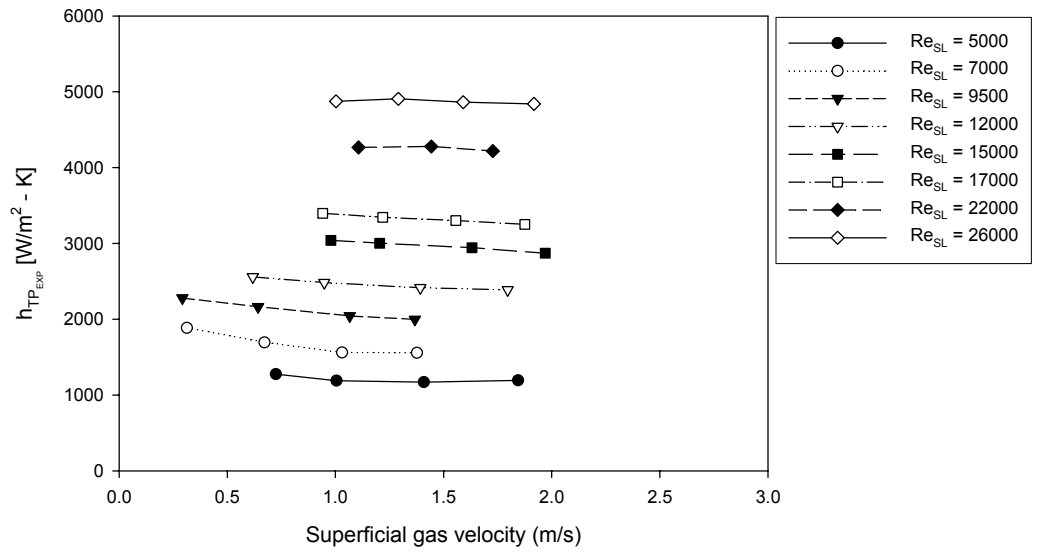


Figure 4.37 Variation of the overall mean heat transfer coefficient with the increase of superficial gas velocity (m/s) for seven degree data

Figure 4.38 shows the variation of superficial gas Reynolds number with the superficial liquid Froude number.

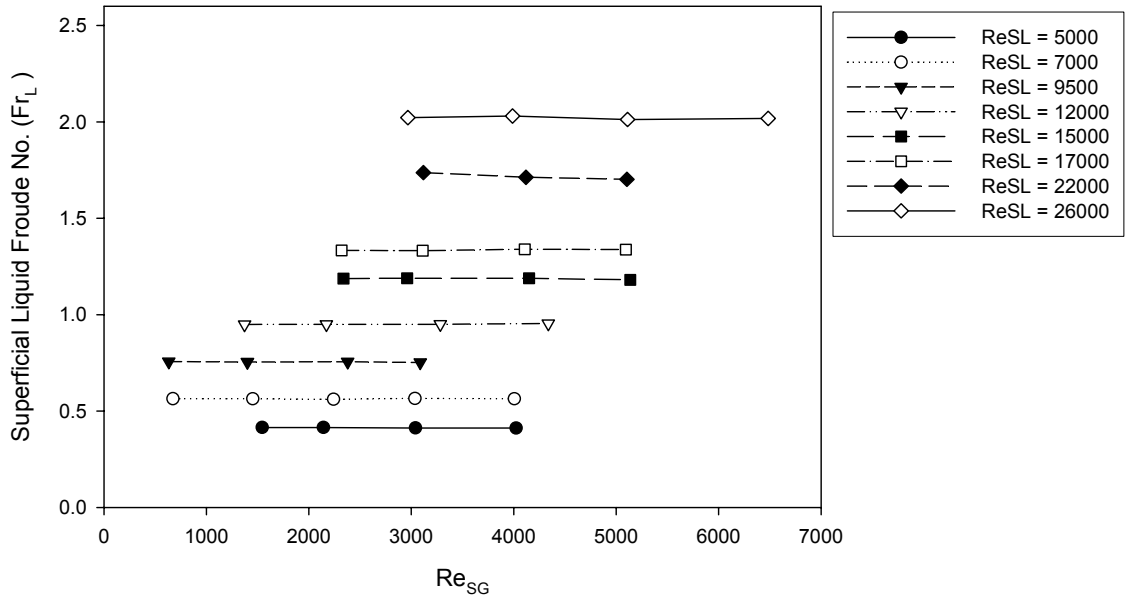


Figure 4.38 Variation of the superficial liquid Froude number with the increase of superficial gas Reynolds number for seven degree data

Comparing Figures 4.35, 4.37 and 4.38, we observe similar trends for overall mean heat transfer coefficient and superficial liquid Froude number with the variation of superficial gas velocity and Reynolds number. It is noted that each superficial liquid Reynolds number series shows its own specific trend with the variation of superficial gas Reynolds number.

Using flow visualization, Figures 4.39 (a) [$Re_{SL}=5000, Re_{SG}=1500$], 4.39(b) [$Re_{SL}=5000, Re_{SG}=3000$] and 4.39(c) [$Re_{SL}=5000, Re_{SG}=5000$] show the selected flow visualization pictures recorded for the seven degree tube position for $Re_{SL}=5000$ series to explain the heat transfer phenomenon.

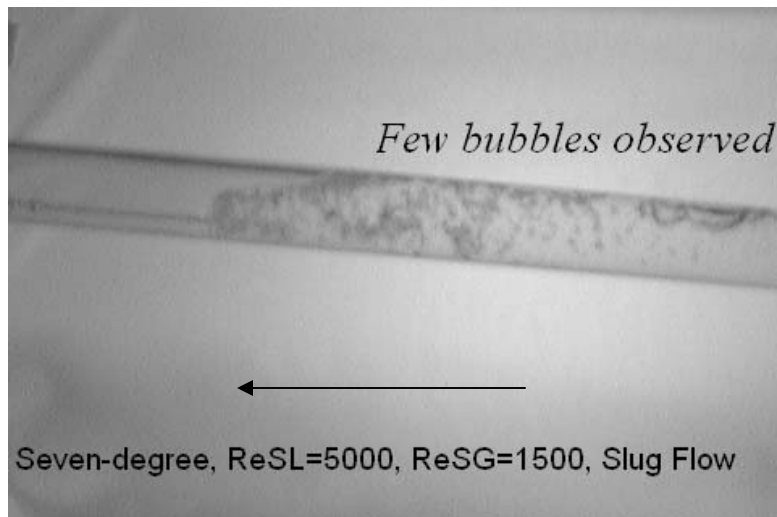


Figure 4.39(a) 7 Degree, $Re_{SL}=5000$, $Re_{SG}=1500$ (Slug flow)

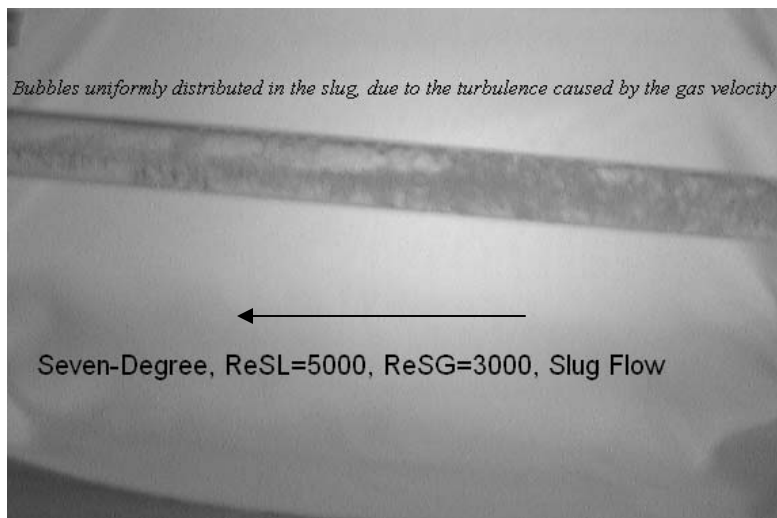


Figure 4.39(b) 7 Degree, $Re_{SL}=5000$, $Re_{SG}=3000$ (Slug flow)

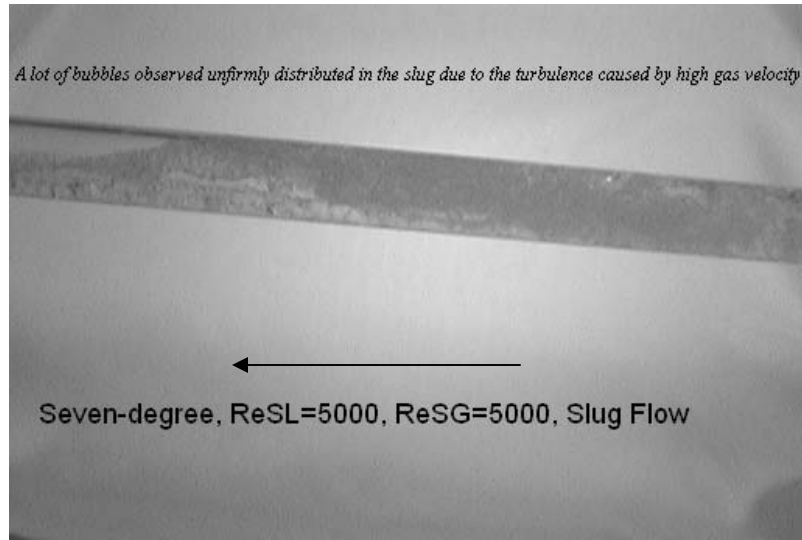


Figure 4.39(c) 7 Degree, $Re_{SL}=5000$, $Re_{SG}=5000$ (Slug flow)

We observe from Figure 4.39(a), a normal slug flow pattern with some formation of bubbles. These formations of bubbles results from the fact that there is a retarded flow observed in this seven degree tube inclination. The retarded flow causes rigorous turbulence with the oncoming fast slug and hence the formation of lots of bubbles. These bubbles are uniformly distributed in the slug, and hence impede the heat transfer characteristics of the slug flow pattern. Figures 4.39(b) and 4.39(c) show an increase of bubbles in the slug flow with the increase in superficial gas velocity. The schematic shown in Figure 4.30 of section 4.1.4 explains the physics of the retarded flow characteristics.

Analysis of back flow and its effect on heat transfer characteristics has been discussed in Section 4.1.3, when a comparative study is done for various Re_{SL} series at the tube inclinations under this study. We shall limit our discussion on the basics in this section.

Similar observations were recorded in this tube inclination position to what we observed in horizontal, two degree and five degree tube inclination. Liquid phase plays a dominant role in the heat transfer analysis, but the effect of gas phase results in the change of flow appearance, which in turn results in the change of heat transfer of the slug. Hence gas phase effect cannot be neglected.

Extra controlled runs were carried out to investigate the effect of superficial gas Reynolds number on the overall mean heat transfer coefficient for other flow patterns for this seven degree tube inclination. Figure 4.40 shows the variation of overall mean heat transfer coefficients of seven degree flow over superficial gas Reynolds numbers with fixed superficial liquid Reynolds number.

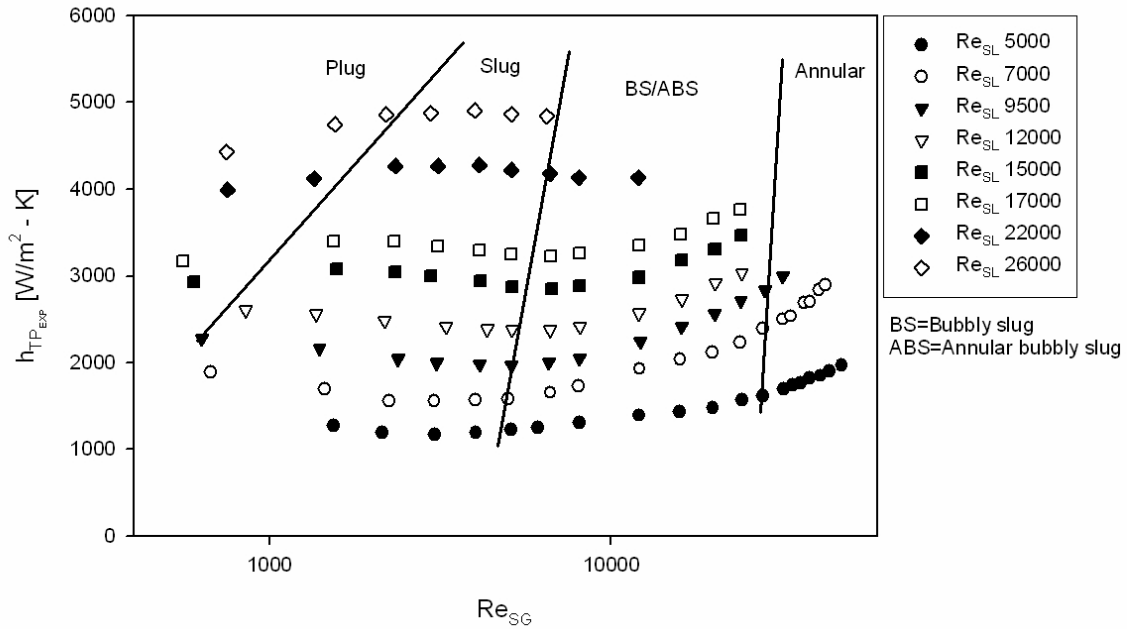


Figure 4.40 Variation of overall mean heat transfer coefficients of seven degree inclined flow over superficial gas Reynolds numbers with fixed superficial liquid Reynolds number

It is observed that the overall mean heat transfer coefficient is dependent on the superficial gas Reynolds number which shows its own trend for different flow patterns. For the slug transitional flow pattern and the annular flow pattern, the overall mean heat transfer coefficient increases with the increase of superficial gas Reynolds number for fixed superficial liquid Reynolds number. However, from Figure 4.35, the slug flow pattern shows a slight decrease in overall mean heat transfer coefficient with the increase of superficial gas Reynolds number.

The combined effect of superficial liquid and superficial gas Reynolds numbers on the overall mean heat transfer characteristics can be better analyzed by the three-dimensional plot with superficial liquid Reynolds number on its abscissa, superficial gas Reynolds number on its ordinate and the overall mean heat transfer coefficient on the “z” axis. The graph can be seen in Figure 4.41.

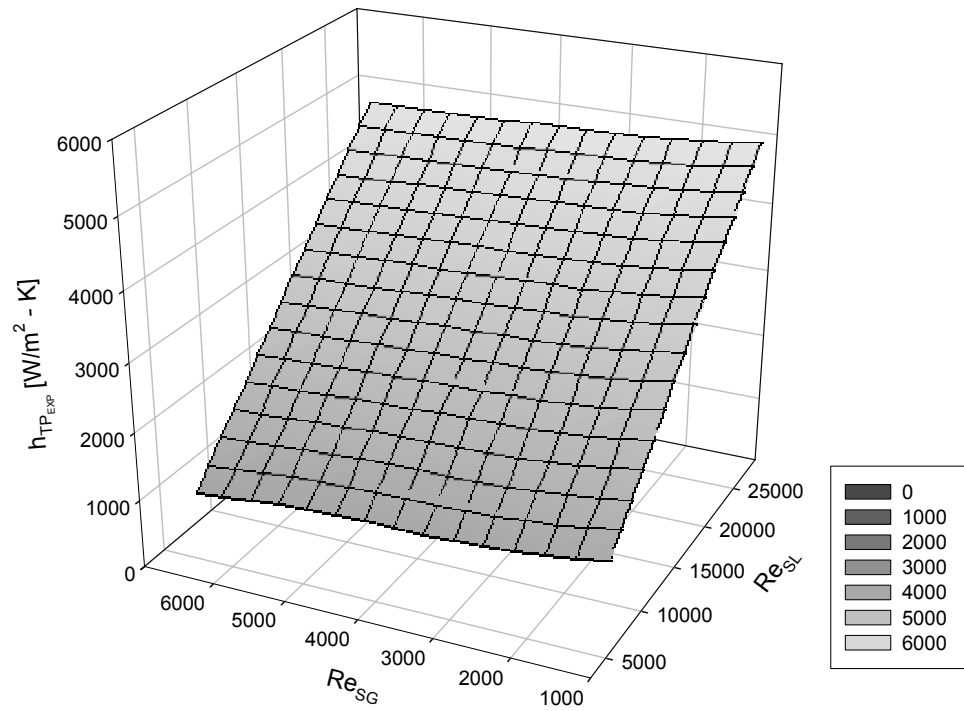


Figure 4.41 Variation of overall mean heat transfer coefficient with the increase of Re_{SL} and Re_{SG} for seven degree data

After observing the heat transfer behavior at individual tube inclination, we shall now build on our analysis by comparing the heat transfer behavior from one tube inclination to the other. We shall carry on a detailed analysis, so as to find an explanation to the intricacies of the slug flow heat transfer behavior.

4.2 Comparison of Slug Flow Data at Different Tube Inclinations

The data for all the four tube inclinations in this study have been recorded and matched in a systematic coordinated way, so that the slug flow heat transfer characteristics could be better understood.

Slug flow shows an average increase of overall mean heat transfer coefficient from horizontal to two degree, five degree and seven degree. Similarly, there is an increase of overall mean heat transfer coefficient from two degree to five degree and seven degree. However, a different heat transfer behavior is observed when the tube is inclined from five degree to seven degree. Table 4.5 below shows the change of overall mean heat transfer coefficient for various tube inclinations for the slug flow.

Table 4.5 Average change of h_{TP} for various tube Inclinations

Index	Description	0 & 2 Degree	0 & 5 Degree	0 & 7 Degree	2 & 5 Degree	2 & 7 Degree	5 & 7 Degree
1	Average Δh_{TP} (%)	18	25	20	9	4	-6
2	Max Δh_{TP} (%)	32	44	46	29	22	6
3	Min Δh_{TP} (%)	3	-1	3	-6	-7	-15

It is observed that five degree is a limiting case for the enhancement of overall mean heat transfer coefficient for slug flow pattern. When five degree tube inclination data is compared to seven degree tube inclination, we observe that for low Re_{SL} values ($5000 \leq Re_{SL} \leq 7000$), there is no substantial increase in the overall mean heat transfer coefficient, but for medium range Re_{SL} values ($9500 \leq Re_{SL} \leq 17000$), we see a decrease in the overall mean heat transfer coefficient. While at high Re_{SL} values

($22000 \leq Re_{SL} \leq 26000$), we again observe no substantial change of the overall mean heat transfer coefficient.

To analyze the complex behavior of the slug flow heat transfer characteristics, for various tube inclinations, we have used flow visualization as a tool, to capture the intricate details of all flow patterns. A 30 sec film was made for all the runs recorded for slug flow pattern used in this research. We used Adobe Premiere Pro v 7.0 to analyze the videos, in which the films were observed at an increment of 0.031 sec in piece-wise photographic form. Intricate details like the shape of the slug, formation of bubbles, back flow characteristics were carefully recorded from one photographic slide to the other.

In our analysis we have used photographic films recorded at an increment of 0.3 sec, since this time increment was deemed appropriate for the representation of slug flow characteristics. The explanation of overall mean heat transfer coefficient for slug flow heat transfer characteristics using flow visualization photographs have been restricted to three important Re_{SL} cases, i.e, low $Re_{SL} = 5000$, medium $Re_{SL} = 15000$ and high $Re_{SL} = 26000$. This approach has been adopted because these superficial Reynolds numbers encompass all the intricacies of slug flow behavior and provide explanation to all heat transfer behavior for various tube inclinations. Providing explanation using more Re_{SL} numbers will be mere repetition.

4.2.1 Low Re_{SL} Analysis ($5000 \leq Re_{SL} \leq 7000$)

Test Case Discussed ($Re_{SL}=5000$ $Re_{SG}=1500$)

Figure 4.42 shows the overall mean heat transfer coefficient behavior for horizontal, two degree, five degree and seven degree with respect to varying superficial gas Reynolds numbers. It is observed that there is an increase of overall mean heat transfer behavior for two degree, five degree when compared to the horizontal, while there is no significant enhancement in the overall mean heat transfer observed for tube inclination from five degree to seven degree.

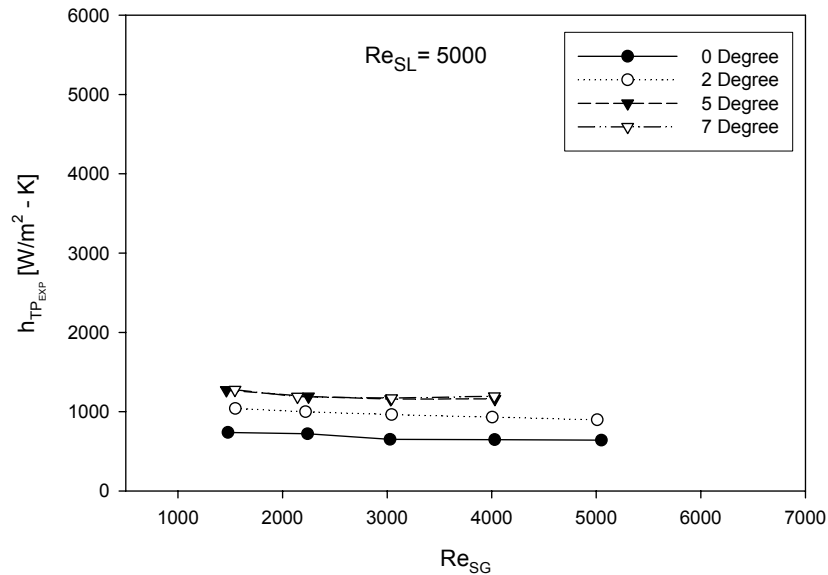


Figure 4.42: Variation of overall mean heat transfer coefficient for $Re_{SL}=5000$ series for varying Re_{SG} values

Figure 4.43 is the summary of the flow visualization photographic slides recorded for $Re_{SL}=5000$, $Re_{SG}=1500$ at a time increment of 0.3 sec for various tube inclinations.

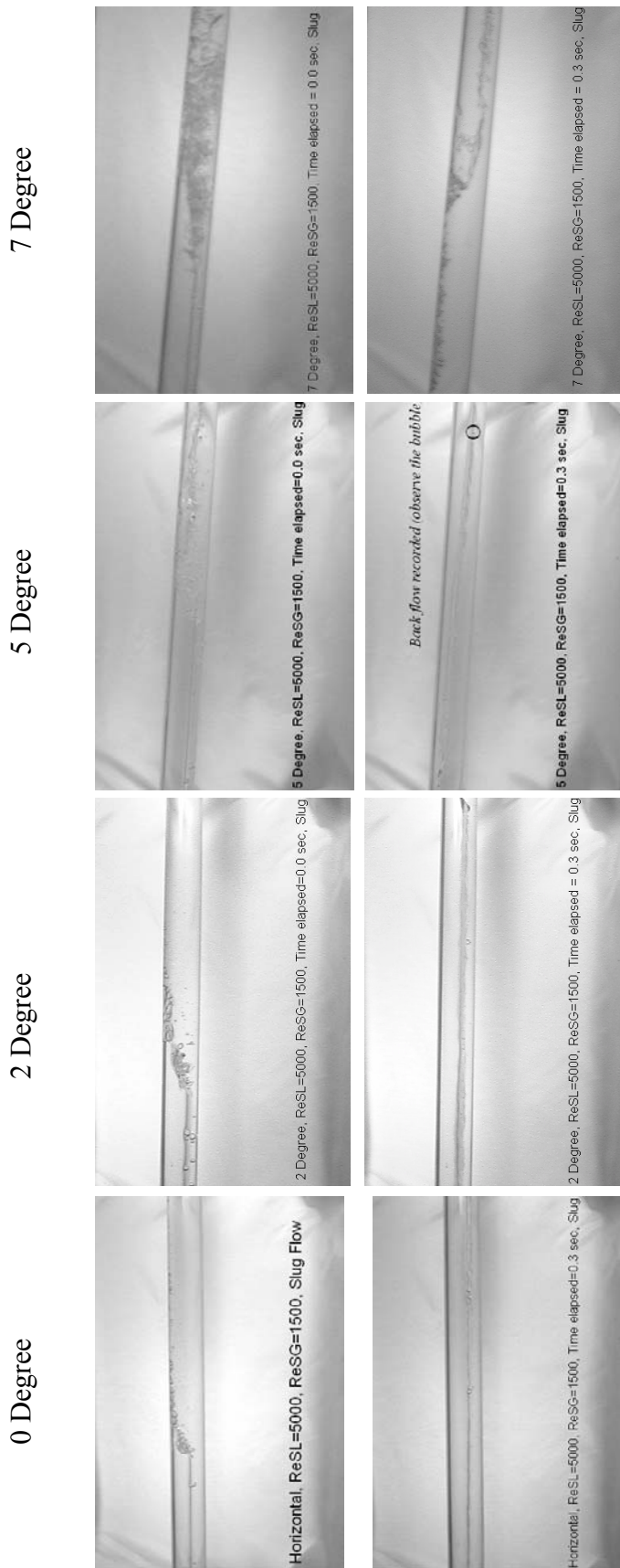
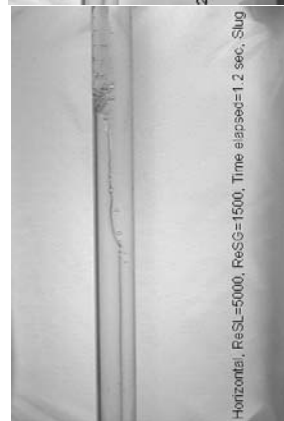
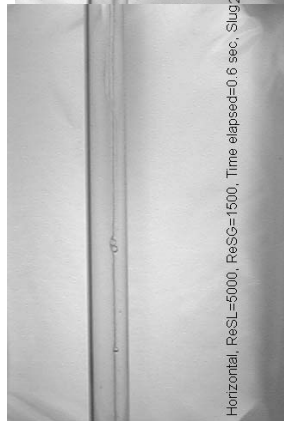
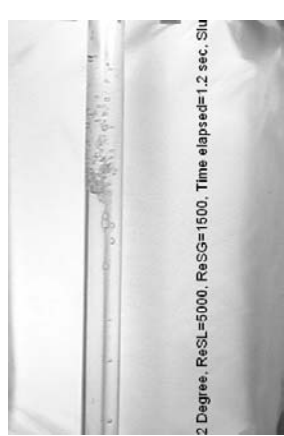


Figure 4.43 Visual observations ($Re_{SL} = 5000$, $Re_{SG} = 1500$, each snap recorded after 0.3 seconds)

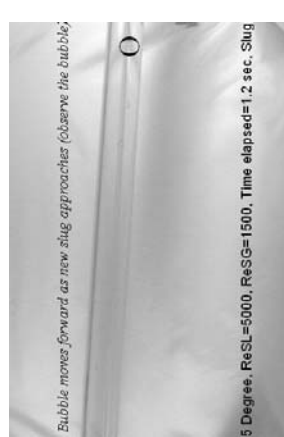
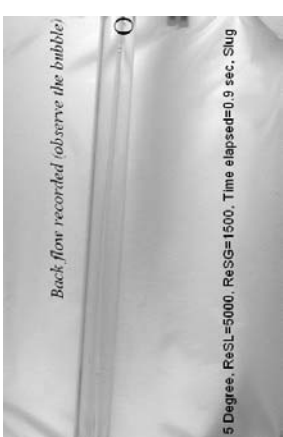
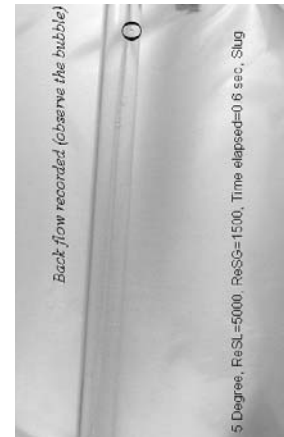
0 Degree



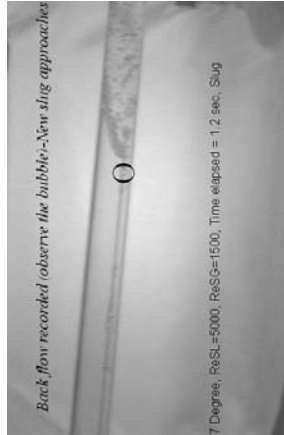
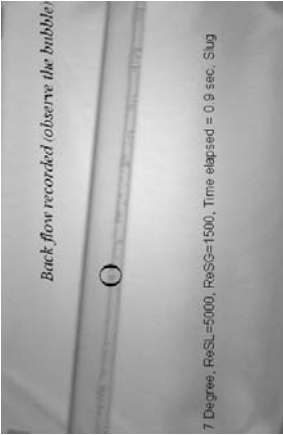
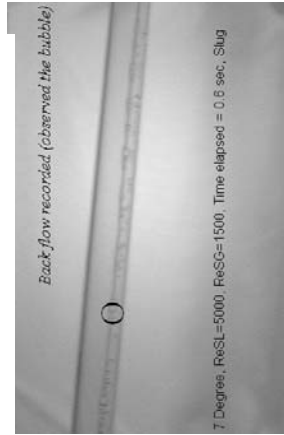
2 Degree



5 Degree



7 Degree



The standard inclination angle used for slug flow heat transfer comparison in this study is the horizontal position. Using the photographic slides for horizontal position, we note that no gravitational forces come into play for the horizontal slug flow, the flow pattern is fairly simple, with regular slugs flowing across the tube, no back flow or retarded flow is observed throughout the flow. Figure 4.44, depicts the horizontal slug flow pattern in simpler terms.

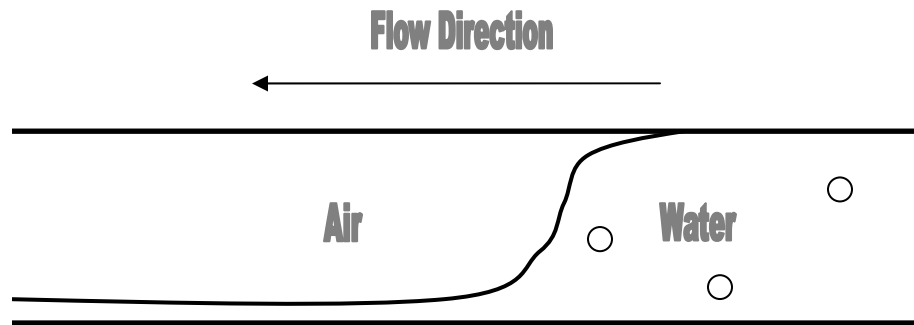


Figure 4.44: Horizontal slug flow pattern

When we move to two degree, five degree and seven degree tube inclinations, we observe an enhancement of heat transfer coefficient, compared to the horizontal tube inclination.

We observe a back flow for two degree tube inclination, this back flow occurs because of the gravitational pull, due to the tube inclination. The new slug which is formed is obstructed by this back flow (or we can say that the back flow causes resistance for this new slug), hence turbulence is caused, which results in better mixing, and thus

enhancement of heat transfer coefficient. Figure 4.20 in section 4.1.3 depicts the inherent physics of the mechanism, which is not visible through flow visualization photographs.

When we analyze the five degree and seven degree data, we observe that there is an enhancement of the overall mean heat transfer coefficient in both cases compared to the horizontal and two degree data. The reason for this is the retarded flow effect (retarded flow is clearly depicted in the flow visualization photographs, refer to Figure 4.43) which causes rigorous turbulence, hence higher heat transfer coefficient. Figure 4.30 in section 4.1.4 shows the inherent physics of how the retarded flow affects the heat transfer characteristics of slug flow.

Although, we observe that there is an enhancement of overall mean heat transfer coefficient until five degree, but we see no substantial enhancement in seven degree data when compared to five degree data. The reason for this being the fact, that when we reach seven degree tube inclination, the back flow causes rigorous turbulence and hence formation of lots of bubbles. These bubbles are uniformly distributed in the slug, and hence impede the heat transfer characteristics of the slug flow pattern.

The same has been presented using the flow visualization photographs depicted in Figure 4.43 (a and b). Figures 4.43 (a and b) are blown up versions of the particular slides shown in Figure 4.43.

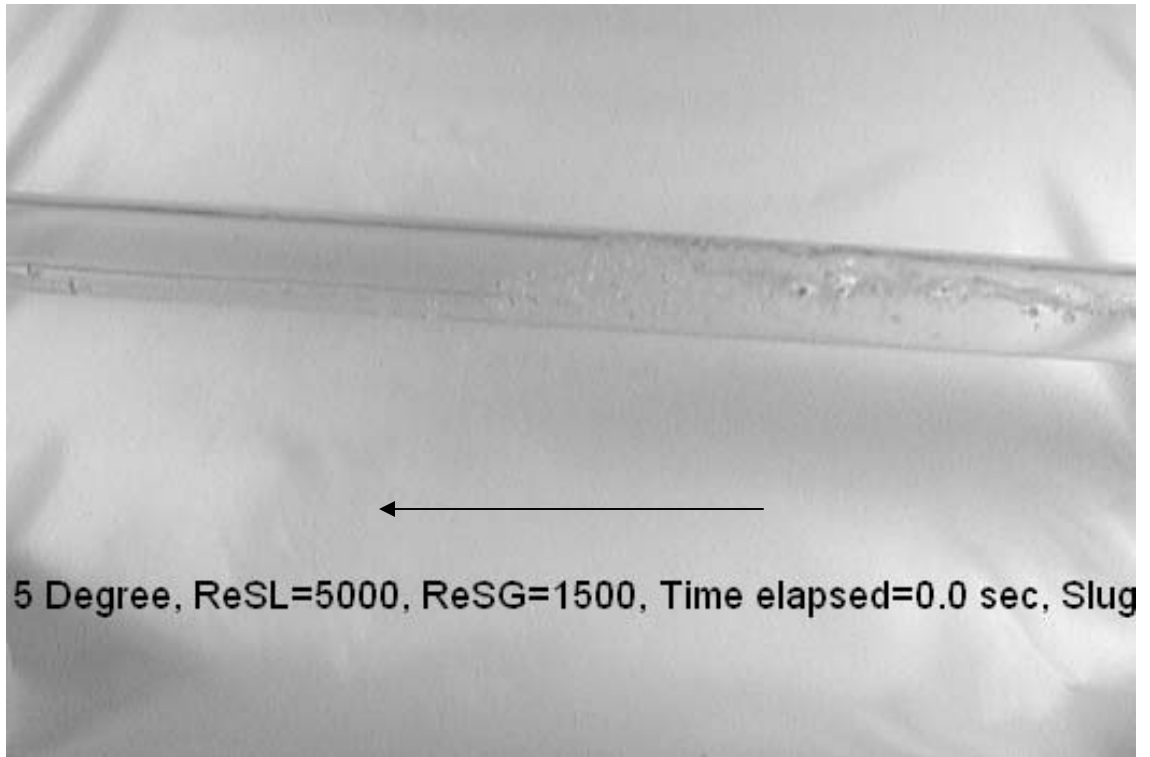


Figure 4.43 (a) – Five degree slug flow at time 0.0 sec ($Re_{SL}=5000$, $Re_{SG}=1500$)

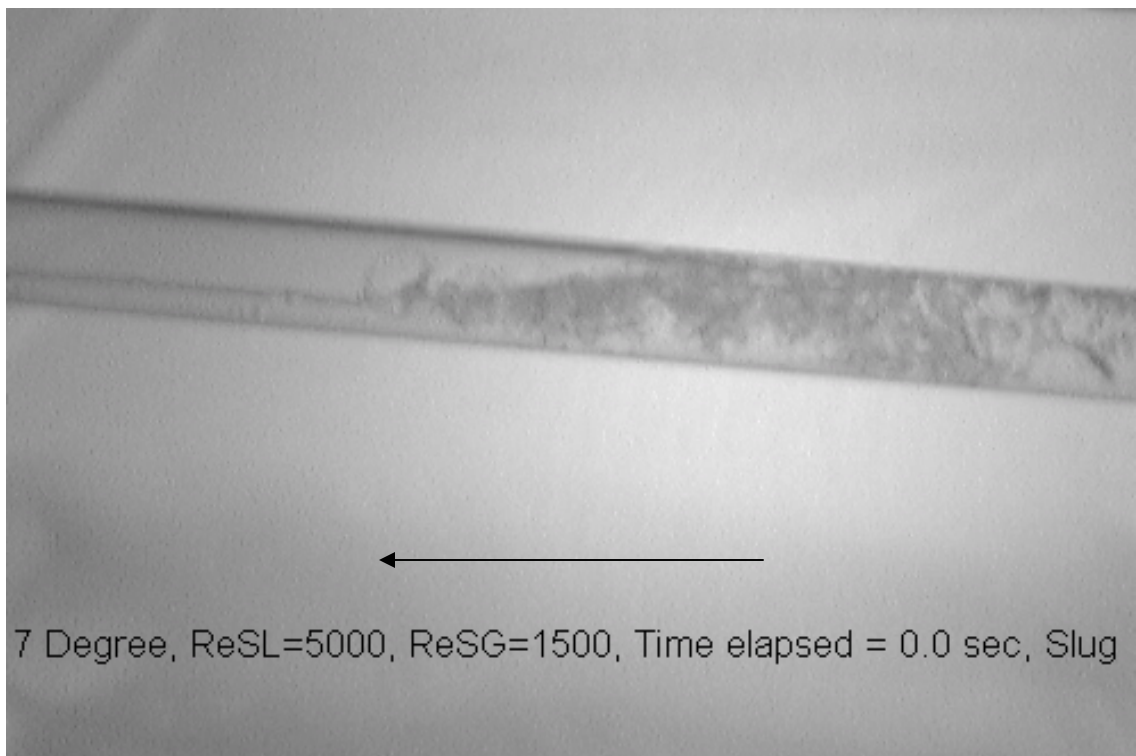


Figure 4.43 (b) – Seven degree slug flow at time 0.0 sec ($Re_{SL}=5000$, $Re_{SG}=1500$)

We can clearly observe from Figure 4.43 (b) that the uniform distribution of bubbles in the seven degree slug impede the heat transfer properties of the slug for this slug flow consideration compared to Figure 4.43(a).

We have further carried out our analysis using the superficial liquid Froude number and plotted its variation at different tube inclinations for various Re_{SL} series. Figure 4.45 shows the variation of superficial liquid Froude number with the variation of superficial gas Reynolds number for $Re_{SL} = 5000$ series.

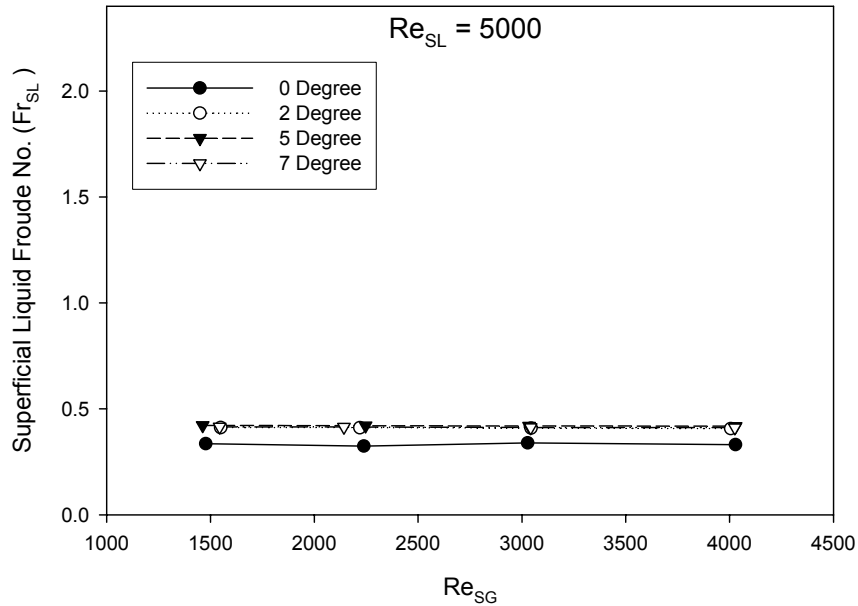


Figure 4.45 Variation of superficial liquid Froude number with the variation of superficial gas Reynolds number for $Re_{SL} = 5000$ series.

As stated earlier superficial liquid Froude number can be stated as a non-dimensional form of superficial liquid velocity. Comparing Figures 4.42 and 4.45, we observe similar trends with the variation of superficial gas Reynolds number. This shows

the dominance of superficial liquid velocity on the heat transfer characteristics of slug flow heat transfer behavior.

We can carry out similar analysis, to other low range Re_{SL} series. Figure 4.46 shows the overall mean heat transfer coefficient behavior for $Re_{SL} = 7000$ series with varying Re_{SG} and Figure 4.47 shows the variation of superficial liquid Froude number with varying superficial gas Reynolds number.

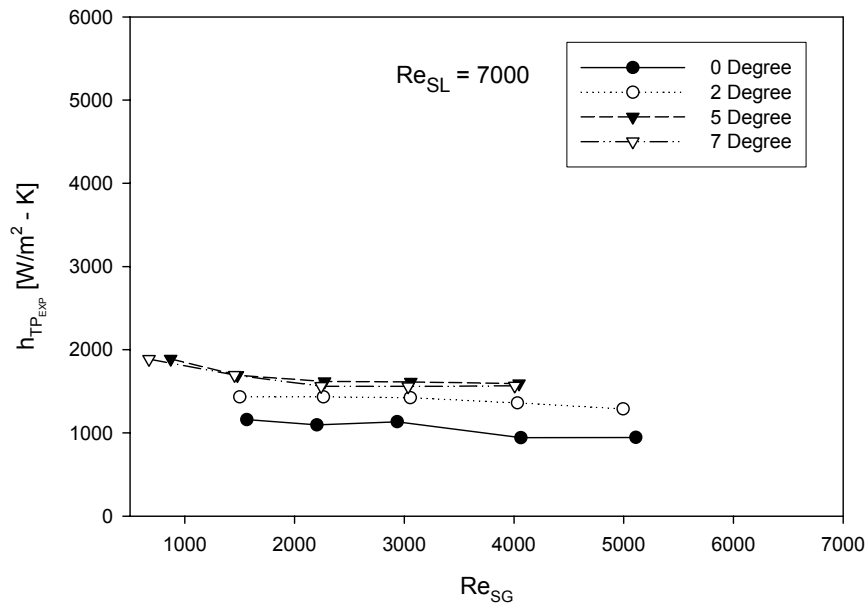


Figure 4.46: Variation of overall mean heat transfer coefficient for $Re_{SL}=7000$ series for varying Re_{SG} values

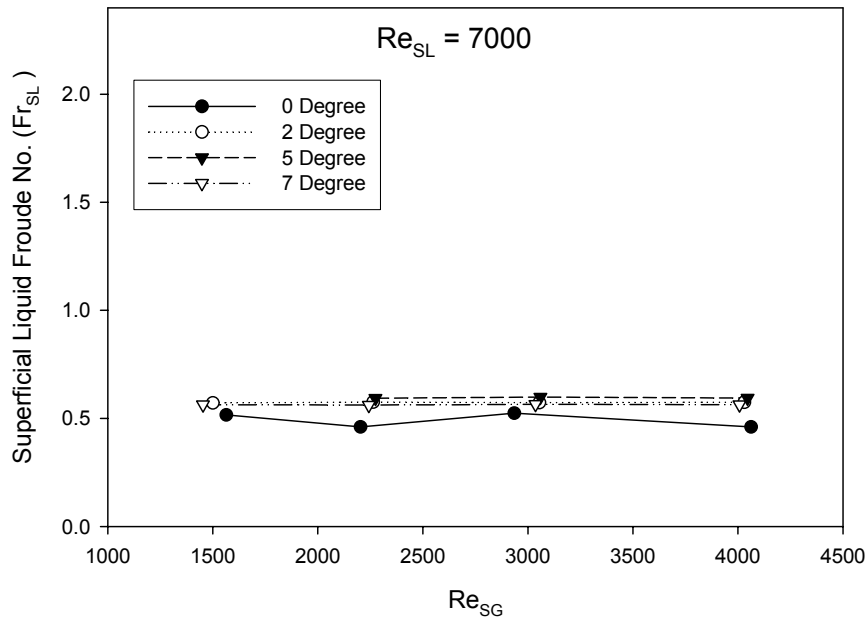


Figure 4.47: Variation of superficial liquid Froude number for $Re_{SL}=7000$ series for varying Re_{SG} values

Since, similar explanation holds for this range of low $Re_{SL} = 7000$ series, no detailed analysis is provided for this series.

4.2.2 Medium Re_{SL} Analysis ($9500 \leq Re_{SL} \leq 17000$),

Test Case Discussed ($Re_{SL}=15000, Re_{SG}=2200$)

The only case when back flow was observed for this range of Reynolds number was for $Re_{SL}=9500, Re_{SG}=750$. No back flow was observed for any other higher Re_{SL} . Figure 4.48 shows the overall mean heat transfer coefficient behavior for horizontal, two degree, five degree and seven degree with respect to varying superficial gas Reynolds numbers for $Re_{SL} = 15000$ series. It is observed that there is an increase of overall mean

heat transfer behavior for two degree, five degree when compared to the horizontal, while there is a drop in the overall mean heat transfer observed for tube inclination from five degree to seven degree for the medium range superficial liquid Reynolds numbers.

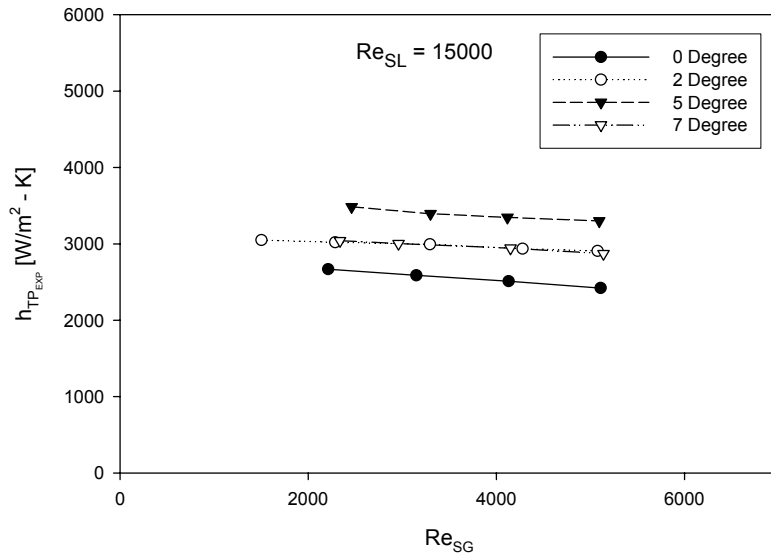


Figure 4.48: Variation of overall mean heat transfer coefficient of $Re_{SL}=15000$ series for varying Re_{SG} values

Figure 4.49 gives the summary of the flow visualization photographic slides recorded for $Re_{SL}=15000$, $Re_{SG}=2200$ at a time increment of 0.3 sec for various tube inclinations. Using the photographic slides for horizontal position, we note that no gravitational forces come into play for the horizontal slug flow. The flow pattern is fairly simple, with regular slugs flowing across the tube, no back flow or retarded flow is observed throughout the flow.

When we move to two degree, five degree and seven degree tube inclinations, we observe an enhancement of heat transfer coefficient, compared to the horizontal degree. The reason for this enhancement is the retarded flow which comes into play due to tube

inclination, and causes turbulence and hence it is responsible for enhancement of heat transfer coefficient. To explain it better, in inclined flow the new slug is obstructed by this retarded flow (or we can say that the retarded flow causes resistance for this new slug), hence turbulence is caused, which results in better mixing, and thus enhancement of heat transfer coefficient. Figures 4.30 in section 4.1.4 and 4.20 in section 4.1.3 depict the physics of heat transfer enhancement for two degree, five degree and seven degree resulting due to back flow and retarded flow.

If we carefully analyze the heat transfer coefficient change from five to seven degree for the medium range Re_{SL} ($9500 \leq Re_{SL} \leq 17000$), we observe a decrease in the overall mean heat transfer coefficient. The reason for this can be explained using the flow visualization photographs.

0 Degree

2 Degree

5 Degree

7 Degree



Figure 4.49 Visual observations (ReSL = 15000, ReSG = 2200, each snap recorded after 0.3 seconds)

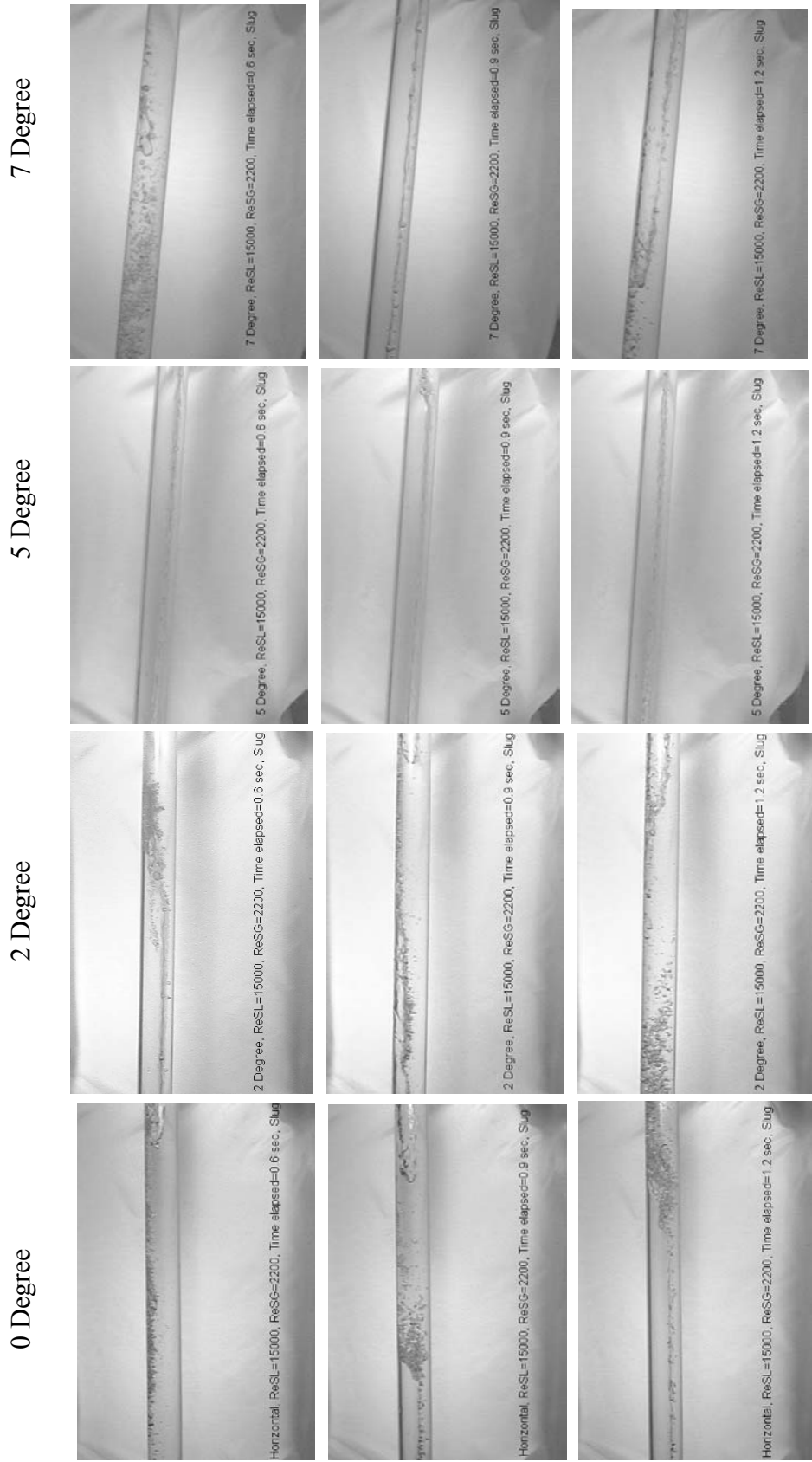


Figure 4.49 Visual observations ($Re_{SL} = 15000$, $Re_{SG} = 2200$, each snap recorded after 0.3 seconds) cont'd

Selecting the following two figures from the series flow-visualization slides shown Figure 4.49, we observe from Figure 4.49 (b) that the slug flow pattern at seven degree tube inclination shows the presence of a lot of bubbles equally distributed in the slug. These bubbles are formed due to high turbulence caused by the interaction of the retarded flow and the oncoming high velocity slug. These bubbles formed impede the heat transfer properties and thus we observe a drop in the overall mean heat transfer coefficient. The slug flow pattern at five degree in Figure 4.49 (a) does not show many evenly distributed bubbles in the slug.

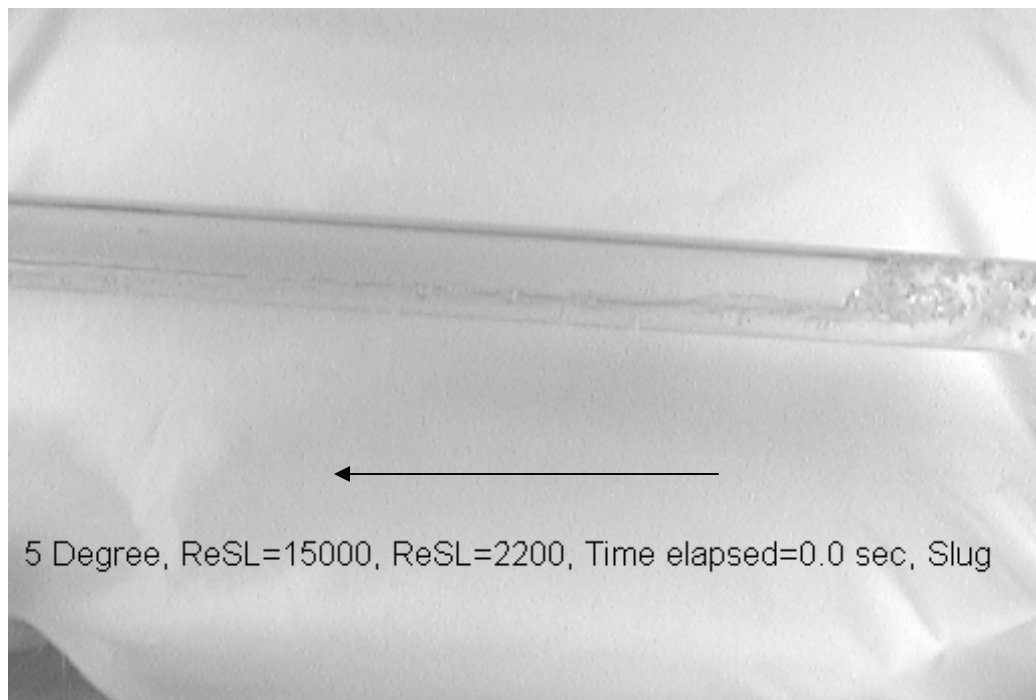


Figure 4.49 (a) – Five degree slug flow at time 0.0 sec ($Re_{SL}=15000$, $Re_{SG}=2200$)



Figure 4.49 (b) – Seven degree slug flow at time 0.0 sec ($Re_{SL}=15000$, $Re_{SG}=2200$)

Analyzing the variation of superficial liquid Froude number with superficial gas Reynolds number, we observe from Figure 4.50, that the trend is similar to what we observed in Figure 4.48. In other words the overall mean heat transfer coefficient behavior is similar to the trend observed for superficial liquid Froude number. This emphasizes the dominance of superficial liquid velocity on the heat transfer behavior.

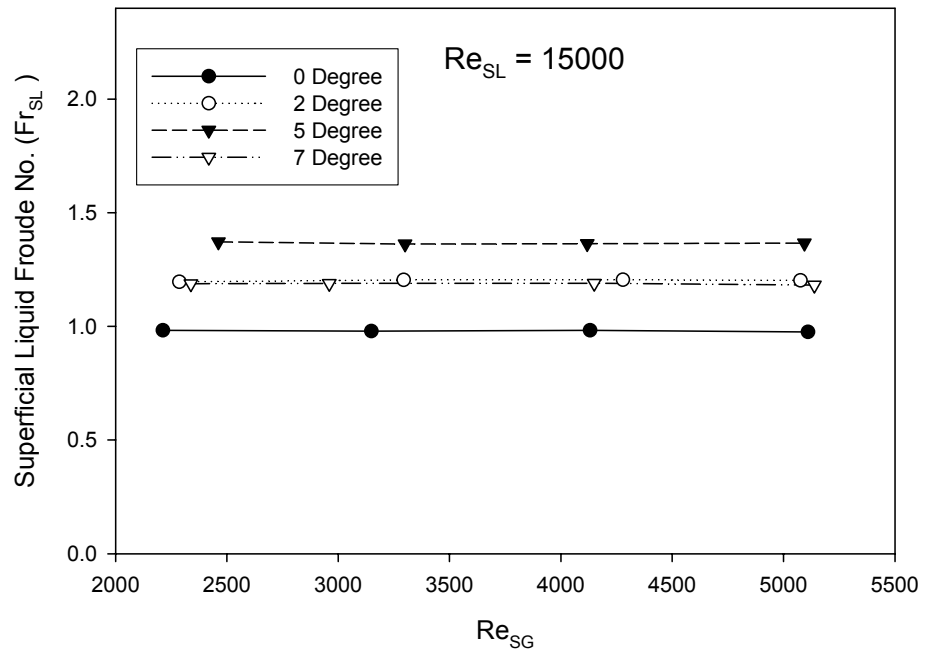


Figure 4.50: Variation of superficial liquid Froude number of $Re_{SL}=15000$ series for varying Re_{SG} values

To understand the heat transfer properties for other Re_{SL} series, we have plotted the graphs for all other medium range superficial liquid Reynolds numbers with the h_{TP} and Fr_{SL} variation with superficial gas Reynolds numbers.

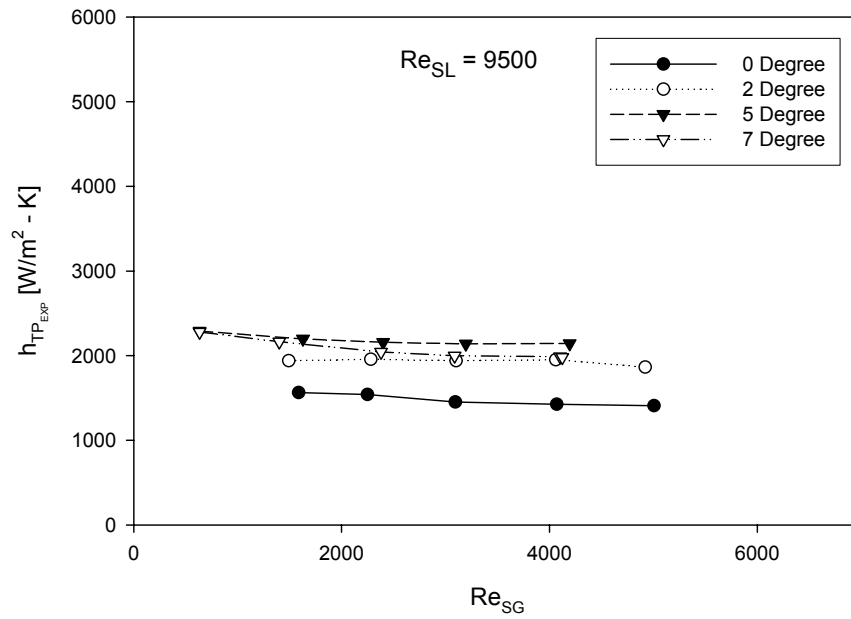


Figure 4.51: Variation of overall mean heat transfer coefficient for $Re_{SL}=9500$ series for varying Re_{SG} values

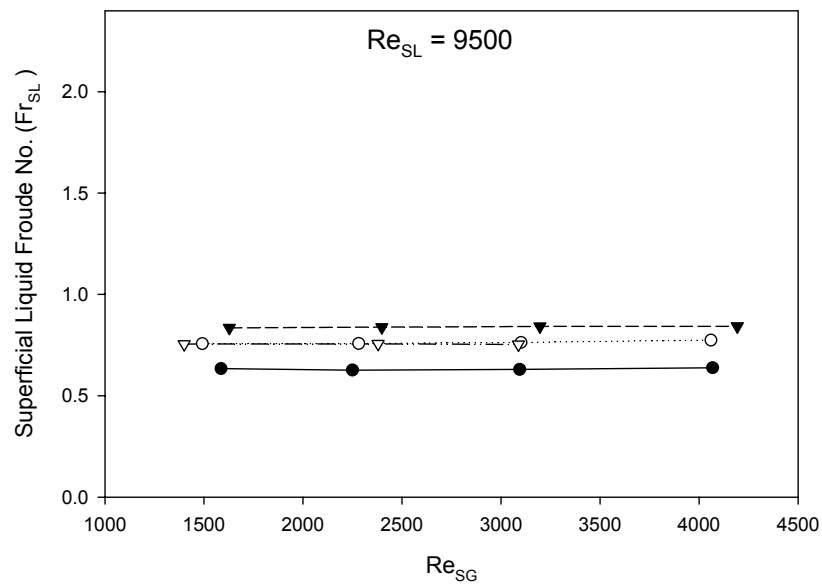


Figure 4.52: Variation of superficial liquid Froude number for $Re_{SL}=9500$ series for varying Re_{SG} values

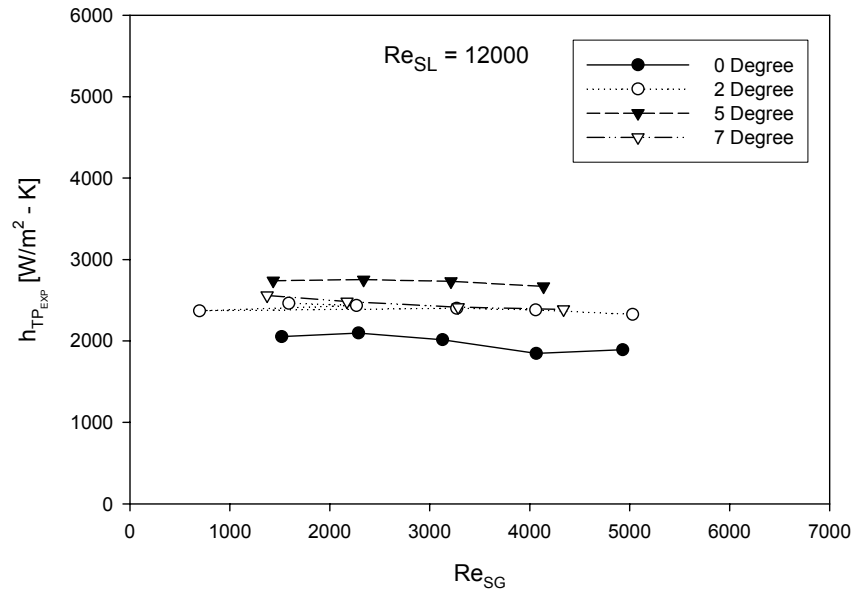


Figure 4.53: Variation of overall mean heat transfer coefficient for $Re_{SL}=12000$ series for varying Re_{SG} values

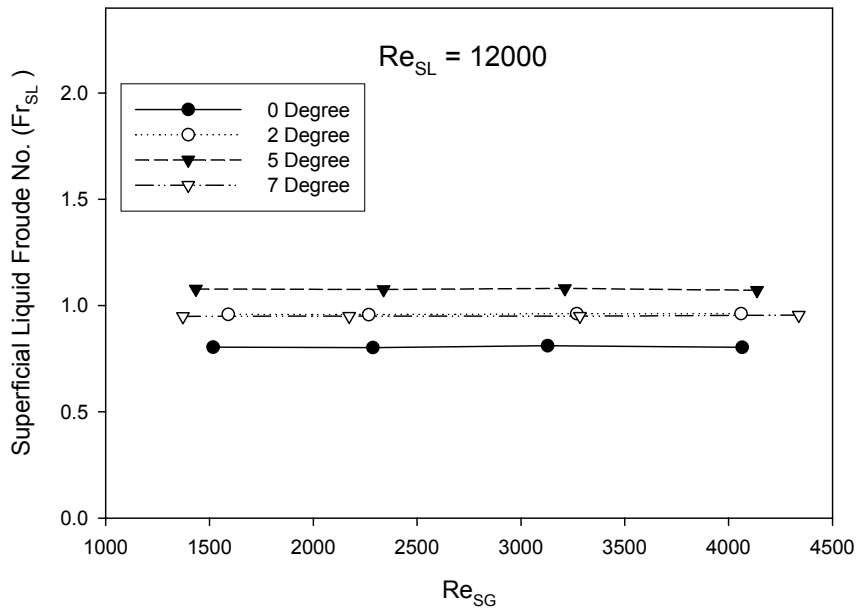


Figure 4.54: Variation of superficial liquid Froude number for $Re_{SL}=12000$ series for varying Re_{SG} values

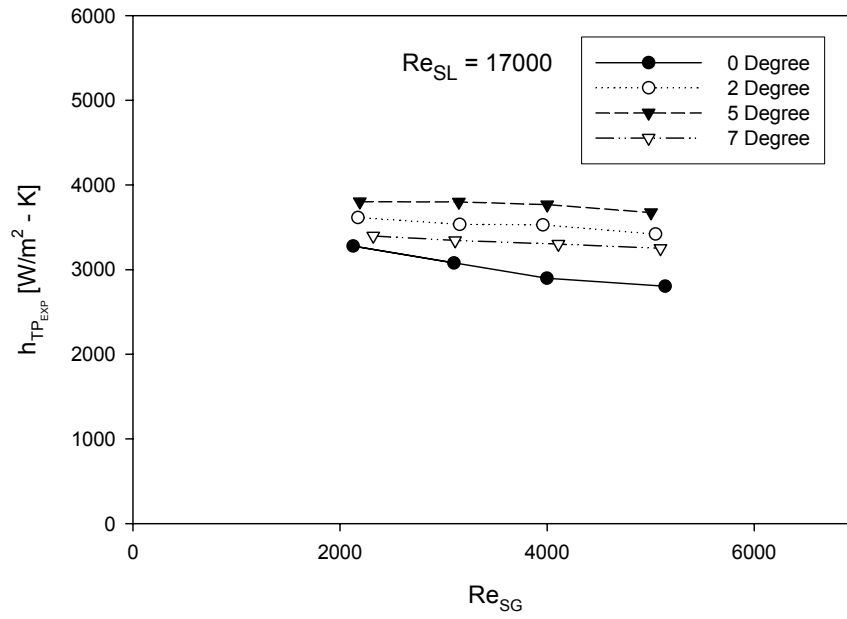


Figure 4.55: Variation of overall mean heat transfer coefficient for $Re_{SL}=17000$ series for varying Re_{SG} values

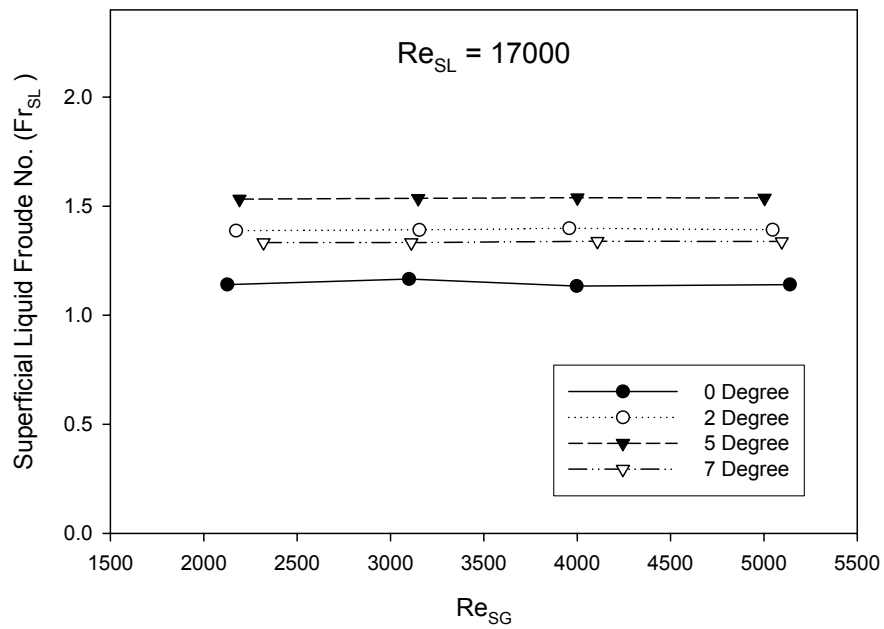


Figure 4.56: Variation of superficial liquid Froude number for $Re_{SL}=17000$ series for varying Re_{SG} values

No detailed analysis has been provided for the $Re_{SL}=9500$, $Re_{SL}=12000$, $Re_{SL}=17000$ series of superficial liquid Reynolds numbers and superficial liquid Froude number, since similar explanation holds for these, what we discussed for $Re_{SL}=15000$ series.

4.2.3 High Re_{SL} Analysis ($22000 \leq Re_{SL} \leq 26000$)

Test Case Discussed ($Re_{SL}=26000$, $Re_{SG}=4000$)

Figure 4.57 shows the overall mean heat transfer coefficient behavior for horizontal, two degree, five degree and seven degree data with respect to varying superficial gas Reynolds numbers. It is observed that there is no substantial increase in the overall mean heat transfer coefficient for the high superficial liquid Reynolds numbers for various tube inclinations under this study.

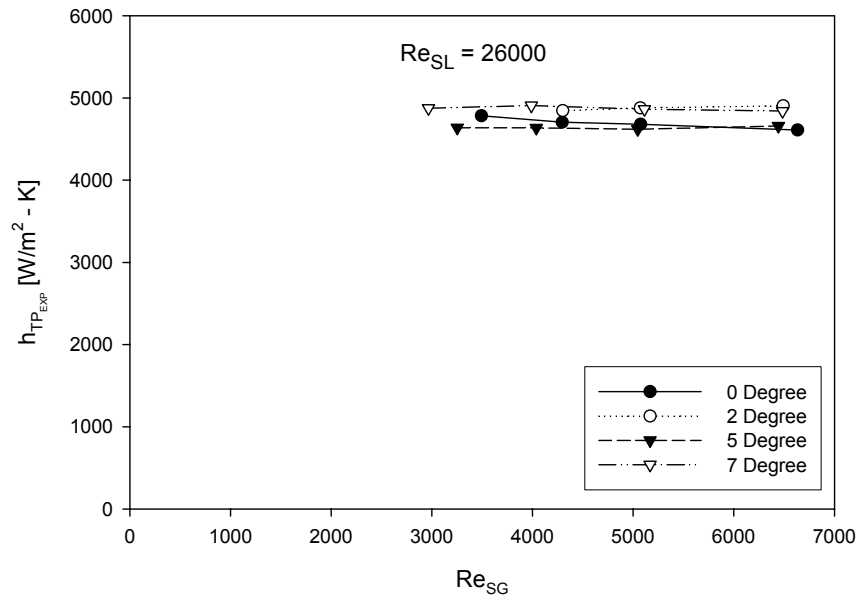


Figure 4.57: Variation of overall mean heat transfer coefficient for $Re_{SL}=26000$ series for varying Re_{SG} values

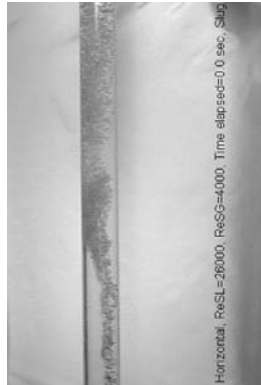
Figure 4.58 gives the summary of the flow visualization photographic slides recorded for $Re_{SL}=26000$, $Re_{SG}=4000$ at a time increment of 0.3 sec for various tube inclinations. Using the photographic slides for horizontal position, we note that no gravitational forces come into play for the horizontal slug flow. The flow pattern is fairly simple, with regular slugs flowing across the tube, no back flow or retarded flow is observed throughout the flow.

When we move to two degree, five degree and seven degree tube inclinations, we observe that there is no substantial increase of the overall mean heat transfer coefficient. The reason for this being the fact that the turbulence is extremely high and similar bubble formation is observed for all tube inclination. The bubbles hinder the heat transfer behavior to similar extent for horizontal and inclined tube position; hence the heat transfer behavior is similar. Detailed analysis has been presented below using flow

visualization. Kim *et al* (2002) observed that in slug flow pattern at high superficial liquid Reynolds numbers the effect of gas phase on heat transfer coefficient is not pronounced since the turbulence level of the liquid is already high.

The flow visual observation for this test case has been presented in a series of photographic slides shown in Figure 4.58. We observe from the flow visualization photographs, that considerable amount of bubbles are formed in this case with high superficial liquid Reynolds numbers, and the bubbles are evenly distributed throughout the slug for all tube inclination. This explains the reason why the heat transfer characteristics are similar for all tube inclinations for this high superficial liquid Reynolds number flow.

0 Degree



2 Degree



5 Degree

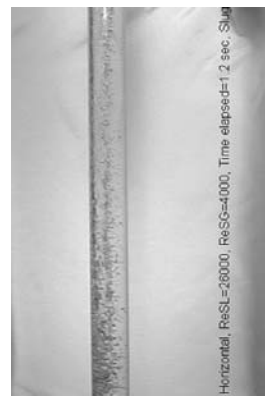
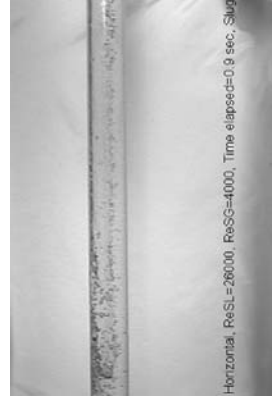
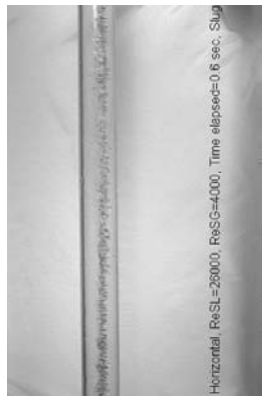


7 Degree



Figure 4.58 Visual observations ($Re_{SL} = 26000$, $Re_{SG} = 4000$, each snap recorded after 0.3 seconds)

0 Degree



2 Degree



5 Degree



7 Degree



Figure 4.58 Visual observations ($Re_{SL} = 26000$, $Re_{SG} = 4000$, each snap recorded after 0.3 seconds) cont'd

Selecting some figures from Figure 4.58, we observe from Figures 4.58(a to d), that the slug flow pattern for this high Re_{SL} series, shows a lot of formation of bubbles for horizontal and all other tube inclination. The formation of bubbles occurs because of the rigorous turbulence created by high liquid velocity. This similarity of formation of bubbles which are equally distributed throughout the slug for all tube inclination, dictates equal heat transfer characteristics. Figure 4.59 shows the variation of superficial liquid Froude number with the variation of superficial gas Reynolds number. We observe that the superficial Froude number shows the same systematic trend that we observed for the overall mean heat transfer coefficient in Figure 4.57. We also observe that the Froude number is dependent on the superficial liquid velocity, which shows slight variation at this high Re_{SL} series, and we observe slight variation in the overall mean heat transfer coefficient. We make similar conclusions to what we observed earlier that the superficial liquid velocity dominates the slug flow heat transfer behavior.

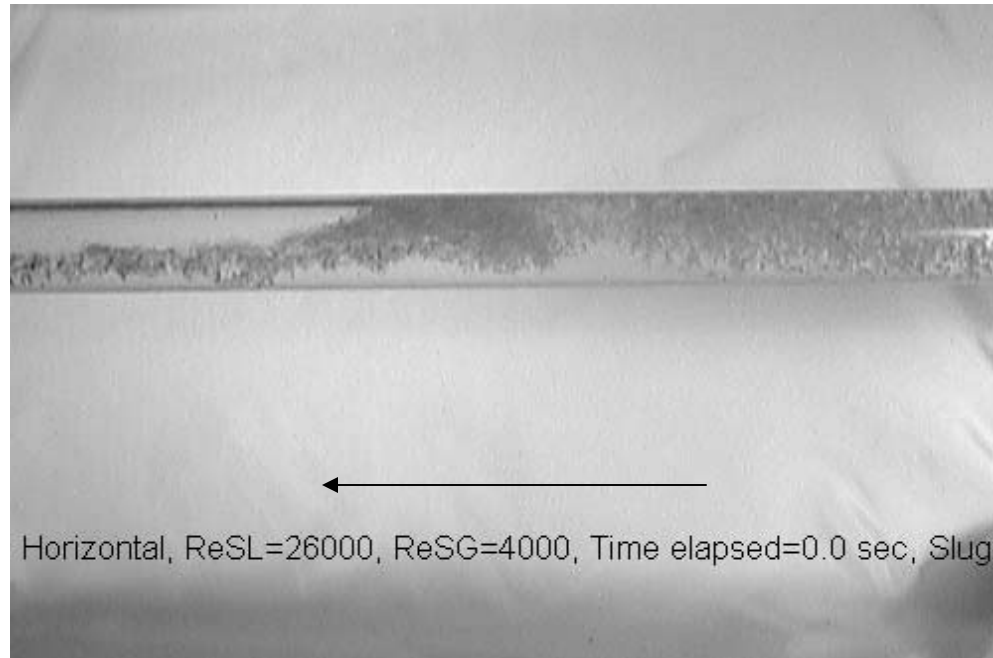


Figure 4.58 (a) – Horizontal slug flow at time 0.0 sec ($Re_{SL}=26000$, $Re_{SG}=4000$)

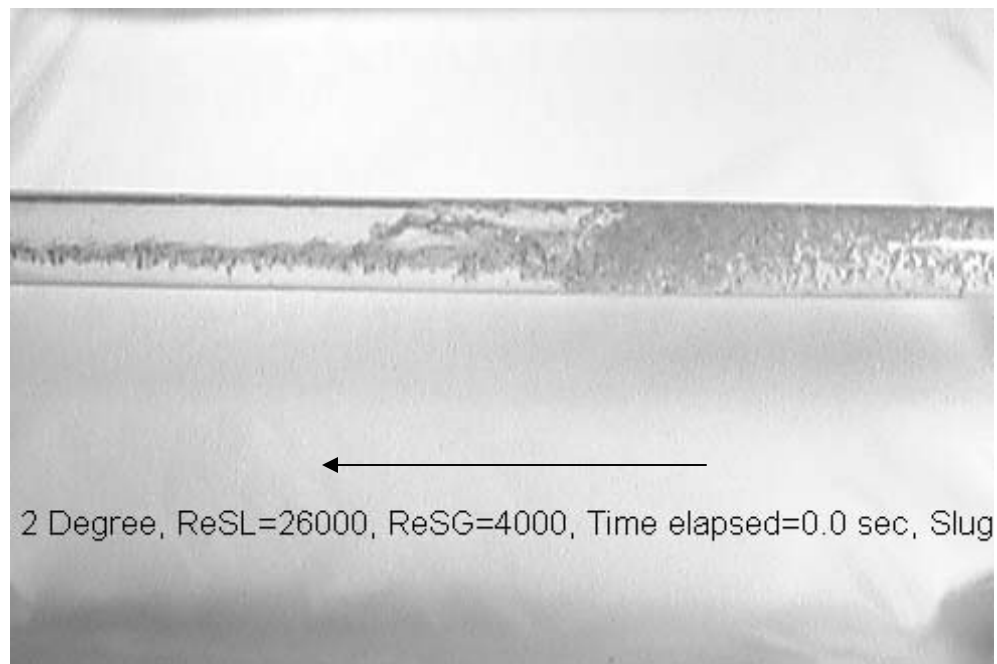


Figure 4.58 (b) – Two degree slug flow at time 0.0 sec ($Re_{SL}=26000$, $Re_{SG}=4000$)

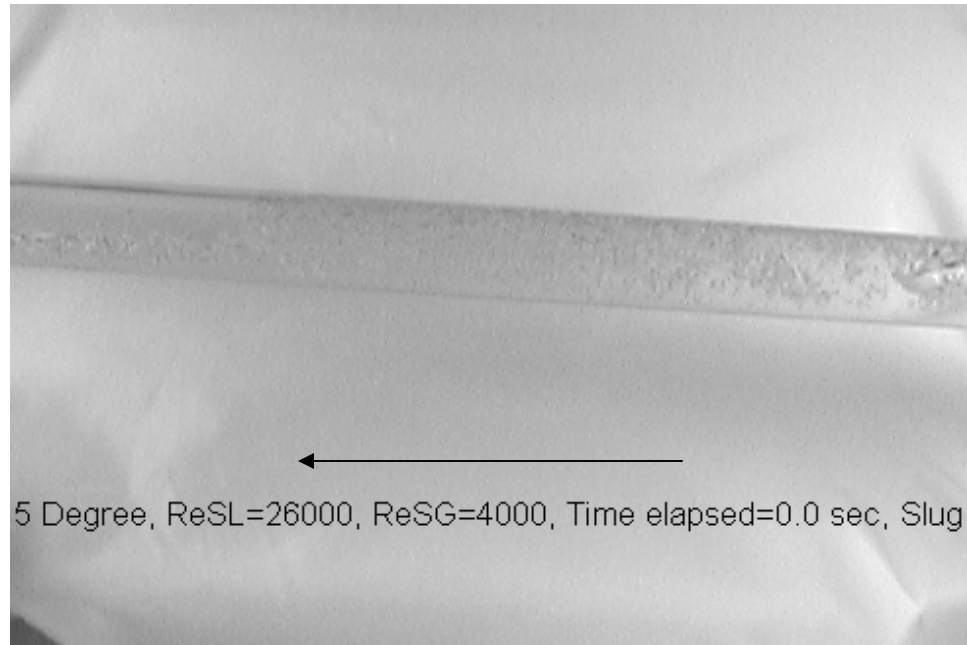


Figure 4.58 (c) – Five degree slug flow at time 0.0 sec ($Re_{SL}=26000$, $Re_{SG}=4000$)

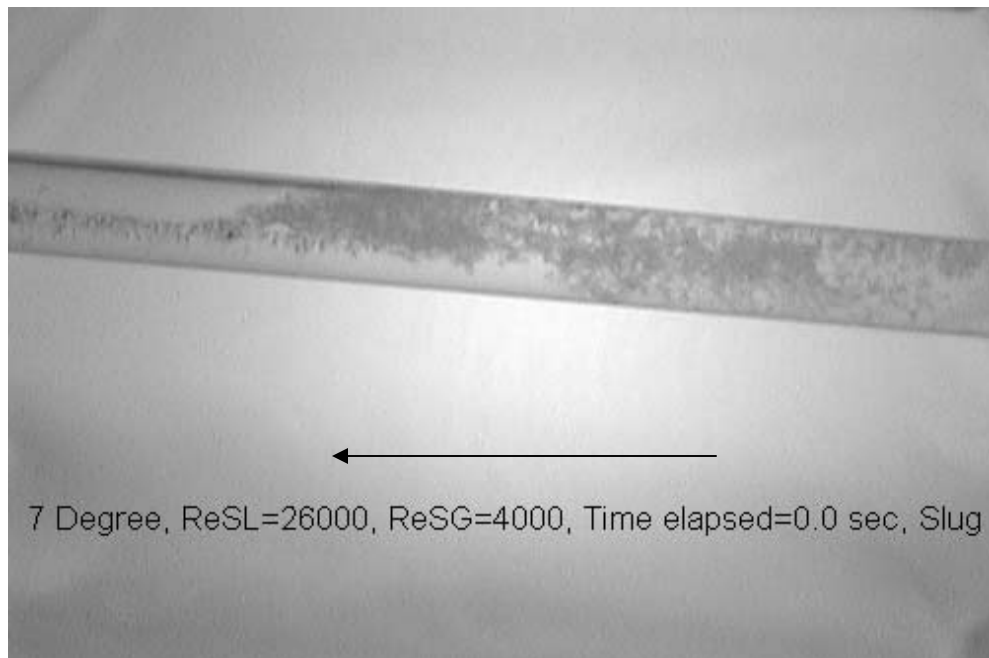


Figure 4.58 (d) – Seven degree slug flow at time 0.0 sec ($Re_{SL}=26000$, $Re_{SG}=4000$)

Figure 4.59 shows the variation of superficial liquid Froude number with varying superficial gas Reynolds number.

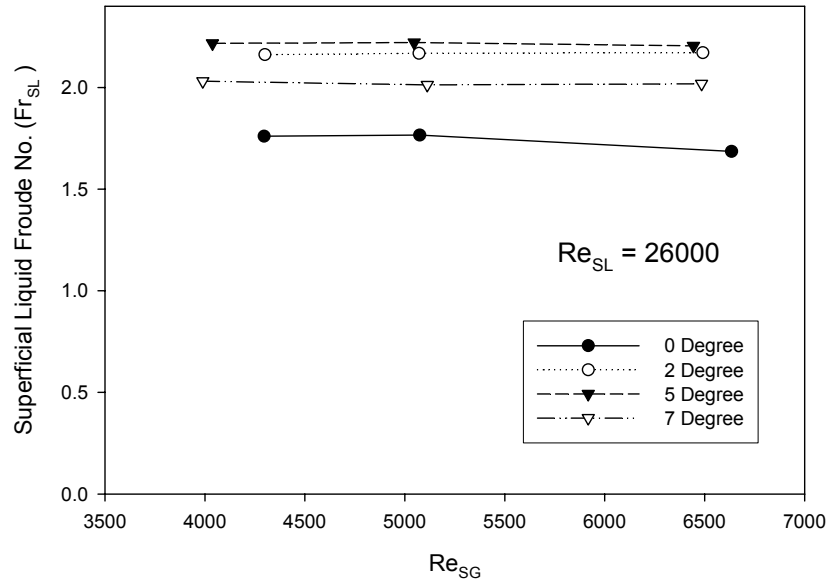


Figure 4.59: Variation of superficial liquid Froude number for $Re_{SL}=26000$ series for varying Re_{SG} values

We observe from Figures 4.578 and 4.59, similar trends of heat transfer behavior and superficial liquid Froude number with varying superficial gas Reynolds number. This emphasizes the dominance of superficial liquid Froude number on the overall mean heat transfer behavior for all tube inclination under study.

Figure 4.60 shows the overall mean heat transfer coefficient characteristics for $Re_{SL}=22000$ series for varying Re_{SG} values.

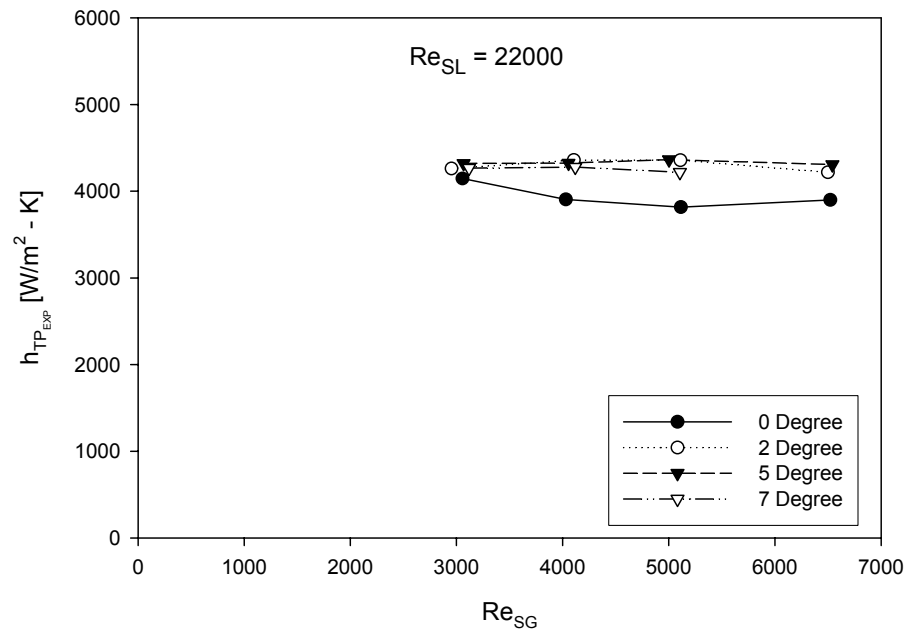


Figure 4.60: Variation of overall mean heat transfer coefficient for $Re_{SL}=22000$ series for varying Re_{SG} values

Figure 4.61 shows the variation of superficial liquid Froude number with varying superficial gas Reynolds number.

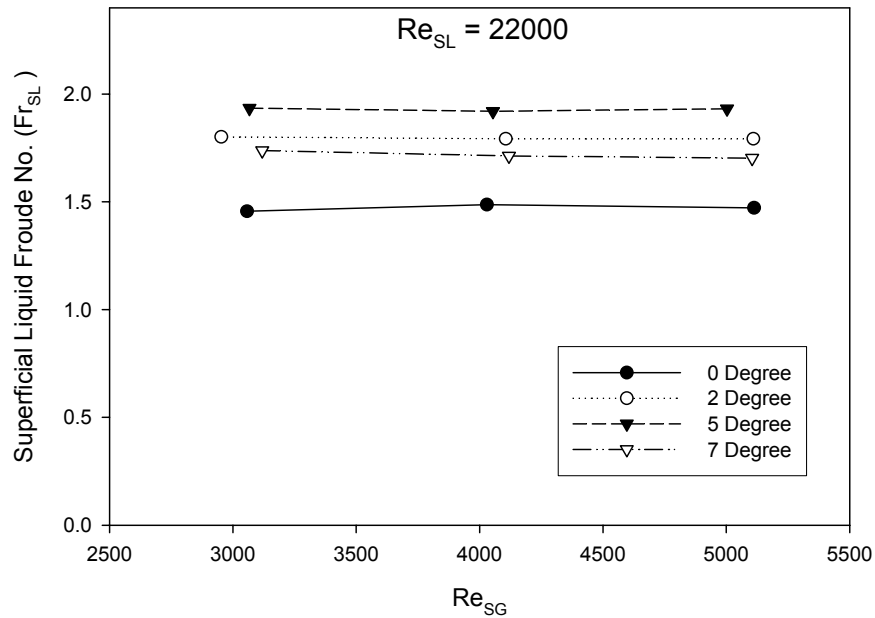


Figure 4.61: Variation of superficial liquid Froude number for $Re_{SL}=22000$ series for varying Re_{SG} values

No detailed analysis has been provided for the $Re_{SL}=22000$ series of superficial liquid Reynolds numbers, since similar explanation holds for these, similar to what we discussed for $Re_{SL}=26000$ series.

Figure 4.62 shows the overall mean heat transfer coefficient increase for increasing values of superficial liquid Reynolds number for all tube inclination positions under this study. We observe that the overall mean heat transfer coefficient is strongly dependent on the liquid phase. It is also observed that the overall mean heat transfer coefficient shows variation for various tube inclination positions. The reason for this has been already extensively discussed in our previous discussions using flow visualization.

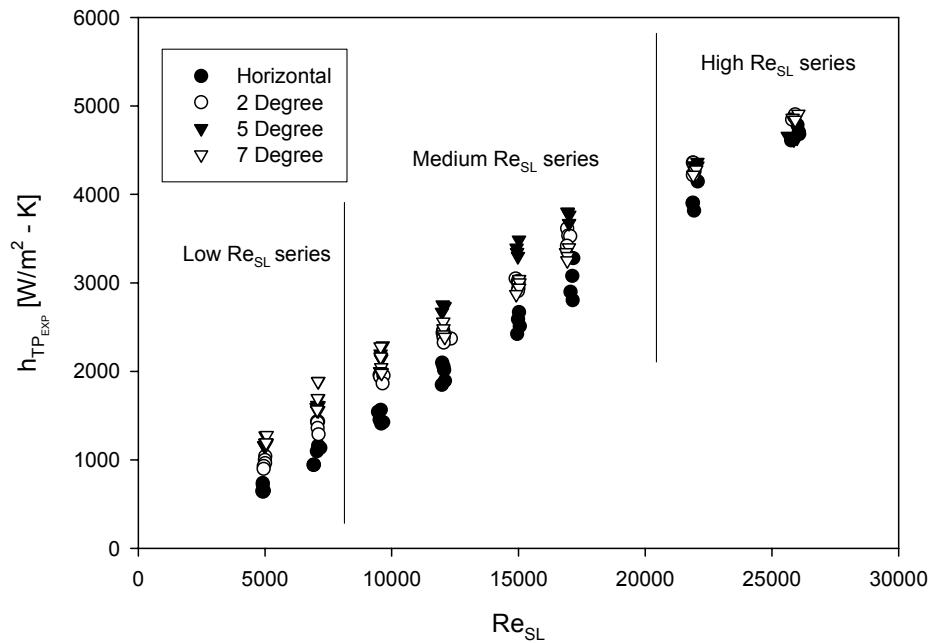


Figure 4.62: Variation of overall mean heat transfer coefficient for varying Re_{SL} values

Figure 4.63 shows the variation of superficial liquid Froude number with overall mean heat transfer coefficient. We observed a linear behavior for increasing values of overall mean heat transfer coefficient with varying superficial liquid Froude number. In all our analysis, we observed similar trends of overall mean heat transfer coefficient and superficial liquid Froude number.

As we stated earlier, superficial liquid Froude number is a non-dimensional representation of superficial liquid velocity. Hence, we can conclude that the heat transfer characteristics in slug flow are dominated by the superficial liquid velocity. This

reinstates the conclusions drawn by Hetsroni *et al* (1998b) and Kago *et al* (1986), that the heat transfer mainly depends on the liquid velocity.

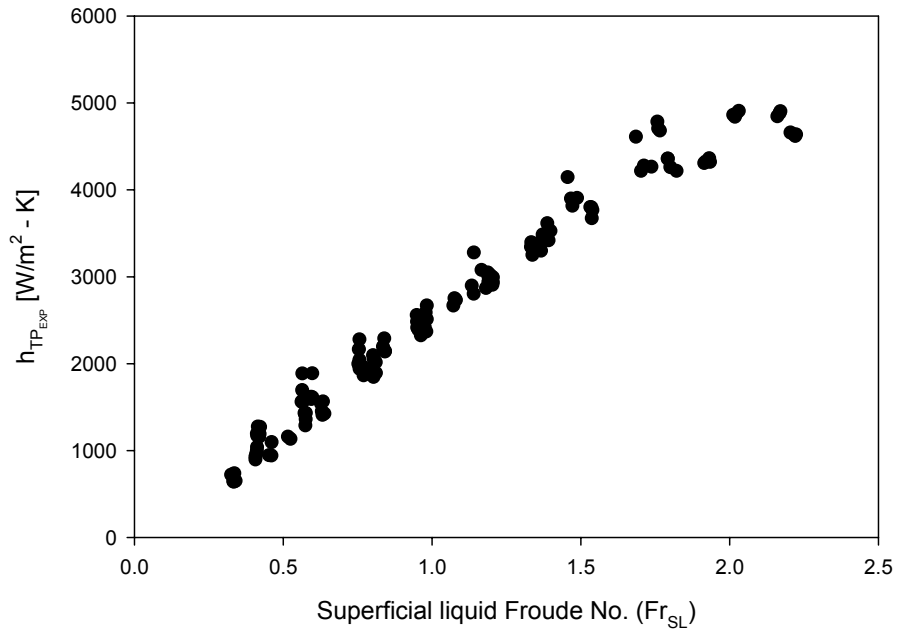


Figure 4.63: Variation of overall mean heat transfer coefficient for varying superficial liquid Froude number for complete slug flow data for 0,2,5,7 degree tube inclinations

Tables 4.6 to 4.11, provide detailed comparison for various tube inclinations, for all data points used in this study, with respect to change of superficial liquid, gas Reynolds numbers, overall mean heat transfer coefficient and superficial liquid Froude number.

We have gone further ahead to modify the existing Froude number so as to bring the effect of inclination on overall mean two-phase heat transfer coefficient. The details of this have been discussed in section 4.2.4.

Table 4.6 Horizontal and two degree comparison

Index	Re _{SL}		ΔRe _{SL} (%)	Re _{SG}		ΔRe _{SG} (%)	h _{hp}		Δh _{hp}	Δh _{hp} (%)	F _{SL}		ΔF _{SL} (%)		
	2 Degr	0 Degr		2 Degr	0 Degr		2 Degr	0 Degr			2 Degr	0 Degr			
1	5007	4911	96	1549	1477	72	4.9	1039	738	301	29	0.4121	0.3358	0.0763	23
2	4996	4912	85	2219	2238	-19	-0.9	999	721	277	28	0.4112	0.3249	0.0862	27
3	4999	4954	45	3044	3028	16	0.5	963	651	311	32	0.4093	0.3396	0.0696	20
4	4956	4891	64	4006	4029	-23	-0.6	931	648	283	30	0.4069	0.3317	0.0751	23
5	7056	7099	-43	1500	1565	-64	-4.1	1432	1159	273	19	0.5716	0.5160	0.0556	11
6	7093	7045	48	2264	2204	60	2.7	1432	1095	337	24	0.5759	0.4606	0.1153	25
7	7062	7180	-118	3055	2935	120	4.1	1422	1133	289	20	0.5729	0.5243	0.0487	9
8	7075	6914	161	4031	4062	-31	-0.8	1361	943	419	31	0.5752	0.4604	0.1148	25
9	9568	9566	2	1492	1586	-95	-6.0	1940	1564	376	19	0.7568	0.6337	0.1232	19
10	9523	9462	61	2282	2250	32	1.4	1956	1542	415	21	0.7572	0.6267	0.1305	21
11	9542	9521	21	3101	3094	7	0.2	1939	1453	486	25	0.7630	0.6296	0.1335	21
12	9677	9663	14	4060	4069	-9	-0.2	1951	1426	525	27	0.7746	0.6383	0.1363	21
13	12029	12041	-12	1590	1518	72	4.8	2463	2052	411	17	0.9585	0.8043	0.1542	19
14	12008	11992	16	2267	2287	-20	-0.9	2436	2097	339	14	0.9571	0.8020	0.1551	19
15	12052	12069	-17	3269	3128	141	4.5	2401	2016	385	16	0.9616	0.8109	0.1507	19
16	12048	11981	66	4060	4065	-5	-0.1	2380	1847	533	22	0.9615	0.8030	0.1585	20
17	14977	15023	-46	2287	2212	75	3.4	3020	2668	351	12	1.1959	0.9821	0.2138	22
18	15005	14985	21	3294	3149	145	4.6	2994	2587	407	14	1.2048	0.9787	0.2261	23
19	14997	15051	-55	4279	4131	148	3.6	2936	2511	425	14	1.2050	0.9825	0.2225	23
20	14978	14950	28	5076	5110	-34	-0.7	2907	2421	486	17	1.2027	0.9753	0.2275	23
21	16925	17162	-237	2173	2126	47	2.2	3614	3279	334	9	1.3874	1.1410	0.2464	22
22	16963	17119	-156	3155	3100	55	1.8	3533	3077	456	13	1.3907	1.1664	0.2243	19
23	17044	17056	-13	3958	3997	-39	-1.0	3526	2898	629	18	1.3983	1.1335	0.2648	23
24	16917	17139	-222	5047	5140	-93	-1.8	3419	2804	615	18	1.3915	1.1404	0.2511	22
25	21942	22073	-130	2953	3057	-104	-3.4	4261	4147	114	3	1.8008	1.4559	0.3449	24
26	21879	21887	-8	4106	4030	76	1.9	4359	3907	453	10	1.7921	1.4872	0.3049	20
27	21900	21928	-28	5110	5113	-3	-0.1	4356	3816	540	12	1.7922	1.4716	0.3206	22
28	25797	26061	-263	4300	4296	4	0.1	4846	4705	140	3	2.1608	1.7599	0.4009	23
29	25881	26070	-189	5071	5074	-3	-0.1	4881	4681	199	4	2.1677	1.7657	0.4019	23
30	25917	25755	163	6491	6634	-144	-2.2	4904	4611	294	6	2.1710	1.6852	0.4858	29

Table 4.7 Horizontal and five degree comparison

Index	Re _{SL}		Δ Re _{SL} (%)	Re _{SG}		Δ Re _{SG} (%)	h _{hp}		Δ h _{hp}	Δ h _{hp} (%)	Fr _{SL}		Δ Fr _{SL}	Δ Fr _{SL} (%)
	5 Degr	0 Degr		5 Degr	0 Degr		5 Degr	0 Degr			5 Degr	0 Degr		
1	5021	4911	110	1462	1477	-15	1271	738	533	42	0.4220	0.3358	0.0862	26
2	5008	4912	96	2247	2238	9	1190	721	469	39	0.4208	0.3249	0.0959	30
3	4987	4954	33	3035	3028	7	1159	651	507	44	0.4191	0.3396	0.0794	23
4	4966	4891	75	4030	4029	1	1161	648	513	44	0.4178	0.3317	0.0861	26
5	7103	7099	4	1480	1565	-85	1693	1159	534	32	0.5969	0.5160	0.0809	16
6	7059	7045	14	2274	2204	70	1618	1095	522	32	0.5937	0.4606	0.1331	29
7	7111	7180	-69	3059	2935	124	1612	1133	479	30	0.5981	0.5243	0.0739	14
8	7038	6914	123	4045	4062	-17	1591	943	649	41	0.5941	0.4604	0.1337	29
9	9563	9566	-2	1629	1586	42	2197	1564	633	29	0.8350	0.6337	0.2013	32
10	9573	9462	111	2398	2250	149	2158	1542	616	29	0.8380	0.6267	0.2112	34
11	9578	9521	57	3196	3094	102	2139	1453	686	32	0.8415	0.6296	0.2120	34
12	9578	9663	-85	4193	4069	124	2143	1426	717	33	0.8423	0.6383	0.2040	32
13	12050	12041	9	1434	1518	-83	2740	2052	688	25	1.0776	0.8043	0.2733	34
14	12009	11992	17	2339	2287	52	2752	2097	655	24	1.0757	0.8020	0.2737	34
15	12090	12069	21	3212	3128	84	2732	2016	717	26	1.0804	0.8109	0.2695	33
16	11984	11981	3	4137	4065	72	2668	1847	822	31	1.0715	0.8030	0.2685	33
17	15022	15023	0	2463	2212	250	3484	2668	816	23	1.3716	0.9821	0.3895	40
18	14927	14985	-57	3300	3149	151	3394	2587	807	24	1.3619	0.9787	0.3832	39
19	14941	15051	-110	4119	4131	-12	3345	2511	834	25	1.3634	0.9825	0.3809	39
20	14977	14950	27	5094	5110	-16	3299	2421	877	27	1.3662	0.9753	0.3910	40
21	16933	17162	-229	2192	2126	66	3802	3279	522	14	1.5325	1.1410	0.3915	34
22	16947	17119	-172	3148	3100	49	3798	3077	721	19	1.5356	1.1664	0.3692	32
23	17002	17056	-55	4001	3997	4	3767	2898	869	23	1.5387	1.1335	0.4052	36
24	16996	17139	-142	5004	5140	-136	3673	2804	869	24	1.5368	1.1404	0.3964	35
25	22058	22073	-15	3067	3057	10	4321	4147	175	4	1.9342	1.4559	0.4783	33
26	21927	21887	40	4054	4030	25	4324	3907	418	10	1.9198	1.4872	0.4326	29
27	22057	21928	129	5003	5113	-110	4364	3816	548	13	1.9313	1.4716	0.4597	31
28	25894	26061	-167	4038	4296	-258	4636	4705	-69	-1	2.2208	1.7599	0.4609	26
29	25871	26070	-199	5046	5074	-28	4618	4681	-63	-1	2.2208	1.7657	0.4551	26
30	25623	25755	-131	6444	6634	-191	4659	4611	48	1	2.2045	1.6852	0.5194	31

Table 4.8 Horizontal and seven degree comparison

Index	Re _{SL}		$\Delta Re_{SL}(\%)$	Re _{SG}		$\Delta Re_{SG}(\%)$	h _{hp}		Δh_{hp}	$\Delta h_{hp}(\%)$	Fr _{SL}		ΔFr_{SL}	$\Delta Fr_{SL}(\%)$
	7 Degr	0 Degr		7 Degr	0 Degr		7 Degr	0 Degr			7 Degr	0 Degr		
1	5068	4911	157	1544	1477	67	1276	738	538	42	0.4149	0.3358	0.0791	24
2	5066	4912	155	2143	2238	-96	1190	721	468	39	0.4148	0.3249	0.0898	28
3	5042	4954	89	3042	3028	14	1169	651	518	44	0.4128	0.3396	0.0731	22
4	5048	4891	157	4025	4029	-4	1193	648	546	46	0.4119	0.3317	0.0802	24
5	7079	7099	-20	1453	1565	-112	1695	1159	535	32	0.5636	0.5160	0.0476	9
6	7053	7045	8	2243	2204	39	1561	1095	466	30	0.5615	0.4606	0.1009	22
7	7103	7180	-77	3036	2935	101	1557	1133	424	27	0.5657	0.5243	0.0414	8
8	7060	6914	146	4007	4062	-55	1567	943	624	40	0.5631	0.4604	0.1027	22
9	9559	9566	-7	1400	1586	-186	2164	1564	601	28	0.7543	0.6337	0.1207	19
10	9585	9462	123	2379	2250	129	2043	1542	501	25	0.7561	0.6267	0.1293	21
11	9545	9521	24	3088	3094	-6	1997	1453	544	27	0.7523	0.6296	0.1227	19
12	9598	9663	-65	4103	4069	35	1987	1426	561	28	0.7555	0.6383	0.1172	18
13	12033	12041	-8	1372	1518	-146	2559	2052	506	20	0.9488	0.8043	0.1444	18
14	12039	11992	47	2173	2287	-115	2483	2097	386	16	0.9499	0.8020	0.1479	18
15	12038	12069	-31	3284	3128	156	2414	2016	398	17	0.9501	0.8109	0.1393	17
16	12095	11981	114	4338	4065	272	2387	1847	541	23	0.9545	0.8030	0.1515	19
17	15028	15023	5	2338	2212	126	3040	2668	371	12	1.1872	0.9821	0.2051	21
18	15040	14985	55	2960	3149	-189	3003	2587	415	14	1.1890	0.9787	0.2103	21
19	15025	15051	-26	4150	4131	19	2943	2511	432	15	1.1891	0.9825	0.2067	21
20	14915	14950	-35	5138	5110	29	2870	2421	449	16	1.1810	0.9753	0.2057	21
21	16990	17162	-171	2320	2126	195	3396	3279	117	3	1.3336	1.1410	0.1926	17
22	16873	17119	-246	3112	3100	12	3344	3077	267	8	1.3327	1.1664	0.1663	14
23	16938	17056	-118	4109	3997	112	3301	2898	403	12	1.3389	1.1335	0.2054	18
24	16930	17139	-209	5096	5140	-44	3251	2804	447	14	1.3372	1.1404	0.1968	17
25	21954	22073	-119	3119	3057	62	4266	4147	119	3	1.7372	1.4559	0.2813	19
26	22020	21887	133	4119	4030	89	4277	3907	371	9	1.7124	1.4872	0.2251	15
27	21896	21928	-32	5105	5113	-8	4218	3816	402	10	1.7021	1.4716	0.2305	16
28	26043	26061	-18	3990	4296	-306	4907	4705	202	4	2.0307	1.7599	0.2708	15
29	25816	26070	-255	5113	5074	38	4862	4681	181	4	2.0124	1.7657	0.2467	14
30	25915	25755	160	6484	6634	-150	4841	4611	230	5	2.0180	1.6852	0.3329	20

Table 4.9 Two degree and five degree comparison

Index	Re _{SL}		ΔRe _{SL} (%)	ΔRe _{SL} (%)	Re _{ESG}		ΔRe _{ESG}	ΔRe _{ESG} (%)	h _{hp}		Δh _{hp}	Δh _{hp} (%)	Fr _{SL}		ΔFr _{SL} (%)	
	5 Degree	2 Degree			5 Degr	2 Degr			5 Degr	2 Degr			5 Degr	2 Degr		
1	5021	5007	14	0.3	1462	1549	-87	-5.6	1271	1039	232	18	0.4220	0.4121	0.0100	2
2	5008	4996	12	0.2	2247	2219	28	1.3	1190	999	192	16	0.4208	0.4112	0.0097	2
3	4987	4999	-12	-0.2	3035	3044	-9	-0.3	1159	963	196	17	0.4191	0.4093	0.0098	2
4	4966	4956	11	0.2	4030	4006	24	0.6	1161	931	230	20	0.4178	0.4069	0.0109	3
5	7103	7056	48	0.7	1480	1500	-20	-1.4	1693	1432	261	15	0.5969	0.5716	0.0253	4
6	7059	7093	-35	-0.5	2274	2264	11	0.5	1618	1432	186	11	0.5937	0.5759	0.0178	3
7	7111	7062	49	0.7	3059	3055	4	0.1	1612	1422	189	12	0.5981	0.5729	0.0252	4
8	7038	7075	-38	-0.5	4045	4031	15	0.4	1591	1361	230	14	0.5941	0.5752	0.0189	3
9	9563	9568	-4	0.0	1629	1492	137	9.2	2197	1940	257	12	0.8350	0.7568	0.0782	10
10	9573	9523	50	0.5	2398	2282	117	5.1	2158	1956	202	9	0.8380	0.7572	0.0808	11
11	9578	9542	37	0.4	3196	3101	95	3.1	2139	1939	199	9	0.8415	0.7630	0.0785	10
12	9578	9677	-99	-1.0	4193	4060	133	3.3	2143	1951	192	9	0.8423	0.7746	0.0677	9
13	12050	12029	21	0.2	1434	1590	-156	-9.8	2740	2463	277	10	1.0776	0.9585	0.1191	12
14	12009	12008	1	0.0	2339	2267	72	3.2	2752	2436	316	11	1.0757	0.9571	0.1186	12
15	12090	12052	38	0.3	3212	3269	-57	-1.8	2732	2401	331	12	1.0804	0.9616	0.1188	12
16	11984	12048	-64	-0.5	4137	4060	78	1.9	2668	2380	289	11	1.0715	0.9615	0.1100	11
17	15022	14977	46	0.3	2463	2287	176	7.7	3484	3020	465	13	1.3716	1.1959	0.1758	15
18	14927	15005	-78	-0.5	3300	3294	6	0.2	3394	2994	400	12	1.3619	1.2048	0.1571	13
19	14941	14997	-56	-0.4	4119	4279	-160	-3.7	3345	2936	409	12	1.3634	1.2050	0.1584	13
20	14977	14978	-1	0.0	5094	5076	18	0.4	3299	2907	392	12	1.3662	1.2027	0.1635	14
21	16933	16925	8	0.0	2192	2173	19	0.9	3802	3614	188	5	1.5325	1.3874	0.1451	10
22	16947	16963	-16	-0.1	3148	3155	-6	-0.2	3798	3533	265	7	1.5356	1.3907	0.1448	10
23	17002	17044	-42	-0.2	4001	3958	43	1.1	3767	3526	241	6	1.5387	1.3983	0.1404	10
24	16996	16917	80	0.5	5004	5047	-43	-0.8	3673	3419	254	7	1.5368	1.3915	0.1453	10
25	22058	21942	116	0.5	3067	2953	115	3.9	4321	4261	60	1	1.9342	1.8008	0.1334	7
26	21927	21879	48	0.2	4054	4106	-51	-1.3	4324	4359	-35	-1	1.9198	1.7921	0.1277	7
27	22057	21900	157	0.7	5003	5110	-107	-2.1	4364	4356	8	0	1.9313	1.7922	0.1391	8
28	25894	25797	96	0.4	4038	4300	-262	-6.1	4636	4846	-210	-5	2.2208	2.1608	0.0600	3
29	25871	25881	-10	0.0	5046	5071	-25	-0.5	4618	4881	-262	-6	2.2208	2.1677	0.0532	2
30	25623	25917	-294	-1.1	6444	6491	-47	-0.7	4659	4904	-245	-5	2.2045	2.1710	0.0336	2

Table 4.10 Two degree and seven degree comparison

Index	Re _{SL}		ΔRe _{SL}	ΔRe _{SL} (%)	Re _{SG}		ΔRe _{SG}	ΔRe _{SG} (%)	h _p		Δh _p	Δh _p (%)	F _{SL}		ΔF _{SL}	ΔF _{SL} (%)
	7 Degr	2 Degr			7 Degr	2 Degr			7 Degr	2 Degr			7 Degr	2 Degr		
1	5068	5007	61	1.2	1544	1549	-5	-0.3	1276	1039	237	19	0.4149	0.4121	0.0028	1
2	5066	4996	70	1.4	2143	2219	-76	-3.4	1190	999	191	16	0.4148	0.4112	0.0036	1
3	5042	4999	44	0.9	3042	3044	-2	-0.1	1169	963	207	18	0.4128	0.4093	0.0035	1
4	5048	4956	92	1.8	4025	4006	19	0.5	1193	931	263	22	0.4119	0.4069	0.0050	1
5	7079	7056	24	0.3	1453	1500	-47	-3.1	1695	1432	262	15	0.5636	0.5716	-0.0081	-1
6	7053	7093	-40	-0.6	2243	2264	-21	-0.9	1561	1432	129	8	0.5615	0.5759	-0.0144	-2
7	7103	7062	41	0.6	3036	3055	-19	-0.6	1557	1422	135	9	0.5657	0.5729	-0.0073	-1
8	7060	7075	-15	-0.2	4007	4031	-24	-0.6	1567	1361	206	13	0.5631	0.5752	-0.0121	-2
9	9559	9568	-9	-0.1	1400	1492	-92	-6.1	2164	1940	224	10	0.7543	0.7568	-0.0025	0
10	9585	9523	62	0.6	2379	2282	97	4.3	2043	1956	86	4	0.7561	0.7572	-0.0011	0
11	9545	9542	3	0.0	3088	3101	-13	-0.4	1997	1939	58	3	0.7523	0.7630	-0.0108	-1
12	9598	9677	-79	-0.8	4103	4060	43	1.1	1987	1951	36	2	0.7555	0.7746	-0.0191	-2
13	12033	12029	4	0.0	1372	1590	-218	-13.7	2559	2463	95	4	0.9488	0.9585	-0.0098	-1
14	12039	12008	30	0.3	2173	2267	-94	-4.2	2483	2436	47	2	0.9499	0.9571	-0.0072	-1
15	12038	12052	-14	-0.1	3284	3269	15	0.4	2414	2401	13	1	0.9501	0.9616	-0.0114	-1
16	12095	12048	48	0.4	4338	4060	278	6.8	2387	2380	8	0	0.9545	0.9615	-0.0070	-1
17	15028	14977	51	0.3	2338	2287	52	2.3	3040	3020	20	1	1.1872	1.1959	-0.0087	-1
18	15040	15005	35	0.2	2960	3294	-334	-10.1	3003	2994	9	0	1.1890	1.2048	-0.0158	-1
19	15025	14997	29	0.2	4150	4279	-129	-3.0	2943	2936	7	0	1.1891	1.2050	-0.0158	-1
20	14915	14978	-63	-0.4	5138	5076	62	1.2	2870	2907	-37	-1	1.1810	1.2027	-0.0217	-2
21	16990	16925	66	0.4	2320	2173	147	6.8	3396	3614	-218	-6	1.3336	1.3874	-0.0538	-4
22	16873	16963	-90	-0.5	3112	3155	-43	-1.4	3344	3533	-189	-6	1.3327	1.3907	-0.0581	-4
23	16938	17044	-105	-0.6	4109	3958	151	3.8	3301	3526	-226	-7	1.3389	1.3983	-0.0594	-4
24	16930	16917	13	0.1	5096	5047	49	1.0	3251	3419	-168	-5	1.3372	1.3915	-0.0543	-4
25	21954	21942	11	0.1	3119	2953	166	5.6	4266	4261	5	0	1.7372	1.8008	-0.0636	-4
26	22020	21879	140	0.6	4119	4106	13	0.3	4277	4359	-82	-2	1.7124	1.7921	-0.0797	-4
27	21896	21900	-4	0.0	5105	5110	-5	-0.1	4218	4356	-138	-3	1.7021	1.7922	-0.0901	-5
28	26043	25797	245	0.9	3990	4300	-310	-7.2	4907	4846	61	1	2.0307	2.1608	-0.1301	-6
29	25816	25881	-65	-0.3	5113	5071	41	0.8	4862	4881	-18	0	2.0124	2.1677	-0.1552	-7
30	25915	25917	-3	0.0	6484	6491	-7	0.1	4841	4904	-63	-1	2.0180	2.1710	-0.1529	-7

Table 4.11 Five degree and seven degree comparison

Index	Re _{SL}		ΔRe _{SL} (%)	ΔRe _{SL} (%)	Re _{SG}		ΔRe _{SG}	ΔRe _{SG} (%)	h _{ip}		Δh _{ip}	Δh _{ip} (%)	F _{SL}		ΔF _{SL}	ΔF _{SL} (%)
	7 Deps	5 Deps			7 Deps	5 Deps			7 Deps	5 Deps			7 Deps	5 Deps		
1	5068	5021	47	0.9	1544	1462	82	5.6	1276	1271	5	0	0.4149	0.4220	-0.0071	-2
2	5066	5008	59	1.2	2143	2247	-104	-4.6	1190	1190	-1	0	0.4148	0.4208	-0.0061	-1
3	5042	4987	56	1.1	3042	3035	7	0.2	1169	1159	11	1	0.4128	0.4191	-0.0063	-2
4	5048	4966	82	1.6	4025	4030	-5	-0.1	1193	1161	33	3	0.4119	0.4178	-0.0059	-1
5	7079	7103	-24	-0.3	1453	1480	-27	-1.8	1695	1693	2	0	0.5636	0.5969	-0.0333	-6
6	7053	7059	-6	-0.1	2243	2274	-31	-1.4	1561	1618	-57	-4	0.5615	0.5937	-0.0322	-5
7	7103	7111	-8	-0.1	3036	3059	-23	-0.8	1557	1612	-55	-4	0.5657	0.5981	-0.0325	-5
8	7060	7038	23	0.3	4007	4045	-39	-1.0	1567	1591	-24	-2	0.5631	0.5941	-0.0310	-5
9	9559	9563	-4	0.0	1400	1629	-229	-14.0	2164	2197	-33	-2	0.7543	0.8350	-0.0807	-10
10	9585	9573	12	0.1	2379	2398	-19	-0.8	2043	2158	-116	-6	0.7561	0.8380	-0.0819	-10
11	9545	9578	-33	-0.3	3088	3196	-108	-3.4	1997	2139	-141	-7	0.7523	0.8415	-0.0893	-11
12	9598	9578	20	0.2	4103	4193	-90	-2.1	1987	2143	-156	-8	0.7555	0.8423	-0.0868	-10
13	12033	12050	-17	-0.1	1372	1434	-62	-4.3	2559	2740	-182	-7	0.9488	1.0776	-0.1289	-12
14	12039	12009	30	0.2	2173	2339	-166	-7.1	2483	2752	-269	-11	0.9499	1.0757	-0.1258	-12
15	12038	12090	-52	-0.4	3284	3212	72	2.2	2414	2732	-318	-13	0.9501	1.0804	-0.1302	-12
16	12095	11984	111	0.9	4338	4137	200	4.8	2387	2668	-281	-12	0.9545	1.0715	-0.1170	-11
17	15028	15022	5	0.0	2338	2463	-124	-5.0	3040	3484	-445	-15	1.1872	1.3716	-0.1845	-13
18	15040	14927	113	0.7	2960	3300	-340	-10.3	3003	3394	-391	-13	1.1890	1.3619	-0.1729	-13
19	15025	14941	84	0.6	4150	4119	31	0.8	2943	3345	-402	-14	1.1891	1.3634	-0.1742	-13
20	14915	14977	-62	-0.4	5138	5094	44	0.9	2870	3299	-429	-15	1.1810	1.3662	-0.1852	-14
21	16990	16933	58	0.3	2320	2192	129	5.9	3396	3802	-406	-12	1.3336	1.5325	-0.1989	-13
22	16873	16947	-74	-0.4	3112	3148	-36	-1.2	3344	3798	-454	-14	1.3327	1.5356	-0.2029	-13
23	16938	17002	-63	-0.4	4109	4001	108	2.7	3301	3767	-467	-14	1.3389	1.5387	-0.1998	-13
24	16930	16996	-67	-0.4	5096	5004	92	1.8	3251	3673	-422	-13	1.3372	1.5368	-0.1996	-13
25	21954	22058	-104	-0.5	3119	3067	52	1.7	4266	4321	-55	-1	1.7372	1.9342	-0.1970	-10
26	22020	21927	93	0.4	4119	4054	64	1.6	4277	4324	-47	-1	1.7124	1.9198	-0.2074	-11
27	21896	22057	-161	-0.7	5105	5003	102	2.0	4218	4364	-146	-3	1.7021	1.9313	-0.2292	-12
28	26043	25894	149	0.6	3990	4038	-48	-1.2	4907	4636	271	6	2.0307	2.2208	-0.1902	-9
29	25816	25871	-56	-0.2	5113	5046	66	1.3	4862	4618	244	5	2.0124	2.2208	-0.2084	-9
30	25915	25623	291	1.1	6484	6444	40	0.6	4841	4659	182	4	2.0180	2.2045	-0.1865	-8

4.2.4 Modified Froude Number:

In order to better analyze the effect of inclination on the overall mean two-phase heat transfer coefficient, we modified the superficial liquid Froude number and defined it as:

$$Fr_{SL} = \frac{u_{SL}}{\sqrt{Dg\sin(\theta)}} \quad (4.6)$$

Mouza *et al* (2002), used a similar form of liquid Froude number to develop a correlation for inclined tubes. Using the modified superficial liquid Froude number a distinct effect of the inclination was observed on the overall mean heat transfer coefficient. Figure 4.64 shows the variation of the overall mean two-phase heat transfer coefficient using the superficial liquid Froude number as defined in equation (4.5). The effect of modified superficial liquid Froude number can be seen in Figure 4.65. For easy distinction between the graphs we have named the superficial liquid Froude number of Eq (4.5) as $Fr_{Horizontal}$, since the calculation of superficial liquid Froude number for all the inclined tube positions have been done using the form used for the calculation of horizontal data. The superficial liquid number of Eq (4.6) has been named as $Fr_{Inclined}$, since we have introduced the $\sin(\Theta)$ term to bring the effect of inclination.

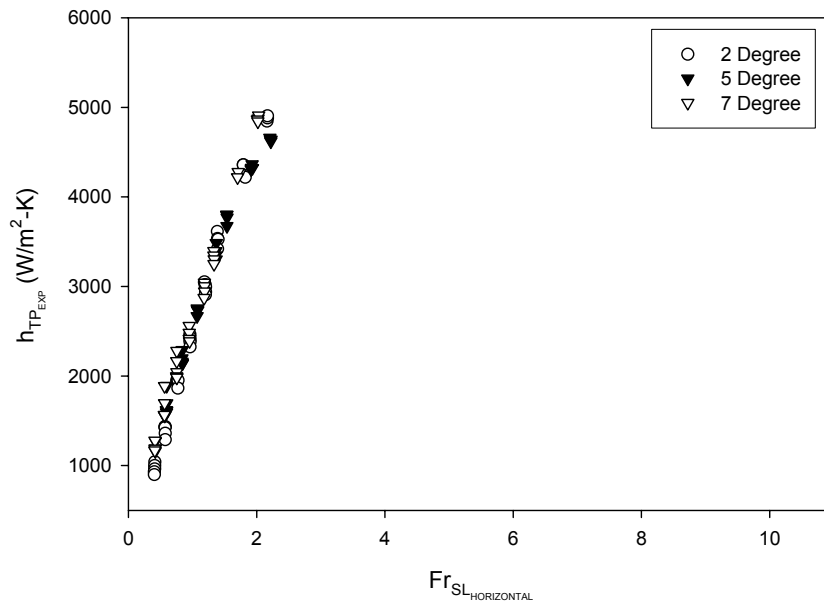


Figure 4.64: Variation of overall mean heat transfer coefficient with changing superficial liquid Froude number (using Eq 4.5 to calculate Fr_{SL})

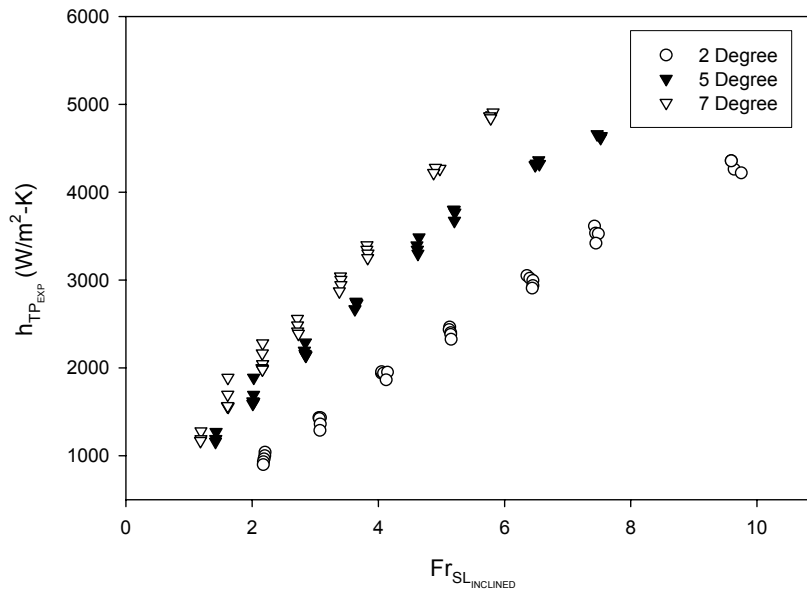


Figure 4.65: Variation of overall mean heat transfer coefficient with changing superficial liquid Froude number (using Eq 4.6 to calculate Fr_{SL})

We observe from Figure 4.64, that the 2 degree, 5 degree and 7 degree data collapses on each other, showing no significant effect of inclination on heat transfer. Figure 4.65, shows a significant effect of inclination on the overall mean two-phase heat transfer coefficient.

Since, we are in the process of evaluating the significance of forms of superficial liquid Froude number on the overall mean two-phase heat transfer coefficient, we infer that the modified superficial liquid Froude can be an important unifying link between the horizontal and inclined data.

As we need to develop a unified correlation for horizontal, 2 degree, 5 degree and 7 degree data, it is felt that the use of a similar form of modified superficial liquid Froude number can be useful in developing a unified correlation for slug flow data.

4.3 Slug Flow Heat Transfer Correlation

After evaluating the important form of superficial liquid Froude number that can contribute as an important unifying link between the horizontal and inclined data, we defined a new term named “Inclination Factor”, which can be used directly in the general correlation of Kim and Ghajar (2002), and a complete unified correlation for horizontal and inclined slug flow data can be obtained.

The Inclination factor is defined as:

$$\text{Inclination factor} = \left(\frac{Dg \sin(\theta)}{u_{sl}^2} \right) \quad (4.7)$$

In this section, new constants were obtained to help predict slug flow heat transfer results using the modified correlation of Kim and Ghajar (2002) by introducing the inclination factor. Also, separate sets of exponents were obtained for only inclined and horizontal slug flow data. The results of the slug flow test runs were fit with new constants using a regression program located within the computer software Sigma Plot.

4.3.1 Slug Flow Heat Transfer Correlation Development:

The 141 slug flow data points measured at the horizontal and inclined positions were used to develop the new constants for the modified equation suggested by Kim and Ghajar (2002). Many trial runs were performed to obtain the best set of constants for the modified Kim and Ghajar (2002) general correlation. The modified correlation with different sets of exponents is presented in Table 4.12.

Figure 4.66 shows the slug flow correlation prediction for the complete set of the horizontal and inclined data points (141 data points). It was observed that 92% of the data points fell within the $\pm 15\%$ deviation band. The prediction had a mean deviation of 6.87 %, with a deviation range of 24.9% and -13.69%. The prediction showed a RMS deviation of 8.69%. From Figure 4.66, we observe that the majority of the data points are clustered towards the 0% deviation reference, showing the quality of the good fit.

Table 4.12 Recommended values for modified Kim and Ghajar (2002) correlation for slug flow data

General Form of the two-phase slug flow heat transfer coefficient correlation:																
$h_{TP} = (1 - \alpha) h_L \left[1 + C \left(\frac{x}{1-x} \right)^m \left(\frac{\alpha}{1-\alpha} \right)^n \left(\frac{Pr_G}{Pr_L} \right)^p \left(\frac{\mu_G}{\mu_L} \right)^q \left(1 + \frac{Dg \sin(\theta)}{u^2 SL} \right)^r \right]$																
Experimental Data	Value of C and Exponents (m, n, p, q, r)					Range of Dev. (%)	Number of Data within $\pm 15\%$	RMS Dev. (%)	Mean Dev. (%)	Range of Parameter						
	C	m	n	p	q					r	$\left(\frac{x}{1-x} \right)$	$\left(\frac{\alpha}{1-\alpha} \right)$	$\left(\frac{Pr_G}{Pr_L} \right)$	$\left(\frac{\mu_G}{\mu_L} \right)$	$\left(\frac{Dg \sin(\theta)}{u^2 SL} \right)$	
Complete slug flow Data from Current Study (141 points) (0.2, 5.7 Deg)	90	1.34	-1.7	0.7	-1.18	-0.7	24.92 and -13.69	129	8.69	6.87	8.69	4912 to 26070	0.5079 to 3.701	0.0744 to 0.1077	0.0132 to 0.0191	0 to 0.715
Inclined Slug flow data (105 data points)	90	1.34	-1.7	0.7	-1.18	-0.7	24.92 and -11.87	98	8.16	6.34	8.16	4948 to 26042	0.4897 to 3.191	0.0744 to 0.0887	0.0132 to 0.0158	0.0074 to 0.718
Horizontal Slug flow data (36 data points)	72	1.29	-1.9	0.7	-1.18	0	16.57 and -10.07	35	7.14	5.84	7.14	4891 to 26070	0.8976 to 3.7013	0.0951 to 0.1077	0.0169 to 0.0191	0

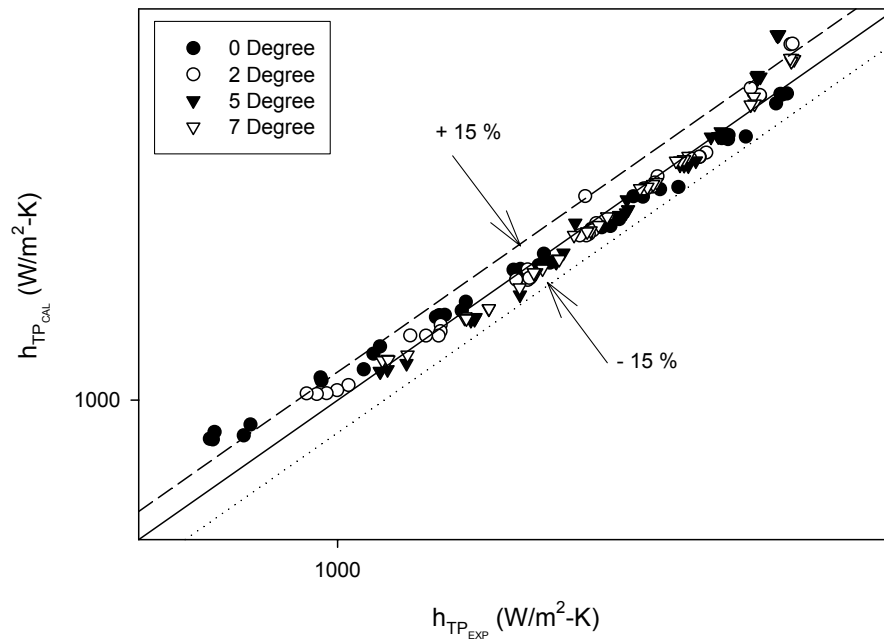


Figure 4.66 Slug flow correlation prediction of complete data set (141 data points) using new constants for the modified Kim and Ghajar (2002) correlation

Individual fit was obtained for the inclined data, in this the horizontal data points were removed. On making many trial runs, it was observed that the exponents obtained for the complete fit of horizontal and inclined data, gave the best results for this individual inclined data fit. Hence, the same set of exponents were retained for this case of individual inclined fit. Figure 4.67 shows the slug flow correlation prediction for the inclined data points (105 data points). It was observed that 93.3% of the data points fell within the $\pm 15\%$ deviation band. The prediction had a mean deviation of 6.34 %, with a deviation range of 24.9% and -11.87%. The prediction showed a RMS deviation of 8.16%. From Figure 4.67, we observe that the majority of the data points are clustered towards the 0% deviation reference, showing the quality of the good fit.

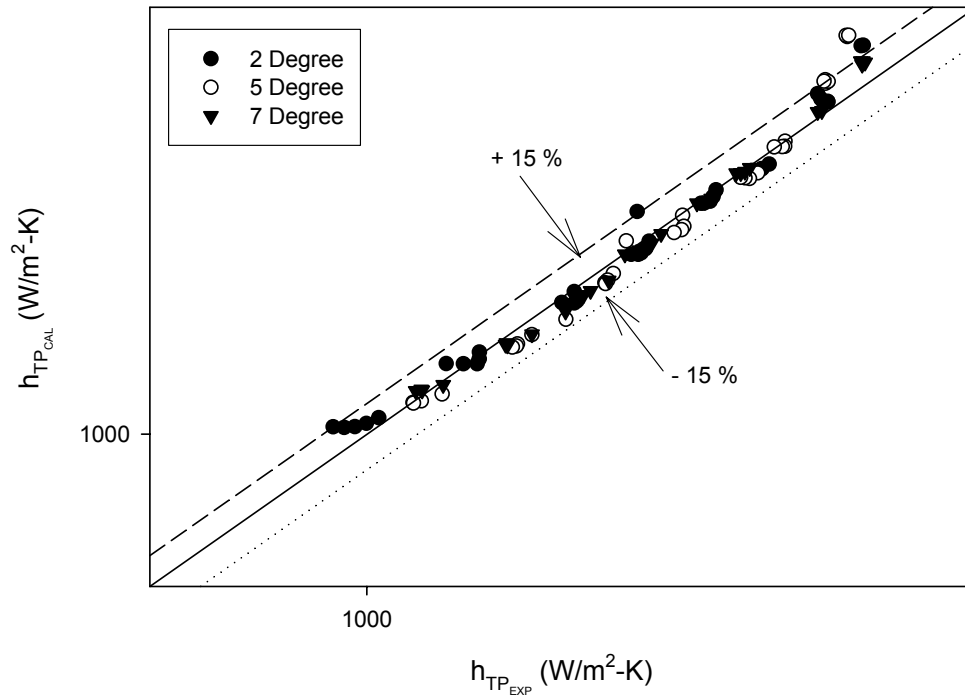


Figure 4.67 Slug flow correlation prediction of inclined data set (105 data points) using new constants for the modified Kim and Ghajar (2002) correlation

Individual fit was also obtained for the horizontal data set (36 data points). A separate set of exponents were obtained which gave the best prediction of the data. Figure 4.68 shows the slug flow correlation prediction for the horizontal data points. It was observed that 97.2% of the data points fell within the $\pm 15\%$ deviation band. The prediction had a mean deviation of 5.84 %, with a deviation range of 16.57% and -10.07%. The prediction showed a RMS deviation of 7.14%.

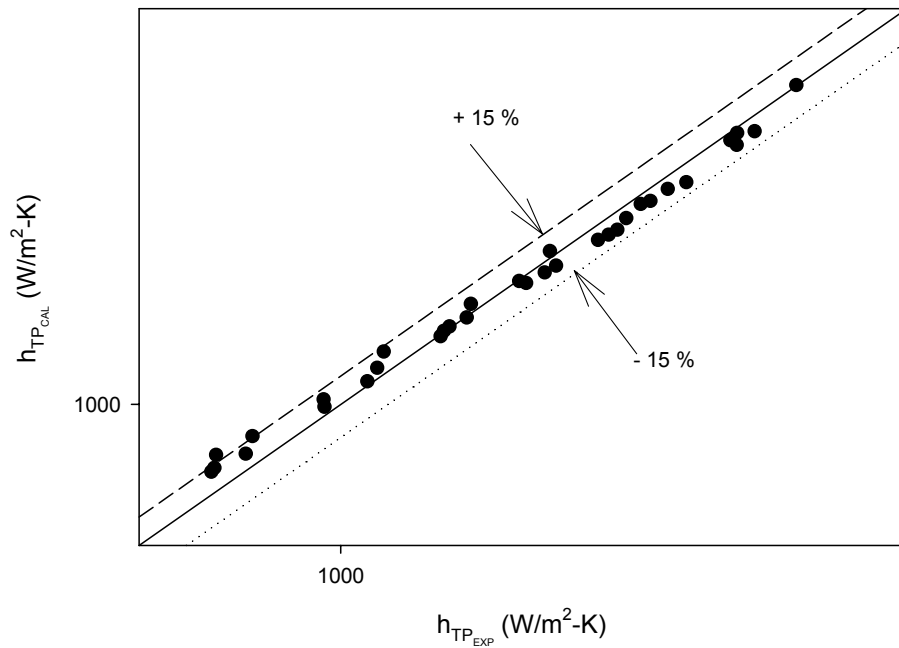


Figure 4.68 Slug flow correlation prediction of horizontal data set (36 data points) using new constants for the modified Kim and Ghajar (2002) correlation

In all the exponents obtained for the modified Kim and Ghajar (2002) general correlation, more than 92% of the data fell within the $\pm 15\%$ in all the cases. The mean deviation ranged from a max. of 6.87% to a min. of 5.84%. The RMS deviation ranged from a max. of 8.69 % to a min. of 7.14%. In all the above correlation predictions, the data was found clustered towards the center of the 0% deviation reference line, showing the quality of the fit.

CHAPTER V

CONCLUSIONS AND RECOMMENDATIONS

A total of 174 slug flow data points were analyzed in this study, of which 141 data points were systematically controlled. Of the systematically controlled data points, 36 data points were at the horizontal position, 37 at the 2-degree position, 34 at the 5-degree position, and 34 at the 7-degree position. The data was then compared against the slug flow data of Kim and Ghajar (2000) and Trimble *et al* (2002) and the results were found in agreement with theirs.

5.1 Conclusions

Detailed explanation fortified by the use of flow visualization pictures was used to explain the physics and the intricacies of the heat transfer behavior. It was observed that the superficial liquid velocity is a dominant factor in the heat transfer of slug flow. On analyzing the inclination effect it was observed that the heat transfer generally increases with the increase of inclination upto 5 degree tube position. At 7 degree tube position, it was observed that the heat transfer decreases. To find the reason for this anomaly in the heat transfer behavior, we utilized the flow visualization. It was observed that the excess formation of bubbles, on some mass flow rates combination, resulted in the drop of heat

transfer. Systematic study was carried out for all Re_{SL} series and detailed explanation was provided for all inclination positions used in this study.

Finally, a modified correlation of Kim and Ghajar (2002) was suggested to predict the heat transfer for this slug flow. It predicted both the horizontal and inclined slug flow heat transfer data and more than 92% of the data points were found within the acceptable deviation range of $\pm 15\%$.

5.2 Recommendations

Further studies upon this subject could allow for a more precise prediction of slug flow heat transfer data. It is recommended that additional systematically controlled runs be performed at higher tube inclinations, so as to fortify the findings of this current study and build a bigger data base.

Additional slug flow heat transfer runs, would benefit the research by allowing for the inclusion in the formulation of the slug heat transfer exponents for the modified Kim and Ghajar (2002) general correlation.

BIBLIOGRAPHY

- Alves, G.E., (1954), "Co-current liquid-gas flow in a pipe-line contractor," Chemical Engineering Progress, Vol. 50, No. 9, pp. 449-456.
- Baker, O. (1954), "Simultaneous Flow of Oil and Gas," Oil and Gas J., Vol. 53, pp. 185-195.
- Barnea, D. and N. Yacoub (1983), "Heat Transfer in Vertical Upwards Gas-Liquid Slug Flow," Int. J. Heat Mass Transfer, Vol. 26, No. 9, pp. 1365-1376.
- Bergelin, O.P., Kegel, P.K., Carpenter, F.G., Gazley, C. Jr. (1949), "Co-current gas liquid flow. II. Flow in vertical tubes," Heat Transfer and Fluid Mechanics Institute, pp. 19-28.
- Colburn, A.P. (1933), "A Method of Correlating Forced Convection Heat Transfer Data and a Comparison with Liquid Friction," Trans. Am. Inst. Chem. Engrs, Vol. 29, pp. 174-210.
- Dukler, A.E. and O. Shaharabany (1977), For Multiphase Processing, Studies in Intermittent (Slug) Flow in Horizontal Tubes: Design Manual I-2, American Institute of Chemical Engineers, New York.
- Durant, W.B., 2003, "Heat Transfer Measurement of Annular Two-Phase Flow in Horizontal and a Slightly Upward Inclined Tube," M.S.Thesis, Oklahoma State University, Stillwater, OK.
- Ewing, M. E., Weinandy, J. J. and Christensen, R. N. (1999), "Observations of Two-Phase Flow Patterns in a Horizontal Circular Channel," Heat Transfer Engineering, Vol. 20, No. 1, pp. 9-14.
- Ghajar, A. J. and Tam, L. M., (1994), "Heat Transfer Measurements and Correlations in the Transition Region for a Circular Tube with Three Different Inlet Configurations," Experimental Thermal and Fluid Science, Vol. 8, No. 1, pp. 79-90.
- Ghajar, A. J. and Zurigat, Y. H., "Microcomputer-Assisted Heat Transfer Measurements/Analysis in a Circular Tube," International Journal of Applied Engineering Education, Vol. 7, No. 2, pp. 125-134, 1991.

- Gnielinski, V. (1976), "New Equations for Heat and Mass Transfer in Turbulent Pipe and Channel Flow," *Int. Chem. Eng.*, Vol. 16, No. 2, pp. 359-368.
- Govier, G.W. and K. Aziz (1972), "The Flow of Complex Mixtures in Pipes". Van Nostrand Reinhold Company, New York.
- Govier, G.W. and Omer. M.M, (1962), "The Horizontal Pipeline Flow of Air-Water Mixtures," *The Canadian Journal of Chemical Engineering*, Vol. 40, pp. 93-104.
- Hestroni, G., Yi, J. H., Hu, B. G., Mosyak, L. P., Ziskind, G. (1998a) "Heat Transfer in Intermittent Air-Water Flows – Part II," *Int. J. Multiphase Flow*, Vol. 24, No. 2, pp. 165-188.
- Hestroni, G., Yi, J. H., Hu, B. G., Mosyak, L. P., Ziskind, G. (1998b) "Heat Transfer in Intermittent Air-Water Flows – Part II," *Int. J. Multiphase Flow*, Vol. 24, No. 2, pp. 189-212, 1998
- Hoogendoorn, C.J., (1959) "Gas liquid flow in horizontal pipes," *Chemical Engineering Science*, Vol. 9, pp. 205 – 217.
- Hubbard, M.G. and A.E. Dukler (1975), "A Model for Gas-Liquid Slug Flow in Horizontal and Near Horizontal Tubes," *Ind. Eng. Che. Fund.*, Vol. 14, No. 4, pp. 337-347.
- Hughmark, G.A. (1965), "Holdup and Heat Transfer in Horizontal Slug Gas Liquid Flow," *Chem. Engng. Sci.*, Vol. 20, pp. 1007-1010.
- Johnson, H. A. and A. H. Abou-Sabe (1952), "Heat Transfer and Pressure Drop for Turbulent Flow of Air-Water Mixture in a Horizontal Pipe," *ASME Trans.*, Vol. 74, pp. 977-987.
- Kago, T., Saruwatari, T., Kashima, M., Marooka, S. and Kato, Y., (1986), "Heat Transfer in Horizontal Plug and Slug Flow for Gas-Liquid and Gas-Slurry Systems," *J.Chem. Eng. Jpn*, Vol. 19, pp. 125-131.
- Kim, D. (2000) "An Experimental and Empirical Investigation of Convective Heat Transfer for Gas-Liquid Two-Phase Flow in Vertical and Horizontal Pipes," Ph.D. Dissertation, Oklahoma State University.
- Kim, D., A.J. Ghajar and R.L. Dougherty, (2000), "Robust Heat Transfer Correlation for Turbulent Gas-Liquid Flow in Vertical Pipes," *Journal of Thermophysics and Heat Transfer*, Vol. 14, No. 4, pp. 574-578.

- Kim, D., A.J. Ghajar, R.L. Dougherty and V.K. Ryali (1999a), "Comparison of Twenty Two-Phase Heat Transfer Correlations with Seven Sets of Experimental Data, Including Flow Pattern and Tube Orientation Effects," *Heat Transfer Engineering*, Vol. 20, No. 1, pp. 15-40.
- Kim, D., and Ghajar, A. J., (2002), "Heat Transfer Measurements and Correlations for Air-Water Flow of Different Flow Patterns in a Horizontal Pipe," *Experimental Thermal and Fluid Science*, Vol. 25, No. 8, pp 659-676.
- Kim, J. (1999) "Construction and Performance Testing of a Uniform Heat Flux Two-Phase Gas-Liquid Experimental Setup Using a Horizontal Circular Tube," M.S. Thesis, Oklahoma State University, Stillwater, OK.
- Kosterin, S.I., (1949), "An investigation of the influence of diameter and inclination of a tube on the hydraulic resistance and flow structure of gas-liquid mixtures," *Izv Akad Nauk SSSR, Otd Tekh Nauk*," Vol. 12, pp. 1824-1835.
- Mandhane, J.M., G.A. Gregory and K. Aziz (1974), "Flow Pattern Map for Gas-Liquid Flow in Horizontal Pipes," *Int. J. Multiphase Flow*, Vol. 1, pp. 537-553.
- Mouza, A.A., Paras, V., Karabelas, A.J., (2002), "Influence of small tube diameter and inclination angle on flooding phenomena," *International congress of chemical and process engineering, Prague*, Aug. 2002.
- Oliver, D. R. and S. J. Wright (1964), "Pressure Drop and Heat Transfer in Gas-Liquid Slug Flow in Horizontal Tubes," *British Chem. Engrg.*, Vol. 9, No. 9, pp. 590 - 596.
- Oliver, D.R. and A. Young Hoon (1968), "Two-Phase Non-Newtonian Flow. Part II: Heat Transfer," *Trans. INSTN Chem. Engrs.*, Vol. 46, pp. T116-T122.
- Ryali, V. K (1999), "Design, Construction and Testing of a Single-Phase and Two-Phase Fluid Flow System in a Horizontal Circular Tube with Constant Heat Flux," MS Thesis, School of Mechanical and Aerospace Engineering, Oklahoma State University, Stillwater, OK.
- Scott, D.S., (1963), "Properties of Co-current Gas-Liquid Flow", *Advances in Chemical Engineering*, Academic Press, New York, Vol. 4, pp. 200-277.
- Shaharabanny, O. (1976), "Experimental Investigation of Heat Transfer in Slug Flow in Horizontal Tubes," M.Sc. Thesis, University of Houston.
- Shoham, O., A.E. Dukler and Y. Taitel (1982), "Heat Transfer During Intermittent/Slug Flow in Horizontal Tubes," *Ind. Eng. Chem. Fundam.*, Vol. 21, pp. 312-319.

- Sieder, E.N. and G.E. Tate (1936), "Heat Transfer and Pressure Drop of Liquids in Tubes," *Ind. Eng. Chem.*, Vol. 28, No. 12, p. 1429.
- Taitel, Y. and A.E. Dukler (1976), "A Model for Predicting Flow Regime Transitions in Horizontal and Near Horizontal Gas-Liquid Flow," *AIChE Journal*, Vol. 22, No. 1, pp. 47-54.
- Taitel, Y. and A.E. Dukler (1977), "Flow Regime Transitions for Vertical Upward Gas-Liquid Flow: A Preliminary Approach through Physical Modeling," Paper Presented at Session on *Fundamental Research in Fluid Mechanics at the 70th AIChE Annual Meeting*, New York.
- Trimble, S., Kim, J., and Ghajar, A. J. (2002), "Experimental Heat Transfer Comparison in Air-Water Slug Flow in a Slightly Upward Inclined Tube," Heat Transfer 2002, *Proceedings of the Twelfth International Heat Transfer Conference*, Elsevier, pp. 569-574, 2002.
- Vijay, M.M., M.A. Aggour and G.E. Sims (1982), "A Correlation of Mean Heat Transfer Coefficients for Two-Phase Two-Component Flow in a Vertical Tube," *Proceedings of 7th Int. Heat Transfer Conference*, Vol. 5, pp. 367-372.
- Vijay, M.M. (1978), "A Study of Heat Transfer in Two-Phase Two-Component Flow in a Vertical Tube," PhD. Thesis, University of Manitoba, Winnipeg Canada, 1978.
- White, P.D., and Huntington, R.L., (1955), "Horizontal Co-Current Two-Phase Flow of Fluids in Pipe Lines," *The Petroleum Engineer*, Vol. 27, No. 9, pp. D40-D45.

APPENDIX A

SOURCE CODE

“2HT03FALL”

(A program to calculate the inside wall temperatures and local heat transfer coefficients for given outside wall temperatures for two-phase heat transfer studies in tubes)
The computer program is developed by Jae-yong Kim (PhD Candidate) based on the work of Ghajar and Zurigat (1991)

```
#include ".\2PhHT.h"  
#include ".\HTCal.h"  
#include ".\ReadData.h"  
#include ".\Properties.h"  
#include ".\PrintData.h"  
#include ".\TPhVars.h"  
#include ".\TPhPress.h"  
#include ".\SetOfData.h"
```

```
const char *HeadLine_SI = "gNum runNum FlowPattern Inclination[deg] ReSL ReSG avgHTC[W/m^2-K]  
OverallHTC[W/m^2-K] QBalErr[%] Tin[C] Tout[C] DT[C] Amp[A] Volt[V] QFlux[W/m^2] QGen[W]  
QTaken[W] LqdVFR[m^3/s] GasVFR[m^3/s] LqdMFR[kg/s] GasMFR[kg/s] LqdMFR[kg/min]  
GasMFR[kg/min] VSL[m/s] VSG[m/s] Pref[Pa] LqdPR GasPR LqdDens[kg/m^3] GasDens[kg/m^3]  
LqdCp[kJ/kg-K] GasCp[kJ/kg-K] LqdVisc[Pa-s] GasVisc[Pa-s] LqdVisc_B/W LqdCond[W/m-K]  
GasCond[W/m-K] Gt[kg/m^2-s] x Kslip alpha ReTP ReL Xtd Ttd Ytd Ftd Ktd Xbr jg";  
//const char *HeadLine_SI = "gNum runNum testDate FlowPattern Inclination[deg] ReSL ReSG  
avgHTC[W/m^2-K] OverallHTC[W/m^2-K] QBalErr[%] Tin[C] Tout[C] DT[C] Amp[A] Volt[V]  
QFlux[W/m^2] QGen[W] QTaken[W] LqdVFR[m^3/s] GasVFR[m^3/s] LqdMFR[kg/s] GasMFR[kg/s]  
LqdMFR[kg/min] GasMFR[kg/min] VSL[m/s] VSG[m/s] Pref[Pa] LqdPR GasPR LqdDens[kg/m^3]  
GasDens[kg/m^3] LqdCp[kJ/kg-K] GasCp[kJ/kg-K] LqdVisc[Pa-s] GasVisc[Pa-s] LqdVisc_B/W  
LqdCond[W/m-K] GasCond[W/m-K] Gt[kg/m^2-s] x Kslip alpha ReTP ReL Xtd Ttd Ytd Ftd Ktd Xbr jg";
```

```
const char *HeadLine_FPS = "gNum runNum FlowPattern Inclination[deg] ReSL ReSG avgHTC[BTU/hr-  
ft^2-F] OverallHTC[BTU/hr-ft^2-F] QBalErr[%] Tin[F] Tout[F] DT[F] Amp[A] Volt[V] QFlux[BTU/hr-  
ft^2] QGen[BTU/hr] QTaken[BTU/hr] LqdVFR[ft^3/hr] GasVFR[ft^3/hr] LqdMFR[lbm/hr]  
GasMFR[lbm/hr] VSL[ft/s] VSG[ft/s] Pref[psi] LqdPR GasPR LqdDens[lbm/ft^3] GasDens[lbm/ft^3]  
LqdCp[BTU/lbm-F] GasCp[BTU/lbm-F] LqdVisc[lbm/hr-ft] GasVisc[lbm/hr-ft] LqdVisc_B/W  
LqdCond[BTU/hr-ft-F] GasCond[BTU/hr-ft-F] Gt[lbm/ft^2-hr] x Kslip alpha ReTP ReL Xtd Ttd Ytd Ftd  
Ktd Xbr jg";  
//const char *HeadLine_FPS = "gNum runNum testDate FlowPattern Inclination[deg] ReSL ReSG  
avgHTC[BTU/hr-ft^2-F] OverallHTC[BTU/hr-ft^2-F] QBalErr[%] Tin[F] Tout[F] DT[F] Amp[A] Volt[V]  
QFlux[BTU/hr-ft^2] QGen[BTU/hr] QTaken[BTU/hr] LqdVFR[ft^3/hr] GasVFR[ft^3/hr]  
LqdMFR[lbm/hr] GasMFR[lbm/hr] VSL[ft/s] VSG[ft/s] Pref[psi] LqdPR GasPR LqdDens[lbm/ft^3]  
GasDens[lbm/ft^3] LqdCp[BTU/lbm-F] GasCp[BTU/lbm-F] LqdVisc[lbm/hr-ft] GasVisc[lbm/hr-ft]
```

LqdVisc_B/W LqdCond[BTU/hr-ft-F] GasCond[BTU/hr-ft-F] Gt[lbm/ft²-hr] x Kslip alpha ReTP ReL
 Xtd Ttd Ytd Ftd Ktd Xbr jg";

```

////////////////////////////////////
int mainFrame(int gNum, char* runNum, char* Pattern, double deg, CSetOfData *aDBLine_SI,
CSetOfData *aDBLine_FPS);
////////////////////////////////////
int main(void)
{
    CSetOfData DBLine_SI, DBLine_FPS;
    CSetOfData *aDBLine_SI = &DBLine_SI;
    CSetOfData *aDBLine_FPS = &DBLine_FPS;

    int groupNum, num_data_pts = 0;
    char *runNum, RNXXXX[10], aLine[300];
    char Pattern[10];
    double ReSL, ReSG, deg;

    char *dbase_SI = "DB2PHT_SI.DAT";
    char *dbase_FPS = "DB2PHT_FPS.DAT";

    ifstream my2PHT_DS;
    ofstream my2PHT_DB_SI;
    ofstream my2PHT_DB_FPS;

    my2PHT_DS.open("DS2PHT.TXT");
    my2PHT_DB_SI.open(dbase_SI);
    my2PHT_DB_FPS.open(dbase_FPS);

    if(!my2PHT_DS)
    {
        cerr<<"cannot open 'DS2PHT.TXT' file"<<endl;
        exit(1);
    }
    if(!my2PHT_DB_SI)
    {
        cerr<<"cannot open 'DB2PHT_SI.DAT' file"<<endl;
        exit(1);
    }
    if(!my2PHT_DB_FPS)
    {
        cerr<<"cannot open 'DB2PHT_FPS.DAT' file"<<endl;
        exit(1);
    }

    my2PHT_DS.getline(aLine, 300, '\n');my2PHT_DS.ignore();
    my2PHT_DS.getline(aLine, 300, '\n');my2PHT_DS.ignore();

    my2PHT_DB_SI << HeadLine_SI << endl;
    my2PHT_DB_FPS << HeadLine_FPS << endl;

    while(!my2PHT_DS.eof())
    {
        my2PHT_DS >> groupNum >> RNXXXX >> ReSL >> ReSG >> Pattern >> deg;
        if (groupNum == 99999) goto to01;
    }
}

```

```

cout << groupNum <<"\t"<< RNXXXX <<"\t"<< ReSL <<"\t"<< ReSG <<"\t"<< Pattern
<<"\t"<< deg <<"\t";
runNum = &RNXXXX[2];
mainFrame(groupNum, runNum, Pattern, deg, aDBLine_SI, aDBLine_FPS);

my2PHT_DB_SI
    << aDBLine_SI->gNum    <<" " << aDBLine_SI->runNum <<" //" <<
aDBLine_SI->testDate <<" "
    << aDBLine_SI->FlwPatn <<" " << aDBLine_SI->Deg    <<" "
    << aDBLine_SI->ReSL    <<" " << aDBLine_SI->ReSG    <<" "
    << aDBLine_SI->JK_HTC  <<" " << aDBLine_SI->DK_HTC  <<" " <<
aDBLine_SI->QBalErr <<" "
    << aDBLine_SI->Tin     <<" " << aDBLine_SI->Tout   <<" " <<
aDBLine_SI->DT        <<" "
    << aDBLine_SI->Amp     <<" " << aDBLine_SI->Volt   <<" "
    << aDBLine_SI->QFlux   <<" " << aDBLine_SI->QGen   <<" " <<
aDBLine_SI->QTaken   <<" "
    << aDBLine_SI->LqdVFR  <<" " << aDBLine_SI->GasVFR  <<" "
    << aDBLine_SI->LqdMFR  <<" " << aDBLine_SI->GasMFR  <<" "
    << aDBLine_SI->LqdMFR*60. <<" " << aDBLine_SI->GasMFR*60. <<" "
    << aDBLine_SI->VSL    <<" " << aDBLine_SI->VSG    <<" " <<
aDBLine_SI->Pref    <<" "
    << aDBLine_SI->LqdPr  <<" " << aDBLine_SI->GasPr  <<" "
    << aDBLine_SI->LqdRho <<" " << aDBLine_SI->GasRho <<" "
    << aDBLine_SI->LqdCp  <<" " << aDBLine_SI->GasCp  <<" "
    << aDBLine_SI->LqdVisc <<" " << aDBLine_SI->GasVisc <<" " <<
aDBLine_SI->LqdVisc_BW <<" "
    << aDBLine_SI->LqdCond <<" " << aDBLine_SI->GasCond <<" "
    << aDBLine_SI->Gt     <<" " << aDBLine_SI->x       <<" "
    << aDBLine_SI->Kslip  <<" " << aDBLine_SI->alpha  <<" "
    << aDBLine_SI->ReTP   <<" " << aDBLine_SI->ReL    <<" "
    << aDBLine_SI->Xtd   <<" " << aDBLine_SI->Ttd   <<" " <<
aDBLine_SI->Ytd     <<" "
    << aDBLine_SI->Ftd   <<" " << aDBLine_SI->Ktd   <<" "
    << aDBLine_SI->Xbr   <<" " << aDBLine_SI->jg    << endl;

my2PHT_DB_FPS
    << aDBLine_FPS->gNum  <<" " << aDBLine_FPS->runNum <<" //" <<
aDBLine_FPS->testDate <<" "
    << aDBLine_FPS->FlwPatn <<" " << aDBLine_FPS->Deg    <<" "
    << aDBLine_FPS->ReSL    <<" " << aDBLine_FPS->ReSG    <<" "
    << aDBLine_FPS->JK_HTC  <<" " << aDBLine_FPS->DK_HTC  <<" " <<
aDBLine_FPS->QBalErr <<" "
    << aDBLine_FPS->Tin     <<" " << aDBLine_FPS->Tout   <<" " <<
aDBLine_FPS->DT        <<" "
    << aDBLine_FPS->Amp     <<" " << aDBLine_FPS->Volt   <<" "
    << aDBLine_FPS->QFlux   <<" " << aDBLine_FPS->QGen   <<" " <<
aDBLine_FPS->QTaken   <<" "
    << aDBLine_FPS->LqdVFR  <<" " << aDBLine_FPS->GasVFR  <<" "
    << aDBLine_FPS->LqdMFR  <<" " << aDBLine_FPS->GasMFR  <<" "
    << aDBLine_FPS->VSL    <<" " << aDBLine_FPS->VSG    <<" " <<
aDBLine_FPS->Pref    <<" "
    << aDBLine_FPS->LqdPr  <<" " << aDBLine_FPS->GasPr  <<" "
    << aDBLine_FPS->LqdRho <<" " << aDBLine_FPS->GasRho <<" "
    << aDBLine_FPS->LqdCp  <<" " << aDBLine_FPS->GasCp  <<" "

```

```

aDBLine_FPS->LqdVisc_BW << "
    << aDBLine_FPS->LqdVisc << " " << aDBLine_FPS->GasVisc << " " <<
    << aDBLine_FPS->LqdCond << " " << aDBLine_FPS->GasCond << " "
    << aDBLine_FPS->Gt << " " << aDBLine_FPS->x << " "
    << aDBLine_FPS->Kslip << " " << aDBLine_FPS->alpha << " "
    << aDBLine_FPS->ReTP << " " << aDBLine_FPS->ReL << " "
    << aDBLine_FPS->Xtd << " " << aDBLine_FPS->Ttd << " " <<
aDBLine_FPS->Ytd << " "
    << aDBLine_FPS->Ftd << " " << aDBLine_FPS->Ktd << " "
    << aDBLine_FPS->Xbr << " " << aDBLine_FPS->jg << endl;

```

```

    num_data_pts++;

```

```

}

```

```

to01:

```

```

    cout << "Total Data Points: " << num_data_pts << endl;

```

```

    my2PHT_DS.close();
    my2PHT_DB_SI.close();
    my2PHT_DB_FPS.close();

```

```

    return 0;

```

```

}

```

```

int mainFrame(int gNum, char* runNum, char* Pattern, double deg, CSetOfData *aDBLine_SI,
CSetOfData *aDBLine_FPS)
{

```

```

    CHTCal dataSet;
    CProperties property;
    CPrintData prnt;
    CTPhVars vars2ph;
    CTPhPress press;

```

```

    int k;
    double Tin, Tout, Tavg;
    double **Tinwall;
    double Tbulk[NUM_ST], Twall[NUM_ST];
    double mdotL, mdotG;
    double Pref;
    double Ampere, Volt;
    double QFluxavg, Qgen, QgenCal, QgenErr;
    double Qtaken, QbalErr;
    double QFlux[NUM_ST], HCoeff[NUM_ST], HCoeffTB[NUM_ST];
    double Nu[NUM_ST];

```

```

    double rhoLavg, kLavg, muLavg, CpLavg;
    double rhoGavg, kGavg, muGavg, CpGavg;

```

```

    double VSLavg, VSGavg;
    double ReSLavg, ReSGavg;
    double PrLavg, PrGavg;

```

```

    double rhoL[NUM_ST], kL[NUM_ST], muL[NUM_ST], CpL[NUM_ST];
    double rhoG[NUM_ST], kG[NUM_ST], muG[NUM_ST], CpG[NUM_ST];

```

```

double ReSL[NUM_ST],ReSG[NUM_ST];
double PrL[NUM_ST], PrG[NUM_ST];

double muLwall[NUM_ST],muGwall[NUM_ST];
double muLBW[NUM_ST], muGBW[NUM_ST];

double **ReSLwall = new double *[NUM_ST]; for(k=0;k<NUM_ST;k++) ReSLwall[k] = new
double[NUM_NT];
double **ReSGwall = new double *[NUM_ST]; for(k=0;k<NUM_ST;k++) ReSGwall[k] = new
double[NUM_NT];

////////////////////////////////////

dataSet.ReadFile(runNum);
dataSet.correctTreading();
dataSet.setGeometry();
dataSet.setTbulk();
dataSet.setTinwall_Power_QFluxIn();
////////////////////////////////////

Tinwall = dataSet.getTinwall();
Tin   = dataSet.getTin();
Tout  = dataSet.getTout();
mdotL = dataSet.getLqdMFR();
mdotG = dataSet.getGasMFR();
Pref  = dataSet.getPref();
Ampere = dataSet.getCurrent();
Volt  = dataSet.getVolt();

////////////////////////////////////

Tavg = (Tin+Tout)/2.0;

rhoLavg = property.Density(Tavg,WATER,SI);
kLavg   = property.Conductivity(Tavg,WATER,SI);
CpLavg  = property.SpecificHeat(Tavg,WATER,SI);
muLavg  = property.Viscosity(Tavg,WATER,SI);

rhoGavg = property.Density(Tavg,Pref,AIR,SI);
kGavg   = property.Conductivity(Tavg,AIR,SI);
CpGavg  = property.SpecificHeat(Tavg,AIR,SI);
muGavg  = property.Viscosity(Tavg,AIR,SI);

VSLavg = mdotL/(rhoLavg*CS_AREA);
VSGavg = mdotG/(rhoGavg*CS_AREA);

ReSLavg = ReNo(mdotL,ID_PIPE,muLavg);
ReSGavg = ReNo(mdotG,ID_PIPE,muGavg);

PrLavg = PrNo(muLavg,CpLavg,kLavg);
PrGavg = PrNo(muGavg,CpGavg,kGavg);

////////////////////////////////////

Qgen = Ampere*Volt;
QgenCal = dataSet.getTotalPower();

```

```

QgenErr = (Qgen-QgenCal)/Qgen*100.0;
// cout << "Q generation Error = " << QgenErr << "%" << endl;

Qtaken = (mdotL*CpLavg + mdotG*CpGavg)*(Tout-Tin);
QbalErr = (Qgen - Qtaken)/Qgen*100.0;
// cout << "Heat Balance Error = " << QbalErr << "%" << endl;
cout << QbalErr << "%" << endl;

QFluxavg = Qgen/(PI*ID_PIPE*HLENGTH);

dataSet.setHTCoeff());

////////////////////////////////////
for(k=0;k<NUM_ST;k++)
    for(int j=0;j<NUM_NT;j++)
        {
            ReSLwall[k][j] =
ReNo(mdotL,ID_PIPE,property.Viscosity(Tinwall[k][j],WATER,SI));
            ReSGwall[k][j] =
ReNo(mdotG,ID_PIPE,property.Viscosity(Tinwall[k][j],AIR,SI));
        }

////////////////////////////////////
/*- CALCULATE FLUID PROPERTIES AT EACH THERMOCOUPLE STATION WITH AVG. TEMP -
*/
// GRNO(IST)=G*BETA*RHO**2*(DIN/12)**3*(TAVG(IST)-TBULK(IST))/VISC**2 *3600.0**2
for(k=0;k<NUM_ST;k++)
    {
        Tbulk[k]=dataSet.getTbulk(k);
        rhoL[k] = property.Density(Tbulk[k],WATER,SI);
        kL[k] = property.Conductivity(Tbulk[k],WATER,SI);
        CpL[k] = property.SpecificHeat(Tbulk[k],WATER,SI);
        muL[k] = property.Viscosity(Tbulk[k],WATER,SI);

        rhoG[k] = property.Density(Tbulk[k],Pref,AIR,SI);
        kG[k] = property.Conductivity(Tbulk[k],AIR,SI);
        CpG[k] = property.SpecificHeat(Tbulk[k],AIR,SI);
        muG[k] = property.Viscosity(Tbulk[k],AIR,SI);

        ReSL[k] = ReNo(mdotL,ID_PIPE,muL[k]);
        ReSG[k] = ReNo(mdotG,ID_PIPE,muG[k]);

        PrL[k] = PrNo(muL[k],CpL[k],kL[k]);
        PrG[k] = PrNo(muG[k],CpG[k],kG[k]);

        Twall[k] = dataSet.getTwall(k);
        muLwall[k] = property.Viscosity(Twall[k],WATER,SI);
        muGwall[k] = property.Viscosity(Twall[k],AIR,SI);

        muLBW[k] = muL[k]/muLwall[k];
        muGBW[k] = muG[k]/muGwall[k];

        QFlux[k] = dataSet.getQFavg(k);
        HCoef[k] = dataSet.getHCoef(k);
        HCoefTB[k] = dataSet.getHCTB(k);
    }

```

```

        Nu[k] = NuNo(HCoeff[k],ID_PIPE,kL[k]);
    }
    ////////////////////////////////////////////////////////////////////
    /*- PRINT THE RESULTS TO 2HI FILE -*/
    prnt.setTemps(dataSet.getTroom(),dataSet.getTin(),dataSet.getTout(),dataSet.getToutwall(),Tinwall,
    Tbulk,Twall);
    prnt.setProps(rhoLavg,rhoGavg,CpLavg,CpGavg,muLavg,muGavg,kLavg,kGavg,muLwall,muGwall,muL,
    muG,muLBW,muGBW,CpL,CpG,kL,kG,rhoL,rhoG);
    prnt.setFDynamics(mdotL,mdotG,VSLavg,VSGavg,ReSLavg,ReSGavg,ReSLwall,ReSGwall,ReSL,
    ReSG);
    prnt.setHTprops(PrLavg,PrGavg,QFluxavg,Qgen,Qtaken,QbalErr,dataSet.getQFluxIn(),dataSet.getHTCcoeff(),
    PrL,PrG,HCoeffTB,QFlux,HCoeff,Nu);
    prnt.setPressures(Pref,dataSet.getDPs());
    prnt.setPower(Ampere, Volt);
    prnt.prntHTI_SI(gNum, runNum,dataSet.getTestDate(),Pattern, aDBLine_SI);
    prnt.prntHTI_FPS(gNum, runNum,dataSet.getTestDate(),Pattern, aDBLine_FPS);
    ////////////////////////////////////////////////////////////////////
    vars2ph.set2PhVars(deg, rhoLavg, rhoGavg, muLavg, muGavg, mdotL, mdotG);
    vars2ph.prnt2PhVarsSI(runNum,dataSet.getTestDate(),Pattern, aDBLine_SI);
    vars2ph.prnt2PhVarsFPS(runNum,dataSet.getTestDate(),Pattern, aDBLine_FPS);
    ////////////////////////////////////////////////////////////////////
    //    press.setdP(dataSet.getDPs());
    //    press.setVelandDens(mdotL,mdotG,rhoLavg,rhoGavg);
    //    press.calFraction(deg);
    //    press.prntFractionSI(runNum,dataSet.getTestDate(),Pattern);
    //    press.prntFractionFPS(runNum,dataSet.getTestDate(),Pattern);
    ////////////////////////////////////////////////////////////////////
    for(k=0;k<NUM_ST;k++) delete[] ReSLwall[k]; delete[] ReSLwall;
    for(k=0;k<NUM_ST;k++) delete[] ReSGwall[k]; delete[] ReSGwall;

    return 0;
}

```

```

#include <string>
#include <sstream>
#include <iostream>
#include <fstream>
#include <cstdlib>
#include <iomanip>
#include <cmath>
//////////////////////////////////////////////////////////////////
using namespace std;
//////////////////////////////////////////////////////////////////
const int NUM_ST=10; //Number of
Thermocouple Station
const int NUM_NT=4; //Number of Thermocouple at a Station
const int NUM_PT=2; //Number of Differential Pressure Tap

const int NUM_LAYER = 30; //Number of
Layer in the radial direction in pipe
const int NUM_ND = NUM_LAYER+1; //Number of Node Point in
the radial direction

```

```

const int TOP    = 0;           //Top Thermocouple
location
const int BOTTOM = 2;         //Bottom Thermocouple
location

const double PI    = 3.14159265359;
const double G_SI  = 9.80665;           //[m/s^2]
const double G_FPS = 32.174;           //[lbf]
const double OD_PIPE = 1.315*.0254;    //[in]*UNIT
FACTOR to [m]
const double ID_PIPE = 1.097*.0254;    //[in]*UNIT
FACTOR to [m]
const double HLENGTH = 104.0*.0254;    //[in]*UNIT
FACTOR to [m]
const double LENGTH = 104.0*.0254;    //[in]*UNIT
FACTOR to [m]
const double DR    = (OD_PIPE-ID_PIPE)/2.0/NUM_LAYER;
const double CS_AREA = PI*ID_PIPE*ID_PIPE/4.0; // [m^2] cross-section Area of pipe
const double DL[2] = {100*0.0254,50*.0254}; //distances [m] from ref. pressure
tap to presure tap No.10 and No.5
const double DX[11] = {7.00*.0254, 17.00*.0254, 27.00*.0254, 37.00*.0254, 47.00*.0254,
57.00*.0254, 67.00*.0254, 77.00*.0254, 87.00*.0254,
97.00*.0254, HLENGTH};
//                               = {6.75, 16.75, 26.75, 36.75, 46.75,
//                               56.75, 66.75, 76.75, 86.75, 96.75};

// Conversion Factors
const double lbm_PER_min_TO_kg_PER_sec = 7.559873e-003; //mass flow rate [lbm/min] to [kg/s]
const double BTU_PER_hr_ft_F_TO_W_PER_m_K = 1.729577; //thermal conductivity [BTU/hr-ft-
F] to [W/m-K]
const double in_TO_m = 0.0254000; //length [in] to
[m]
const double psi_TO_Pa = 6894.757293; //pressure [psi] to [Pa]
const double ft3_PER_sec_TO_m3_PER_sec = 2.831685e-2; //volumetric flow rate [m^3/s] to [ft^3/s]
const double lbm_PER_sec_TO_kg_PER_sec = 4.535924e-1; //mass flow rate [lbm/s] to [kg/s]

inline double CtoF(double TC)
{
    return 1.8*(TC)+32.0;
}
inline double FtoC(double TF)
{
    return ((TF)-32.0)/1.8;
}
inline double ReNo(double mdot, double d, double mu)
{
    return d*(mdot/(PI*d*d/4.0))/mu;
}
inline double PrNo(double mu, double Cp, double k)
{
    return mu*Cp/k;
}
inline double NuNo(double h, double d, double k)
{
    return h*d/k;
}

```



```

double EqResist;
double Ohm;
double Amp;

double **Tpipe = new double *[NUM_ND]; for(i=0;i<NUM_ND;i++) Tpipe[i] = new
double[ NUM_NT];
double **Condk = new double *[NUM_ND]; for(i=0;i<NUM_ND;i++) Condk[i] = new
double[ NUM_NT];
double **Resivy= new double *[NUM_ND]; for(i=0;i<NUM_ND;i++) Resivy[i]= new
double[ NUM_NT];
double **Resist= new double *[NUM_ND]; for(i=0;i<NUM_ND;i++) Resist[i]= new
double[ NUM_NT];
double **Currnt= new double *[NUM_ND]; for(i=0;i<NUM_ND;i++) Currnt[i]= new
double[ NUM_NT];

double Tcheck;
double *Told = new double[ NUM_NT];
double *Tnew = new double[ NUM_NT];

for(k=0;k<NUM_ST;k++)
{
    int count = 0;

    for(i=0;i<NUM_ND;i++)
        for(j=0;j<NUM_NT;j++)
            Tpipe[i][j] = m_dToutwall[k][j];

    do
    {
        EqResist = 0.;
        Amp = 0.;
        Tcheck = 0.;

        for(i=0;i<NUM_ND;i++)
            for(j=0;j<NUM_NT;j++)
            {
                Condk[i][j] =
(07.27+0.0038*(1.8*Tpipe[i][j]+32.))*BTU_PER_hr_ft_F_TO_W_PER_m_K; //[W/m-K]
                Resivy[i][j] =
(27.67+0.0213*(1.8*Tpipe[i][j]+32.))*in_TO_m/1.e+06; // [ohm-m]
                Resist[i][j] = Resivy[i][j]*m_dDZ[k]/m_dXArea[i];
                EqResist += 1.0/Resist[i][j];
            }
        Ohm = 1.0/EqResist;
        for(i=0;i<NUM_ND;i++)
            for(j=0;j<NUM_NT;j++)
            {
                Currnt[i][j] = m_dCurrent*Ohm/Resist[i][j];
                Amp += Currnt[i][j];
            }

        for(i=0;i<NUM_LAYER;i++)
            for(j=0;j<NUM_NT;j++)
            {

```

```

jm = j-1; jp = j+1; im = i-1; ip = i+1;

if(jm==-1) jm = NUM_NT-1;
if(jp==NUM_NT) jp = 0;

A = Currnt[i][j]*Currnt[i][j]*Resivy[i][j]/m_dXArea[i];
if(i==0)
{
    B = 0.0;
    C =
NUM_NT*DR*(Condk[i][j]+Condk[i][jp])*(Tpipe[i][j]-Tpipe[i][jp])/(8.0*PI*m_dRad[i]);
    D =
NUM_NT*DR*(Condk[i][j]+Condk[i][jm])*(Tpipe[i][j]-Tpipe[i][jm])/(8.0*PI*m_dRad[i]);
}
else
{
    B =
PI*(m_dRad[i]+DR/2.0)*(Condk[i][j]+Condk[im][j])*(Tpipe[i][j]-Tpipe[im][j])/(NUM_NT*DR);
    C =
NUM_NT*DR*(Condk[i][j]+Condk[i][jp])*(Tpipe[i][j]-Tpipe[i][jp])/(4.0*PI*m_dRad[i]);
    D =
NUM_NT*DR*(Condk[i][j]+Condk[i][jm])*(Tpipe[i][j]-Tpipe[i][jm])/(4.0*PI*m_dRad[i]);
}

X = PI*(m_dRad[i]-
DR/2.0)*(Condk[i][j]+Condk[ip][j])/(NUM_NT*DR);
Tpipe[ip][j] = Tpipe[i][j] - (A-B-C-D)/X;
}

for(j=0;j<NUM_NT;j++)
{
    Tnew[j] = Tpipe[NUM_ND-1][j];
    Tcheck += fabs(Tnew[j] - Told[j]);
}

for (j=0;j<NUM_NT;j++)
    Told[j] = Tnew[j];

count ++;

} while(Tcheck >0.00001);

for(j=0;j<NUM_NT;j++)
    m_dTinwall[k][j] =Tpipe[NUM_ND-1][j];

for(i=0;i<NUM_ND;i++)
    for(j=0;j<NUM_NT;j++)
        m_dPower[k] += Currnt[i][j]*Currnt[i][j]*Resist[i][j];

m_dTPower += m_dPower[k];

double Q1=0.,Q2=0.,Q4=0.,QGen=0;
i=NUM_ND-1;

for(j=0;j<NUM_NT;j++)

```

```

        {
            jm = j-1; jp = j+1; im = i-1; ip = i+1;

            if(jm==-1) jm = NUM_NT-1;
            if(jp==NUM_NT) jp = 0;

            Q1=PI*(Condk[im][j]+Condk[i][j])*(m_dRad[im]-DR/2.0)*(Tpipe[i][j]-
Tpipe[im][j])/(NUM_NT*DR);
            Q2=NUM_NT*(Condk[i][jp]+Condk[i][j])*DR*(Tpipe[i][j]-
Tpipe[i][jp])/(PI*m_dRad[i]*8.0);
            Q4=NUM_NT*(Condk[i][j]+Condk[i][jm])*DR*(Tpipe[i][j]-
Tpipe[i][jm])/(PI*m_dRad[i]*8.0);
            QGen=Currrnt[i][j]*Currrnt[i][j]*Resivy[i][j]/m_dXArea[i];

            m_dQFluxIn[k][j]=(QGen-Q1-Q2-Q4)*NUM_NT/(2.0*PI*m_dRad[i]);
        }

        for(j=0;j<NUM_NT;j++)
        {
            m_dTavg[k] += m_dTinwall[k][j];
            m_dQavg[k] += m_dQFluxIn[k][j];
        }

        m_dTavg[k] /= NUM_NT;
        m_dQavg[k] /= NUM_NT;
    }

    for(i=0;i<NUM_ND;i++) delete[] Tpipe[i]; delete[] Tpipe;
    for(i=0;i<NUM_ND;i++) delete[] Condk[i]; delete[] Condk;
    for(i=0;i<NUM_ND;i++) delete[] Resist[i]; delete[] Resist;
    for(i=0;i<NUM_ND;i++) delete[] Resivy[i]; delete[] Resivy;
    for(i=0;i<NUM_ND;i++) delete[] Currrnt[i]; delete[] Currrnt;

    delete[] Told;
    delete[] Tnew;
}

void CHTCal::setHTCoeff()
{
    int j,k;

    /*- CALCULATION OF PERIPHERAL HEAT TRANSFER COEFFICIENT -*/
    for(k=0;k<NUM_ST;k++)
        for(j=0;j<NUM_NT;j++)
            m_dHTCoeff[k][j] = m_dQFluxIn[k][j]/(m_dTinwall[k][j]-m_dTbulk[k]);

    for(k=0;k<NUM_ST;k++)
    {
        /*- CALCULATE RATIO OF TOP/BOTTOM HEAT TRANSFER COEFFICIENTS -*/
        m_dHTCoeffTB[k]=m_dHTCoeff[k][TOP]/m_dHTCoeff[k][BOTTOM];
        /*- CALCULATION OF OVERALL HEAT TRANSFER COEFFICIENT -*/
        m_dHTCavg[k] = m_dQavg[k]/(m_dTavg[k]-m_dTbulk[k]);
        // for(j=0;j<NUM_NT;j++)
        // m_dHTCavg[k] += m_dHTCoeff[k][j]/NUM_NT;
    }
}

```

```

    }
}

void CHTCal::setGeometry()
{
    int i,k;

    double sum = m_dLgthNCV[0] = DX[0];

    for(k=1;k<NUM_ST;k++)
    {
        m_dLgthNCV[k]=DX[k]-DX[k-1];
        sum += m_dLgthNCV[k];
    }

    m_dLgthNCV[NUM_ST] = HLENGTH - sum;

    for(k=0;k<NUM_ST;k++)
        m_dDZ[k] = DX[k] + (DX[k+1] - DX[k])/2.0;

    m_dRad[0] = OD_PIPE/2.0;
    for(i=0;i<NUM_LAYER;i++)
        m_dRad[i+1] = m_dRad[i] -DR;

    m_dXArea[0] = (m_dRad[0]-DR/4.0)*PI*DR/NUM_NT;
    for(i=1;i<NUM_LAYER;i++)
        m_dXArea[i] = 2.0*m_dRad[i]*PI*DR/NUM_NT;
    m_dXArea[NUM_LAYER] = (m_dRad[NUM_LAYER]+DR/4.0)*PI*DR/NUM_NT;
}

void CHTCal::setTbulk()
{
    m_dTbulk[0] = m_dTin+(m_dTout-m_dTin)*m_dLgthNCV[0]/LENGTH;
    for(int k=1;k<NUM_ST;k++)
        m_dTbulk[k] = m_dTbulk[k-1]+(m_dTout-m_dTin)*m_dLgthNCV[k]/LENGTH;
}

// HTCal.h: interface for the CHTCal class.
#pragma once

#include ".\ReadData.h"

class CHTCal:public CReadData
{
public:

protected:
    double **m_dTinwall;
    double **m_dQFluxIn;
    double **m_dHTCcoeff;

    double m_dXArea[NUM_ND];
}

```

```

double m_dRad[NUM_ND];
double m_dDZ[NUM_ST];
double m_dLgthNCV[NUM_ST+1];

double m_dTPower;
double m_dPower[NUM_ST];

double m_dTbulk[NUM_ST];
double m_dTavg[NUM_ST];
double m_dQavg[NUM_ST];
double m_dHTCavg[NUM_ST];
double m_dHTCcoeffTB[NUM_ST];

public:
double getTin(){return m_dTin;};
double getTout(){return m_dTout;};
double getTroom(){return m_dTroom;};
double getTbulk(int k){return m_dTbulk[k];};
double getTwall(int k){return m_dTavg[k];};
double getQFavg(int k){return m_dQavg[k];};
double getHCoeff(int k){return m_dHTCavg[k];};
double getHCTB(int k){return m_dHTCcoeffTB[k];};

double getLqdMFR(){return m_dLqdMFR;};
double getGasMFR(){return m_dGasMFR;};
double getPref(){return m_dPref;};
double getCurrent(){return m_dCurrent;};
double getVolt(){return m_dVolt;};
double getTotalPower(){return m_dTPower;};

double **getTinwall(){return m_dTinwall;};
double **getQFluxIn(){return m_dQFluxIn;};
double **getHTCcoeff(){return m_dHTCcoeff;};

void setTbulk();
void setTinwall_Power_QFluxIn();
void setHTCcoeff();
void setGeometry();

CHTCal();
virtual ~CHTCal();

};

// PrintData.cpp: implementation of the CPrintData class.
//
//
//
//
// Construction/Destruction
//
CPrintData::CPrintData()
{

```



```

my2HTFile << "\t\t\tINLET TEMPERATURE      : " << setiosflags( ios::right )<<setfill('
')<<setprecision(2)<<setw(9)<< TinAvg          << " [C]" << endl;
my2HTFile << "\t\t\tOUTLET TEMPERATURE      : " << setiosflags( ios::right )<<setfill('
')<<setprecision(2)<<setw(9)<< ToutAvg         << " [C]" << endl;
my2HTFile << "\t\t\tAVG REFERENCE GAGE PRESSURE : " << setiosflags( ios::right
)<<setfill(' ')<<setprecision(2)<<setw(9)<< PrefAvg*psi_TO_Pa << " [Pa]" << endl;
my2HTFile << "\t\t\tAVG LIQUID RE_SL        : " << setiosflags( ios::right )<<setfill('
')<<setprecision(0)<<setw(9)<< RESLAvg         << endl;
my2HTFile << "\t\t\tAVG GAS RE_SL           : " << setiosflags( ios::right )<<setfill('
')<<setprecision(0)<<setw(9)<< RESGAvg        << endl;
my2HTFile << "\t\t\tAVG LIQUID PR          : " << setiosflags( ios::right )<<setfill('
')<<setprecision(3)<<setw(9)<< LqdPRAvg       << endl;
my2HTFile << "\t\t\tAVG GAS PR            : " << setiosflags( ios::right )<<setfill('
')<<setprecision(3)<<setw(9)<< GasPRAvg       << endl;
my2HTFile << "\t\t\tAVG LIQUID DENSITY      : " << setiosflags( ios::right )<<setfill('
')<<setprecision(1)<<setw(9)<< LqdDensAvg      << " [kg/m^3]" << endl;
my2HTFile << "\t\t\tAVG GAS DENSITY        : " << setiosflags( ios::right )<<setfill('
')<<setprecision(3)<<setw(9)<< GasDensAvg      << " [kg/m^3]" << endl;
my2HTFile << "\t\t\tAVG LIQUID SPECIFIC HEAT : " << setiosflags( ios::right )<<setfill('
')<<setprecision(3)<<setw(9)<< LqdCpAvg/1000.   << " [kJ/kg-K]" << endl;
my2HTFile << "\t\t\tAVG GAS SPECIFIC HEAT  : " << setiosflags( ios::right )<<setfill('
')<<setprecision(3)<<setw(9)<< GasCpAvg/1000.   << " [kJ/kg-K]" << endl;
my2HTFile << "\t\t\tAVG LIQUID VISCOSITY     : " << setiosflags( ios::right )<<setfill('
')<<setprecision(2)<<setw(5)<< LqdViscAvg*1e+5   << "e-05 [Pa-s]" << endl;
my2HTFile << "\t\t\tAVG GAS VISCOSITY       : " << setiosflags( ios::right )<<setfill('
')<<setprecision(2)<<setw(5)<< GasViscAvg*1e+6   << "e-06 [Pa-s]" << endl;
my2HTFile << "\t\t\tAVG LIQUID CONDUCTIVITY   : " << setiosflags( ios::right )<<setfill('
')<<setprecision(3)<<setw(9)<< LqdCondAvg      << " [W/m-K]" << endl;
my2HTFile << "\t\t\tAVG GAS CONDUCTIVITY     : " << setiosflags( ios::right )<<setfill('
')<<setprecision(2)<<setw(5)<< GasCondAvg*1e+3   << "e-03 [W/m-K]" << endl;
my2HTFile << "\t\t\tCURRENT TO TUBE          : " << setiosflags( ios::right )<<setfill('
')<<setprecision(2)<<setw(9)<< AmpAvg          << " [A]" << endl;
my2HTFile << "\t\t\tVOLTAGE DROP IN TUBE        : " << setiosflags( ios::right )<<setfill('
')<<setprecision(2)<<setw(9)<< VoltAvg         << " [V]" << endl;
my2HTFile << "\t\t\tAVG HEAT FLUX              : " << setiosflags( ios::right )<<setfill('
')<<setprecision(2)<<setw(9)<< QFluxAvg        << " [W/m^2]" << endl;
my2HTFile << "\t\t\tQ = AMP*VOLT              : " << setiosflags( ios::right )<<setfill('
')<<setprecision(2)<<setw(9)<< QGenAvg         << " [W]" << endl;
my2HTFile << "\t\t\tQ = M*C*(T2 -T1)           : " << setiosflags( ios::right )<<setfill('
')<<setprecision(2)<<setw(9)<< QTakenAvg       << " [W]" << endl;
my2HTFile << "\t\t\tHEAT BALANCE ERROR          : " << setiosflags( ios::right )<<setfill('
')<<setprecision(2)<<setw(9)<< QBalErrAvg      << " [%]" << endl;
// my2HTFile << "\t\t\tCALCULATED QIN          : " << setiosflags( ios::right )<<setfill('
')<<setprecision(2)<<setw(9)<< QINCAL         << endl;
// my2HTFile << "\t\t\tQIN CALCULATION ERROR       : " << setiosflags( ios::right )<<setfill('
')<<setprecision(2)<<setw(9)<< QINBAL         << endl;
// my2HTFile << "\t\t\tGAS PRESSURE              : " << setiosflags( ios::right )<<setfill('
')<<setprecision(2)<<setw(9)<< GasPsig        << " [psig]" << endl;
// my2HTFile << "\t\t\tATMOSPHERE PRESSURE          : " << setiosflags( ios::right )<<setfill('
')<<setprecision(2)<<setw(9)<< AtmPress       << " [mmHg]" << endl;

char *StNoStrip = "\n 1 2 3 4 5 6 7 8 9 10";

my2HTFile << "\n          OUTSIDE SURFACE TEMPERATURE OF TUBE [C]" <<
StNoStrip << endl;
for(IPR=0;IPR<NUM_NT;IPR++)

```

```

    {
        my2HTFile << IPR+1;
        for(IST=0;IST<NUM_ST;IST++)
            my2HTFile << " " << setfill(' ') <<setprecision(2) <<setw(7) <<
Tosurf[IST][IPR];
            my2HTFile << endl;
        }

    my2HTFile << "\n                INSIDE SURFACE TEMPERATURES [C]" << StNoStrip
<< endl;
    for(IPR=0;IPR<NUM_NT;IPR++)
    {
        my2HTFile << IPR+1;
        for(IST=0;IST<NUM_ST;IST++)
            my2HTFile << " " << setfill(' ') <<setprecision(2) <<setw(7) <<
Tisurf[IST][IPR];
            my2HTFile << endl;
        }

    my2HTFile << "\n                SUPERFICIAL REYNOLDS NUMBER OF GAS AT THE
INSIDE TUBE WALL" << StNoStrip << endl;
    for(IPR=0;IPR<NUM_NT;IPR++)
    {
        my2HTFile << IPR+1;
        for(IST=0;IST<NUM_ST;IST++)
            my2HTFile << " " << setfill(' ') <<setprecision(0) <<setw(7) <<
RESGisurf[IST][IPR];
            my2HTFile << endl;
        }

    my2HTFile << "\n                SUPERFICIAL REYNOLDS NUMBER OF LIQUID AT THE
INSIDE TUBE WALL" << StNoStrip << endl;
    for(IPR=0;IPR<NUM_NT;IPR++)
    {
        my2HTFile << IPR+1;
        for(IST=0;IST<NUM_ST;IST++)
            my2HTFile << " " << setfill(' ') <<setprecision(0) <<setw(7) <<
RESLisurf[IST][IPR];
            my2HTFile << endl;
        }

    my2HTFile << "\n                INSIDE SURFACE HEAT FLUXES [W/m^2]" <<
StNoStrip << endl;
    for(IPR=0;IPR<NUM_NT;IPR++)
    {
        my2HTFile << IPR+1;
        for(IST=0;IST<NUM_ST;IST++)
            my2HTFile << " " << setfill(' ') <<setprecision(0) <<setw(7) <<
QFluxisurf[IST][IPR];
            my2HTFile << endl;
        }

```



```

        my2HTFile << setiosflags( ios::right ) << setfill(' ') << setprecision(3) << setw(7) <<
GasDens[IST]      << endl ;
//
        my2HTFile << setiosflags( ios::right ) << setfill(' ') << setprecision(4) << setw(9) <<
LqdBlkBeta[IST]  << " " ;
//
        my2HTFile << setiosflags( ios::right ) << setfill(' ') << setprecision(4) << setw(9) <<
GasBlkBeta[IST]  << endl ;

        MuBW_Lqd += LqdViscBulk[IST]/LqdViscWall[IST];
    }
    my2HTFile << "\n" << endl;

    double avgHTCcoeff = 0.;

    my2HTFile << "ST  X/D  RESL  RESG  PRL  PRG  MUB/W(L)  MUB/W(G)  HT/HB
HFLUX  TB[C]  TW[C]  HCOEFF  NU_L" << endl;
    for(IST=0;IST<NUM_ST;IST++)
    {
        my2HTFile << setiosflags( ios::right ) << setfill(' ') << setw(2) << IST+1 << " " ;
        my2HTFile << setiosflags( ios::right ) << setfill(' ') << setprecision(2) << setw(6) <<
DX[IST]/ID_PIPE << " " ;
        my2HTFile << setiosflags( ios::right ) << setfill(' ') << setprecision(0) << setw(6) <<
RESL[IST]      << " " ;
        my2HTFile << setiosflags( ios::right ) << setfill(' ') << setprecision(0) << setw(5) <<
RESG[IST]      << " " ;
        my2HTFile << setiosflags( ios::right ) << setfill(' ') << setprecision(2) << setw(4) <<
LqdPR[IST]    << " " ;
        my2HTFile << setiosflags( ios::right ) << setfill(' ') << setprecision(3) << setw(5) <<
GasPR[IST]    << " " ;
        my2HTFile << setiosflags( ios::right ) << setfill(' ') << setprecision(3) << setw(5) <<
LqdViscBW[IST] << " " ;
        my2HTFile << setiosflags( ios::right ) << setfill(' ') << setprecision(3) << setw(7) <<
GasViscBW[IST] << " " ;
        my2HTFile << setiosflags( ios::right ) << setfill(' ') << setprecision(3) << setw(6) <<
HTCcoeffTB[IST] << " " ;
        my2HTFile << setiosflags( ios::right ) << setfill(' ') << setprecision(0) << setw(5) <<
QFlux[IST]    << " " ;
        my2HTFile << setiosflags( ios::right ) << setfill(' ') << setprecision(2) << setw(5) <<
Tbulk[IST]    << " " ;
        my2HTFile << setiosflags( ios::right ) << setfill(' ') << setprecision(2) << setw(5) <<
Twall[IST]    << " " ;
        my2HTFile << setiosflags( ios::right ) << setfill(' ') << setprecision(1) << setw(7) <<
HTCcoeff[IST] << " " ;
        my2HTFile << setiosflags( ios::right ) << setfill(' ') << setprecision(2) << setw(6) <<
Nu[IST]       << endl;

        avgHTCcoeff += HTCcoeff[IST];
    }

    aDBLine_SI->gNum   = gNum;
    aDBLine_SI->runNum = runNum;
    aDBLine_SI->testDate = testDate;
    aDBLine_SI->LqdVFR = LqdMFRAvg/LqdDensAvg;
    aDBLine_SI->GasVFR = GasMFRAvg/GasDensAvg;
    aDBLine_SI->LqdMFR = LqdMFRAvg;
    aDBLine_SI->GasMFR = GasMFRAvg;

```

```

aDBLine_SI->VSL    = VSLAvg;
aDBLine_SI->VSG    = VSGAvg;
aDBLine_SI->Tin    = TinAvg;
aDBLine_SI->Tout   = ToutAvg;
aDBLine_SI->DT     = ToutAvg-TinAvg;
aDBLine_SI->Pref   = PrefAvg*psi_TO_Pa;
aDBLine_SI->ReSL   = RESLAvg;
aDBLine_SI->ReSG   = RESGAvg;
aDBLine_SI->LqdPr  = LqdPRAvg;
aDBLine_SI->GasPr  = GasPRAvg;
aDBLine_SI->LqdRho = LqdDensAvg;
aDBLine_SI->GasRho = GasDensAvg;
aDBLine_SI->LqdCp  = LqdCpAvg/1000.;
aDBLine_SI->GasCp  = GasCpAvg/1000.;
aDBLine_SI->LqdVisc = LqdViscAvg;
aDBLine_SI->GasVisc = GasViscAvg;
aDBLine_SI->LqdCond = LqdCondAvg;
aDBLine_SI->GasCond = GasCondAvg;
aDBLine_SI->Amp    = AmpAvg;
aDBLine_SI->Volt   = VoltAvg;
aDBLine_SI->QFlux  = QFluxAvg;
aDBLine_SI->QGen   = QGenAvg;
aDBLine_SI->QTaken = QTakenAvg;
aDBLine_SI->QBalErr = QBalErrAvg;
aDBLine_SI->JK_HTC = avgHTCcoeff/10.;
aDBLine_SI->DK_HTC = overallHTC;
aDBLine_SI->LqdVisc_BW = MuBW_Lqd/10.;

    my2HTFile.close();
}

void CPrintData::prntHTI_FPS(int gNum, char *runNum, char *testDate, char *Pattern, CSetOfData
*aDBLine_FPS)
{
    int  IST,IPR;
    char fileName[20];
    ofstream my2HTFile;

    strcpy(fileName,"RN");strcat(fileName,runNum);strcat(fileName,"FPS.2HT");
    my2HTFile.open(fileName);
    if(!my2HTFile)
    {
        cerr<<"cannot open "<< fileName <<" file"<<endl;
        exit(1);
    }

    my2HTFile << "\t\t\t======" << endl;
    my2HTFile << "\t\t\t    RUN NUMBER " << runNum << endl;
    my2HTFile << "\t\t\t    FLOW PATTERN: " << Pattern << endl;
    my2HTFile << "\t\t\t    Air-Water Two-phase Heat Transfer" << endl;
    my2HTFile << "\t\t\t    Test Date: " << testDate << endl;
    my2HTFile << "\t\t\t    FPS UNIT VERSION" << endl;
    my2HTFile << "\t\t\t======" << endl;
    // my2HTFile << "\t\t\tTEST FLUIDS - LIQUID    : ";
    // if (LqdIs == WATER) my2HTFile << "\t\t\tDISTILLED WATER" << endl;
    // else if (LqdIs == GLYCOL) my2HTFile << LqdConcent*100 << "% GLYCOL" << endl;

```



```

my2HTFile << "\t\t\tAVG LIQUID CONDUCTIVITY   : " << setiosflags( ios::right )<<setfill('
')<<setprecision(3)<<setw(9)<< LqdCondAvg/1.729577          << " [BTU/hr-ft-F]" << endl;
my2HTFile << "\t\t\tAVG GAS  CONDUCTIVITY   : " << setiosflags( ios::right )<<setfill('
')<<setprecision(2)<<setw(5)<< GasCondAvg*1000/1.729577      << "e-03 [BTU/hr-ft-F]" << endl;
my2HTFile << "\t\t\tCURRENT TO TUBE       : " << setiosflags( ios::right )<<setfill('
')<<setprecision(2)<<setw(9)<< AmpAvg                          << " [A]"          << endl;
my2HTFile << "\t\t\tVOLTAGE DROP IN TUBE    : " << setiosflags( ios::right )<<setfill('
')<<setprecision(2)<<setw(9)<< VoltAvg                          << " [V]"          << endl;
my2HTFile << "\t\t\tAVG HEAT FLUX         : " << setiosflags( ios::right )<<setfill('
')<<setprecision(2)<<setw(9)<< QFluxAvg/3.152481                << " [BTU/hr-ft^2]" << endl;
my2HTFile << "\t\t\tQ = AMP*VOLT          : " << setiosflags( ios::right )<<setfill('
')<<setprecision(2)<<setw(9)<< QGenAvg/2.928751e-1              << " [BTU/hr]"      << endl;
my2HTFile << "\t\t\tQ = M*C*(T2 -T1)         : " << setiosflags( ios::right )<<setfill('
')<<setprecision(2)<<setw(9)<< QTakenAvg/2.928751e-1            << " [BTU/hr]"      << endl;
my2HTFile << "\t\t\tHEAT BALANCE ERROR       : " << setiosflags( ios::right )<<setfill('
')<<setprecision(2)<<setw(9)<< QBalErrAvg                       << " [%]"          << endl;
// my2HTFile << "\t\t\tCALCULATED QIN      : " << setiosflags( ios::right )<<setfill('
')<<setprecision(2)<<setw(9)<< QINCAL                            << endl;
// my2HTFile << "\t\t\tQIN CALCULATION ERROR  : " << setiosflags( ios::right )<<setfill('
')<<setprecision(2)<<setw(9)<< QINBAL                            << endl;
// my2HTFile << "\t\t\tGAS  PRESSURE        : " << setiosflags( ios::right )<<setfill('
')<<setprecision(2)<<setw(9)<< GasPsig                          << " [psig]"      << endl;
// my2HTFile << "\t\t\tATMOSPHERE PRESSURE     : " << setiosflags( ios::right )<<setfill('
')<<setprecision(2)<<setw(9)<< AtmPress                        << " [mmHg]"      << endl;

```

```

char *StNoStrip = "\n  1  2  3  4  5  6  7  8  9  10";

```

```

my2HTFile << "\n          OUTSIDE SURFACE TEMPERATURE OF TUBE [F]" <<
StNoStrip << endl;

```

```

for(IPR=0;IPR<NUM_NT;IPR++)
{
    my2HTFile << IPR+1;
    for(IST=0;IST<NUM_ST;IST++)
        my2HTFile << " " << setfill(' ') <<setprecision(2) <<setw(7) <<
Tosurf[IST][IPR]*1.8+32.0;
    my2HTFile << endl;
}

```

```

my2HTFile << "\n          INSIDE SURFACE TEMPERATURES [F]" << StNoStrip
<< endl;

```

```

for(IPR=0;IPR<NUM_NT;IPR++)
{
    my2HTFile << IPR+1;
    for(IST=0;IST<NUM_ST;IST++)
        my2HTFile << " " << setfill(' ') <<setprecision(2) <<setw(7) <<
Tisurf[IST][IPR]*1.8+32.0;
    my2HTFile << endl;
}

```

```

my2HTFile << "\n          SUPERFICIAL REYNOLDS NUMBER OF GAS AT THE
INSIDE TUBE WALL" << StNoStrip << endl;

```

```

for(IPR=0;IPR<NUM_NT;IPR++)
{

```

```

        my2HTFile << IPR+1;
        for(IST=0;IST<NUM_ST;IST++)
            my2HTFile << " " << setfill(' ') <<setprecision(0) <<setw(7) <<
RESGisurf[IST][IPR];
        my2HTFile << endl;
    }

    my2HTFile << "\n          SUPERFICAL REYNOLDS NUMBER OF LIQUID AT THE
INSIDE TUBE WALL" << StNoStrip << endl;
    for(IPR=0;IPR<NUM_NT;IPR++)
    {
        my2HTFile << IPR+1;
        for(IST=0;IST<NUM_ST;IST++)
            my2HTFile << " " << setfill(' ') <<setprecision(0) <<setw(7) <<
RESLisurf[IST][IPR];
        my2HTFile << endl;
    }

    my2HTFile << "\n          INSIDE SURFACE HEAT FLUXES [BTU/hr-ft^2]" <<
StNoStrip << endl;
    for(IPR=0;IPR<NUM_NT;IPR++)
    {
        my2HTFile << IPR+1;
        for(IST=0;IST<NUM_ST;IST++)
            my2HTFile << " " << setfill(' ') <<setprecision(0) <<setw(7) <<
QFluxisurf[IST][IPR]/3.152481;
        my2HTFile << endl;
    }

    double overallHTC = 0.;
    my2HTFile << "\n          PERIPHERAL HEAT TRANSFER COEFFICIENT [BTU/hr-
ft^2-F]" << StNoStrip << endl;
    for(IPR=0;IPR<NUM_NT;IPR++)
    {
        my2HTFile << IPR+1;
        for(IST=0;IST<NUM_ST;IST++)
        {
            my2HTFile << " " << setfill(' ') <<setprecision(0) <<setw(7) <<
HTCisurf[IST][IPR]/5.674466;
            overallHTC += HTCisurf[IST][IPR]/5.674466;
        }
        my2HTFile << endl;
    }

    overallHTC /= IST*IPR;

    my2HTFile << "\n\n\n" << endl;

    my2HTFile << "\t\t\t======" << endl;
    my2HTFile << "\t\t\t  RUN NUMBER " << runNum << " continued" << endl;
    my2HTFile << "\t\t\t  FLOW PATTERN: " << Pattern << endl;
    my2HTFile << "\t\t\t  Air-Water Two-phase Heat Transfer" << endl;
    my2HTFile << "\t\t\t  Test Date: " << testDate << endl;
    my2HTFile << "\t\t\t  FPS UNIT VERSION" << endl;

```



```

RESG[IST]      my2HTFile << setiosflags( ios::right ) << setfill(' ') << setprecision(0) << setw(5) <<
               << " ";
LqdPR[IST]    my2HTFile << setiosflags( ios::right ) << setfill(' ') << setprecision(2) << setw(4) <<
               << " ";
GasPR[IST]    my2HTFile << setiosflags( ios::right ) << setfill(' ') << setprecision(3) << setw(5) <<
               << " ";
LqdViscBW[IST] my2HTFile << setiosflags( ios::right ) << setfill(' ') << setprecision(3) << setw(5) <<
               << " ";
GasViscBW[IST] my2HTFile << setiosflags( ios::right ) << setfill(' ') << setprecision(3) << setw(7) <<
               << " ";
HTCcoeffTB[IST] my2HTFile << setiosflags( ios::right ) << setfill(' ') << setprecision(3) << setw(6) <<
               << " ";
QFlux[IST]/3.152481 my2HTFile << setiosflags( ios::right ) << setfill(' ') << setprecision(0) << setw(5) <<
               << " ";
Tbulk[IST]*1.8+32.0 my2HTFile << setiosflags( ios::right ) << setfill(' ') << setprecision(2) << setw(5) <<
               << " ";
Twall[IST]*1.8+32.0 my2HTFile << setiosflags( ios::right ) << setfill(' ') << setprecision(2) << setw(5) <<
               << " ";
HTCcoeff[IST]/5.674466 my2HTFile << setiosflags( ios::right ) << setfill(' ') << setprecision(1) << setw(7) <<
               << " ";
Nu[IST]        my2HTFile << setiosflags( ios::right ) << setfill(' ') << setprecision(2) << setw(6) <<
               << endl ;

               avgHTCcoeff += HTCcoeff[IST];
    }

aDBLine_FPS->gNum    = gNum;
aDBLine_FPS->runNum  = runNum;
aDBLine_FPS->testDate = testDate;
aDBLine_FPS->LqdVFR  = LqdMFRAvg/LqdDensAvg/ft3_PER_sec_TO_m3_PER_sec*3600.;
aDBLine_FPS->GasVFR  = GasMFRAvg/GasDensAvg/ft3_PER_sec_TO_m3_PER_sec*3600.;
aDBLine_FPS->LqdMFR  = LqdMFRAvg/lbm_PER_sec_TO_kg_PER_sec*3600.;
aDBLine_FPS->GasMFR  = GasMFRAvg/lbm_PER_sec_TO_kg_PER_sec*3600.;
aDBLine_FPS->VSL     = VSLAvg/3.048000e-1;
aDBLine_FPS->VSG     = VSGAvg/3.048000e-1;
aDBLine_FPS->Tin     = CtoF(TinAvg);
aDBLine_FPS->Tout    = CtoF(ToutAvg);
aDBLine_FPS->DT      = CtoF(ToutAvg-TinAvg);
aDBLine_FPS->Pref    = PrefAvg;
aDBLine_FPS->ReSL    = RESL Avg;
aDBLine_FPS->ReSG    = RESG Avg;
aDBLine_FPS->LqdPr   = LqdPRAvg;
aDBLine_FPS->GasPr   = GasPRAvg;
aDBLine_FPS->LqdRho  = LqdDensAvg/1.601846e+1;
aDBLine_FPS->GasRho  = GasDensAvg/1.601846e+1;
aDBLine_FPS->LqdCp   = LqdCpAvg/1000./4.184000;
aDBLine_FPS->GasCp   = GasCpAvg/1000./4.184000;
aDBLine_FPS->LqdVisc = LqdViscAvg/4.133789e-4;
aDBLine_FPS->GasVisc = GasViscAvg/4.133789e-4;
aDBLine_FPS->LqdCond = LqdCondAvg/1.729577;
aDBLine_FPS->GasCond = GasCondAvg/1.729577;
aDBLine_FPS->Amp     = AmpAvg;
aDBLine_FPS->Volt    = VoltAvg;
aDBLine_FPS->QFlux   = QFluxAvg/3.152481;
aDBLine_FPS->QGen    = QGenAvg/2.928751e-1;
aDBLine_FPS->QTaken  = QTakenAvg/2.928751e-1;

```

```

aDBLine_FPS->QBalErr = QBalErrAvg;
aDBLine_FPS->JK_HTC = avgHTCcoeff/10./5.674466;
aDBLine_FPS->DK_HTC = overallHTC;
aDBLine_FPS->LqdVisc_BW = MuBW_Lqd/10.;

    my2HTFile.close();
}

void CPrintData::setTemps(double Troom, double Tin, double Tout, double **Tos, double **Tis, double
*Tb, double *Tw)
{
    TroomAvg = Troom;
    TinAvg = Tin;
    ToutAvg = Tout;
    Tosurf = Tos;
    Tisurf = Tis;
    Tbulk = Tb;
    Twall = Tw;
}

void CPrintData::setProps(double LDensAvg, double GDensAvg, double LCpAvg, double GCpAvg, double
LViscAvg, double GViscAvg, double LCondAvg, double GCondAvg,
                        double *LViscWall, double *GViscWall, double
*LViscBulk, double *GViscBulk, double *LViscBW, double *GViscBW,
                        double *LCp, double *GCp, double *LCond, double
*GCond, double *LDens, double *GDens)
{
    LqdDensAvg = LDensAvg; GasDensAvg = GDensAvg;
    LqdCpAvg = LCpAvg; GasCpAvg = GCpAvg;
    LqdViscAvg = LViscAvg; GasViscAvg = GViscAvg;
    LqdCondAvg = LCondAvg; GasCondAvg = GCondAvg;

    LqdViscWall = LViscWall, GasViscWall = GViscWall;
    LqdViscBulk = LViscBulk, GasViscBulk = GViscBulk;
    LqdViscBW = LViscBW; GasViscBW = GViscBW;

    LqdCp = LCp; GasCp = GCp;
    LqdCond = LCond; GasCond = GCond;
    LqdDens = LDens; GasDens = GDens;
}

void CPrintData::setFDynamics(double LMFRAvg, double GMFRAvg, double LVAvg, double GVAvg,
double LReAvg, double GReAvg,
                        double **LReisurf, double **GReisurf, double
*LRe, double *GRe)
{
    LqdMFRAvg = LMFRAvg; GasMFRAvg = GMFRAvg;
    VSLAvg = LVAvg; VSGAvg = GVAvg;
    RESLavg = LReAvg; RESGavg = GReAvg;
    RESLisurf = LReisurf; RESGisurf = GReisurf;
    RESL = LRe; RESG = GRe;
}

void CPrintData::setPressures(double pAvg, double *dp)
{
    PrefAvg = pAvg;
}

```

```

        DPAvg = dp;
    }

void CPrintData::setHTprops(double LPrAvg, double GPrAvg, double QFAvg, double QGAvg, double
QTAvg, double QBErrAvg,
                        double **QFis, double **HTCis, double *LPr, double *GPr, double
*HTCTB, double *QF, double *HTC, double *NU)
{
    LqdPRAvg = LPrAvg; GasPRAvg = GPrAvg;
    QFluxAvg = QFAvg;
    QGenAvg = QGAvg; QTakenAvg = QTAvg; QBalErrAvg = QBErrAvg;
    QFluxisurf = QFis; HTCisurf = HTCis;
    LqdPR = LPr; GasPR = GPr; HTCcoeffTB = HTCTB; QFlux = QF; HTCcoeff = HTC; Nu = NU;
}
void CPrintData::setPower(double amp, double volt)
{
    AmpAvg = amp; VoltAvg = volt;
}

```

```

// PrintData.h: interface for the CPrintData class.
#pragma once

```

```

#include ".\SetOfData.h"

```

```

class CPrintData
{
private:
    double TroomAvg, TinAvg, ToutAvg;
    double PrefAvg, *DPAvg;
    double AmpAvg, VoltAvg;

    double LqdVFRAvg, GasVFRAvg;
    double LqdMFRAvg, GasMFRAvg;
    double VSLAvg, VSGAvg;
    double RESLAvg, RESGAvg;
    double LqdPRAvg, GasPRAvg;
    double LqdDensAvg, GasDensAvg;
    double LqdCpAvg, GasCpAvg;
    double LqdViscAvg, GasViscAvg;
    double LqdCondAvg, GasCondAvg;

    double QFluxAvg, QGenAvg, QTakenAvg, QBalErrAvg;

    double **Tosurf, **Tisurf;
    double **RESLisurf, **RESGisurf;
    double **QFluxisurf, **HTCisurf;

    double *Tbulk, *Twall;

    double *LqdViscWall, *GasViscWall;
    double *LqdViscBulk, *GasViscBulk;
    double *LqdViscBW, *GasViscBW;
    double *LqdCp, *GasCp;
    double *LqdCond, *GasCond;
}

```

```

    double *LqdDens,   *GasDens;

    double *RESL,     *RESG;
    double *LqdPR,    *GasPR;

    double *HTCcoeffTB, *QFlux;
    double *HTCcoeff,  *Nu;

public:
    void setPower(double amp, double volt);
    void setHTprops(double LPrAvg, double GPrAvg, double QFAvg, double QGAvg, double
    QTAvg, double QBErrAvg,
        double **QFis, double **HTCis, double *LPr, double *GPr, double *HTCTB,
    double *QF, double *HTC, double *NU);
    void setPressures(double pAvg, double *dp);
    void setFDynamics(double LMFRAvg, double GMFRAvg, double LVAvg, double GVAvg, double
    LReAvg, double GReAvg,
        double **LReisurf, double **GREisurf, double *LRe, double *GRE);
    void setProps(double LDensAvg, double GDensAvg, double LCpAvg, double GCpAvg, double
    LViscAvg, double GViscAvg, double LCondAvg, double GCondAvg,
        double *LViscWall, double *GViscWall, double *LViscBulk, double *GViscBulk,
    double *LViscBW, double *GViscBW,
        double *LCp, double *GCp, double *LCond, double *GCond, double
    *LDens, double *GDens);
    void setTemps(double Troom, double Tin, double Tout, double **Tosurf, double **Tisurf, double
    *Tbulk, double *Twall);

    void prntHTI_SI(int gNum, char *runNum, char *testDate, char *Pattern, CSetOfData
    *aDBLine_SI);
    void prntHTI_FPS(int gNum, char *runNum, char *testDate, char *Pattern, CSetOfData
    *aDBLine_FPS);

    CPrintData();
    virtual ~CPrintData();

};

```

```

// Properties.cpp: implementation of the CProperties class.

```

```

//

```

```

////////////////////////////////////

```

```

#include "..\2PhHT.h"

```

```

#include "..\Properties.h"

```

```

////////////////////////////////////

```

```

// Construction/Destruction

```

```

////////////////////////////////////

```

```

CProperties::CProperties()

```

```

{

```

```

}

```

```

CProperties::~CProperties()

```

```

{

```

```

}

```

```

double CProperties::Viscosity(double TC, enum fluid FLUID, enum unit UNIT)

```

```

{

```

```

double Visco;
double TF=CtoF(TC);
//Calculated Viscosity is in [lbm/hr-ft]
switch(FLUID)
{
    case WATER:
        Visco = 1.0/(1.207e-5*TF*TF+3.863e-3*TF+0.09461);
        break;
    case AIR:
        Visco = -2.673e-8*TF*TF+6.819e-5*TF+0.03936;
        break;
    default:
        {
            cout << "FLUID is not WATER nor AIR in 'Viscosity' calculation" <<endl;
            exit(1);
        }
        break;
}

switch(UNIT)
{
    case FPS:
        return Visco;
        break;
    case SI:
        //Converting Viscosity in [Pa-s]
        return Visco*4.133789e-4;
        break;
    default:
        {
            cout << "UNIT is not SI nor FPS in 'Viscosity' calculation" <<endl;
            exit(1);
        }
        break;
}
}

double CProperties::Density(double TC, fluid FLUID, enum unit UNIT)
{
    if(FLUID!=WATER)
    {
        cout << "FLUID is not WATER in 'Density' calculation for water" <<endl;
        exit(1);
    }
    double TF=CtoF(TC);
    //Calculated Density in [lbm/ft^3]
    double Dens = 1.0/(2.101e-8*TF*TF-1.303e-6*TF+0.01602);

    switch(UNIT)
    {
        case FPS:
            return Dens;
            break;
        case SI:
            //Converting Density in [kg/m^3]
            return Dens*16.018463;
    }
}

```

```

        break;
    default:
    {
        cout << "UNIT is not SI nor FPS in 'Density' calculation for water" <<endl;
        exit(1);
    }
    break;
}
}

```

```

double CProperties::Density(double TC, double Psi, enum fluid FLUID, enum unit UNIT)
{
    if(FLUID!=AIR)
    {
        cout << "FLUID is not AIR in 'Density' calculation for air" <<endl;
        exit(1);
    }

    double TR=CtoF(TC)+459.67;
    double Psia = Psi + ATM_psi;
    //Calculated Density in [lbm/in^3]
    double Dens = Psia/(TR*R_fps);

    switch(UNIT)
    {
        case FPS:
            //Density in [lbm/ft^3]
            return Dens*1728.;
            break;
        case SI:
            //Converting Density in [kg/m^3]
            return Dens*2.76799e+04;
            break;
        default:
            {
                cout << "UNIT is not SI nor FPS in 'Density' calculation for air" <<endl;
                exit(1);
            }
            break;
    }
}

```

```

double CProperties::Conductivity(double TC, enum fluid FLUID, enum unit UNIT)
{
    double Cond;
    double TF=CtoF(TC);
    //Calculated Conductivity is in [BTU/ft-hr-F]
    switch(FLUID)
    {
        case WATER:
            Cond = 4.722e-4*TF+0.3149;
            break;
        case AIR:
            Cond = -6.154e-9*TF*TF+2.591e-5*TF+0.01313;
            break;
    }
}

```

```

        default:
            {
                cout << "FLUID is not WATER nor AIR in 'Conductivity' calculation" <<endl;
                exit(1);
            }
            break;
    }

switch(UNIT)
{
    case FPS:
        return Cond;
        break;
    case SI:
        //Converting Conductivity in [J/m-s-K]
        return Cond*1.730735;
        break;
    default:
        {
            cout << "UNIT is not SI nor FPS in 'Conductivity' calculation" <<endl;
            exit(1);
        }
        break;
}
}

double CProperties::SpecificHeat(double TC, enum fluid FLUID, enum unit UNIT)
{
    double SpHt;
    double TF=CtoF(TC);
    //Calculated SpecificHeat is in [BTU/lbm-F]
    switch(FLUID)
    {
        case WATER:
            SpHt = 1.337e-6*TF*TF-3.374e-4*TF+1.018;
            break;
        case AIR:
            SpHt = 7.540e-6*TF+0.2401;
            break;
        default:
            {
                cout << "FLUID is not WATER nor AIR in 'SpecificHeat' calculation" <<endl;
                exit(1);
            }
            break;
    }

    switch(UNIT)
    {
        case FPS:
            return SpHt;
            break;
        case SI:
            //Converting Conductivity in [J/kg-K]
            return SpHt*4186.8;
            break;
    }
}

```

```

        default:
            {
                cout << "UNIT is not SI nor FPS in 'SpecificHeat' calculation" <<endl;
                exit(1);
            }
            break;
    }
}

// Properties.h: interface for the CProperties class.
#pragma once

enum fluid {WATER, AIR};
enum unit {SI, FPS};

const double R_fps = 53.34*12;           //Air-Gas Constant in [in-lbf/lbm-R]
const double R_si = 0.28700e+3;        //Air-Gas Constant in [J/kg-K]
const double ATM_psi = 14.695985;     //atmosphere in [psi]
const double ATM_Pa = 1.013252e+5;    //atmosphere in [Pa]

class CProperties
{
public:
    double SpecificHeat(double TC, enum fluid FLUID, enum unit UNIT);
    double Conductivity(double TC, enum fluid FLUID, enum unit UNIT);
    double Density(double TC, enum fluid FLUID, enum unit UNIT);
    double Density(double TC, double Psi, enum fluid FLUID, enum unit UNIT);
    double Viscosity(double TC, enum fluid FLUID, enum unit UNIT);

    CProperties();
    virtual ~CProperties();
};

// ReadData.cpp: implementation of the CReadData class.
//
////////////////////////////////////////////////////////////////////
#include ".\2PhHT.h"
#include ".\ReadData.h"
////////////////////////////////////////////////////////////////////
// Construction/Destruction
////////////////////////////////////////////////////////////////////
CReadData::CReadData()
{
    int k,j;

    m_iDataNum = 0;
    m_dToutwall = new double*[NUM_ST];for(k=0;k<NUM_ST;k++) m_dToutwall[k] = new
double [NUM_NT];
    m_dDP = new double [NUM_PT];

    for(k=0;k<NUM_ST;k++)
        for(j=0;j<NUM_NT;j++)
            m_dToutwall[k][j]=0.;
}

```

```

m_dTin =0.;
m_dTout =0.;
m_dTCout=0.;
m_dTroom=0.;

for(k=0;k<NUM_PT;k++) m_dDP[k]=0.;

m_dLqdMFR =0.;
m_dGasMFR =0.;
m_dPref =0.;
m_dCurrent=0.;
m_dVolt =0.;

}

CReadData::~CReadData()
{
    for(int k=0;k<NUM_ST;k++) delete[] m_dToutwall[k]; delete[] m_dToutwall;
    delete[] m_dDP;
}

bool CReadData::ReadFile(char *runNum)
{
    if(runNum==NULL) return false;

    char fileName[20];
    char aLine[600];
    char dummy[20];
    double aData;

    int k=0,j=0;

    ifstream myDatFile;

    strcpy(fileName,"RN");strcat(fileName,runNum);strcat(fileName, ".DAT");

    myDatFile.open(fileName);
    if(!myDatFile) return false;

    myDatFile.getline(aLine, 599,'\n');
    myDatFile.getline(aLine, 599,'\n');
    while(!myDatFile.eof())
    {
        m_iDataNum++;
        myDatFile.getline(aLine, 599,'\n');
        istringstream aDataSet(aLine);
        aDataSet >> dummy;
        if(m_iDataNum == 1) for(int i=0;i<11;i++) m_cTestDate[i] = dummy[i];
        aDataSet >> dummy;
        for(k=0;k<NUM_ST;k++)
            for(j=0;j<NUM_NT;j++)
            {
                aDataSet >> aData; m_dToutwall[k][j] += aData;
            }
        aDataSet >> aData; m_dTin += aData;
    }
}

```

```

        aDataSet >> aData; m_dTout += aData;
        aDataSet >> aData; m_dTCout += aData;
        aDataSet >> aData; m_dTroom += aData;
        for(k=0;k<NUM_PT;k++)
        {
            aDataSet >> aData; m_dDP[k]+= aData;
        }
    aDataSet >> aData; m_dLqdMFR += aData;
    aDataSet >> aData; m_dGasMFR += aData;
    aDataSet >> aData; m_dPref += aData;
    aDataSet >> aData; m_dCurrent+= aData;
    aDataSet >> aData; m_dVolt += aData;
}

// In order to deal with logic error in while state
m_iDataNum -= 1;
for(k=0;k<NUM_ST;k++)
    for(j=0;j<NUM_NT;j++)
    {
        m_dToutwall[k][j] -= aData;
    }
    m_dTin -= aData;
    m_dTout -= aData;
    m_dTCout -= aData;
    m_dTroom -= aData;
    for(k=0;k<NUM_PT;k++)
    {
        m_dDP[k]-= aData;
    }
m_dLqdMFR -= aData;
m_dGasMFR -= aData;
m_dPref -= aData;
m_dCurrent-= aData;
m_dVolt -= aData;

// In order to deal with logic error in while state

for(k=0;k<NUM_ST;k++)
    for(j=0;j<NUM_NT;j++)
        m_dToutwall[k][j]/=m_iDataNum;

m_dTin /=m_iDataNum;
m_dTout /=m_iDataNum;
m_dTCout/=m_iDataNum;
m_dTroom/=m_iDataNum;

    for(k=0;k<NUM_PT;k++)
        m_dDP[k]/=m_iDataNum;

m_dLqdMFR /=m_iDataNum;
m_dGasMFR /=m_iDataNum;
m_dPref /=m_iDataNum;
m_dCurrent/=m_iDataNum;
m_dVolt /=m_iDataNum;

// Convert mass flow rate from [lbm/min] to [kg/s]
m_dLqdMFR *= lbm_PER_min_TO_kg_PER_sec;

```

```

    m_dGasMFR *= lbm_PER_min_TO_kg_PER_sec;

    if (m_dGasMFR < 0.0) m_dGasMFR = 0.0;

myDatFile.close();
return true;
}

void CReadData::correctTreading()
{
    /*
    Brian's Thermocouple and Thermoprobe correaction

    m_dToutwall[0][0] = 1.0040*m_dToutwall[0][0] - 0.0764 + 0.139199;
    m_dToutwall[0][1] = 1.0015*m_dToutwall[0][1] - 0.2317 - 0.028216;
    m_dToutwall[0][2] = 1.0047*m_dToutwall[0][2] - 0.3761 + 0.305399;
    m_dToutwall[0][3] = 1.0051*m_dToutwall[0][3] - 0.3862 + 0.046863;
    m_dToutwall[1][0] = 1.0039*m_dToutwall[1][0] - 0.3806 + 0.148761;
    m_dToutwall[1][1] = 1.0008*m_dToutwall[1][1] - 0.3413 - 0.112462;
    m_dToutwall[1][2] = 1.0039*m_dToutwall[1][2] - 0.3294 - 0.222726;
    m_dToutwall[1][3] = 1.0048*m_dToutwall[1][3] - 0.3506 - 0.121098;
    m_dToutwall[2][0] = 1.0011*m_dToutwall[2][0] - 0.3858 + 0.087733;
    m_dToutwall[2][1] = 1.0003*m_dToutwall[2][1] - 0.6256 - 0.246509;
    m_dToutwall[2][2] = 1.0028*m_dToutwall[2][2] - 0.7137 + 0.029774;
    m_dToutwall[2][3] = 1.0064*m_dToutwall[2][3] - 0.8922 - 0.178193;
    m_dToutwall[3][0] = 0.9978*m_dToutwall[3][0] - 0.6054 - 0.234388;
    m_dToutwall[3][1] = 0.9939*m_dToutwall[3][1] - 0.6378 - 1.043430;
    m_dToutwall[3][2] = 0.9957*m_dToutwall[3][2] - 0.5758 + 0.428277;
    m_dToutwall[3][3] = 1.0018*m_dToutwall[3][3] - 0.8015 + 0.225467;
    m_dToutwall[4][0] = 0.9932*m_dToutwall[4][0] - 0.5485 - 0.681605;
    m_dToutwall[4][1] = 0.9938*m_dToutwall[4][1] - 0.6867 + 0.559943;
    m_dToutwall[4][2] = 0.9971*m_dToutwall[4][2] - 0.7887 + 0.764959;
    m_dToutwall[4][3] = 0.9975*m_dToutwall[4][3] - 0.8152 - 0.117427;
    m_dToutwall[5][0] = 0.9962*m_dToutwall[5][0] - 0.9077 - 0.963670;
    m_dToutwall[5][1] = 0.9948*m_dToutwall[5][1] - 0.8795 - 0.437326;
    m_dToutwall[5][2] = 0.9954*m_dToutwall[5][2] - 0.7124 + 0.287850;
    m_dToutwall[5][3] = 0.9987*m_dToutwall[5][3] - 0.5191 + 0.439340;
    m_dToutwall[6][0] = 1.0029*m_dToutwall[6][0] - 0.2257 - 0.982640;
    m_dToutwall[6][1] = 0.9997*m_dToutwall[6][1] - 0.2532 - 0.257222;
    m_dToutwall[6][2] = 1.0010*m_dToutwall[6][2] - 0.3428 - 0.283510;
    m_dToutwall[6][3] = 1.0021*m_dToutwall[6][3] - 0.3593 - 0.308606;
    m_dToutwall[7][0] = 0.9975*m_dToutwall[7][0] - 0.3873 + 0.346080;
    m_dToutwall[7][1] = 0.9982*m_dToutwall[7][1] - 0.0011 + 0.201090;
    m_dToutwall[7][2] = 1.0026*m_dToutwall[7][2] - 0.4375 + 0.315210;
    m_dToutwall[7][3] = 1.0021*m_dToutwall[7][3] - 0.4041 + 0.090750;
    m_dToutwall[8][0] = 1.0013*m_dToutwall[8][0] - 0.3741 + 0.524680;
    m_dToutwall[8][1] = 1.0018*m_dToutwall[8][1] - 0.5177 + 0.197680;
    m_dToutwall[8][2] = 1.0020*m_dToutwall[8][2] - 0.4327 + 0.478860;
    m_dToutwall[8][3] = 1.0038*m_dToutwall[8][3] - 0.5192 + 0.179750;
    m_dToutwall[9][0] = 1.0037*m_dToutwall[9][0] - 0.4770 + 0.277360;
    m_dToutwall[9][1] = 0.9986*m_dToutwall[9][1] - 0.4291 - 0.325489;
    m_dToutwall[9][2] = 0.9991*m_dToutwall[9][2] - 0.6143 - 0.024244;
    m_dToutwall[9][3] = 1.0015*m_dToutwall[9][3] - 0.7760 + 0.025080;

    m_dTin = 1.0003*m_dTin - 0.7934 + 0.50279;
    m_dTout = 1.0010*m_dTout - 0.7931 + 0.22984;

```

```

m_dTCout = 0.9984*m_dTCout - 0.9653 - 0.26398;
m_dTroom = 1.0046*m_dTroom - 0.9480 + 0.262674;
*/

m_dToutwall[0][0] = m_dToutwall[0][0] + 0.1010;
m_dToutwall[0][1] = m_dToutwall[0][1] - 0.4030;
m_dToutwall[0][2] = m_dToutwall[0][2] - 0.1572;
m_dToutwall[0][3] = m_dToutwall[0][3] - 0.4620;
m_dToutwall[1][0] = m_dToutwall[1][0] - 0.3000;
m_dToutwall[1][1] = m_dToutwall[1][1] - 0.6924;
m_dToutwall[1][2] = m_dToutwall[1][2] - 0.5713;
m_dToutwall[1][3] = m_dToutwall[1][3] - 0.5813;
m_dToutwall[2][0] = m_dToutwall[2][0] - 0.4489;
m_dToutwall[2][1] = m_dToutwall[2][1] - 1.1983;
m_dToutwall[2][2] = m_dToutwall[2][2] - 1.0205;
m_dToutwall[2][3] = m_dToutwall[2][3] - 1.2603;
m_dToutwall[3][0] = m_dToutwall[3][0] - 1.3060;
m_dToutwall[3][1] = m_dToutwall[3][1] - 2.2812;
m_dToutwall[3][2] = m_dToutwall[3][2] - 0.7072;
m_dToutwall[3][3] = m_dToutwall[3][3] - 1.1057;
m_dToutwall[4][0] = m_dToutwall[4][0] - 1.8094;
m_dToutwall[4][1] = m_dToutwall[4][1] - 0.8171;
m_dToutwall[4][2] = m_dToutwall[4][2] - 0.4108;
m_dToutwall[4][3] = m_dToutwall[4][3] - 1.3168;
m_dToutwall[5][0] = m_dToutwall[5][0] - 2.3338;
m_dToutwall[5][1] = m_dToutwall[5][1] - 1.7675;
m_dToutwall[5][2] = m_dToutwall[5][2] - 0.6858;
m_dToutwall[5][3] = m_dToutwall[5][3] - 0.3088;
m_dToutwall[6][0] = m_dToutwall[6][0] - 1.2369;
m_dToutwall[6][1] = m_dToutwall[6][1] - 0.6994;
m_dToutwall[6][2] = m_dToutwall[6][2] - 0.8643;
m_dToutwall[6][3] = m_dToutwall[6][3] - 0.7819;
m_dToutwall[7][0] = m_dToutwall[7][0] - 0.3051;
m_dToutwall[7][1] = m_dToutwall[7][1] + 0.0301;
m_dToutwall[7][2] = m_dToutwall[7][2] - 0.2518;
m_dToutwall[7][3] = m_dToutwall[7][3] - 0.5146;
m_dToutwall[8][0] = m_dToutwall[8][0] - 0.0533;
m_dToutwall[8][1] = m_dToutwall[8][1] - 0.4474;
m_dToutwall[8][2] = m_dToutwall[8][2] - 0.0370;
m_dToutwall[8][3] = m_dToutwall[8][3] - 0.4376;
m_dToutwall[9][0] = m_dToutwall[9][0] - 0.2316;
m_dToutwall[9][1] = m_dToutwall[9][1] - 1.0484;
m_dToutwall[9][2] = m_dToutwall[9][2] - 0.9408;
m_dToutwall[9][3] = m_dToutwall[9][3] - 1.0629;

m_dTin = 1.0003*m_dTin - 0.7934;
m_dTout = m_dTout - 1.0496;
m_dTCout = 0.9984*m_dTCout - 0.9653;
m_dTroom = m_dTroom - 0.9401;

}

// ReadData.h: interface for the CReadData class.
#pragma once

class CReadData

```

```

{
public:

protected:
    int    m_iDataNum;
    char   m_cTestDate[15];

    double **m_dToutwall;
    double *m_dDP;

        double m_dTin;
        double m_dTout;
double m_dTCout;
        double m_dTroom;
        double m_dLqdMFR;
        double m_dGasMFR;
double m_dPref;
        double m_dCurrent;
        double m_dVolt;

public:
    void correctTreading();

    char *getTestDate(){return m_cTestDate;};

    double **getToutwall(){return m_dToutwall;};
    double *getDPs(){return m_dDP;};

    double getTin(){return m_dTin;};
    double getTout(){return m_dTout;};
    double getTroom(){return m_dTroom;};
    double getLqdMFR(){return m_dLqdMFR;};
    double getGasMFR(){return m_dGasMFR;};
    double getPref(){return m_dPref;};
    double getCurrent(){return m_dCurrent;};
    double getVolt(){return m_dVolt;};

    bool ReadFile(char *runNum);

    CReadData();
    virtual ~CReadData();

};

```

```

#include ".\setofdata.h"

```

```

CSetOfData::CSetOfData(void)
{
    gNum    = 99999;
    runNum   = "9999";
    testDate = "03-14-1971";
    FlwPatn  = "FlwPatn";
    Deg      = 0.;
    ReSL     = 0.;
}

```

```

    ReSG    = 0.;
    JK_HTC  = 0.;
    DK_HTC  = 0.;
    QBalErr = 0.;
    Tin     = 0.;
    Tout    = 0.;
    DT      = 0.;
    Amp     = 0.;
    Volt    = 0.;
    QFlux   = 0.;
    QGen    = 0.;
    QTaken  = 0.;
    LqdVFR  = 0.;
    GasVFR  = 0.;
    LqdMFR  = 0.;
    GasMFR  = 0.;
    VSL     = 0.;
    VSG     = 0.;
    Pref    = 0.;
    LqdPr   = 0.;
    GasPr   = 0.;
    LqdRho  = 0.;
    GasRho  = 0.;
    LqdCp   = 0.;
    GasCp   = 0.;
    LqdVisc = 0.;
    GasVisc = 0.;
    LqdVisc_BW = 0.;
    LqdCond = 0.;
    GasCond = 0.;
    Gt      = 0.;
    x       = 0.;
    Kslip   = 0.;
    alpha   = 0.;
    ReTP    = 0.;
    ReL     = 0.;
    Xtd     = 0.;
    Ttd     = 0.;
    Ytd     = 0.;
    Ftd     = 0.;
    Ktd     = 0.;
    Xbr     = 0.;
    jg      = 0.;
}

CSetOfData::~CSetOfData(void)
{
}

#pragma once

class CSetOfData
{
public:
    int gNum;
    char *runNum, *testDate, *FlwPatn;

```

```

        double Deg, ReSL, ReSG;
        double JK_HTC, DK_HTC, QBalErr, Tin, Tout, DT, Amp, Volt, QFlux, QGen, QTaken;
        double LqdVFR, GasVFR, LqdMFR, GasMFR, VSL, VSG, Pref;
        double LqdPr, GasPr, LqdRho, GasRho, LqdCp, GasCp, LqdVisc, GasVisc, LqdVisc_BW,
LqdCond, GasCond;
        double Gt, x, Kslip, alpha, ReTP, ReL, Xtd, Ttd, Ytd, Ftd, Ktd, Xbr, jg;

        CSetOfData(void);
        ~CSetOfData(void);
};

// TPhPress.cpp: implementation of the CTPHPress class.
//
//
//
#include ".\2PhHT.h"
#include ".\TPhPress.h"

//
// Construction/Destruction
//
CTPhPress::CTPhPress()
{
    m_fTP = new double[NUM_PT];
}

CTPhPress::~CTPhPress()
{
    delete[] m_fTP;
}

void CTPHPress::calFraction(double deg)
{
    double theta = PI*deg/180.;
    double hf;
    for(int i=0;i<NUM_PT;i++)
    {
        hf = DL[i]*sin(theta)+(m_dP[i]*6894.757293)/(m_rhoTP*G_SI);
        m_fTP[i]=hf/(DL[i]/ID_PIPE*m_VTP*m_VTP/2.0/G_SI);
    }
}

void CTPHPress::setVelandDens(double mdotL, double mdotG, double rhoL, double rhoG)
{
    double QL = mdotL/rhoL;
    double QG = mdotG/rhoG;
    m_VTP = (QL+QG)/CS_AREA;
    m_rhoTP = (mdotL+mdotG)/(QL+QG);
}

void CTPHPress::prntFractionSI(char *runNum, char* testDate, char* Pattern)
{
    int i;
    char fileName[20];
    char *StNoStrip = "\n\t\t\t\t\t PT# 5 10";
    fstream my2HTFile;

```

```

strcpy(fileName,"RN");strcat(fileName,runNum);strcat(fileName,"SI.2HT");

my2HTFile.open(fileName, ios::app);
if(!my2HTFile)
{
    cerr<<"cannot open and append 2HT file"<<endl;
    exit(1);
}

my2HTFile <<"\n\n" << endl;
my2HTFile << "\t\t\t======" << endl;
my2HTFile << "\t\t\t    RUN NUMBER " << runNum << " continued" << endl;
my2HTFile << "\t\t\t    FLOW PATTERN: "<< Pattern << endl;
my2HTFile << "\t\t\t    Two-phase flow Darcy Friction factor " << endl;
my2HTFile << "\t\t\t    Test Date: " << testDate << endl;
my2HTFile << "\t\t\t======" << endl;

my2HTFile << setiosflags( ios::fixed );

my2HTFile << "\n\t\t\t\tPRESSURE DROP ALONG TUBE [psia]" << StNoStrip << endl;
my2HTFile << "\t\t\t\t\t";
for(i=NUM_PT-1;i>=0;i--) my2HTFile << " " << setfill(' ') <<setprecision(4) <<setw(7) <<
m_dP[i];
my2HTFile << endl;

my2HTFile << "\n\t\t\t\t TWO-PHASE FLOW FRICTION FACTOR TUBE" << StNoStrip <<
endl;
my2HTFile << "\t\t\t\t\t";
for(i=NUM_PT-1;i>=0;i--) my2HTFile << " " << setfill(' ') <<setprecision(4) <<setw(7) <<
m_fTP[i];
my2HTFile << endl;

my2HTFile.close();
}

void CTPhPress::prntFractionFPS(char *runNum, char* testDate, char* Pattern)
{
    int i;
    char fileName[20];
    char *StNoStrip = "\n\t\t\t\t PT# 5 10";
    fstream my2HTFile;

    strcpy(fileName,"RN");strcat(fileName,runNum);strcat(fileName,"FPS.2HT");

    my2HTFile.open(fileName, ios::app);
    if(!my2HTFile)
    {
        cerr<<"cannot open and append 2HT file"<<endl;
        exit(1);
    }

    my2HTFile <<"\n\n" << endl;
    my2HTFile << "\t\t\t======" << endl;

```



```

////////////////////////////////////
// Construction/Destruction
////////////////////////////////////

CTPhVars::CTPhVars()
{
    m_theta = 0.;
    m_ReSL = 0.;
    m_ReSG = 0.;
    m_VSL = 0.;
    m_VSG = 0.;
    m_ReTP = 0.;
    m_x = 0.;
    m_Gt = 0.;
    m_Kslip = 0.;
    m_rhoH = 0.;
    m_alpha = 0.;
    m_Xtd = 0.;
    m_Ktd = 0.;
    m_Ftd = 0.;
    m_Ttd = 0.;
    m_Ytd = 0.;
    m_Xbr = 0.;
    m_jg = 0.;
}

CTPhVars::~~CTPhVars()
{
}

void CTPHVars::set2PhVars(double deg, double rhoL, double rhoG, double muL, double muG, double
mdotL, double mdotG)
{
    double mdotT;
    double dPL, fL, BL, nL;
    double dPG, fG, BG, nG;

    m_theta = PI*deg/180.;
    mdotT = mdotG + mdotL;
    m_x = mdotG/mdotT;
    m_Gt = mdotT/CS_AREA;

    m_rhoH = 1./((1.-m_x)/rhoL + m_x/rhoG);
    m_Kslip = pow(rhoL/m_rhoH, 0.5);
    m_alpha = 1./(1. + m_Kslip*(1.-m_x)/m_x*rhoG/rhoL);

    m_VSL = mdotL/(rhoL*CS_AREA);
    m_VSG = mdotG/(rhoG*CS_AREA);

    m_ReSL = m_Gt*(1.-m_x)*ID_PIPE/muL;
}

```



```

my2HTFile << "\t\t\t\tQUALITY(x)      : " << setiosflags( ios::right )<<setfill('
')<<setprecision(3)<<setw(9)<< m_x      << endl;
my2HTFile << "\t\t\t\tSLIP RATIO(K)   : " << setiosflags( ios::right )<<setfill('
')<<setprecision(3)<<setw(9)<< m_Kslip   << endl;
my2HTFile << "\t\t\t\tVOID FRACTION(alpa): " << setiosflags( ios::right )<<setfill('
')<<setprecision(3)<<setw(9)<< m_alpha   << endl;
my2HTFile << "\t\t\t\tV_SL           : " << setiosflags( ios::right )<<setfill('
')<<setprecision(3)<<setw(9)<< m_VSL     << " [m/s]" << endl;
my2HTFile << "\t\t\t\tV_SG           : " << setiosflags( ios::right )<<setfill('
')<<setprecision(3)<<setw(9)<< m_VSG     << " [m/s]" << endl;
my2HTFile << "\t\t\t\tRE_SL          : " << setiosflags( ios::right )<<setfill('
')<<setprecision(0)<<setw(9)<< m_ReSL    << endl;
my2HTFile << "\t\t\t\tRE_SG          : " << setiosflags( ios::right )<<setfill('
')<<setprecision(0)<<setw(9)<< m_ReSG    << endl;
my2HTFile << "\t\t\t\tRE_TP          : " << setiosflags( ios::right )<<setfill('
')<<setprecision(0)<<setw(9)<< m_ReTP    << endl;
my2HTFile << "\t\t\t\tX(Taitel & Dukler) : " << setiosflags( ios::right )<<setfill('
')<<setprecision(3)<<setw(9)<< m_Xtd     << endl;
my2HTFile << "\t\t\t\tT(Taitel & Dukler) : " << setiosflags( ios::right )<<setfill('
')<<setprecision(3)<<setw(9)<< m_Ttd     << endl;
my2HTFile << "\t\t\t\tY(Taitel & Dukler) : " << setiosflags( ios::right )<<setfill('
')<<setprecision(3)<<setw(9)<< m_Ytd     << endl;
my2HTFile << "\t\t\t\tF(Taitel & Dukler) : " << setiosflags( ios::right )<<setfill('
')<<setprecision(3)<<setw(9)<< m_Ftd     << endl;
my2HTFile << "\t\t\t\tK(Taitel & Dukler) : " << setiosflags( ios::right )<<setfill('
')<<setprecision(3)<<setw(9)<< m_Ktd     << endl;
my2HTFile << "\t\t\t\tX (Breber)      : " << setiosflags( ios::right )<<setfill('
')<<setprecision(3)<<setw(9)<< m_Xbr     << endl;
my2HTFile << "\t\t\t\tj*g(Breber)     : " << setiosflags( ios::right )<<setfill('
')<<setprecision(3)<<setw(9)<< m_jg      << endl;

```

```

aDBLine_SI->Deg   = m_theta*180./PI;
aDBLine_SI->Gt    = m_Gt;
aDBLine_SI->x     = m_x;
aDBLine_SI->Kslip = m_Kslip;
aDBLine_SI->alpha = m_alpha;
aDBLine_SI->ReTP  = m_ReTP;
aDBLine_SI->ReL   = m_ReL;
aDBLine_SI->Xtd   = m_Xtd;
aDBLine_SI->Ttd   = m_Ttd;
aDBLine_SI->Ytd   = m_Ytd;
aDBLine_SI->Ftd   = m_Ftd;
aDBLine_SI->Ktd   = m_Ktd;
aDBLine_SI->Xbr   = m_Xbr;
aDBLine_SI->jg    = m_jg;
aDBLine_SI->FlwPatn = Pattern;

```

```

my2HTFile.close();

```

```

}

```

```

void CTPHVars::prnt2PhVarsFPS(char *runNum, char* testDate, char* Pattern, CSetOfData
*aDBLine_FPS)

```

```

{
    char fileName[20];
    fstream my2HTFile;

```

```

strcpy(fileName,"RN");strcat(fileName,runNum);strcat(fileName,"FPS.2HT");
my2HTFile.open(fileName, ios::out|ios::app);
    if(!my2HTFile)
    {
        cerr<<"cannot open and append 2HT file in void CTPHVars::prnt2PhVarsFPS()"<<endl;
        exit(1);
    }

my2HTFile <<"\n\n" << endl;
my2HTFile << "\t\t\t=====" << endl;
my2HTFile << "\t\t\t    RUN NUMBER " << runNum << " continued" << endl;
my2HTFile << "\t\t\t    FLOW PATTERN: "<< Pattern << endl;
my2HTFile << "\t\t\t    Air-Water Two-phase Heat Transfer" << endl;
my2HTFile << "\t\t\t    QUANTITIES OF MAIN PARAMETERS" << endl;
my2HTFile << "\t\t\t    Test Date: " << testDate << endl;
my2HTFile << "\t\t\t=====" << endl;

my2HTFile << setiosflags( ios::fixed );

my2HTFile << "\t\t\t\tINCLINATION ANGLE : " << setiosflags( ios::right )<<setfill('
')<<setprecision(3)<<setw(9)<< m_theta*180./PI << " [DEG]" << endl;
my2HTFile << "\t\t\t\tTOTAL MASS FLUX(Gt): " << setiosflags( ios::right )<<setfill('
')<<setprecision(3)<<setw(9)<< m_Gt/1.259979/9.290304e-2 << " [lbm/ft^2-hr]" << endl;
my2HTFile << "\t\t\t\tQUALITY(x)      : " << setiosflags( ios::right )<<setfill('
')<<setprecision(3)<<setw(9)<< m_x << endl;
my2HTFile << "\t\t\t\tSLIP RATIO(K)      : " << setiosflags( ios::right )<<setfill('
')<<setprecision(3)<<setw(9)<< m_Kslip << endl;
my2HTFile << "\t\t\t\tVOID FRACTION(alpa): " << setiosflags( ios::right )<<setfill('
')<<setprecision(3)<<setw(9)<< m_alpha << endl;
my2HTFile << "\t\t\t\tV_SL      : " << setiosflags( ios::right )<<setfill('
')<<setprecision(3)<<setw(9)<< m_VSL/3.048000e-1 << " [ft/s]" << endl;
my2HTFile << "\t\t\t\tV_SG      : " << setiosflags( ios::right )<<setfill('
')<<setprecision(3)<<setw(9)<< m_VSG/3.048000e-1 << " [ft/s]" << endl;
my2HTFile << "\t\t\t\tRE_SL      : " << setiosflags( ios::right )<<setfill('
')<<setprecision(0)<<setw(9)<< m_ReSL << endl;
my2HTFile << "\t\t\t\tRE_SG      : " << setiosflags( ios::right )<<setfill('
')<<setprecision(0)<<setw(9)<< m_ReSG << endl;
my2HTFile << "\t\t\t\tRE_TP      : " << setiosflags( ios::right )<<setfill('
')<<setprecision(0)<<setw(9)<< m_ReTP << endl;
my2HTFile << "\t\t\t\tX(Taitel & Dukler) : " << setiosflags( ios::right )<<setfill('
')<<setprecision(3)<<setw(9)<< m_Xtd << endl;
my2HTFile << "\t\t\t\tT(Taitel & Dukler) : " << setiosflags( ios::right )<<setfill('
')<<setprecision(3)<<setw(9)<< m_Ttd << endl;
my2HTFile << "\t\t\t\tY(Taitel & Dukler) : " << setiosflags( ios::right )<<setfill('
')<<setprecision(3)<<setw(9)<< m_Ytd << endl;
my2HTFile << "\t\t\t\tF(Taitel & Dukler) : " << setiosflags( ios::right )<<setfill('
')<<setprecision(3)<<setw(9)<< m_Ftd << endl;
my2HTFile << "\t\t\t\tK(Taitel & Dukler) : " << setiosflags( ios::right )<<setfill('
')<<setprecision(3)<<setw(9)<< m_Ktd << endl;
my2HTFile << "\t\t\t\tX (Breber)      : " << setiosflags( ios::right )<<setfill('
')<<setprecision(3)<<setw(9)<< m_Xbr << endl;
my2HTFile << "\t\t\t\ttj*g(Breber)     : " << setiosflags( ios::right )<<setfill('
')<<setprecision(3)<<setw(9)<< m_jg << endl;

aDBLine_FPS->Deg = m_theta*180./PI;
aDBLine_FPS->Gt = m_Gt/1.259979/9.290304e-2;

```

```

aDBLine_FPS->x      = m_x;
aDBLine_FPS->Kslip  = m_Kslip;
aDBLine_FPS->alpha  = m_alpha;
aDBLine_FPS->ReTP   = m_ReTP;
aDBLine_FPS->ReL    = m_ReL;
aDBLine_FPS->Xtd    = m_Xtd;
aDBLine_FPS->Ttd    = m_Ttd;
aDBLine_FPS->Ytd    = m_Ytd;
aDBLine_FPS->Ftd    = m_Ftd;
aDBLine_FPS->Ktd    = m_Ktd;
aDBLine_FPS->Xbr    = m_Xbr;
aDBLine_FPS->jg     = m_jg;
aDBLine_FPS->FlwPatn = Pattern;

my2HTFile.close();
}

```

```

// TPhVars.h: interface for the CTPHVars class.
#pragma once

```

```

#include ".\SetOfData.h"

```

```

class CTPHVars

```

```

{

```

```

protected:

```

```

    double m_theta;
    double m_ReSL, m_ReSG; //superficial Reynolds number
    double m_VSL, m_VSG; //superficial Velocity
    double m_ReTP; //two-phase Reynolds number
    double m_ReL; //in-sity Reynolds number
    double m_Kslip; //slip ratio
    double m_x; //quality
    double m_Gt; //total mass flux
    double m_rhoH; //homogenous density
    double m_alpha; //void fraction
    double m_Xtd; //Martinelli parameter
    double m_Ktd; //wavy flow, dimensionless parameter
    double m_Ftd; //modified Froude number
    double m_Ttd; //dispersed bubble flow dimensionless parameter
    double m_Ytd; //inclination dimensionless parameter
    double m_Xbr; //Martinelli parameter (Breber et al.)
    double m_jg; //dimensionless gas velocity (Breber et al.)

```

```

public:

```

```

    void prnt2PhVarsSI(char *runNum, char* testDate, char* Pattern, CSetOfData *aDBLine_SI);
    void prnt2PhVarsFPS(char *runNum, char* testDate, char* Pattern, CSetOfData *aDBLine_FPS);
    void set2PhVars(double deg, double rhoL, double rhoG, double muL, double muG, double mdotL,
double mdotG);

```

```

    CTPHVars();
    virtual ~CTPHVars();

```

```

};

```

APPENDIX B

UNCERTAINTY ANALYSIS

An analysis of the probable error involved in the experimental data of the two-phase annular flow heat transfer coefficients is calculated and explained in this Appendix. Calculation of the uncertainties is based on the method proposed by Kline and McClintock (1953).

Uncertainty Analysis of Heat Transfer Coefficient

The heat transfer coefficient is defined as:

$$h = \frac{\dot{q}''}{T_{wi} - T_b} \quad (1)$$

The percent probable error for h is given by:

$$w_h = \left[\left(\frac{d\dot{q}''}{\dot{q}''} \right)^2 + \left(\frac{dT}{\Delta T} \right)^2 \right]^{1/2} \quad (2)$$

The heat flux is the product of the voltage drop across the test section and the current carried by the tube. Therefore, the heat flux can be written as:

$$\dot{q}'' = \frac{V_D I}{\pi D_i L} \quad (3)$$

The uncertainty in the heat flux can then be calculated using the following equation:

$$U_{\dot{q}''} = \left[\left(\frac{dV_D}{V_D} \right)^2 + \left(\frac{dI}{I} \right)^2 + \left(\frac{dD_i}{D_i} \right)^2 + \left(\frac{dL}{L} \right)^2 \right]^{1/2} \quad (4)$$

The uncertainty of each variable was then estimated as follows:

dV_D The voltage was measured by the National Instruments Data Acquisition System and the error of the terminal block was 0.05%. The two-phase flow heat transfer experimental data had a voltage range of 2.19 to 4.91 volts, and it gives an average error of 0.03545 volts.

dI The amperage was also measured by the National Instruments Data Acquisition System and the error of the terminal block was 0.05%. The two-phase flow heat transfer experimental data had a current range of 288 to 508 amps, and it gives an average error of 3.98 amps.

dD_i The inside diameter of the test section was measured accurately to 0.001 inch using a caliper, and the inside diameter was 1.097 inches.

dL The heated length of the test section was 110 inches and was measured to within 0.0625 inch.

To evaluate the inside wall temperature, T_{wi} , using the appropriate boundary conditions, the heat diffusion equation was solved to render equation 5.

$$T_{wi} = T_{wo} - \left(\frac{\dot{q}}{2\pi \frac{(D_o^2 - D_i^2)}{4} kL} \right) \left[D_o^2 \ln \left(\frac{D_o}{D_i} \right) - \left(\frac{D_o^2 - D_i^2}{2} \right) \right] \quad (5)$$

The bulk temperature at the desired location x is determined by using the following equation:

$$T_b = T_{b,out} - [(T_{b,out} - T_{b,in})(L - x)]/L \quad (6)$$

The uncertainty associated with the quantity $(T_{wi} - T_b)$ can be estimated from the following equation:

$$U_i = \left[\left(\frac{|dT_{wo}| + |dT_b| + |dT_2| + |dT_1|}{T_{wi} - T_b} \right)^2 \right]^{1/2} \quad (7)$$

where

$$T_1 = - \left(\frac{\dot{q}}{2\pi \frac{(D_o^2 - D_i^2)}{4} kL} \right) \left[D_o^2 \ln \left(\frac{D_o}{D_i} \right) - \left(\frac{D_o^2 - D_i^2}{2} \right) \right] \quad (8)$$

$$T_2 = (T_{b,out} - T_{b,in})(L - x)/L \quad (9)$$

For this analysis, the following uncertainties of each term are as follows:

dT_{wo} The assumed error in the outside wall temperature was estimated to be 0.5°C within a range of 0 to 40 °C, which was an ordinary temperature variation during the test run, from the calibration runs for the thermocouples.

dT_b The average bulk temperature deviation was assumed to be 0.5 °C within a range of 0 to 40 °C, which was an ordinary temperature variation during the test run, from the calibration runs for the inlet thermal probe and the outlet thermal probe.

dT_2 The deviation ratio, dT_2/T_2 was assumed to be 0.02 °C.

dT_1 The deviation ratio, dT_1/T_1 was assumed to be 0.02 °C.

Using a typical two-phase flow heat transfer run (at TC station no. 6 of RN4108):

$$\dot{q} = 2115.16 \text{ W} \quad \dot{q}'' = 9147.17 \text{ W/m}^2$$

$$V_D = 4.5725 \text{ volts} \quad I = 462.58 \text{ amps}$$

$$T_{bin} = 13.95 \text{ } ^\circ\text{C} \quad T_{b,out} = 18.77 \text{ } ^\circ\text{C}$$

$$\begin{aligned}
 D_o &= 0.028854 \text{ m} & D_i &= 0.02786 \text{ m} \\
 T_{wo} &= 28.03 \text{ }^{\circ}\text{C} & k &= 13.1186 \text{ W/m-}^{\circ}\text{K} \\
 x &= 1.4478 \text{ m} & L &= 2.7941 \text{ m}
 \end{aligned}$$

Substituting all of the above values into the proper equations, we have

$$T_1 = -0.729 \text{ }^{\circ}\text{C}$$

$$T_2 = 2.32 \text{ }^{\circ}\text{C}$$

$$(T_{wi} - T_b) = 10.84 \text{ }^{\circ}\text{C}$$

These values result in the expected experimental uncertainties of:

$$\begin{aligned}
 U_t &= \{[(0.5 + 0.5 + 0.02 + 0.02/10.84)^2]\}^{1/2} \\
 &= 0.0959
 \end{aligned}$$

$$\begin{aligned}
 U_{\dot{q}''} &= [(0.03545/4.57)^2 + (3.98/462.58)^2 + (0.001/1.097)^2 + (0.0625/110)^2]^{1/2} \\
 &= 0.0116
 \end{aligned}$$

$$U_h = [(0.0959)^2 + (0.0116)^2]^{1/2}$$

Finally, the uncertainty for heat transfer coefficient calculations is

$$U_h = 9.65 \%$$

From the uncertainty analysis, it can be seen that the maximum error corresponding to the experimental heat transfer coefficient is 9.65 %. As shown in this analysis, the uncertainty in heat transfer coefficient is dominated by the accuracy of the measurement of temperatures.

In our analysis a more representative value of dT_{wo} and dT_b would have been 0.3°C . Using this value in our calculations, the uncertainty was found to be 6.01 %.

VITA

Kapil Malhotra

Candidate for the Degree of

Master of Science

Thesis: HEAT TRANSFER MEASUREMENT OF SLUG TWO-PHASE FLOW IN A
HORIZONTAL AND A SLIGHTLY UPWARD INCLINED TUBE

Major Field: Mechanical Engineering

Biographical:

Personal Data: Born in Lucknow (India), on July 31, 1978, the son of
Mr. J.L.Malhotra and Mrs. Neeru Malhotra.

Education: Received the Bachelor of Science degree in Mechanical Engineering,
Siddaganga Institute of Technology, Karnataka (India), in October 2000.
Completed the requirements for the Master of Science degree at Oklahoma
State University, Stillwater (USA), in December 2004.

Professional Experience: Worked as a Senior Projects Engineer for Triveni
Engineering and Industries Limited (A Turbine Manufacturing Group),
Bangalore, India from 2000 to 2002. Graduate Teaching and Research
Assistant, School of Mechanical and Aerospace Engineering, Oklahoma State
University, 2003 to 2004.

Professional Membership: American Society of Mechanical Engineers (ASME)